

MODELING AND OPTIMIZATION OF HYBRID ELECTRIC VEHICLES

A THESIS SUBMITTED TO  
THE GRADUATE SCHOOL OF NATURAL AND APPLIED SCIENCES  
OF  
MIDDLE EAST TECHNICAL UNIVERSITY

BY

BURAK ŞAMİL ÖZDEN

IN PARTIAL FULFILLMENT OF THE REQUIREMENTS  
FOR  
THE DEGREE OF MASTER OF SCIENCE  
IN  
MECHANICAL ENGINEERING

FEBRUARY 2013



Approval of the thesis:

**MODELING AND OPTIMIZATION OF HYBRID ELECTRIC VEHICLES**

submitted by **BURAK ŞAMİL ÖZDEN** in partial fulfillment of the requirements for the degree of **Master of Science in Mechanical Engineering Department, Middle East Technical University** by,

Prof. Dr. Canan Özgen  
Dean, Graduate School of **Natural and Applied Sciences**

\_\_\_\_\_

Prof. Dr. Süha Oral  
Head of Department, **Mechanical Engineering**

\_\_\_\_\_

Prof. Dr. Y. Samim Ünlüsoy  
Supervisor, **Mechanical Engineering Dept., METU**

\_\_\_\_\_

**Examining Committee Members:**

Prof. Dr. Tuna Balkan  
Mechanical Engineering Dept., METU

\_\_\_\_\_

Prof. Dr. Y. Samim Ünlüsoy  
Mechanical Engineering Dept., METU

\_\_\_\_\_

Assoc. Prof. Dr. İlhan Konukseven  
Mechanical Engineering Dept., METU

\_\_\_\_\_

Asst. Prof. Dr. Buğra Koku  
Mechanical Engineering Dept., METU

\_\_\_\_\_

Asst. Prof. Dr. Kutluk Bilge Arıkan  
Mechatronics Engineering Dept., Atılım University

\_\_\_\_\_

Date: 01.02.2013

**I hereby declare that all information in this document has been obtained and presented in accordance with academic rules and ethical conduct. I also declare that, as required by these rules and conduct, I have fully cited and referenced all material and results that are not original to this work.**

Name, Last name: Burak Şamil Özden

Signature:

## ABSTRACT

### MODELING AND OPTIMIZATION OF HYBRID ELECTRIC VEHICLES

Özden, Burak Şamil  
M.S., Department of Mechanical Engineering  
Supervisor: Prof. Dr. Y. Samim Ünlüsoy

February 2013, 135 pages

The main goal of this thesis study is the optimization of the basic design parameters of hybrid electric vehicle drivetrain components to minimize fuel consumption and emission objectives, together with constraints derived from performance requirements. In order to generate a user friendly and flexible platform to model, select drivetrain components, simulate performance, and optimize parameters of series and parallel hybrid electric vehicles, a MATLAB based graphical user interface is designed. A basic sizing procedure for the internal combustion engine, electric motor, and battery is developed. Pre-defined control strategies are implemented for both types of hybrid configurations. To achieve better fuel consumption and emission values, while satisfying nonlinear performance constraints, multi-objective gradient based optimization procedure is carried out with user defined upper and lower bounds of optimization parameters. The optimization process is applied to a number of case studies and the results are evaluated by comparison with similar cases found in literature.

Keywords: Hybrid Electric Vehicles, Vehicle Modeling, Optimization, Component Sizing, Graphical User Interface.

## ÖZ

### ELEKTRİKLİ HİBRİT ARAÇLARIN MODELLENMESİ VE OPTİMİZASYONU

Özden, Burak Şamil  
Yüksek Lisans, Makine Mühendisliği Bölümü  
Tez Yöneticisi: Prof. Dr. Y. Samim Ünlüsoy

Şubat 2013, 135 sayfa

Bu tez çalışmasının ana hedefi, elektrikli hibrit araç aktarma organlarına ait temel parametrelerin tanımlanmış performans değerlerini sağlayacak ve yakıt sarfiyatı ve emisyon amaç fonksiyonlarını en aza indirmek üzere optimizasyonunun gerçekleştirilmesidir. Aktarma organları parametrelerinin belirlenmesi, araç performansının elde edilmesi ve seri ve paralel elektrikli araç parametrelerinin optimizasyonu için kullanımı kolay ve esnek bir platform oluşturmak üzere MATLAB tabanlı bir grafik arayüz tasarlanmıştır. Elektrik motoru, içten yanmalı motor ve batarya için temel boyutlandırma işlemi için bir prosedür geliştirilmiştir. Her iki hibrit araç konfigürasyonu için önceden belirlenen kontrol stratejileri uygulanmıştır. Kullanıcı tarafından girilen alt ve üst tasarım parametreleri sınırları ve performans değerleri sağlanırken, daha iyi yakıt tüketimi ve emisyon değerleri elde etmek için, çok amaçlı, gradyan tabanlı optimizasyon prosedürü kullanılmıştır. Optimizasyon işlemi değişik tipte araçlar için uygulanmış ve elde edilen sonuçlar literatürde bulunan benzer uygulamalarla karşılaştırılarak değerlendirilmiştir.

Anahtar Kelimeler: Hibrit Elektrikli Araçlar, Araç Modelleme, Optimizasyon, Komponent Boyutlandırma, Grafik Kullanıcı Arayüzü

*To my lovely family*

## ACKNOWLEDGEMENTS

First, I would like to thank to my Supervisor Prof. Dr. Y. Samim Ünlüsoy for his guidance and advice for working discipline and for my thesis study.

I would like to state my appreciation to my dear friends and colleagues Akif Hacıncıpođlu, Hasan Ölmöz, Rasim Aşkın Dilan, Ferhat Sağlam, and Kamil Özden for their assistance and support. Financial support of TÜBİTAK is also gratefully acknowledged.

Finally I would like to thank my lovely family for their understanding, endless support, encouragement, and faith in me and to my love and intended wife Gülçin for her priceless love.

## TABLE OF CONTENTS

ABSTRACT.....	v
ÖZ.....	vi
ACKNOWLEDGEMENTS.....	viii
TABLE OF CONTENTS.....	ix
LIST OF FIGURES.....	xi
LIST OF TABLES.....	xiv
LIST OF ABBREVIATIONS.....	xv
 CHAPTERS	
INTRODUCTION.....	1
1.1 HYBRID ELECTRIC VEHICLE (HEV).....	1
1.2 HYBRID ELECTRIC VEHICLES COMPONENTS.....	2
1.3 HEV DRIVETRAIN ARCHITECTURES.....	3
1.3.1 Parallel Drivetrain.....	3
1.3.2 Series Drivetrain.....	4
1.3.3 Series-Parallel Drivetrain.....	4
1.3.4 Complex Drivetrain.....	5
1.4 POWER CONTROL SYSTEM.....	5
1.5 HYBRIDNESS.....	6
LITERATURE SURVEY.....	9
2.1 INTRODUCTION.....	9
2.2 LITERATURE SURVEY.....	9
SYSTEM MODELING.....	17
3.1 INTRODUCTION.....	17
3.2 VEHICLE MODELING.....	17
3.2.1 Drivetrain Configuration Selection.....	18
3.2.2 Component Modeling.....	19
3.2.3 Vehicle Model.....	37
3.3 POWER COMPONENT SIZING.....	39
3.3.1 Parallel Drive Train Power Component Sizing.....	40
3.3.2 Series Drive Train Power Component Sizing.....	45
3.4 CONTROL STRATEGY IMPLEMENTATION.....	50
3.4.1 Parallel Hybrid Control Strategy Parameters and Rules.....	51
3.4.2 Series Hybrid Control Strategy Parameters and Rules.....	56
GUI DEVELOPMENT.....	59
4.1 INTRODUCTION.....	59
4.2 INTERFACE DEVELOPMENT.....	59
4.2.1 Type Selection Screen.....	59
4.2.2 Parameters Screen.....	60
4.2.3 Optimization Screen.....	62
4.2.4 Results Screen.....	63
OPTIMIZATION PROCESS.....	67
5.1 INTRODUCTION.....	67
5.2 METHOD.....	67
5.3 OPTIMIZATION VARIABLES AND CONSTRAINTS.....	70
5.4 CASE STUDIES and Results.....	74
5.4.1 Case 1, 2 & 3.....	82
5.4.2 Case 4 & 5.....	85
5.4.3 Case 6.....	88

5.4.4 Case 7 & 8 .....	89
5.4.5 Case 9 .....	92
5.4.6 Case 10 .....	95
5.4.7 Case 11 .....	98
5.4.8 Case 12 & 13 .....	99
5.4.9 Case 14 & 15 .....	102
DISCUSSION AND CONCLUSION .....	105
REFERENCES .....	109
APPENDICIES	
A. SIZING PROCEDURE FLOWCHARTS .....	113
B. OPTIMIZATION PROCESS RESULT DATA .....	119
C. SIMULATION RESULTS FOR CONVENTIONAL VEHICLES .....	131

## LIST OF FIGURES

### FIGURES

Figure 1-1: HEV Components [3].....	2
Figure 1-2: Drivetrain configurations [3].....	4
Figure 1-3: Hybrid vehicle control scheme and strategy example [4].....	6
Figure 1-4: Hybridness value and related HEV name for parallel configuration [5] .....	7
Figure 1-5: Available techniques for different hybridness values [5] .....	8
Figure 3-1: ADVISOR Forward/Backward facing model [10] .....	18
Figure 3-2: Pre-transmission (a) and Post-transmission (b) configurations [2].....	19
Figure 3-3: Internal combustion engine block diagram [27].....	20
Figure 3-4: Fuel usage and emission block diagram [27] .....	21
Figure 3-5: Engine maps block diagram [27].....	22
Figure 3-6: Schematic of engine thermal model [12].....	22
Figure 3-7: Block diagram of top level exhaust catalyst model [27].....	24
Figure 3-8: Thermal resistance model of the catalytic converter [27].....	24
Figure 3-9: Rint and RC model comparison with experimental result for SOC [31] .....	26
Figure 3-10: Internal resistance model electrical schematic [31].....	27
Figure 3-11: Energy storage model [27] .....	27
Figure 3-12: Charging power limit for battery [32] .....	28
Figure 3-13: Battery thermal model schematic [31].....	29
Figure 3-14: Electric motor model block diagram .....	31
Figure 3-15: Gearbox upshift and downshift lines in engine torque-speed map [27] .....	34
Figure 3-16: Wheel/axle block diagram.....	35
Figure 3-17: Braking strategy and fractions [27] .....	35
Figure 3-18: Vehicle model block diagram.....	38
Figure 3-19: Forces acting on a vehicle acceleration up a slope .....	39
Figure 3-20: Parallel drivetrain power component sizing flow diagram.....	41
Figure 3-21: Comparison between acceleration times as published by manufacturers (crosses) and values calculated with (3.32) for $V = 100$ kph. (solid line).....	41
Figure 3-22: Block diagram representation of parallel drivetrain components sizing.....	44
Figure 3-23: Series drivetrain power component sizing flow diagram .....	46
Figure 3-24: Typical characteristics of traction motor .....	47
Figure 3-25: Block diagram representation of series drivetrain components sizing .....	48
Figure 3-26: Block diagram representation of series drivetrain components sizing .....	49
Figure 3-27: Block diagram representation of series drivetrain components sizing .....	50
Figure 3-28: Control strategy when $SOC > \text{low limit}$ [43].....	52
Figure 3-29: Battery resistance vs. SOC [27].....	55
Figure 3-30: ICE Efficiency map and $cs\_off\_trq\_frac$ and $cs\_min\_trq\_frac$ values.....	55
Figure 3-31: Series configuration controller block diagram.....	56
Figure 3-32: Series control strategy [27].....	58
Figure 4-1: Type Selection Screen GUI.....	60
Figure 4-2: Parameters Screen GUI .....	61
Figure 4-3: Optimization Screen GUI for series configuration .....	62
Figure 4-4: Optimization Screen GUI for parallel configuration .....	63
Figure 4-5: Results Screen GUI for parallel configuration .....	63
Figure 4-6: Flow diagram of the optimization process (a) .....	65
Figure 4-7: Flow diagram of the optimization process (b).....	66
Figure 5-1: Fuel economy and emission tradeoffs for a SI engine [43] .....	70
Figure 5-2: Fuel economy and emission tradeoffs for a CI engine [43].....	71
Figure 5-3: SOC correction procedure graphical representation.....	72
Figure 5-4: Speed profile of the UDDS drive cycle .....	75
Figure 5-5: Speed profile of the HWFET drive cycle .....	76
Figure 5-6: Speed profile of the J1015 drive cycle .....	76
Figure 5-7: ADVISOR result screen for simulation with case 1 initial parameters .....	82

Figure 5-8: ADVISOR result screen for simulation with case 2 initial parameters .....	83
Figure 5-9: ADVISOR result screen for simulation with case 3 initial parameters .....	83
Figure 5-10: ADVISOR result screen for simulation with case 1 optimized parameters.....	84
Figure 5-11: ADVISOR result screen for simulation with case 2 optimized parameters.....	85
Figure 5-12: ADVISOR result screen for simulation with case 3 optimized parameters.....	85
Figure 5-13: ADVISOR result screen for simulation with case 4 initial parameters .....	86
Figure 5-14: ADVISOR result screen for simulation with case 5 initial parameters .....	86
Figure 5-15: ADVISOR result screen for simulation with case 4 optimization result parameters.....	87
Figure 5-16: ADVISOR result screen for simulation with case 5 optimization result parameters.....	88
Figure 5-17: ADVISOR result screen for simulation with case 6 initial parameters .....	89
Figure 5-18: ADVISOR result screen for simulation with case 6 optimization result parameters.....	89
Figure 5-19: ADVISOR result screen for simulation with case 7 initial parameters .....	91
Figure 5-20: ADVISOR result screen for simulation with case 8 initial parameters .....	91
Figure 5-21: ADVISOR result screen for simulation with case 7 optimization result parameters.....	92
Figure 5-22: ADVISOR result screen for simulation with case 8 optimization result parameters.....	92
Figure 5-23: ADVISOR result screen for simulation with case 9 initial parameters .....	93
Figure 5-24: J1015 Drive cycle results for reference study .....	94
Figure 5-25: J1015 Drive cycle results for reference study with hot initial conditions.....	94
Figure 5-26: ADVISOR result screen for simulation with case 10 initial parameters .....	95
Figure 5-27: ADVISOR result screen for simulation with case 10 optimization result parameters.....	96
Figure 5-28: HWFET Drive Cycle without SOC correction.....	96
Figure 5-29: UDDS Drive cycle without SOC correction.....	97
Figure 5-30: UDDS Drive cycle without SOC correction and initial SOC = 0.8.....	97
Figure 5-31: ADVISOR result screen for simulation with case 11 initial parameters .....	99
Figure 5-32: ADVISOR result screen for simulation with case 11 optimization result parameters.....	99
Figure 5-33: ADVISOR result screen for simulation with case 12 initial parameters .....	101
Figure 5-34: ADVISOR result screen for simulation with case 13 initial parameters .....	101
Figure 5-35: ADVISOR result screen for simulation with case 12 optimization result parameters....	102
Figure 5-36: ADVISOR result screen for simulation with case 13 optimization result parameters....	102
Figure A-1: Flowchart for parallel drivetrain sizing procedure – part1 .....	113
Figure A-2: Flowchart for parallel drivetrain sizing procedure – part2 .....	114
Figure A-3: Flowchart for parallel drivetrain sizing procedure – part3 .....	115
Figure A-4: Flowchart for series drivetrain sizing procedure – part1 .....	116
Figure A-5: Flowchart for series drivetrain sizing procedure – part2 .....	117
Figure A-6: Flowchart for series drivetrain sizing procedure – part3 .....	118
Figure B-1: Case 1 cost function value change during optimization .....	119
Figure B-2: Case 2 cost function value change during optimization .....	119
Figure B-3: Case 3 cost function value change during optimization .....	120
Figure B-4: Case 4 cost function value change during optimization .....	120
Figure B-5: Case 5 cost function value change during optimization .....	121
Figure B-6: Case 6 cost function value change during optimization .....	121
Figure B-7: Case 7 cost function value change during optimization .....	122
Figure B-8: Case 8 cost function value change during optimization .....	122
Figure B-9: Case 9 cost function value change during optimization .....	123
Figure B-10: Case 10 cost function value change during optimization.....	123
Figure B-11: Case 11 cost function value change during optimization.....	124
Figure B-12: Case 12 cost function value change during optimization.....	124
Figure B-13: Case 13 cost function value change during optimization.....	125
Figure B-14: Case 14 – Run #1 cost function value change during optimization.....	125
Figure B-15: Case 14 – Run #2 cost function value change during optimization.....	126
Figure B-16: Case 14 – Run #3 cost function value change during optimization.....	126
Figure B-17: Case 14 – Run #4 cost function value change during optimization.....	127
Figure B-18: Case 14 – Run #5 cost function value change during optimization.....	127
Figure B-19: Case 15 – Run #1 cost function value change during optimization.....	128
Figure B-20: Case 15 – Run #2 cost function value change during optimization.....	128
Figure B-21: Case 15 – Run #3 cost function value change during optimization.....	129
Figure B-22: Case 15 – Run #4 cost function value change during optimization.....	129
Figure B-23: Case 15 – Run #5 cost function value change during optimization.....	130

Figure C-1: Results for UDDS - 85kW SI - 1625 kg .....	131
Figure C-2: Results for UDDS - 85kW SI - 1265 kg .....	132
Figure C-3: Results for J1015 - 85kW SI - 1265 kg.....	133
Figure C-4: Results for HWFET - 102kW SI - 1265 kg .....	134
Figure C-5: Results for UDDS - 85kW CI - 1200 kg.....	135

## LIST OF TABLES

### TABLES

Table 3-1: Fuel converter basic variables [27].....	25
Table 3-2: Fuel converter base data files .....	25
Table 3-3: Battery data files .....	29
Table 3-4: Energy storage system variables [27] .....	30
Table 3-5: Electric motor data files.....	32
Table 3-6: Electric motor variables [27] .....	32
Table 3-7: 5-Speed gearbox and final drive ratios .....	33
Table 3-8: Wheel/axle variables [27].....	36
Table 3-9: Baseline control strategy variables [27].....	52
Table 3-10: Base values of control strategy parameters.....	56
Table 3-11: Series control strategy parameters [27] .....	57
Table 5-1: Fmincon function parameters .....	69
Table 5-2: Parallel configuration optimization variables .....	72
Table 5-3: Series configuration optimization variables .....	73
Table 5-4: Base vehicle parameters .....	74
Table 5-5: Base power components specifications .....	75
Table 5-6: Case 1 data.....	77
Table 5-7: Case 2 data.....	77
Table 5-8: Case 3 data.....	77
Table 5-9: Case 4 data.....	78
Table 5-10: Case 5 data.....	78
Table 5-11: Case 6 data.....	78
Table 5-12: Case 7 data.....	79
Table 5-13: Case 8 data.....	79
Table 5-14: Case 9 data.....	79
Table 5-15: Case 10 data.....	80
Table 5-16: Case 11 data.....	80
Table 5-17: Case 12 data.....	80
Table 5-18: Case 13 data.....	81
Table 5-19: Case 14 data.....	81
Table 5-20: Case 15 data.....	81
Table 5-21: Case 1, 2 & 3 optimization results .....	84
Table 5-22: Case 4 & 5 optimization results .....	87
Table 5-23: Case 6 optimization results .....	88
Table 5-24: Case 7 & 8 optimization results.....	90
Table 5-25: Case 9 optimization results .....	93
Table 5-26: Case 10 optimization results .....	95
Table 5-27: Case 11 optimization results .....	98
Table 5-28: Case 12 optimization results .....	100
Table 5-29: Case 13 optimization results .....	100
Table 5-30: Case 14 and case 15 weighting factors .....	103
Table 5-31: Case 14 results .....	103
Table 5-32: Case 15 Results.....	104

## LIST OF ABBREVIATIONS

ADVISOR	Advanced Vehicle Simulator
AER	All Electric Range
CI	Compression Ignition
CIDI	Compression Ignition Direct Injection
CV	Conventional Vehicle
DIRECT	Divided Rectangles
DMI	Driving Mode Identifier
DTI	Driving Trend Identifier
ECU	Electronic Control Unit
EM	Electric Motor
EM/G	Electric Motor/Generator
EPA	Environmental Protection Agency
EV	Electric Vehicle
FLC	Fuzzy Logic Control
FTP	Federal Test Procedure
GPS	Global Positioning System
GUI	Graphical User Interface
HEV	Hybrid Electric Vehicle
HF	Hybridness Factor
HWFET	Highway Fuel Economy Test
HWY	Highway
ICE	Internal Combustion Engine
ICEV	Internal Combustion Engine Vehicle
LA92	California Unified Cycle
NEDC	New European Drive Cycle
NREL	National Research Laboratory
NSGA	Non-dominated Sorting Genetic Algorithm
PHEV	Plug-in Hybrid Electric Vehicle
PI	Proportional Integral
PID	Proportional Integral Derivative
PM	Permanent Magnet
PM	Particulate Matter
PNGV	Partnership of New Generation Vehicles
PSAT	Powertrain Analysis Toolkit
RCF	Resistive Companion Form
SA	Simulated Annealing
SAE	Society of Automotive Engineers
SI	Spark Ignition
SOC	State of Charge
SUV	Sport Utility Vehicle
UDDS	Urban Dynamometer Driving Schedule
USCAR	United States Consortium for Automotive Research
ZEV	Zero Emission Vehicle



## CHAPTER 1

### INTRODUCTION

#### 1.1 HYBRID ELECTRIC VEHICLE (HEV)

Increasing oil prices and emphasis on reducing emissions for environmental protection have forced and generated a new challenge for the automotive industry in 21<sup>st</sup> century. The ultimate aim is to reach zero emission vehicles (ZEV). However, battery and fuel cell technologies have not yet been adequately developed to meet essentials such as speed, driving range, and the development of the required infrastructure is neither easy nor economically feasible as yet. Although the hybrid electric vehicle (HEV) has been introduced as an interim solution just before full electric vehicle takes over the market, HEV has already proved to be a practical solution for commercialization of super-ultra-low-emission vehicles [1].

Early studies about hybridization of the energy for the propulsion of the vehicles start with 1916-1919 Woods gas electric car, although electric vehicle history goes to 1800s [2]. However, because of uncompetitive prices, lack of sufficient technologies such as electro mechanics, computer technology, and mismatch of adequate electrical energy storage unit, hybrid technology had to wait for about a century.

In 1970s, with the first oil crisis, it was realized that fossil fuels were not endless. In parallel with developing technologies and warnings about air pollution due to traffic, research on hybrid vehicles accelerated.

Some organizations have been launched to support the technology such as Partnership for New Generation of Vehicles (PNGV) which has a goal of mid-size sedan that could achieve 80 mpg (34 km/l) [2].

The main idea behind the hybrid technology is the combination of two or more power sources together in order to utilize the advantageous of the different characteristics of the sources and overcome the disadvantageous of separate systems. Starting from this idea, HEV which combines conventional internal combustion engine (ICE) and electric motor as propulsion units have advantages of both ICE vehicle and EV and overcome the some disadvantages of the individual systems. Due to high energy density of petroleum fuels, conventional ICE vehicles have long range and good driving performance while they have some disadvantages such as poor fuel economy and excessive pollutant emission. The reasons for poor performance in fuel economy are changing of the operation range of ICE according to driving conditions and dissatisfaction of maximum energy range operation, low efficiency of the engine and transmission in stop-and-go driving cycles. On the other hand battery powered electric vehicles have a distinctive advantage in “regenerative braking” which is defined as the storage instead of dissipation of the kinetic energy in the brakes during braking action. Moreover, electric motor has high efficiency by its nature. However pure electric vehicles suffer problems related to energy storage and the issue “State of Charge” (SOC) which shows the level of charge and it effects the efficiency of the battery operations together with the charging and discharging power levels.

Optimization of the ICE operation gives extra advantages in addition to reduction of emission and fuel consumption such as the extended maintenance periods and reduced cost due to reduced oil changes, exhaust repairs, brake pad replacements.

The main limitation for HEV is the battery technology which is the bottleneck of hybrid technology. Energy storage system adds extra cost and weight to the vehicle. There are further limitations due to cost of additional electric motor, power converters, and complex circuits for controllers. Moreover,

there are safety concerns due to high voltage applications in the system, electromagnetic field caused by high current changes with high frequency. To these, one can add probable problems, such as long term warranty and lack of specially trained employees for maintenance in service stations.

### 1.2 HYBRID ELECTRIC VEHICLES COMPONENTS

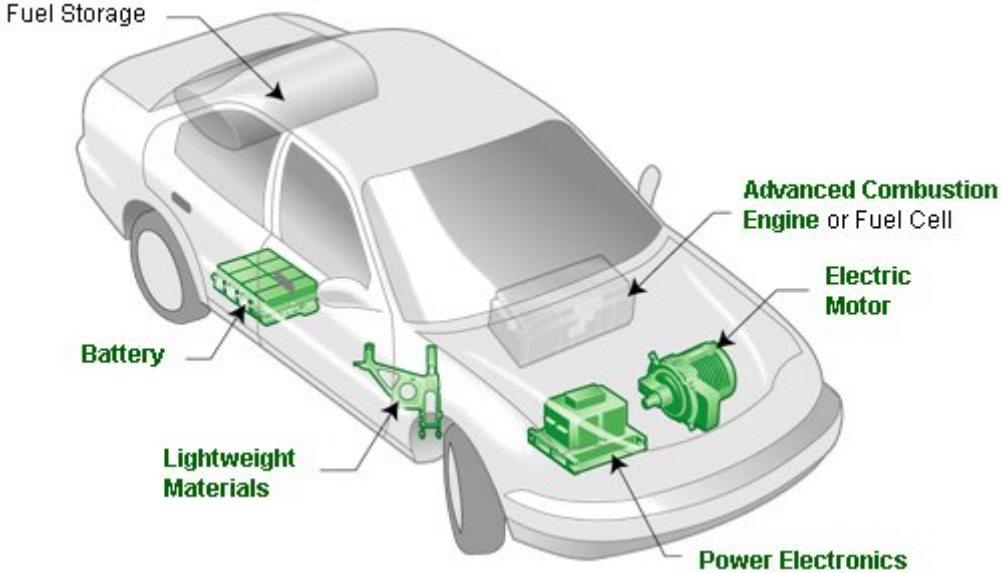


Figure 1-1: HEV Components [3]

HEVs include complex technologies compared to commercial vehicles. The system needs additional components which are not used in conventional vehicles. These components, shown in Figure 1-1, are electric motor, power converters, hybrid control unit, battery and ultracapacitors. In addition to them, lightweight materials for chassis such as magnesium alloys, improved and specially designed transmission system for speed and torque coupling are also included in HEV.

Brief descriptions of the key HEV technologies are as follows:

- *Propulsion System:* The propulsion system consists of two main elements: electric motor(s) and an internal combustion engine. There are 4 main types of electric motors used in HEVs: 1. DC Motors (brushed), 2. Induction Motors, 3. PM Synchronous or Brushless Motors, 4. Switch Reluctance Motors. These motor types have different characteristics, but the main requirements for a HEV are high torque/power density, high efficiency and the ability to sustain constant power and torque in a wide speed range. Moreover compactness, cost, reliability, and robustness are the other criteria for electric motor selection. Besides the electric motor specifications, innovations for the internal combustion engine are also possible such that downsizing the engine, adjustment of valve timing, and narrowed speed range for better fuel efficiency and emission characteristics.
- *Power Converters:* General power electronic circuits are rectifiers, dc/dc converters, inverters, etc. Whole system electrical power transmission characteristic is one of the major parts of the HEV. These characteristics include determination of current type (AC or DC), voltage value, cable size, thermal considerations, magnetic influences, frequency effects, safety precautions, and overall transmission efficiency. Since the subject is high electrical power transmission while protecting the system components such as batteries from fluctuations and undesirable situations

while bidirectional conduction of energy from EM/G to batteries or vice versa, all parameters have to be considered in design stage.

- *Hybrid Control Unit*: This is the “head” of the whole system which works in cooperation with the ECU unit for other systems of the car such as air conditioning, cooling, lighting, etc. It controls the hybrid system in order to achieve maximum fuel efficiency/minimum emission besides drive performance, comfort, and safety. This hardware unit runs the applied algorithm and controller strategies.
- *Energy Storage*: HEV basically has two storage units: fuel tank and electrical storage unit. The electrical energy storage has crucial importance for hybrid technology. It is essential for regenerative braking, electric only propulsion, electric propulsion assistance, and charging during coasting. Batteries and ultracapacitors are used to store energy. But the main difference is capacitor’s high specific power (W/kg) against battery’s high specific energy (Wh/kg). There are a wide variety of batteries include lead/acid, nickel/cadmium, nickel/metal hydride, zinc/bromine, lithium-ion and lithium polymer. As basic design parameters, energy storage capacity in other word specific energy value, supplied peak power, cycle life, efficiency, self-discharge value, and of course its cost have deterministic role.

### 1.3 HEV DRIVETRAIN ARCHITECTURES

Classification of hybrid electric vehicles could be organized according to different specifications and technologies such as connection type of electric motor and engine by means of transmission, or power ratio of electric motor and engine. The most common classification is in terms of connection between the components which define the energy flow routes and control action of the flow. Conventionally, drivetrain classification is made as two basic types: “Parallel” and “Series”. In the following a total of 4 kinds of drivetrain architectures are defined:

- Parallel HEV
- Series HEV
- Series-Parallel HEV
- Complex HEV

#### 1.3.1 Parallel Drivetrain

Parallel drive train is constructed by means of mechanical coupling of electric motor and internal combustion engine with two separate clutches via the drive shaft. Different from the conventional ICE vehicle, electric motor assist the ICE in order to achieve common HEV performances such as low emission or fuel economy. On Figure 1-2 (a) schematic of parallel drive train and power flow line types and elements are given. The mechanical coupling between the motor and the engine could be in two different format named as “speed coupling” and “torque coupling” in order achieve different design requirements and this basic criteria works with the more complex systems given in following drivetrain types separately or both on the same system. Compared to series type applications, parallel drivetrain has the advantage of only one extra motor need moreover smaller electric motor and also smaller engine could be used which results in weight reduction and more space.

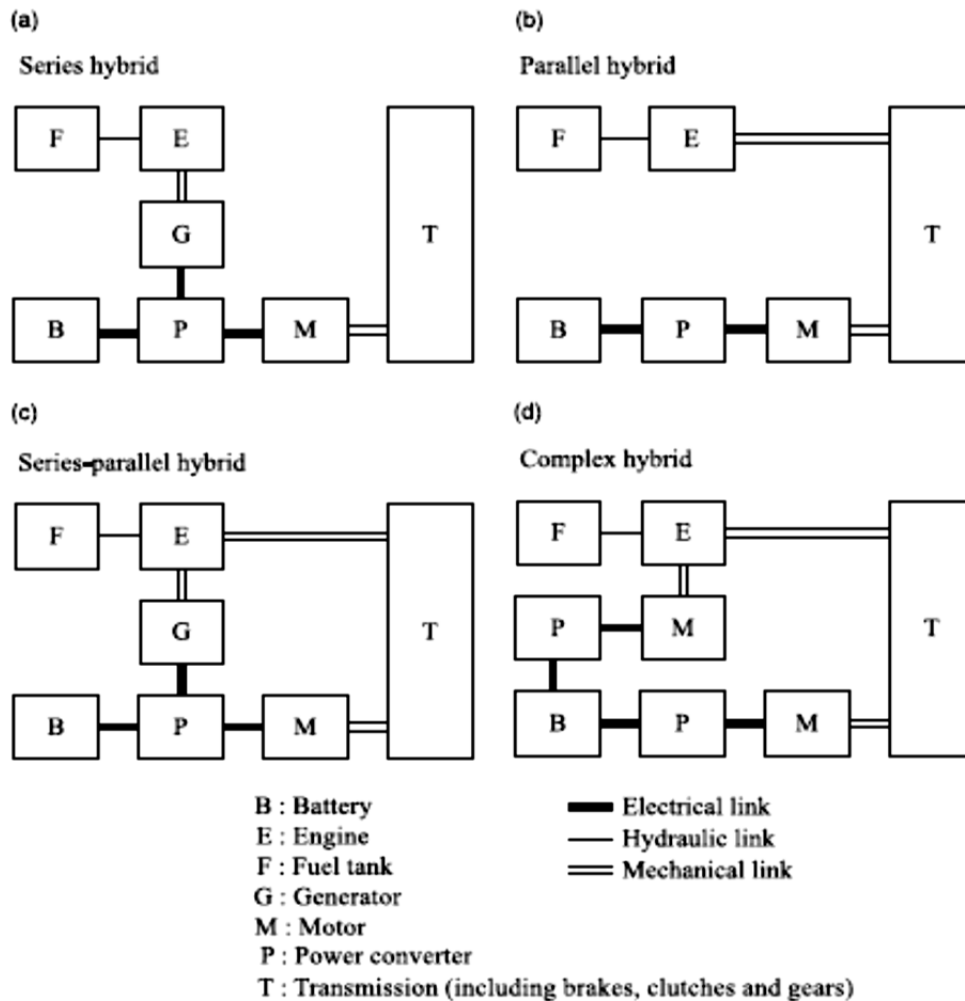


Figure 1-2: Drivetrain configurations [3]

### 1.3.2 Series Drivetrain

This is the simplest and a basic type of HEV drivetrains. Two separate power sources fuel and battery feed an ICE and an electric motor which propels the vehicle. The ICE is directly coupled with a generator and produces electrical energy which is transmitted to the battery or directly to electric motor connected to the drive shaft. The diagram for series drivetrain is given on Figure 1-2 (b). The series HEV is more like an EV with internal combustion engine assistance for charging the battery. It has similar advantages with parallel drivetrain such as engine operating region adjustment. In addition mechanical transmission free design adds more space to vehicle and direct electric propulsion of the wheels gives opportunities such as differential free four wheel drive. Compared to parallel one the system is simpler, thus elementary control algorithms could be adequate. On the other hand, the engine, generator, and electric motor have to sustain enough power during high torque demands.

### 1.3.3 Series-Parallel Drivetrain

Series parallel hybrid uses the advantageous of both series and parallel configurations. As shown on the Figure 1-2 (c), it includes an extra generator different from the parallel configuration and unlike the series configuration the engine has mechanical coupling directly with electric motor. Although from the cost point of view it seems disadvantageous, with a successful control design it may become more profitable.

### 1.3.4 Complex Drivetrain

The system shown in Figure 1-2 (d) is slightly different from the previous series-parallel configuration. A motor is connected to the engine with a planetary gear set. It could be both used as a generator and traction motor. Main advantage of this system is that it gives additional chance of third propulsive source and based on those new modes of operation with successive control application.

## 1.4 POWER CONTROL SYSTEM

The fundamental configurations listed above have all different characteristics with some common principles with varied complexities, additional components, and cost differences. As the system gets more complex the control strategy that has to be applied becomes more complicated by bringing new and versatile operation modes and better performance. Thus for each drivetrain configuration, a different control system implementation is needed in order to run the hybrid technology.

Different control systems vary from the very simple such as “on-off control” to those with high complexity including real time optimization and driving characteristic estimation. The main principle of the applied strategy is energy management or power split with the help of many separate sub elements like motor, engine, brake, transmission, and clutch controllers. While the aim is get the best optimized energy management, on the way to achieve the goal some basic considerations could be named as:

- Getting the maximum efficiency or minimum emission region/point of ICE on the torque/speed map according to demand.
- Satisfying the maximum battery efficiency related with energy demand rate and SOC
- Safe battery region satisfaction, keeping the SOC above from a certain value and below the maximum permissible value while propulsion, charging and regenerative braking.
- Power split between the electric motor (so the battery) and the engine according to system parameters.
- Determination of task of the electric motor whether to work as motor or generator considering the power demand, engine speed, and SOC.
- Engine shut down below a specified limit, avoiding low efficiency region.
- Avoiding/minimizing engine start operation and sudden speed changes to keep efficiency on the desired level.
- Some additional, nontraditional methods such as driving characteristic calculation and parameter optimization related to it, road characteristic prediction by a help of GPS and built-in map database and changing system parameters by global real time optimization.

These control actions differ according to each powertrain configuration and system elements' specifications. By the application of control actions to the system, general working modes could be observed:

- Engine Only Mode
- Electric Motor Only Mode
- Hybrid Mode
- Regenerative Braking Mode
- Engine Propulsion and Charging Mode
- Charging Only Mode
- Hybrid Propulsion and Charging Mode

The schematic of a typical control scheme example is given Figure 1-3. The main inputs are the accelerator and brake pedal positions. Together with these, vehicle velocity, selected gear, battery SOC, other sensor inputs to the system should be considered. Hierarchically, the main controller is named as vehicle controller which works together with sub-controllers engine, motor, brake, clutch and transmission. There are two main action modes named as “traction” and “braking”.

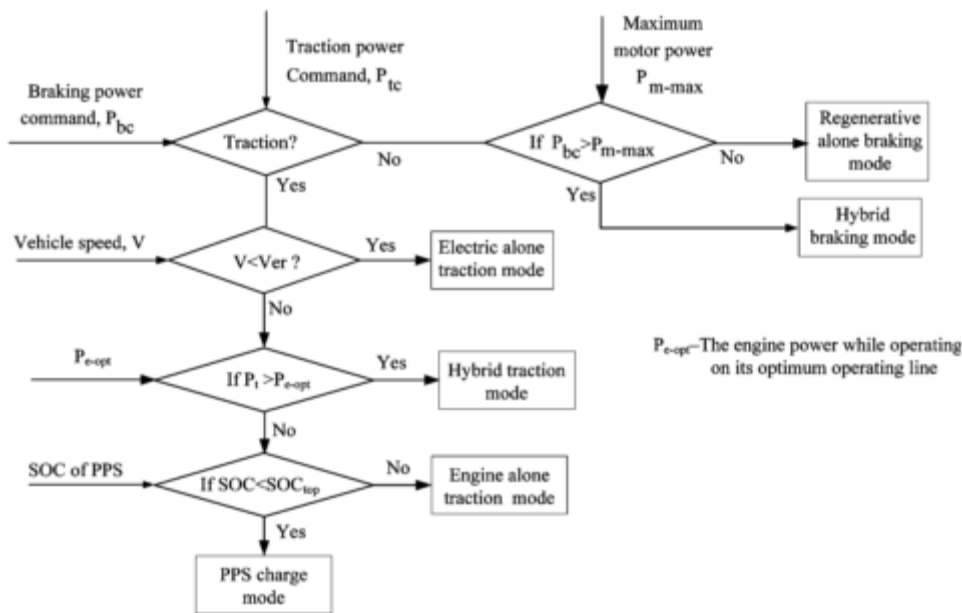
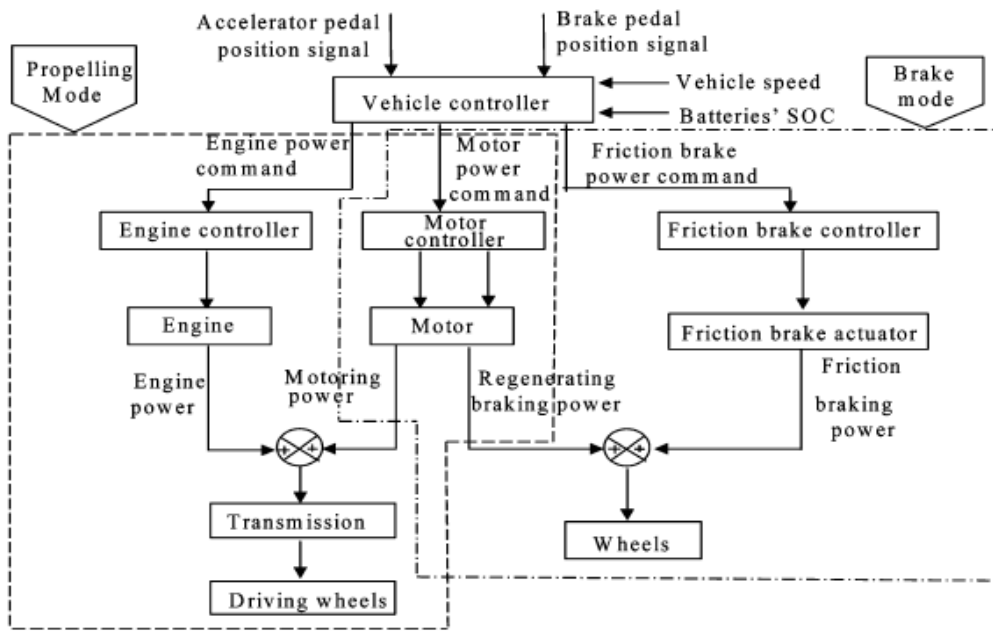


Figure 1-3: Hybrid vehicle control scheme and strategy example [4]

### 1.5 HYBRIDNESS

Hybridness is a value that gives an insight into the overall character of the hybrid vehicle. It can also be named as “hybridization factor”. The value is defined as the ratio of electric motor power to total vehicle propulsion power (ICE power + EM power) [5].

$$HF = \frac{\text{Sum of power of all traction motors}}{\text{Sum of all traction motors + Engine power}}$$

With changing hybridization factor, the prefix of HEV also changes. In Figure 1-4, a hybrid vehicle with parallel drivetrain configuration is given for different HFs. The three primary classifications are mild, full, and plug-in hybrids.

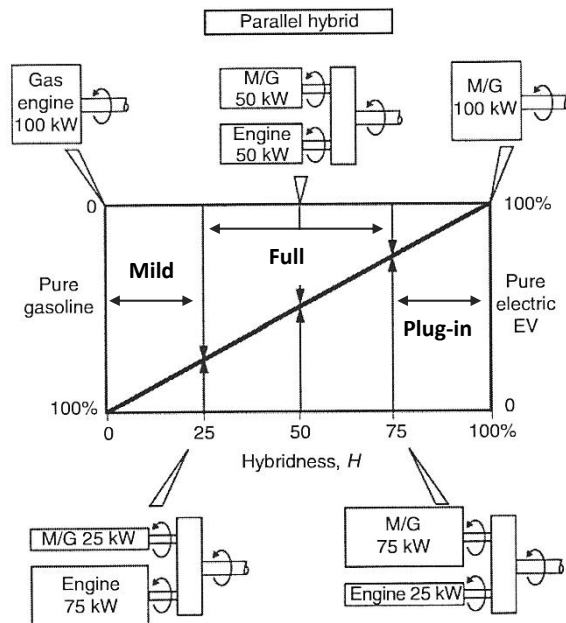


Figure 1-4: Hybridness value and related HEV name for parallel configuration [5]

HF value shows the hybridization implementation is applied for the purpose of which available techniques for hybrid vehicles. These could be sorted by increasing hybridness value starting from only start-stop ability, overcome engine oscillations, regenerative braking, electric only propulsion and up to considerably downsized engine with reduced fuel consumption. Various techniques to enhance hybrid performance arrayed with hybridness are given in Figure 1-5.

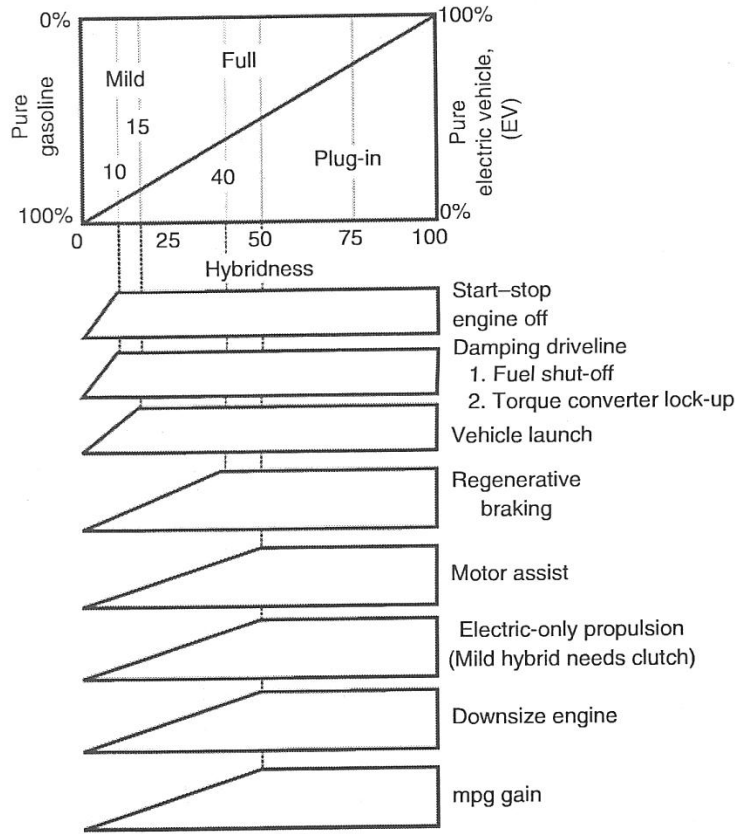


Figure 1-5: Available techniques for different hybridness values [5]

As a fundamental design decision, the hybridization factor value determination and optimization is one of the primary goals of the studies [6]. The optimization process of hybridness value could also be evaluated as power rating adjustment for propulsion systems since it is the ratio between electric motor and total power. The studies show that especially fuel consumption local minimization could be achieved around some specific hybridness value which gives an insight.

## CHAPTER 2

### LITERATURE SURVEY

#### 2.1 INTRODUCTION

Studies focused on drive train hybridization configurations and optimization of the structure elements according to their types, sizes, operating regions and working areas have vital effect especially on vehicle fuel consumption and emission values. The combination of the two propulsion systems gives additional degrees of freedom for designing components in order get better fuel and emission values. Thus, an optimization procedure for component selection and sizing and also for the control strategy with respect to defined constraints and optimization objectives defined respect to demands will be needed to reach a well-designed hybrid vehicle. Starting with this idea, a large number of studies have been reported in journal papers, theses and conference articles and graduate thesis in literature about this topic.

In the following section, the literature will be examined as the steps that constitute hybrid vehicle parameters optimization procedure. The main branches of the routine could be classified as

- Selection of the drivetrain configuration
- Modeling and sizing of the vehicle components
- Control strategy
- Optimization of the parameters

Selection of the drivetrain configuration is the basic decision parameter for a hybrid vehicle. For different configurations all design and simulation steps have to be modified and considerably large differences could be obtained. In the literature, comparison of the configurations with respect to fuel consumption and emission and also other aspects such as cost are given.

In the modeling section, starting from designing the vehicle by using Newton's second order law for the sizing according to performance needs which states the vehicle as a simple mass having an acceleration and velocity; continuing with inclusion of inertial effects of drivetrain parts and loses and finally reaching up to detailed models of each element with performances, internal dynamics, nonlinearities and loses. As the complexity of the model increases, its accuracy also increases; yet computational effort to get result also increases. In order to handle the complexity different platforms are investigated.

A wide variety of control strategy options are available in order to satisfy efficient engine operating point, correct SOC, regenerative braking, etc. Optimization of such control variables and new generation neural network and generic algorithm strategy implementations covered in the following.

Last branch, optimization of the design variables is the main focus of this study. Although optimization of the vehicle involves hundreds of design variables, it is difficult to optimize all the variables in an integrative manner. Thus only some basic parameters that have crucial effect on HEV performance are investigated.

#### 2.2 LITERATURE SURVEY

There is a considerable number of studies on HEV drivetrain configurations with respect to different design goals. Dominik et al. [7] investigated three different configurations (parallel, series, and split) for Plug-in Hybrid Electric Vehicles sized to have a similar all-electric range (AER), performance, and towing capacity in order to observe fuel consumption (L/100 km) and electrical energy consumption (Wh/km). The test is handled with 30% final SOC, 25% final and 91% initial SOC, 9.3

seconds 0-100 kph acceleration, 177 kph maximum speed and 6% grade at 105 kph constraint values. The simulations are handled by using three different driving cycles UDDS, HWY, and LA92. The simulated data shows that for different driving schedules different drivetrain configuration becomes advantageous. From the fuel consumption point of view, it is found that parallel configuration gives better performance with a smaller electric motor size, similar engine size, and nearly same battery capacity.

Vincent et al. [8] published another paper about powertrain configurations comparison for 10 AER and 40 AER PHEVs. The test carried out for charge sustaining mode in 10 AER, both for UDDS and HWFET driving cycles showed that parallel configuration gives superior results in fuel consumption (5.14 and 5 L/100 km, while series configuration gives 5.57 and 5.79 L/100 km and power split gives 5.43 and 5 L/100 km. When it comes to 40 AER case, as the battery capacity increased, power split configuration achieves better fuel consumption value such as 4.6 L/100 km while parallel configuration could reach 5.48 and series configuration could only get 5.69 L/100 km values in UDDS cycle. Although engine efficiency has the lowest value, 27.5% for parallel configuration, while series could operate around 32.5% and series configuration could reach up to 34.5% configuration and loses due mechanical transmission reach up to 6% in parallel selection, this configuration gives better results with power-split alternative compared to series one especially in regular hybrid electric vehicle working procedure.

Cuddy and Wipke [9] have made a feasibility analysis of parallel and series drivetrain by using comparison between the configurations and also with the conventional diesel-powered vehicle. The effects of vehicle components' specifications and efficiency values are investigated. Moreover the study includes sensitivity of different drivetrains according to changing vehicle parameter values for fuel economy aspect. An examined sensitivity of the vehicle economy is handled with vehicle component efficiencies change. This is carried basically in order to see the effects of uncertain component efficiency assumptions. For example changing the battery efficiency from 87.6% to 80% will result in 1.3% decrease in series configuration which is equal to 0.38 km/L degradation of the fuel economy while it will result in 1.1% decrease which is equal to 0.34 km/L performance loss in fuel consumption. The analysis could be repeated for different parameter efficiencies such as motor average efficiency, motor as generator efficiency, coefficient of rolling resistance, regenerative braking fraction. The analysis can be performed with a good accuracy changes up to  $\pm 10$ . As well as the battery efficiency effect on fuel economy, battery specific power effect also examined through a sensitivity analysis for fuel economy. Batteries in this comparison were assumed to have a power density of 800 W/kg, which results in a baseline battery mass of 78.4 kg for the series hybrid and 39.7 kg for the parallel hybrid. If a more conservative assumption is made such that the specific power becomes 400W/kg doubles the battery mass for the vehicles. The effect on fuel consumption in series configuration is calculated as 3.8% decrease while in parallel it will result in 2.1%. Again the parallel gives a better performance in response to changes in parameters. Also transmission design changes like connecting motor directly differential and different drive cycle alternatives are also investigated. The main conclusions of this paper are could be stated as: Parallel configuration gives 24% better fuel economy compared to conventional ICEV and 4% better fuel economy compared to series one; A lightweight midsize hybrid vehicle can achieve 30 km/L (gasoline equivalent); and different configuration has different sensitivity for fuel economy aspect.

In order to construct a valid system for fuel consumption, emission and such parameters optimization, a mathematical model based platforms have crucial role in design, simulation and validation stages. The tools than can model embedded software as well as components, and could automate the details of hybrid vehicle, need to be developed.

David W. G. et al. [10] have examined the modeling and simulation tools and method depending on the level of details of how each component is modeled. Basically they are categorized the vehicle model that it may be steady- state, quasi-steady, or dynamic model. Advanced Vehicle Simulator (ADVISOR) program which is developed by National Research Laboratory and Powertrain System Analysis Toolkit (PSAT) are the examples of the static and quasi-static simulation tools. They are based on experimental models in the form of look-up tables and efficiency maps. The main advantage of using steady-state model is getting faster response with a simpler model yet on the other hand compromising accuracy by neglecting the dynamic effects of the system. In order to include all

internal dynamics, physics-based models are developed such as VTB, PSIM, V-Elph and Simplorer where all state variables are modeled according to the physical laws and principals. Especially Resistive Companion Form (RCF) modeling is widely used in modeling platforms providing that physics-based models of each component in a modular way which could be easily integrated with input and output ports. In addition to these simulation platforms, Bond Graph method is also defined as a design tool alternative. Particularly, the method is used for multi domain systems including power exchanges. Its main advantage is showing systems in a simpler form and represent physical system in basic passive elements with resistance, capacitance and inertias and power as effort and flow. As the author stated the tradeoff between engineering assumptions and model setting up effort and also simulation run time and model detail. According to analysis performance demands, modeling and simulation platform should be constructed.

Wipke et al. [11] have surveyed ADVISOR as a vehicle modeling and system analysis tool. The capabilities and limitations of the platform are examined. Battery, fuel converter, transmission systems modeling and control strategy implementation techniques are investigated. The study shows the modeling approach techniques forward and backward approach and combination of them with advantageous and disadvantageous of them and evaluated based on optimized execution and prediction of performance demands from the vehicle. The backward-facing approach calculates each component needs to satisfy the desired performance by assuming vehicle can met the required criteria. Driver behavior is not included and system does not check whether the components could operate at desired point. Starting from the wheels with speed and acceleration demands, the calculation goes step by step with differential, transmission, coupling and finally to energy storage and converter units. The procedure is against the power flow direction. This method gives a fast response and very suitable for the application of efficiency implementations gathered from tested components yet the main weakness of the approach lack of controlling mechanism in order check whether the system is well-suited for the application demands and could not model the dynamic effects of the system. In forward-facing model, driver model is included into system generally by using PI controller and throttle opening and brake force is calculated according to speed demand and current speed values. The calculation direction coincides with the power flow. Based on the define throttle opening, current engine torque could be calculated and calculations are handled till the vehicle resultant acceleration is computed. The model gives chance to include dynamic effects and gives maximum effort calculations. The major disadvantageous of the approach is high simulation time due to integration routines used in speed calculations. ADVISOR uses a combination of these two approaches and it is closely related to backward-facing modeling. The main idea behind the strategy is stated as “1. No drivetrain component will require more torque or power from its upstream neighbor than it can use. 2. A component is as efficient in the forward-facing calculations as it was computed to be in the backward-facing calculations”. By using this type of approach and detailed look-up tables and component models, the program could achieve get accuracy within 0.8% while the calculation of acceleration for 0-100 kph and energy use is US06 cycle is predicted within 1.9% accuracy.

Brooker et al. [12] presented the five battery model alternatives used in ADVISOR simulation platform. Battery models' accuracy has importance on hybrid vehicle performance analysis and they are used in order to determine battery's voltage, current, state of charge and temperature. The purpose of the accurate modeling is to answer the questions “Is it better to regenerate electrical energy at high or low current to maximize regenerative braking and energy efficiency in the overall vehicle system and how can a control strategy optimally heat od cool the batteries to get their best performance”. The used 5 model is named as internal resistance model, resistance-capacitance model, capacitance model for PNGV, neural network lead acid model and fundamental lead acid model. The first, internal resistance model is based on a simple resistive circuit with a voltage source. Although it gives fast and reasonable results, the load voltage fluctuates dramatically and best performance approach is not achieved. To overcome that problem capacitor addition to system model is considered in the second and third, resistance-capacitance model and capacitance model for PNGV. Smoother results are received for the load voltage. The neural network approach is used for a purpose that modeling the battery with limited data set without limiting the system into standard models. However, to ensure a precise and accurate prediction and use the advantage of the model, considerably largo amount of data number is needed. The fifth one, fundamental lead acid model, gives chance to model the battery very close to the real lead acid battery but it needs extensive knowledge of battery parameters.

Assanis D. et al. [13] offered a methodology for the sizing and scaling the internal combustion engine for hybrid vehicle simulations. In order to increase the accuracy of the predictions, high-fidelity engine models are implemented. Engine modeling platform named as TDES is used for Volkswagen 1.9L turbo diesel engine. After validation of the TDES by using experimental data, comparison with direct linear scaling is made. The torque values for 1.0 L 32.6 kW engine differs from each other within 5% range. Also brake specific fuel consumption values are compared with the changing engine displacement by 1.0 L, 1.5 L and original one 1.9 L. Although it is same for all displacements for linear scaling, in TDES results it shows significant discrepancies.

Salmasi F.R. [14] classified and made comparison between the possible control strategies that could be applied to HEVs. The strategies for parallel drivetrain are only discussed because of series hybrid simplicity compared to parallel one. The strategies are classified in two main categories as rule-based and optimization-based. Rule based algorithms include deterministic and fuzzy approaches. In deterministic approach, starting from the on/off controller, power follower, modified power follower and state machine based strategies are examined. Fuzzy approaches are given in the order of conventional, predictive and adaptive fuzzy algorithms. Optimization based strategies are also investigated in two main groups: global and real-time optimization. They include linear programming, control theory approach, dynamic programming, stochastic dynamic programming and genetic algorithm in sub group of global optimization while the real time optimization consist of robust control, optimal predictive control and decoupling control. Although lots of alternatives are investigated through the studies, some of them are only theoretical ones and impossible to real time implementation and due to robustness and adaptation capabilities fuzzy rule-based and taking dynamic effects into account in real time application analytical optimal methods are chosen as feasible ones. While fuzzy provide more robust to model uncertainties, variations and adaptation to complex structures, analytical optimization uses the advantage of competence in computational complexity and dynamic effects inclusion.

Schouten et al. [15] offered fuzzy logic control system for parallel HEV taking the efficiencies of the components EM and battery into account. The most efficient operating regions are defined as for 55kW CIDI engine 230-320 rad/s and 30-50kW range, 320-430 rad/s and 9-12kW EM range and battery is stated as it has high efficiency in high SOC and low power discharging and charging cases. According to the results the a base control strategy is constructed such that if the power demand is below 6 kW only EM is in use, in the range 6 to 50 kW internal combustion engine is used to propel the vehicle and if necessary produce additional power to charge the batteries and if the demand is over 50 kW, EM helps to propel the vehicle. Then fuzzy rule based strategy is implemented on the base strategy. It checks and controls SOC, power demand from driver, electric motor speed and generator power. The typical rules are given 1) If SOC is low,  $P_{\text{driver}}$  is normal, and  $\omega_{\text{em}}$  is low, then  $P_{\text{gen}}$  is 5 kW 2) If SOC is low,  $P_{\text{driver}}$  is normal, and  $\omega_{\text{em}}$  is not low, then  $P_{\text{gen}}$  is 15 kW. The main purpose of this study is to optimize the efficiencies not only internal combustion engine but also EM and batteries. FLC provides a 7.7% improvement compared to baseline only control implementation in simulation handled in SAE J1711 standard.

Rajagopalan A. et al. [16] published a report in National Research Laboratory based on a fuzzy logic controller with an instantaneous optimization procedure for emission and fuel consumption reduction and include the tradeoff between them by defining a cost function with different weights of each optimization parameters. The basic fuzzy logic calculates the SOC and torque demand membership functions. According to the instantaneous ICE working speed, the optimization procedure is carried out with normalized efficiency and emission values according to max of the values at that speed which is received from look-up tables. Relative to different scenarios such as cold start, inadequate torque, different weighting factors are examined. The standard weighting factors are given as 0.7 for efficiency and 0.3, 0.1 and 0.1 values for  $\text{NO}_x$ , CO and HC emissions. Once the optimal torque curve is defined according to weights, fuzzy control aims to shift operating point about optimal based on SOC. By the application of two different methods simultaneously, the optimal operating point of the engine and so the torque value is determined at an instant with a specific engine rotation speed. The simulations are made in three different drive cycles comparing the standard power split strategy applied in ADVISOR. In UDDS, the values of fuel economy as mpg, CO, HC and  $\text{NO}_x$  emission values as g/mi are given in order, first for standard base line strategy, 59.3, 0.113, 0.044, 0.988 and

then for the new fuzzy logic strategy 63.9, 0.107, 0.036, 0.784. It shows that the improvement in fuel consumption 8% while it is 5% for CO, and 20% for HC and NO<sub>x</sub> emissions for UDDS cycle.

Langari et al. [17] suggest an intelligent method for parallel HEV based of roadway specifications identification using neural networks and according to the trained results override torque distribution factors used fuzzy logic based control algorithm. The study also includes driver characterization and updates the fuzzy membership functions. Up to 62 characteristic parameters which could define drive cycle and with a further classification they could be collected in 16 groups. The 9 of the factors directly affects the fuel usage and emission. Different identifier blocks are implemented in order to classify the driving trends, modes, style etc. For instance DTI (Driving Trend Identifier) block defines the transient moves which describes driving trends and by average velocity and acceleration. DMI (Driving Mode Identifier) unit decides whether the vehicle operating in start-up, cruise, acceleration, stationary or deceleration. This advance approach, which incorporated many identified parameters for controller design, is the most detailed fuzzy logic energy management system. However, driveline efficiencies are not included into the calculations.

The last step is for the process which constitutes the focus of the thesis is the optimization of the HEV component sizes by their powers and finding optimum hybridization factor which is named as power ratios of internal combustion engine and electric motor.

Lukic S. M. and Emadi A. [18] examined the hybridness value starting from mild hybrid up to full hybrid effect on fuel consumption and performance and also calculate the optimal value of the hybridization factor for a typical passenger car. The study uses ADVISOR's baseline control strategy as being flexible and easy to apply. Predefined performance criteria set by U.S. Consortium for Automotive Research for the PNGV are used for performance limitations. By keeping the total power and performance constant, sizing the batteries so they do not limit the performance and not impose any additional weight, the fuel consumption values are examined with the changing hybridness value. The change in the value of performance criteria within %10 range is accepted as constant. 100 kW and 150 kW powered two passenger cars that have 336V and 560V batteries are used for the analysis. In analysis, except for gradeability and maximum speed, other performance criteria parameters remain in %10 range. The gradeability is descending with increasing hybridness factor since gradeability quantifies the performance of the vehicle during long power-intensive driving and so with a larger ICE full power could be provided longer as fuel exists in the tank. Since the max speed does not change in a steady pattern in order to get rational results, its effect is not included. For both vehicles, the fuel consumption pattern has local maximum. The vehicles give the best fuel consumption performance while satisfying the gradeability constraint with HF = 0.3 for 150 kW powered-car and HF = 0.48 for 100 kW powered one and the HF values are very close to ones those at local maximums. The results could be explained as if the ICE is small; the motor is not used to its full capacity. ICE does not operate in the most efficient region. On the other hand, if the engine is large, the operating points are below the optimum torque; therefore, the efficiency is low. It should also be noted that the fuel consumption values at local max. are not the absolute maximum values. However vehicles have high hybridization factor have low gradeability and require very large batteries.

Fang L. et al. [19] offered simultaneous optimization of HEV control strategy parameters and vehicle parameters by using genetic algorithm. Different from the literature works which use gradient based algorithms or derivative free methods such as swarm optimization by converting multi-objective optimization into single one by writing them in the form of weighted sums or one main objective where the others defined as constraints, this study optimizes powertrain component sizes and control system parameters since they are coupled. In the Pareto front gives chance to get the optimized results in a single run without giving effort to change the weighting factors in in each simulation or redefining the priorities by using the genetic algorithm steps Initialization, Crossover, Mutation, Elitist Strategy, Evaluation, Non-dominated sorting, Crowding-distance computation, Selection and Termination test and the procedure works simultaneous with ADVISOR platform. The default parallel vehicle and CYC\_1015 cycle is used in order simulate the strategy. The vehicle parameters ICE peak power, rating power of electric motor, final drive ratio and battery pack number are calculated and moreover the control parameters: low and high state of charge, engine off speed and torque, min charge torque and torque fraction of charge are calculated also as design variables. With starting values 7.5 L/100 km fuel, 2.601 g/km CO, 0.401 g/km HC and 0.357 NO<sub>x</sub>, the results after

optimization is observed as Fuel: [5.9, 6.5] (L/100km) CO: [1.960, 3.179] (g/km) HC: [0.291, 0.374] (g/km) NO<sub>x</sub>: [0.289, 0.329] (g/km). The simulation results demonstrate that the proposed approach can improve fuel economy and reduce emissions without sacrificing the performance of the HEV.

Hu, X. et al. [20] used a multi-objective optimization method using an initial static control strategy parameters and initial power sizing parameters by implementing NSGA-II method in order to optimize not only fuel consumption but also basic emission values for parallel HEV. Total four objectives and seven variables 3 of which are components sizing values and the rest is control strategy parameters. For the simulation 1994 Saturn SL1 vehicle is used on ADVISOR platform. The variables are defined in the ADVISOR platform also as for the component sizing parameters, fuel converter power scale, motor torque scale and energy storage system capacity scale, and for control strategy parameters, min torque fraction and off torque fraction for the engine, charging torque and electric only launch speed. Delta SOC is kept within [-0.5%, +0.5%] so the entire output energy for the cycle is considered to be solely from the engine. With the application of the performance constraints such as 0 to 96.5 km/h in 12s and 6.5% grade ability at 88.5 km/h for 20 minutes with 408 kg extra mass for passenger and cargo simulation. After 3030 ADVISOR simulations with total of 38.5 hours elapsed time, 30 tradeoff solutions for Pareto set are given. The ranges for the set is given as fuel: [5.155, 6.137] L/100km, no<sub>x</sub>: [0.246, 0.322] g/km, hc: [0.341, 0.391] g/km, co: [1.253, 3.008] g/km. By considering one of the trade-off solutions, the procedure reduces the fuel consumption by 31%, NO<sub>x</sub> emissions by 19%, HC emissions by 12.7% and CO emissions by 37%, respectively, compared with the baseline vehicle and considering the flexibility of the design the four objectives have a variation of 16%, 23.6%, 12.8% and 58.4%, respectively, and six of the seven design variables have a variation of 8.5%, 25%, 69.5%, 61%, 56.3% and 75%, respectively while the battery capacity sizing factor is not changed.

Gao W. et al. [21] compares three different derivative free optimization methods and suggests a hybrid algorithm of MATLAB derivative based function `fmincon` and non-derivative Divided RECTangles method. DIRECT Algorithm, Simulate Annealing and Genetic Algorithm are all the derivative free algorithms used in the simulation and all of them are designed to overcome stuck around a local max/min value while searching for global optimization. In addition to engine, electric motor, battery power and final drive ratio, minimum and maximum state of charge values are also considered as design variables. The simulations are carried with combination of FTP-75 and HWFT driving cycles and using PSAT midsize cavalier pre-defined vehicle parameters. After 100 hours of computation progress of each algorithm and 400 function evaluations, the fuel consumption starting value 35.1 mpg improved up to 40.37 mpg by Simulate Annealing process while DIRECT method gets a very close to that with 39.64 mpg value and Genetic Algorithm could only rise up to 36.6 mpg because of bad initial population. Moreover performance improvements are also observed and SA gives far better increase compared to the two others. In addition to this comparison, a hybrid methodology in order to decrease the time spent for the simulation process by using MATLAB platform and `fmincon` function working simultaneous with DIRECT method since derivative based method gives faster convergence.

A review of the previous work in the literature about HEV powertrain configuration design parameters and optimization routines shows that component sizing and working range optimization has the descent role in fuel consumption and emission reduction. Although the studies include much work on control strategies from the basic on-off control to real time optimization studies, most of them are carried with standard vehicles supplied in simulation platforms such as ADVISOR and PSAT. There exist hardly any study that could satisfy flexibility and simplicity for vehicle selection and sizing according to performance demands.

In literature, there are also comparison of different drivetrain configurations named as parallel, series, complex etc. according to their especially fuel consumption performance and design and controllability complexity. Parallel configuration is found as the most promising configuration since series gives a limited design alternatives and complex drivetrain has many parameters that should be optimized simultaneously. With the addition of hybridness value and sensitivity analysis over parallel configuration, most of the optimization studies are based on that drivetrain configuration. Moreover, recent optimization studies working on component sizing focus on non-derivative based algorithms such as genetic algorithm to overcome stuck around local minimum while searching the global

optimum point for minimum fuel consumption and emission values. However the simulation procedures time requirements are extremely high and there are not so much work on gradient based algorithms performance analysis and somehow comparison with non-derivative based ones or combination of them.

The aim of this study is to model and simulate the performance of hybrid electric vehicles (HEV) and optimize the power component specifications. The battery package, electric motor, and internal combustion engine sizing, an optimization process is implemented by developing an easy to use GUI platform on MATLAB software. Appropriate control strategies for vehicles with different characteristics is simulated in order to search for improved fuel economy and reduced emission potential of HEV without sacrificing its performance and reliability. In the study, fuel economy potential of special purpose vehicles such as a dump truck, sports car, shuttle bus etc. will be investigated by using standard driving cycles. In order to get successive analysis of hybrid vehicles' performance, there are some design stages and criteria to be decided which offer unprecedented possibilities in fuel consumption and emission reduction purposes. Hence, firstly an introduction to hybrid vehicles, advantageous and disadvantageous of hybrid technology, their drive train architectures to satisfy effective split of the power between power plants, basic elements, functions and key technologies of hybrid electric vehicle (HEV) will be given, then another basic decision "hybridness" will be given in the following sections.

In this thesis, by using graphical user interface design, a better and easier way to choose and change vehicle parameters and put performance criteria and optimize vehicle components' sizes and some control parameters is developed and final fuel consumption and emission values improvements referenced to base vehicle and performance criteria satisfaction is investigated.



## CHAPTER 3

### SYSTEM MODELING

#### 3.1 INTRODUCTION

The first step for an investigation of vehicle performance, fuel consumption, emission values, and application of optimization is the model construction process. In modeling, the level of detail is the key factor. There is always a trade-off between the amount of engineering assumptions and the time required constructing the model of the system, and between model detail and simulation time.

In HEV design, with increasing number of components and simultaneous multi-directional power flows and coupling of the two main energy systems make the modeling process complex and complicated. In order to satisfy the flexibility, accuracy, and fast response requirements, components are modeled separately in detail including efficiency, saturation limits, dynamic behavior and discontinuities by using experimental data and engineering knowledge.

In addition to component separated modeling, the HEV model needs a pre-selection of drive train configuration between the basic alternatives of series, parallel, or complex in order to determine the components needed and construction of components order in vehicle system.

#### 3.2 VEHICLE MODELING

In vehicle modeling it is desired to observe acceleration performance, fuel consumption, and emission values as output according to some standard driving cycle. Hybrid electric vehicle powertrain modeling could be handled in two basic approaches; namely the Backward-Facing Approach and the Forward Facing Approach. Backward approach assumes that vehicle could satisfy the desired performance and how each component should operate is calculated going from wheel to engine. Generally drive cycle inputs with velocity and time data are directly applied to wheel and submitted as its speed. On the other hand forward facing approach uses a PI or PID (could also be another strategy) controller in order to translate the velocity demand into the throttle command of the vehicle. Then the calculation flows from power converter to wheels and final wheel speed is calculated [22].

To combine both strategies with their advantages, Backward/Forward based method which used also in ADVISOR is constructed [11]. The integration of the component models were achieved as forward/backward modeling where each component takes the previous component's desired velocity and torque output value as input. This flow named as backward flow and starts from vehicle model and goes to power sources, engine and battery. Then achievable speed and torque values those calculated in power source models are fed back to the components. Again the flow occurs in component based. At each component calculations are made with model losses and some control algorithms and new value is sent to next component. This flow is named as forward flow. Final step is to calculate the vehicle speed with achievable torque and speed values. So it could be stated that all components have basically 2 input and 2 output ports both including speed and torque information. Figure 3-1 shows the ADVISOR vehicle model for a parallel hybrid vehicle drivetrain.

Before going into component based modeling, drive train alternatives should be examined as a primary design selection. After the drivetrain selection is clarified, the vehicle components formation frame could be constructed.

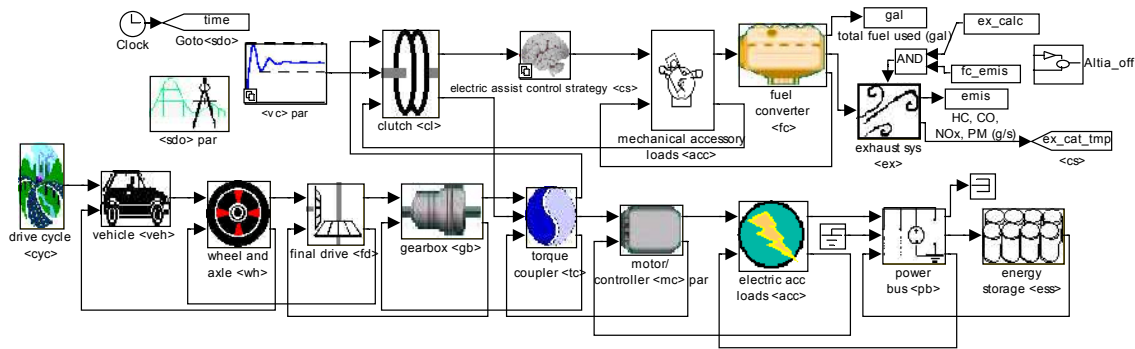


Figure 3-1: ADVISOR Forward/Backward facing model [10]

### 3.2.1 Drivetrain Configuration Selection

The parallel and series configurations mainly differ from each other in energy transfer line of the vehicle. While series configuration is constructed in a way very similar to purely electric vehicle with the addition of an electrical energy source composed as ICE and generator combination; parallel configuration is close to conventional vehicle in energy transferring aspect since it uses mechanical energy transmitting line, while electrical energy is included with a battery and an electric motor with a torque coupler. In addition to these, series-parallel configuration is designed to combine the advantages of both configurations.

Tamor [23] shows that hybridization of the powertrain gives up to 50 % increase in fuel economy. Here the problem is deciding the tradeoff between better fuel economy and emission performance, and complex model structure and control algorithm. The parallel configuration satisfies a balanced choice of fuel economy since it has superior fuel economy to series configuration and design detail. Further it is easier to design compared to complex hybrid drivetrain [24]. On the other hand some studies show that series hybrid can provide better fuel economy compared to the parallel alternative [25]. More recent studies carried by NREL (National Research Laboratory) shows that both configurations have similar fuel economy potential with different strategies and on different driving schedules [24]. In the light of these reference studies, both series and parallel drive train configurations are selected as base analysis structures. Then series configuration is also used for simulations and comparisons of the two configurations are made in the case studies.

If the selection of parallel configuration is made, there is another design selection related to the position of the electric motor; namely pre-transmission and post-transmission. The Figure 3-2 shows parallel drivetrain configuration with pre and post-transmission alternatives.

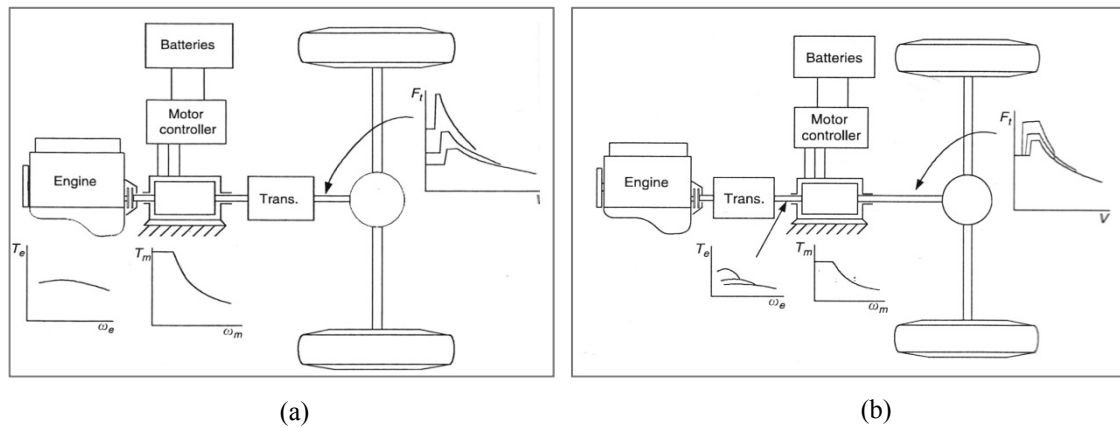


Figure 3-2: Pre-transmission (a) and Post-transmission (b) configurations [2]

The pre-transmission configuration is selected since the configuration gives chance to work the electric motor as generator, engine assistance, and regenerative braking for motors and engines have similar speed range and transmission modify both engine torque and motor torque. Previous studies indicate that pre-transmission configurations gives better performance with mild hybrid vehicles [26].

### 3.2.2 Component Modeling

As mentioned in the introduction, each component is modeled in MATLAB Simulink suitable to forward/backward simulation of the vehicle. Component blocks work simultaneously with m-files to construct structure variables and give opportunity to be modified over workspace which provides high flexibility especially in optimization procedures. Also look-up tables and losses linked to torque and speed parameters formed by using experimental results are included as data files. Internal combustion engine, battery, electric motor engine, and gearbox with losses are taken from ADVISOR simulation platform with some modifications.

#### 3.2.2.1 Internal Combustion Engine Model

Internal combustion engine is one of the energy sources in a hybrid drive system. A model is needed to simulate generated power from the fuel as mechanical shaft work and it should be easily implemented to different drivetrain configurations as a black box power source for the calculation of vehicle performance, fuel consumption, and emission values. A look up table based model is used which is provided by ADVISOR in MATLAB Simulink platform.

As stated in the previous section the flow in the forward/backward system transferred as torque and speed demand, by including inertial affects, accessory loads and losses the model determines the engine operating point which satisfy these requirements. Moreover emission and fuel consumption values are stored as lookup a table which is indexed by engine speed and torque. Figure 3-3 shows the fuel converter block diagram used in Simulink.

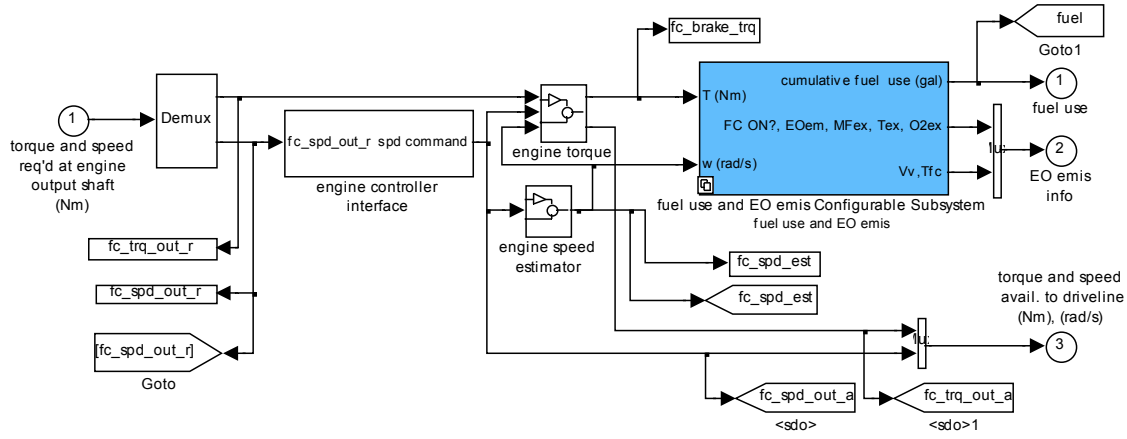


Figure 3-3: Internal combustion engine block diagram [27]

The first step is to estimate the engine speed and the torque that could be supplied by engine at estimated operation speed in present time step according to engine controller input. The desired speed and torque input are taken directly from clutch output port in backward system. So the engine speed and torque values are related to each other and calculated at each time step starting with the available torque and speed values.

$$T_{avail.} = T_{eng} - T_{acc.} \quad (3.1)$$

$$T_{eng} = \max(T_{ct}, \min(T_{req}, T_{max})) \quad (3.2)$$

$$T_{req} = T_{req,clutch} + T_{inertia} + T_{acc.} \quad (3.3)$$

$$T_{inertia} = \frac{d\omega_{avail}}{dt} * I_{engine} \quad (3.4)$$

$$T_{acc.} = P_{acc.}/\omega_{avail} \quad (3.5)$$

and

$$\omega_{avail} = \min(\omega_{req}, \omega_{eng,max}) * (clutch\ state) + \omega_{spin-down} * (clutch\ state) \quad (3.6)$$

$$\omega_{spin-down} = \max(\omega_{idle}, \omega_{closed}) \quad (3.7)$$

$$\omega_{closed} = \frac{(T_{closed} - T_{acc.})}{I_{engine}} * t_{step} \quad (3.8)$$

Where

$T_{avail.}$  = Available Torque For Driveshaft

$T_{eng}$  = Engine Torque Available

$T_{acc.}$  = Accessories Torque

$T_{req.}$  = Requested Torque at Clutch

$T_{max}$  = Maximum Engine Torque

$T_{inertia}$  = Inertial Torque of The Engine

$T_{closed}$  = Closed Throttle Torque

$P_{acc.}$  = Accessories Mechanical Power

$I_{engine}$  = Engine Inertia

$\omega_{avail}$  = Speed Available at Driveshaft

$\omega_{req}$  = Requested Speed at Clutch

$\omega_{eng,max}$  = Maximum Engine Speed

$\omega_{idle}$  = Idle Speed

$\omega_{closed}$  = Closed Throttle Speed  
 clutch state = 1 (engaged) or 0 (disengaged)  
 $t_{step}$  = Time Step

After calculating the engine operating speed and torque referenced to requested values at that time step, fuel use and emission calculations could be handled by using a coupled system consisting of engine heat model and exhaust model. The block named as “fuel use and EO emission” is generated to calculate the fuel usage and emission values with thermal correction which includes scaling of the fuel use and changes especially in emission while cold start case. The second block named as “engine controller interface” takes the speed needed from the engine output as an input and gives a speed command output to engine torque and speed calculation and estimation blocks. In Figure 3-4 fuel end emission block is given with HOT engine maps block which is shown in Figure 3-5 in open form with look-up table blocks and with thermal correction blocks.

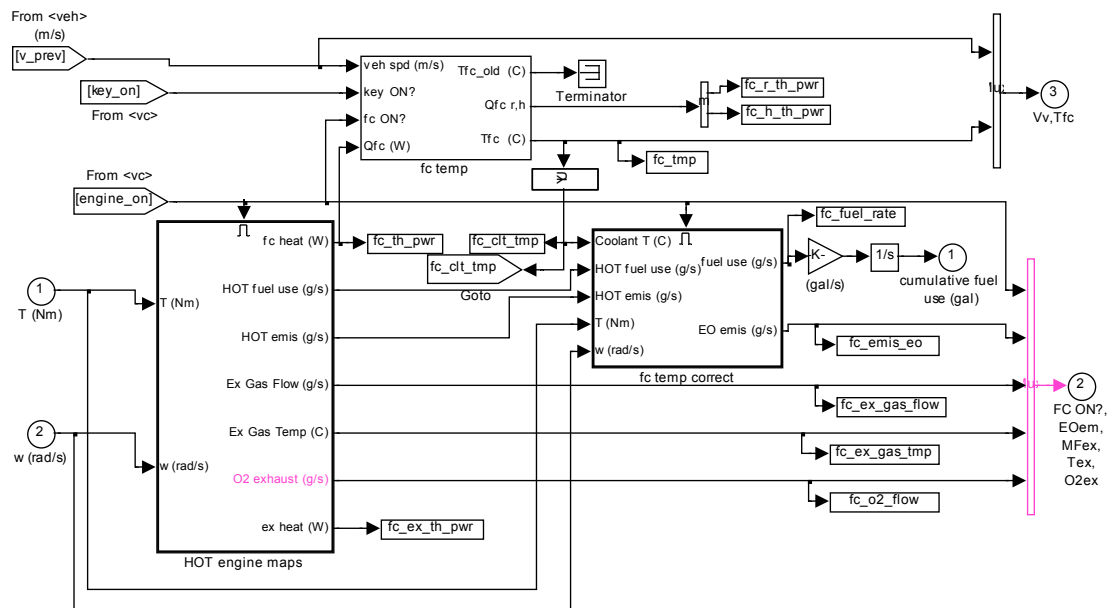


Figure 3-4: Fuel usage and emission block diagram [27]

The thermal model is based on four different temperatures of the engine and vehicle parts namely the cylinder, the engine block, the exterior engine accessories and the hood. The generation of the heat starts with the combustion process, then it is conducted to the engine block, and then some of the heat generated is removed through forced liquid cooling, conduction, natural convection, and radiation and this is process is schematically shown in Figure 3-6. The block diagram configurations of the thermal model subsystem blocks are given in Appendix.

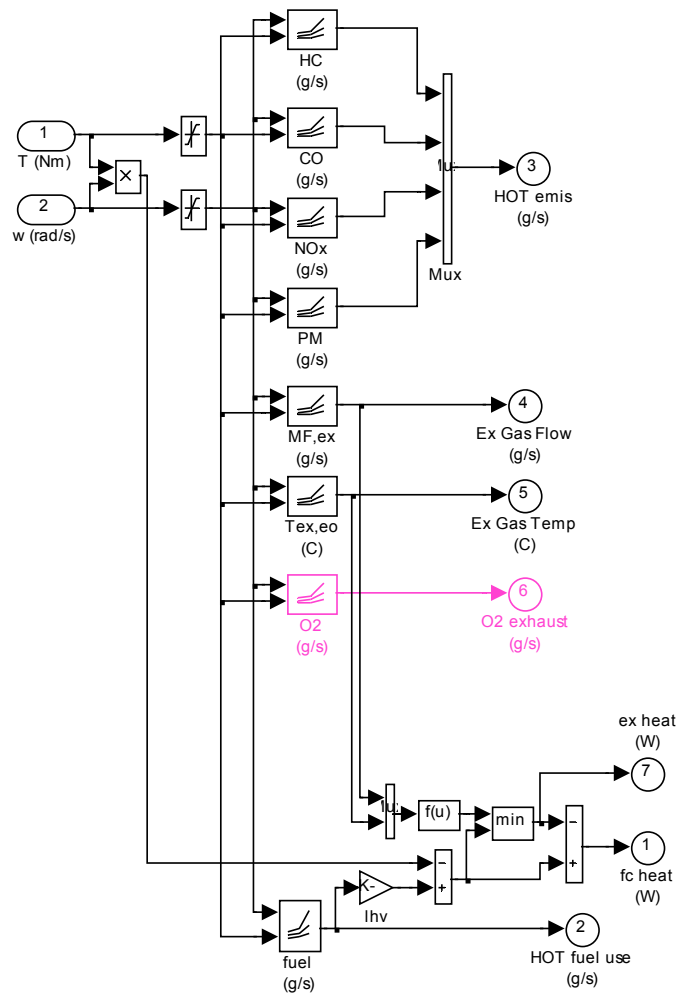


Figure 3-5: Engine maps block diagram [27]

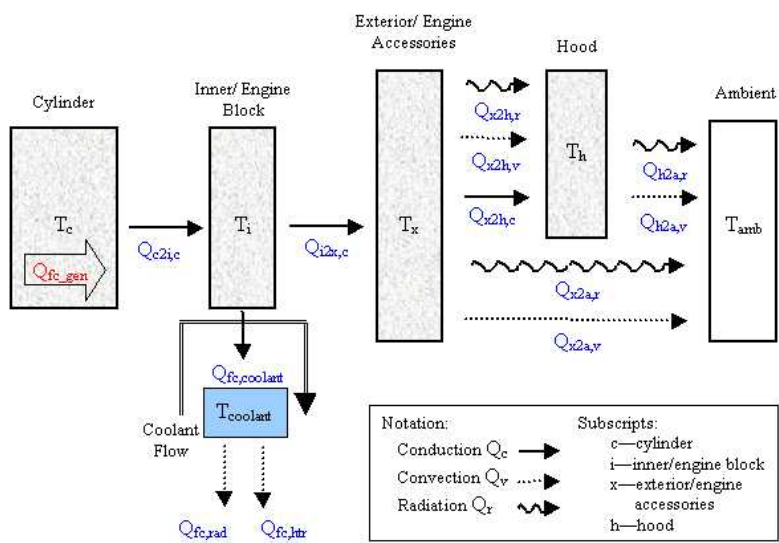


Figure 3-6: Schematic of engine thermal model [12]

The heat generation simply calculated as the net heat transfer to cylinders during the combustion process. The equation of the base energy source for hybrid vehicle could be stated as:

$$Q_{fuel} = P_{vehicle} + Q_{fc\_gen} + Q_{exhaust} \quad (3.9)$$

As mentioned above the correction factors for emissions at engine outlet are calculated according to temperature values found from heat transfer model. The correction factor has been incorporated based on normalized engine temperature factor,  $\gamma$ , which is related to the engine cooling system's thermostat set point,  $T_{Engtstat}$ , and the coolant temperature,  $T_{coolant}$ . The correction factor formula is given in [28] and it is formed as ColdUse = HotUse\*Cold Factor where:

$$Cold\ Factor = \begin{cases} (1 + \gamma^{3.1}) & fuel \\ (1 + 7.4\gamma^{3.072}) & HC \\ (1 + 9.4\gamma^{3.21}) & CO \\ (1 + 0.6\gamma^{7.3}) & NOx \end{cases} \quad (3.10)$$

and

$$\gamma = \frac{T_{Engtstat} - T_{coolant}}{T_{Engtstat} - 20} \quad (3.11)$$

Where

$\gamma$  = Normalised Engine Temperature Factor

$T_{Engtstat}$  = Thermostat Preset Temperature [ $C^\circ$ ]

$T_{coolant}$  = Engine Coolant Temperature [ $C^\circ$ ]

The second structure modeled to calculate the emission values is exhaust system that works coupled with the main fuel converter structure. The exhaust system model simulates an engine exhaust after-treatment system for the vehicle in order to get close values of exhaust emissions (HC, CO, NOx, and PM) in g/s, as a function of time. It is composed of the exhaust manifold, downpipe, catalytic converter, and muffler. In Figure 3-7 the catalyst system block diagram is given.

Catalyst conversion efficiencies as a function of temperature are stored as vectors in source data files. Catalyst temperature is calculated by using a lumped-capacitance approach. Figure 3-8 shows the thermal model and heat transfers to components and to air by radiation and convection as connected resistances representation.



Those variables that can be modified by the user are defined as basic workspace variables. Basically the engine thermal and exhaust model variables are used as default values from prepared data files. However, some of the engine parameters are implemented as adjustable parameters and also design variables through the user interface. These parameters are given in Table 3-1 with definitions.

Table 3-1: Fuel converter basic variables [27]

Variable Name	Unit	Explanation
fc_map_trq	N*m	engine torque range
fc_fuel_map	g/s	fuel use indexed by fc_map_spd and fc_map_trq
fc_co_map	g/s	engine out CO indexed by fc_map_spd and fc_map_trq
fc_hc_map	g/s	engine out HC indexed by fc_map_spd and fc_map_trq
fc_nox_map	g/s	engine out NOx indexed by fc_map_spd and fc_map_trq
fc_pm_map	g/s	engine out PM indexed by fc_map_spd and fc_map_trq
fc_inertia	kg*m <sup>2</sup>	rotational inertia of the engine
fc_max_trq	N*m	maximum torque output indexed by fc_map_spd
fc_trq_scale	--	scaling factor for torque range
fc_pwr_scale	--	scaling factor for power=fc trq scale*fc spd scale
fc_max_pwr	kW	engine peak power in kW
fc_mass	kg	mass of the fuel converter and fuel system

Some of the variables are determined directly according to user selections such as fuel type, fuel density, and fuel converter description, while the rest of the values are assigned by user selections and performance demands. Moreover, the torque scale and power scale values are treated as design variables during sizing and optimization process in order to adjust power source sizing.

In ADVISOR platform there are numbers of data m-files prepared over MATLAB by using test values gathered from test results by some laboratories. All variable values including the ones stated in Table 3-1 are stored in those files. The files are indexed according to fuel converter type: compression ignition and spark ignition as “CI” and “SI” and also power rating of the engine in terms of kilowatts. The data files generate the base vehicle engine parameter values during selection, sizing and optimization procedures are given in Table 3-2 with file names and specifications.

Table 3-2: Fuel converter base data files

File Name	Explanation
FC_CI60_emis.m	60kW - compression ignition engine with emission data
FC_CI92_emis.m	92kW - compression ignition engine with emission data
FC_SI41_emis.m	41kW - spark ignition engine with emission data
FC_SI63_emis.m	63kW - spark ignition engine with emission data
FC_SI102_emis.m	102kW - spark ignition engine with emission data

### 3.2.2.2 Energy Storage System Model

Battery model is the most difficult part of the whole vehicle model. Although it seems like simple energy storage device like a capacitor in a simple electric circuit, while in energy delivery from and to the battery, dynamical model balancing, simulation in reasonable time, and details including nonlinear functions become the key points since battery goes thermally dependent electrochemical process.

There are four different battery models provided by the ADVISOR platform named as RC Model, Rint Model, Fundamental Lead Acid Model and Neural Network Model. RC model states “R” for resistance and “C” for capacitance and it is based on an electrical circuit with resistors and capacitors while Rint only consist of a resistor with a power supply so the name shortened from “internal resistance”. They both have the similar thermal model for the battery. RC model is developed over Rint model in order eliminate the internal resistance fluctuations due to discharge rate changes and it gives a better SOC estimation over a simulation period [29]. Although RC gives better estimation for SOC over time, Rint model is used for the HEV simulation since sufficient amount of data are not available for the RC model. Besides internal resistance also gives acceptable voltage predictions within 3 % error limit over fifteen US06 drive cycles (maximum 12 % error is observed) [30]. Moreover Rint model SOC accuracy is also examined for 15 cycles and the result given in the Figure 3-9 indicates a close approximation.

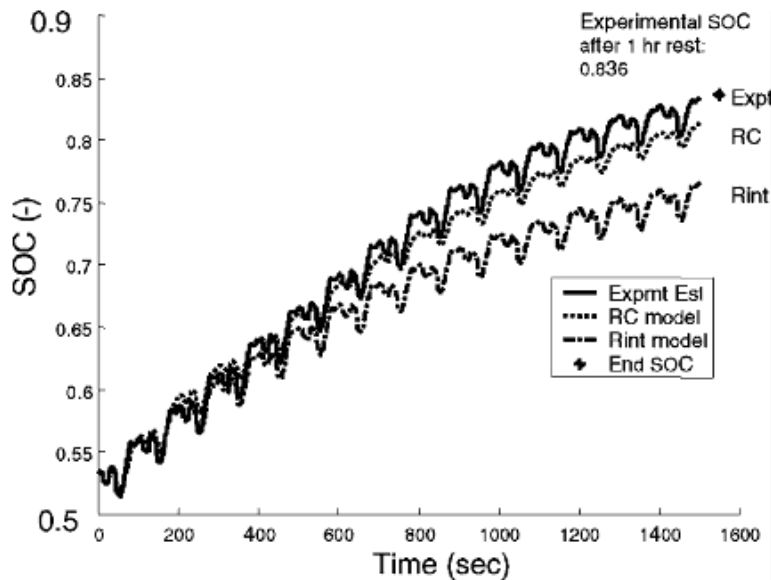


Figure 3-9: Rint and RC model comparison with experimental result for SOC [31]

The Rint model consists of an open voltage source and a resistor whose values vary with SOC, temperature and direction of current flow (charge/discharge). The electrical schematic of the internal resistance model is given in Figure 3-10. SOC calculation, power limitations, coulombic efficiencies and losses with battery temperature calculations are included to the model. The Rint model includes characterized datasets for Lithium-ion (LI), Nickel Metal Hydride (NiMH) and Lead acid (PB) batteries.

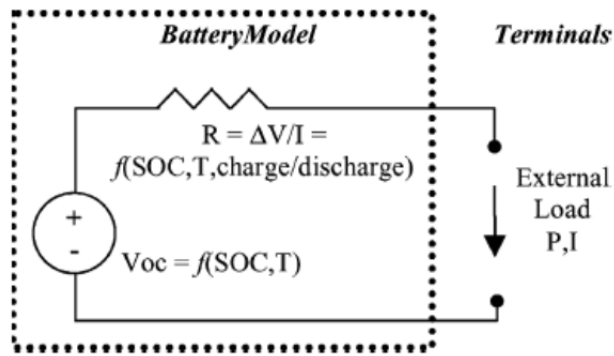


Figure 3-10: Internal resistance model electrical schematic [31]

There are 5 main structures formed in Rint model constructed in Simulink platform. These are shown in Figure 3-11.

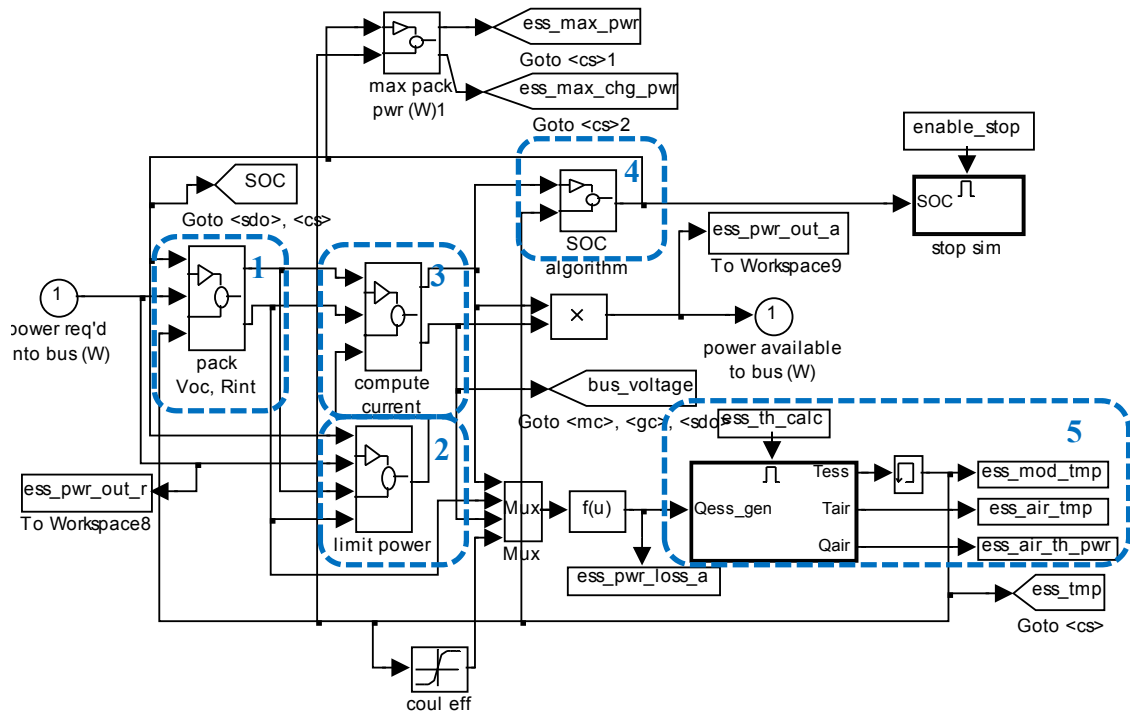


Figure 3-11: Energy storage model [27]

Each of the sub-structures is explained step by step as follows:

1. The battery is modeled as a circuit with an open circuit voltage source ( $V_{oc}$ ) and with an effective internal resistance ( $R_{int}$ ) in series.  $V_{oc}$  and  $R_{int}$  are functions of SOC value and they are calculated according to it. Also the discharge and charge states resistances are calculated according to different data. These data are implemented to model as interpolated look-up tables referenced to data files. After the calculation of data from tables they are scaled with number of battery modules.
2. The maximum power that the battery could deliver is determined according to battery operating voltage which is compared with battery's minimum voltage, motor's minimum voltage or  $V_{oc}/2$  value. When the operating voltage drops, either of these limits the maximum power supplied to the system and the value is calculated as:

$$P = V_{bus} * \frac{V_{OC} - V_{bus}}{R} \quad (3.12)$$

Since the open circuit voltage changes with SOC value available power changes with changing SOC [32]. Charging and discharging power limits for one module is given in Figure 3-12.

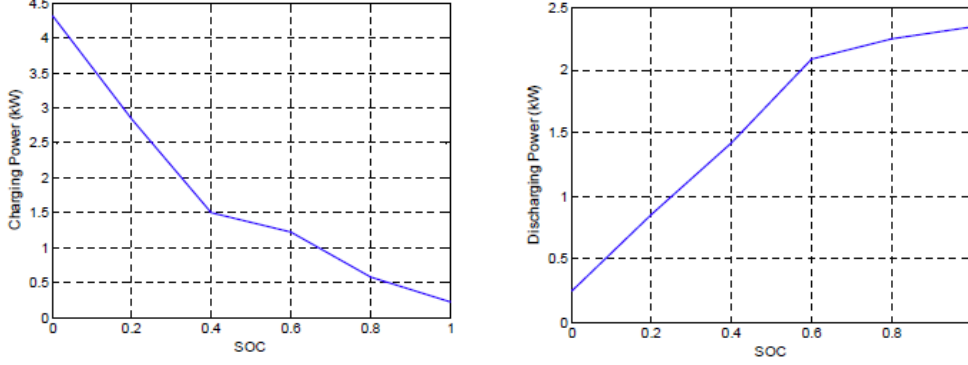


Figure 3-12: Charging power limit for battery [32]

3. The current of the equivalent circuit which is given in Figure 3-10 is determined by using  $V_{oc}$ ,  $R_{int}$  and power values. The current is determined by using the equation given below.

$$P + RI^2 - (V_{OC} * I) = 0 \quad (3.13)$$

4. Then the effective SOC of the battery is determined by using the calculated current. While doing the calculation the model uses coulombic efficiencies and maximum capacity values which are functions of temperature in order to calculate the residual battery capacity in units of ampere-hours (Ah). SOC estimation is made according to:

$$SOC = \frac{Ah_{max} - Ah_{used}(\eta_{coulomb})}{Ah_{max}} \quad (3.14)$$

where

$$Ah_{used} = \int_0^t A, \quad \text{for } A > 0 \text{ discharge,} \quad (3.15)$$

$$\int_0^t \eta_{coulomb} A dt, \quad \text{for } A < 0 \text{ charge.}$$

5. Finally, the thermal model of the battery accounts for the temperature effects on performance parameters, efficiencies and maximum capacity value and the effects are implemented as lookup tables indexed by operating temperature. A schematic of the model is given in Figure 3-13.

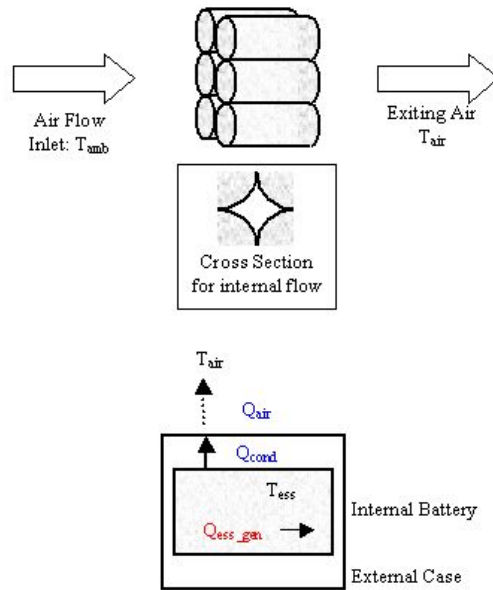


Figure 3-13: Battery thermal model schematic [31]

In simulations, ADVISOR’s battery data files are used for look-up tables while in pack number determination and optimization process. There are two main battery type: Nickel Metal Hydride (NiMH) and Lead Acid (PB) modeled by using Rint model approach. Due to its convenience with its characteristics and better performance, NiMH type battery is used for HEV analysis.

The data files are named with battery type, one cell capacity in terms of “Ah” and battery brand. In order to satisfy the appropriate capacity scaling while optimizing the module number, elasticity is supplied with four different battery files given in Table 3-1.

Table 3-3: Battery data files

File Name	Explanation
ESS_NIMH28_OVONIC.m	28 Ah, NiMH Ovonic Brand Battery
ESS_NIMH45_OVONIC.m	45 Ah, NiMH Ovonic Brand Battery
ESS_NIMH60_OVONIC.m	60 Ah, NiMH Ovonic Brand Battery
ESS_NIMH90_OVONIC.m	90 Ah, NiMH Ovonic Brand Battery

The given data files and also in Simulink model there are plenty of parameters effecting the power flow from and to the batteries during the operation. While some of them directly implemented to the simulation, some of them are monitored and/or modified before and/or during the simulation. The variables are given in Table 3-4 with their names and explanations.

Table 3-4: Energy storage system variables [27]

Variable Name	Unit	Explanation
ess_coulombic_eff	--	average Coulombic efficiency of the energy storage system (ESS)
ess_init_soc	--	initial state of charge of the ESS
ess_max_ah_cap	Ah	maximum A-h capacity the ESS can have, no matter how slowly it is drained
ess_module_mass	kg	mass of one energy storage module
ess_module_num	--	number of modules in a pack; assumed to be strung in <u>series</u>
ess_min_volts	V	minimum battery operating voltage, not to be exceeded during discharge
ess_max_volts	V	maximum battery operating voltage, not to be exceeded during charge
ess_r_chg	ohms	module's resistance to being charged; indexed by ess_soc and ess_tmp
ess_r_dis	ohms	module's resistance to being discharged; indexed by ess_soc and ess_tmp
ess_soc	--	vector of SOCs used to index other variables
ess_voc	volts	module's open-circuit voltage; indexed by ess_soc and ess_tmp
battery_mass	kg	the mass of the batteries
ess_pwr_out_a	W	power out of ess available
ess_pwr_out_r	W	power out of ess requested
ess_soc_hist	--	state of charge history
ess_eff	--	round-trip efficiency
ess_in_kj	kJ	total energy into energy storage system over the drive cycle
ess_loss_kj	kJ	total energy into the energy storage system not stored or used as output over the drive cycle
ess_stored_kj	kJ	energy stored in the energy storage system over the drive cycle
ess_out_kj	kJ	useful energy leaving the batteries over the drive cycle
eta_ess_chg	kJ	recharge efficiency
eta_ess_dis	kJ	discharge efficiency
into_storage_kj	kJ	useful energy coming into the batteries over the drive cycle.
ess_cap_scale	--	scale factor for module max ah capacity

### 3.2.2.3 Electric Motor Model

The second primary element of the electrical energy system of HEV is electric motor which works as motor for propelling and generator while regenerative braking and charging from internal combustion engine. The model block provides the transition between torque and speed requests to electric power requests which is sent to batter model and from power input comes from battery to torque and speed output to driveline. Its block diagram is given in Figure 3-14.

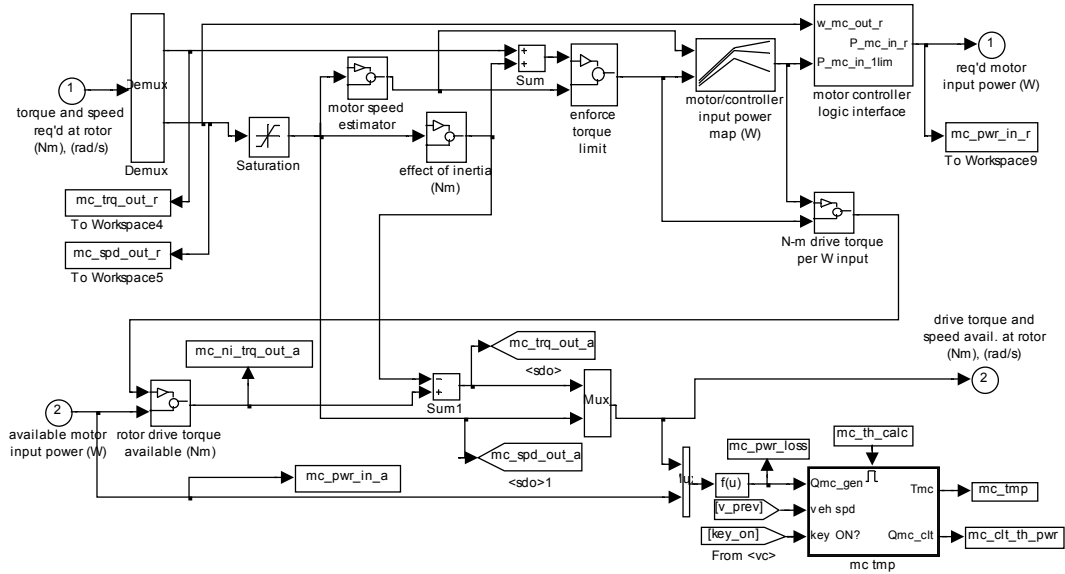


Figure 3-14: Electric motor model block diagram

The EM model calculates the torque and speed capability at the operating point by using lookup tables which are indexed by motor speed and it also includes the loss as lookup table also which is indexed by torque and speed and inertia effects. The EM's maximum torque is determined using a lookup table indexed by current speed. Moreover, motor control blocks at the outside of the block checks for the maximum current and ensures that it is not exceeded.

The output power calculation could be simply shown as:

$$P_{m,req} = P_{m,out} + P_{m,loss}(T_{m,out}, \omega_m) \quad (3.16)$$

and

$$P_{m,req} = (T_{m,req} + T_{m,inertia}) * \omega_m \quad (3.17)$$

$$T_{m,inertia} = I_{m,inertia} * \frac{d\omega_m}{dt} \quad (3.18)$$

where

$P_{m,req}$  = Motor power required at electrical side

$P_{m,out}$  = Motor power output

$P_{m,loss}(T_{m,out}, \omega_m)$  = Motor power loss (function of motor torque & speed)

$T_{m,out}$  = Motor torque output

$T_{m,req}$  = Motor torque required

$T_{m,inertia}$  = Motor torque needed due to inertail effect

$I_{m,inertia}$  = Motor inertia

Similar to other components electric motor model is simulated over prepared data files. There two alternatives given for motor types: "induction" and "permanent magnet". The permanent magnet type has advantages over induction even though it is costly. Although it has a significant advantage in efficiency [33] permanent magnet is not used through the simulations since most of the studies are done based on AC motors and so in order get a better comparison of the results AC motors are used in the simulations. There are 3 different data files for the model and they are given in Table 3-5.

Table 3-5: Electric motor data files

File Name	Explanation
MC_AC59.m	59 kW, Alternating Current Motor
MC_AC75.m	75 kW, Alternating Current Motor
MC_AC187.m	187 kW, Alternating Current Motor

The variables used in the data files and Simulink models are given in Table 3-6.

Table 3-6: Electric motor variables [27]

Variable Name	Unit	Explanation
mc_map_spd	rad/s	speed range of the motor
mc_map_trq	N*m	torque range of the motor
mc_eff_map	--	efficiency map of the motor indexed by mc_map_spd and mc_map_trq
mc_inertia	kg*m <sup>2</sup>	rotational inertia of the motor
mc_inpwr_map	W	input power map, indexed by mot_map_spd and mot_map_trq
mc_mass	kg	mass of the motor/controller
mc_max_crnt	A	max. current allowed in motor/controller
mc_max_trq	N*m	maximum torque curve of the motor indexed by mc_map_spd
mc_min_volts	V	min. voltage allowed in motor/controller
mc_trq_scale	--	torque scaling factor
mc_max_cont_trq	N*m	maximum continuous torque curve of the motor indexed by mc_map_spd
mc_outpwr_map	W	used to compute mc_inpwr_map as mc_inpower_map = mc_outpwr_map + mc_losspwr_map
mc_pwr_in_r	W	power requested from the motor
mc_spd_out_a	rad/s	available speed out of the motor
mc_trq_out_a	N*m	available torque out of the motor
mc_pwr_loss	W	power lost by the motor/controller
mc_map_spd	rad/s	speed range of the motor
mc_map_trq	N*m	torque range of the motor

### 3.2.2.4 Transmission System Model

The transmission system consists of gearbox and differential of the vehicle which are connected between wheels and propulsion system. Especially in parallel configuration the fuel consumption value, and maximum speed and acceleration ratings are highly affected by gear and final drive ratios. In the model three effects of transmission system on torque and speed of the vehicle are included.

- torque multiplication and speed reduction according to the current gear ratio
- torque loss due to the acceleration of rotational inertia
- torque loss due to friction

The ratios, loss tables and other parameters such as inertia are supplied as data files. The torque equation of the transmission system is

$$T_{r,in} = \frac{T_{r,out}}{i_{gear}} + T_{inertia} + T_{gb,loss} \quad (3.19)$$

where

$$T_{inertia} = I_{gb,inertia} \frac{d\omega_{gb}}{dt} \quad (3.20)$$

$T_{r,in}$  = Torque required at the input side of the gearbox

$T_{r,out}$  = Gearbox output torque required

$T_{gb,loss}(T_{r,out}, \omega_{gb,out}, i_{gear})$  = Gearbox torque loss (as a lookup table)

$\omega_{gb}$  = Gearbox speed

$i_{gear}$  = Gearbox current ratio

$I_{gb,inertia}$  = Gearbox inertia

The final drive ratio is directly added to gearbox ratio and so the differential ratio is directly taken as “1”. Differential losses and inertial effects are not included into the model.

There are two basic transmissions are used for the vehicles. One of these is a 5 speed gearbox which is implemented to parallel drivetrain and a 1-speed gearbox for series drivetrain. The gear ratios of the 5-speed transmission systems are given in Table 3-7.

Table 3-7: 5-Speed gearbox and final drive ratios

Description	Gear Ratios					Differential Ratio
5 Speed Gearbox	3.46	1.94	1.29	0.97	0.81	3.67

Moreover the 1-Speed gearbox gear ratio is directly determined according to vehicle specifications. Since it is designed for series drivetrain, ratio is calculated from the maximum speed availability by the electric motor. The equation simply written as

$$i_{gear} = \frac{\omega_{em,max} * r_{wheel} * 1.1}{190 * 0.278} \quad (3.21)$$

Where

$\omega_{em,max}$  = Maximum electric motor speed [rad/s]

$i_{gear}$  = Desired gearbox ratio

The “190” indicates the maximum speed of 190 kph and 1.1 is used to include a 10 % tire sleep condition.

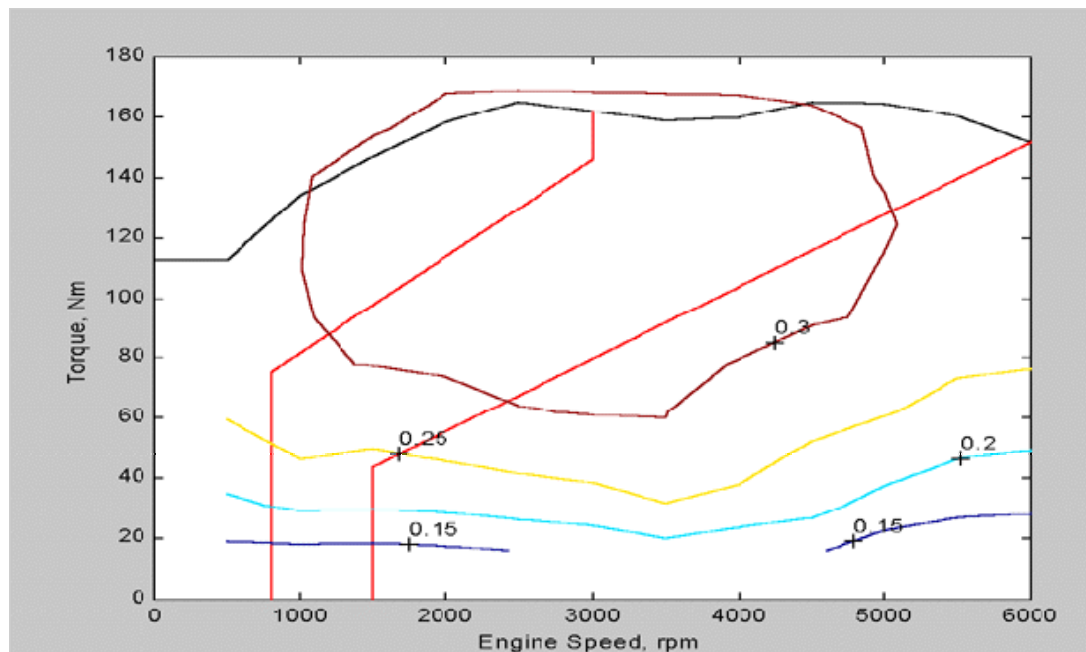


Figure 3-15: Gearbox upshift and downshift lines in engine torque-speed map [27]

Another property of the model is the control action of the up and down shift command determination for the 5-speed gear box. There are 4 variables which are one dimensional matrices defined for each gear ratio. The variables are named as

- GearX\_Upshift Speed
- GearX\_Upshift Load
- GearX\_Downshift Speed
- GearX\_Downshift Load

The upshift and downshift loads are determined as fractional engine load current torque/maximum engine torque at current speed. The values of the downshift and upshift torque fraction values indexed by upshift and downshift speeds are given as

$$\text{Downshift\_load\_fraction} = [0 \ 0.6 \ 0.9 \ 1]$$

$$\text{Upshift\_load\_fraction} = [0 \ 0.3 \ 1]$$

And the upshift and downshift speed values are defined as

$$\omega_{downshift} = \min(\omega_{engine}) + [0.01 \ 0.05 \ 0.10 \ 0.15] * (\max(\omega_{engine}) - \min(\omega_{engine})) \quad (3.22)$$

$$\omega_{upshift} = \min(\omega_{engine}) * [0.20 \ 0.30 \ 0.98] * (\max(\omega_{engine}) - \min(\omega_{engine})) \quad (3.23)$$

The approximate upshift and downshift lines in engine speed and torque space are given as red lines in Figure 3-15.

### 3.2.2.5 Wheel/Axle Model

The wheel and axle model similar to other blocks works with two input and output ports and it transmits the torque and speed requested from the vehicle block and available torque and speed from the final drive and feeds it back to the tire as a propulsion torque at current speed. In addition to that, the wheel and axle model includes the losses in the axle bearings, wheel and also axle inertia and tire slip by using lookup tables indexed by speed and torque request. Moreover the action of braking as a distribution of front and rear brakes and also regenerative (driveline) and friction braking is determined. Traction control block controls the limits of the torque transmitted to wheels while braking and traction. The block diagram representation is given in Figure 3-16.

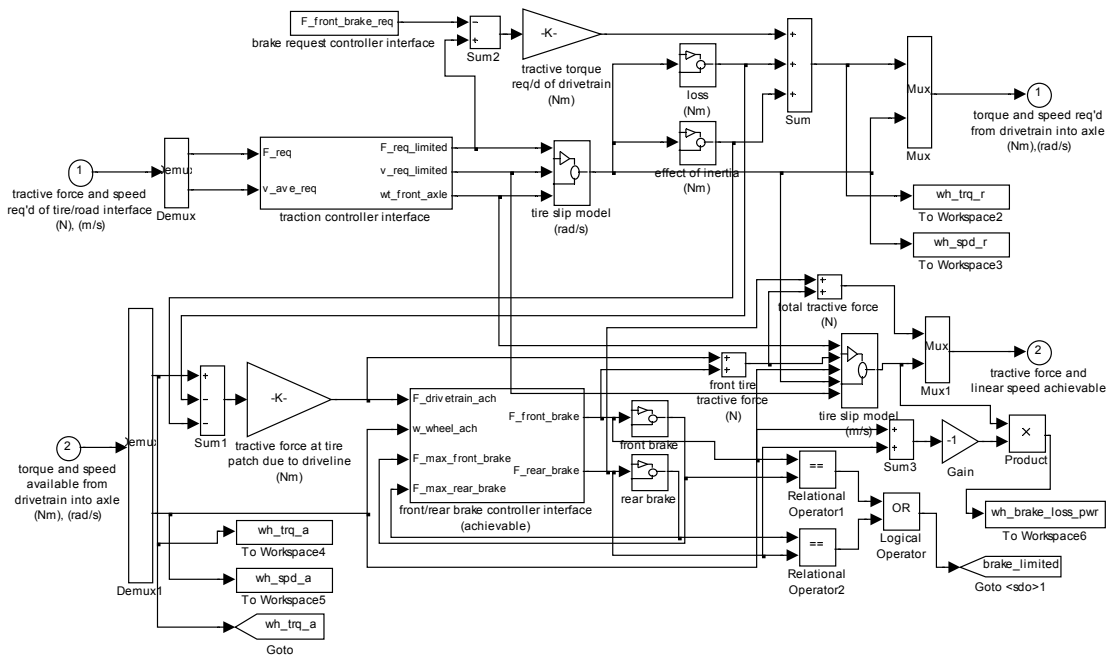


Figure 3-16: Wheel/axle block diagram

As stated above wheel/axle model includes brake distribution for the vehicle and it is important for regenerative braking used in HEV. Since regenerative braking is one of the aspects that satisfies better fuel economy over conventional vehicles, the braking strategy and brake distribution between driveline (regenerative) and friction braking gets important. The braking force needed to satisfy the deceleration demand is supplied with front axle braking with a fraction including driveline and friction braking and rear axle friction braking with a fraction. The driveline and friction braking has fractions changing with vehicle speed. They are implemented as a 1-D look-up table and the values are gathered over 94 model Taurus wheel test estimations [27]. A schematic for brake distribution is given below in Figure 3-17.

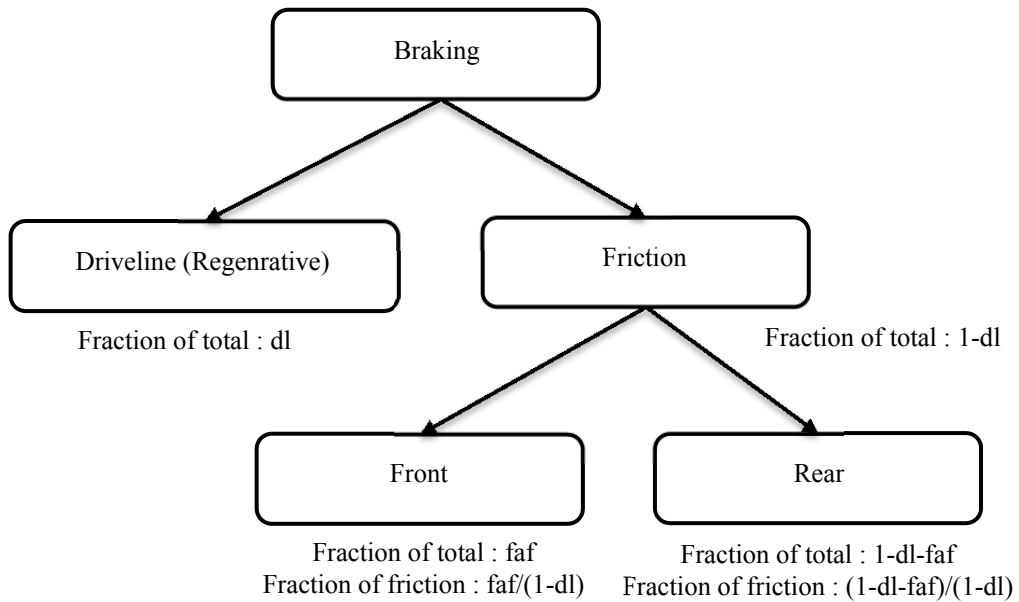


Figure 3-17: Braking strategy and fractions [27]

The equations for the braking strategy could be written step by step as [27]:

1. “(braking force required at tire patch from front friction brakes) = (braking force required from all friction brakes) \* (fraction of braking supposed to be done by front friction brakes) / [ 1 – (fraction of braking supposed to be done by driveline) ]”
2. “unless (fraction of braking supposed to be done by driveline)=1, in which case (braking force required at tire patch from front friction brakes) = 0.6”
3. “(braking force supplied at tire patch by front friction brakes) = max( (braking force required at tire patch from front friction brakes), (most negative braking force front brakes can supply)”
4. “(braking force required at tire patch required from rear friction brakes) = (braking force required from all friction brakes) – (braking force supplied at tire patch by front friction brakes)”
5. “(braking force supplied at tire patch by rear friction brakes) = max( (braking force required at tire patch from rear friction brakes), (most negative braking force rear brakes can supply) )”

The fractions of the braking are mapped according to vehicle speed and the default values of the front axle fractions are given as 1x5 matrices:

- dl\_fa\_frac = [0 0 0.5 0.8 0.8]
- dl\_fa\_mph = [-1 0 15 100 1500]
- fric\_fa\_frac = [0.8 0.8 0.4 0.1 0.1]
- fric\_fa\_mph = [-1 0 15 100 1500]

The speed 1500 kph indicates the speed higher than 100 kph will have the same fraction value of 0.8 and the speed -1 simulates the point that vehicle does not move. The rest of the braking fraction is fulfilled by rear brakes.

Table 3-8: Wheel/axle variables [27]

Variable Name	Unit	Explanation
wh_axle_loss_mass	kg	vehicle test mass, used to index wh_axle_loss_trq
wh_axle_loss_trq	N*m	front brake and axle bearing drag torque
wh_fa_dl_brake_frac	--	fraction of braking done by driveline via front axle
wh_fa_dl_brake_mph	kph	vehicle speed, used to index wh_fa_dl_brake_frac
wh_fa_fric_brake_frac	--	fraction of braking done by front axle friction brakes
wh_fa_fric_brake_mph	kph	vehicle speed, used to index wh_fa_fric_brake_frac
wh_inertia	kg*m <sup>2</sup>	rotational inertia of the wheels
wh_radius	m	radius of the wheel
wh_slip	--	wheel slip of drive wheels
wh_slip_force_coeff	--	(tractive force on front tires)/(vehicle weight on front tires), used to index wh_slip
wh_1st_rrc	--	1st coefficient of rolling resistance such that force of rolling resistance is (wh_1st_rrc+v*wh_2nd_rrc)*M*g*cos(theta) [where Mgc*cos(theta) is the weight normal over the axle
wh_2nd_rrc	s/m	2nd coefficient of rolling resistance
wh_slip_r	rad	amount of slip requested at wheels
wh_brake_loss_pwr	N*m/s	amount of power loss from braking
wh_loss_kj	kJ	the difference between the total energy into the wheel and the useful energy transmitted by the wheel over the drive cycle
wh_out_kj	kJ	the useful energy output of the wheel during the drive cycle--used to maintain the achieved force and speed
wh_out_regen_kj	kJ	the useful energy transmitted up the drive train by the wheel for regeneration during the drive cycle
wh_regen_eff	kJ	the efficiency of the wheel with respect to regeneration

In order to determine the fractions, losses in the axles and inertial effects are included, slip and traction limitations are calculated, and regenerative braking performances are monitored. Variables defined are given in Table 3-8.

A second control block is formed for traction control. As mentioned before, the block controls the limits of the tractive force and also speed. The maximum achievable speed is computed by solving “F = ma” equation by using two consecutive time steps for maximum speed, and while the acceleration changes the weight on the tire also changes due to load transfer which also effects the maximum tractive force. Then the maximum tractive force is computed by using the limited requested speed. The limited values of velocity and force by the controller are defined according to equations given below. The details of the resistive forces with their equation are given in the next section.

$$\begin{aligned}
V_{max} = & [\max(S) * M_v * g * w_f - M_v * g * (a + \sin(\text{atan}(\theta))) - 1/2 * M_v * g * b \\
& * V_{init} - 1/8 * \rho_{air} * C_D * A_f * (V_{init})^2 + \max(S) * M_v * h/L \\
& * V_{init}/t_{step} + M_v * V_{init}/t_{step}] / [3/8 * \rho_{air} * C_D * A_f * V_{init} + 1/2 \\
& * M_v * g * b + M_v/t_{step} + \max(S) * M_v * h/L]
\end{aligned} \tag{3.24}$$

$$F_{max} = \max(S) * [M_v * g * w_f - M_v * h/L * 2 * (V_{req} - V_{init})/t_{step}] \tag{3.25}$$

Where

$V_{max}$  = Maximum achivable speed

$F_{max}$  = Maximum force

$M_v$  = Vehicle mass

$g$  = Gravitational Acceleration

$w_f$  = Front axle weight distribuion ratio

$\theta$  = Grade percent

$V_{init}$  = Vehicle speed at the begining of time step

$t_{step}$  = Duration of time step

$h$  = Height of center of gravity of the vehicle

$L$  = Vehicle base

$\rho_{air}$  = Air density

$C_D$  = Aeodynamic drag coefficient

$A_f$  = Frontal area of the vehicle

$a$  = First rolling resistance coefficient

$b$  = Second rolling resistance coefficient

$S$  = Wheel tire slip

$V_{req}$  = Vehicle speed required at the output of wheel block

### 3.2.3 Vehicle Model

The model calculates the required acceleration forces including the forces to overcome resistances (grade, rolling, and air) and inertial effects, at the desired speed defined in drive cycle data. It uses basic vehicle longitudinal dynamics equations. The average speed is calculated over the two consecutive time steps and it is taken as the average speed at the beginning of the time step to calculate the forces and the speed required at the end of the time step. The block diagram representation of the model is given in Figure 3-18.

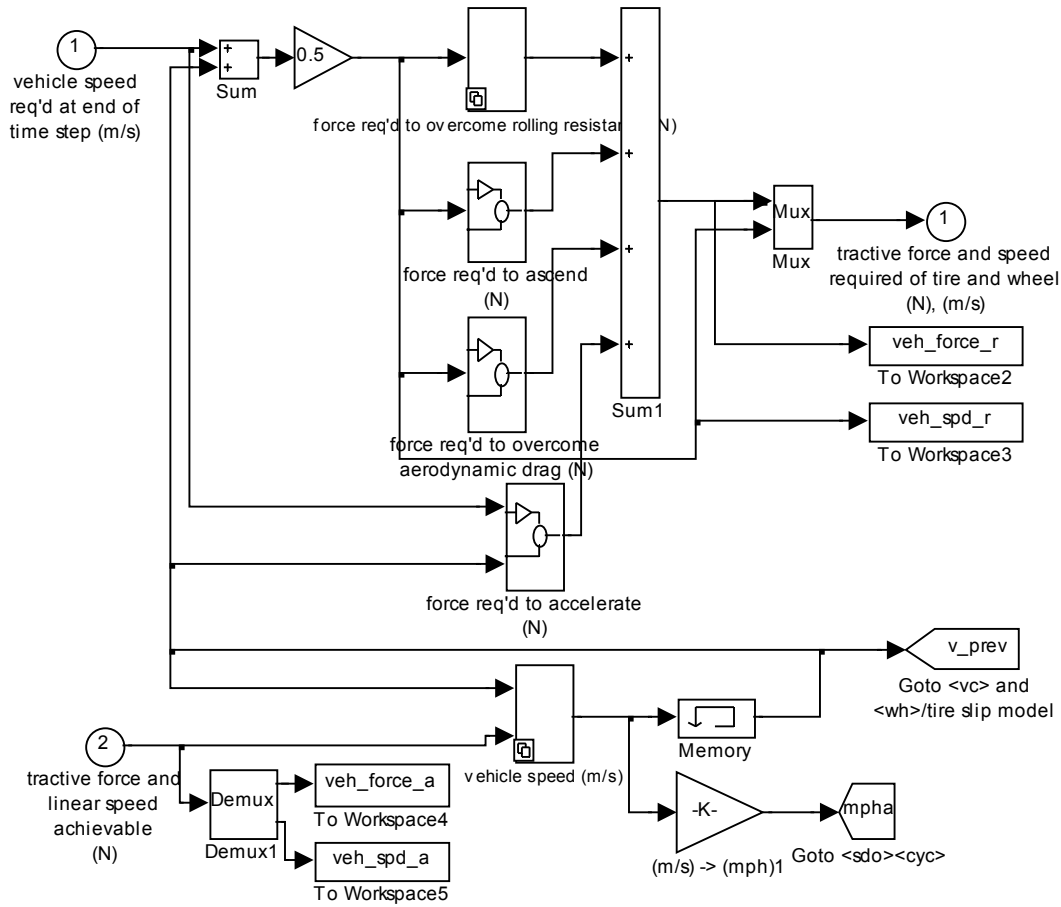


Figure 3-18: Vehicle model block diagram

The fundamental dynamical equation including rolling, air and grade resistances and inertial effects is given below and the resultant forces on the vehicle are shown in Figure 3-19. As shown on the figure, rolling resistances are calculated for each axle similar as traction forces in simulations. Also air resistance and acceleration effects on load distribution are also included. On the other hand initial power sizing process uses a simpler vehicle model which assumes all forces are applied at vehicle center of gravity and load distribution effects are not considered. The model of power sizing will be given in the next part in detail.

$$M_v \frac{dV}{dt} = \underbrace{(F_{tf} + F_{tr})}_{F_t} - \underbrace{(F_{rf} + F_{rr} + F_a + F_g)}_{F_{res}} \quad (3.26)$$

Where

$F_t$  = Traction forces

$F_{res}$  = Resistive forces

$F_{tf}$  = Front axle tractive force

$F_{tr}$  = Rear axle tractive force

$F_{rf}$  = Front axle rolling resistance force

$F_{rr}$  = Rear axle rolling resistance force

$F_a$  = Air resistance force

$F_g$  = Grade resistance force

$F_r$  = Rolling resistance force

$$F_r = \frac{(a + bV) * M_v * g}{f_r} \quad (3.27)$$

$$F_g = M_v * g * \sin(\alpha) \quad (3.28)$$

$$F_a = \frac{1}{2} \rho_{air} C_d A_f V^2 \quad (3.29)$$

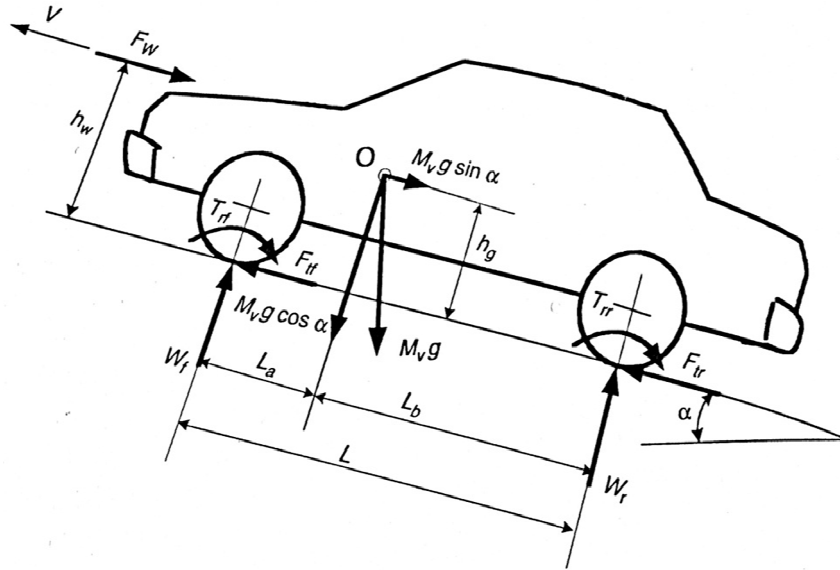


Figure 3-19: Forces acting on a vehicle acceleration up a slope

### 3.3 POWER COMPONENT SIZING

The parameters of the drivetrain such as engine power, electric motor power, energy capacity and power of battery are key parameters and exert a considerable influence on vehicle performance and efficiency of the vehicle. Before going through the optimization process, as an initial step in the design, these parameters should be estimated based on the performance requirements determined by the user over designed GUI. These initially sized parameter values are used optimization procedure as starting values.

There are two different drive train configuration series and parallel to be designed and analyzed. The sizing strategy for series and parallel configurations should be handled separately since the power flow directions and methods are different from energy source to the wheels. For this reason this section is prepared in two main sections as parallel drive train component sizing and series drive train component sizing. In both configurations inertial effects are not included while calculating the acceleration ratings since for some of the components inertial data are missing. The existing ones are included in the full model. In addition to that, loss effects are included as constant and added to sizing procedure simply as product of the final power ration with a gain of 1.2 which includes clutch, gearbox and final drive losses. They are given as 0.92, 0.95 and 0.94 which results in

$$loss\_factor\_const = \frac{1}{0.92 * 0.95 * 0.94} \cong 1.2 \quad (3.30)$$

### 3.3.1 Parallel Drive Train Power Component Sizing

As described in the previous sections, parallel hybrid configuration differs from series one in allowing both engine and traction motor supply their mechanical power to the wheels. With this fundamental difference it has major advantages over series in that there is no need for a generator motor, a smaller traction motor can be used and there is no need of multi conversion of energy while transmitting to the wheels [34]. Starting with these specifications of parallel configuration, power sizing procedure is constructed. There are different design methodologies for parallel configuration; however power sizing strategy will differ for each strategy implementation. In this thesis, sizing is based on electrical power peaking strategy; that is engine supply the power needed during cruise on a flat road or a mild grade or mean power during stop and go driving pattern, while electric motor with battery supplies the power to meet the load at peak.

In order to determine the power demand, there are 5 different types of input to be supplied over GUI. These are defined as:

- 1) Vehicle Maximum Speed
- 2) 0 – 100 kph Acceleration
- 3) Maximum Acceleration
- 4) Maximum Grade at Low Speed
- 5) Maximum Grade at High Speed

These input variables are used for electric motor power and engine power determination process. As stated above, maximum vehicle speed and maximum grade at high speed value (the speed value should be between 80-120 kph and the grade value should be between 0-8 % values) are used for internal combustion engine sizing. Then from the maximum acceleration and maximum grade at low speed input values total maximum torque value is calculated for the overall drivetrain. Then by using the 0 – 100 acceleration performance maximum power sizing estimation is made where the overall power demand is determined by using internal combustion engine sizing approach [35] for the whole vehicle. The detailed flow diagram of the sizing process is shown in Figure 3-20.

As a requirement in cruising with maximum speed or cruising on a mild grade, the power needed could be expressed as

$$P_e = \frac{V}{\eta_{t,e}} \left( M_v g f_r + \frac{1}{2} \rho_{air} C_d A_f V^2 + M_v g \sin(\alpha) \right) \quad (3.31)$$

From 0-100 acceleration performance which is given in seconds, total vehicle power could be estimated as

$$P_{veh} = \frac{V^2 * M_v}{t_0} \quad (3.32)$$

The comparison between the estimated and the test results of the manufacturers are shown in Figure 3-21.

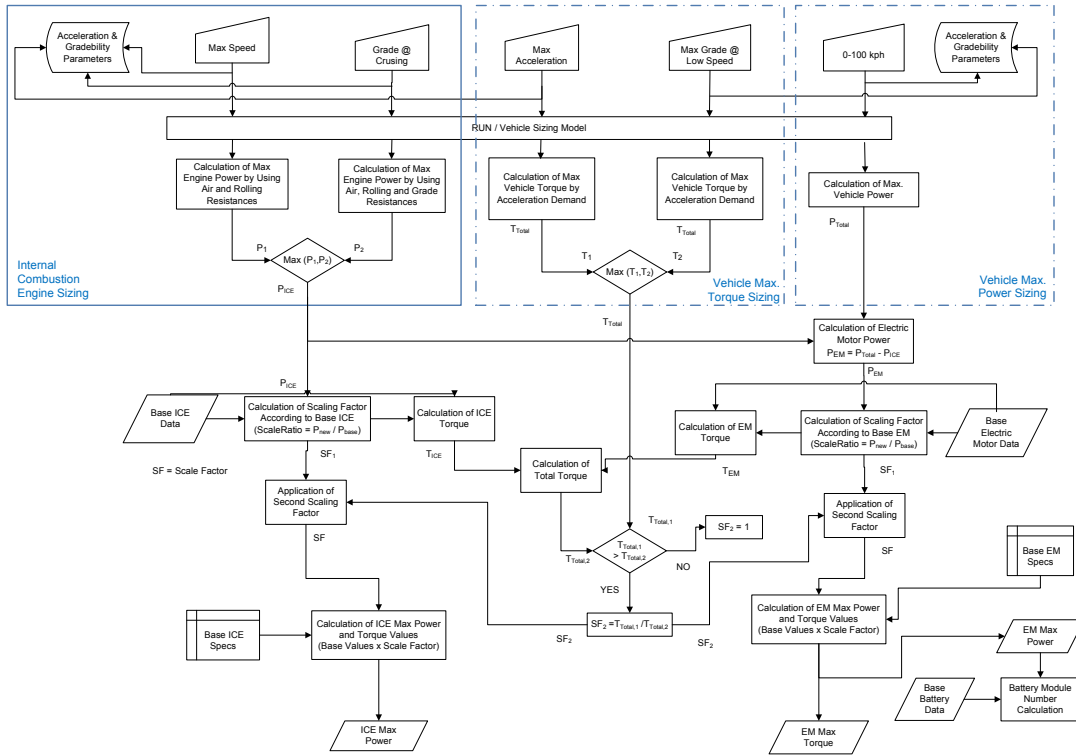


Figure 3-20: Parallel drivetrain power component sizing flow diagram

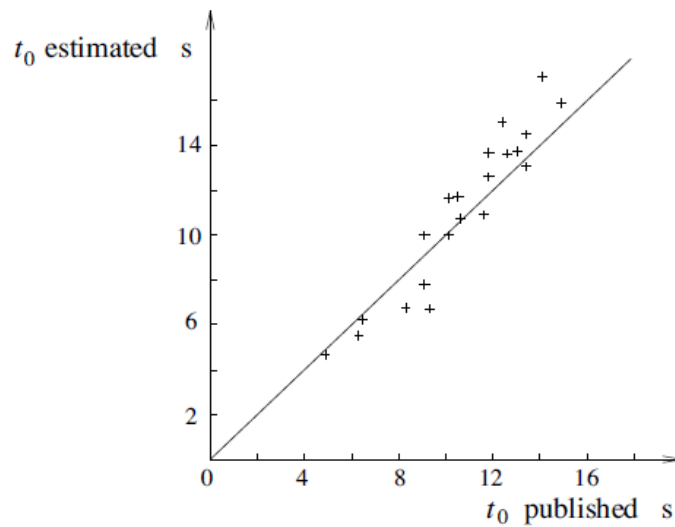


Figure 3-21: Comparison between acceleration times as published by manufacturers (crosses) and values calculated with (3.32) for  $V = 100$  kph. (solid line)

After performance requirements in 0-100 kph acceleration, grade at high speed and maximum vehicle speed are defined as power needs, component sizing according to their maximum torque values is carried by using the values defined in maximum acceleration and maximum grade at low speeds demands.

While evaluating the maximum acceleration, basic dynamical equation is used for the estimation for the acceleration as a mean value.

$$F_{max} = M_v * a_{max} \quad (3.33)$$

where

$$F_{max} = \frac{T_{max}}{r_{wheel}} \quad (3.34)$$

$$T_{max} = (T_{em,max} * i_{tc} + T_{ic,max}) * i_{gb,1} * i_d \quad (3.35)$$

$F_{max}$  = Maximum force needed for the acceleration

$a_{max}$  = Maximum acceleration needed

$T_{max}$  = Maximum torque at the wheel

$r_{wheel}$  = Wheel radius

$T_{em,max}$  = Electric motor maximum torque

$T_{ic,max}$  = Internal combustion engine maximum torque

$i_{tc}$  = Torque coupler ratio

$i_{gb,1}$  = Gear box ratio at first gear

$i_d$  = Differential ratio

While calculating the maximum torque at the wheels as a summation of maximum torque value of the engine and electric motor, it is assumed that both operate close to the maximum torque region in their torque-speed range. It is also assumed in the same way also for maximum gradeability which is given below. Since speed of the vehicle is close to zero, the air resistance will also be close to zero and the rolling resistance will be relatively too small compared to grade resistance, the force and the torque required for maximum gradeability is given as

$$F_{max} = M_v * g * \sin(\text{atan}(\alpha)) \quad (3.36)$$

and

$$F_{max} = \frac{T_{max}}{r_{wheel}} \quad (3.37)$$

$$T_{max} = (T_{em,max} * i_{tc} + T_{ic,max}) * i_{gb,1} * i_d \quad (3.38)$$

Totally five power sizing values are calculated according to defined performance criteria. By using maximum acceleration and maximum gradeability ratings maximum total torque of the vehicle is calculated. The 0-100 kph rating is used to find the maximum total power of the vehicle. On the other hand, grade at high speed and maximum speed values provide for engine only power sizing. In order to calculate electric motor and internal combustion engine power sizing separately and move to the battery power and capacity sizing, the steps shown in Figure 3-22 should be evaluated.

First comparison is made between the maximum power values of engine found in gradeability at high speed and maximum vehicle speed and the larger one is specified as the internal combustion engine maximum power. Then this value is subtracted from the value found from the power rating for 0-100 kph acceleration, and the maximum power value of the electric motor is determined. This is a rough estimation for electric motor and better estimation could be made using the electric motor power sizing formula given in the following section and calculating the resistive forces through the acceleration process instead of using a mean value as an approximation.

After the internal combustion and electric motor are sized according to their maximum power ratings, a comparison should be carried out to check whether the components with specified power rating could satisfy the maximum torque values found. The specifications of the engine and electric motor are supplied by the data files given in sections 3.2.2.1 and 3.2.2.3. These files include maximum power and torque rating of base engine and electric motor and the base data file selection is made respect to vehicle type selection on the GUI.

Since the calculated power ratings for the engine and electric motor are different from the base component specifications, a scaling procedure is applied by using a factor named as “torque scaling

factor” which is defined as “mc\_trq\_scale” for electric motor and “fc\_trq\_scale” and directly applied to base component maximum torque value by production [13].

$$T_{ic,max} = T_{ic,base,max} * fc\_trq\_scale \quad (3.39)$$

$$T_{em,max} = T_{em,base,max} * mc\_trq\_scale \quad (3.40)$$

$T_{ic,base,max}$  = Maximum torque rating of the base engine

$T_{em,base,max}$  = Maximum torque rating of the base motor

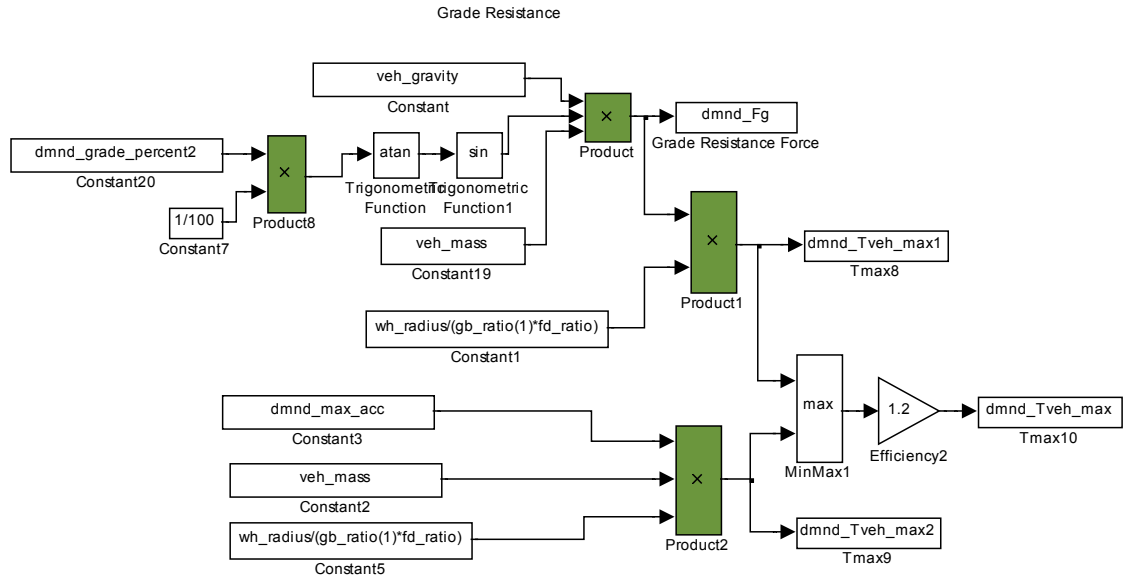
Since same type of ICE (spark or compression ignition) with close power rating have similar maximum torque curve characteristics, in the same speed region, the maximum power could be changed only by using torque scaling [13] [36]. So for ease of implementation of power value of the engine, in the optimization process torque scaling is directly used and the power value is calculated as

$$P_{ic} = \frac{(T_{ic,base} * fc\_trq\_scale)}{T_{ic}} * n_{ic} \quad (3.41)$$

Using the same approach, electric motor power rating could also be included to the sizing and also optimization process as only torque scaling factor [37].

$$P_{em} = \frac{(T_{em,base} * mc\_trq\_scale)}{T_{em}} * n_{em} \quad (3.42)$$

As a result power and torque ratings of the engine and electric motor are expressed as two scaling factors with base data file ratings, and a comparison between resultant power and torque ratings from different performance demands could be made. There are two ratings for engine maximum torque and maximum power and also two ratings for electric motor maximum torque and maximum power which need to be compared to decide the final rating of power components. The Simulink diagram of parallel drivetrain sizing procedure is given in Figure 3-22.



(a)



After engine and electric motor power sizing is completed, the next step is to estimate the battery power and capacity sizing. In parallel configuration, battery should deliver sufficient power that will meet the demand from the traction motor at any time. Moreover it should store sufficient energy to avoid discharging up to critical region for battery life. So there are two parameters to be decided in the sizing process: battery power capacity and energy capacity.

Power capacity of the battery could be determined by using electric motor power calculated at the second step of the sizing procedure. The power of the battery as power peaking source can be expressed as

$$P_{bat} \geq P_{em} \quad (3.43)$$

After power rating determination, the second parameter, energy capacity of the batteries should also be determined. However, the capacity scaling is directly related to drive cycle stop and go patterns and acceleration and grade properties and their durations. So the procedure for capacity determination starts with a base value which is taken directly from the reference data file given in Table 3-3. Then in the optimization process it becomes the third optimization parameter as “battery capacity scale factor”. Similar to power scaling of EM and ICE, the expression simply formed as

$$C_{bat} = C_{bat,base} * ess\_cap\_scale \quad (3.44)$$

and the power rating of the battery is calculated in the form of module number. By using the known base battery data on module power rating, total power becomes

$$P_{bat} = ess\_module\_num * P_{bat,base} \quad (3.45)$$

All scaling and number of module effects, such as mass and resistance changes are implanted to the battery model and it satisfies the related connection to effects on fuel economy and emission values.

### 3.3.2 Series Drive Train Power Component Sizing

The concept of series drivetrain configuration is based on pure electric vehicle as described in the previous sections. In power sizing aspect, it is very similar to pure electric vehicle since the only direct traction power is transmitted to the wheels by the electric motor. But, on the other hand it has another power source; internal combustion engine with a generator connected to its output shaft in addition to the standard battery pack. Also as named in parallel configuration, peaking power source will replace the battery pack as in hybrid strategy, it is used for supplying peaking power demands and used for regenerative braking. So as a control strategy, sustaining maximum SOC of peaking power source is going to be implemented and it is explained in detail in the next section.

Similar to parallel one, in order to determine the power demand, there are 5 different type of inputs to be supplied over GUI. These are defined as:

- 1) 0 – 100 kph Acceleration
- 2) Maximum Acceleration
- 3) Maximum Grade at Low Speed
- 4) Maximum Grade at High Speed
- 5) Maximum Speed

Again similar to parallel configuration, these input variables are used for electric power and combustion power determination process. As the power is in the form of electrical energy flow, in series configuration sizing procedure of the elements differs in some performance demands. As mentioned above, the only traction power to the wheels transmitted by electrical motor. So its power and torque values should satisfy all performance demands. Starting from this rule, 0-100 kph acceleration gives the maximum power of the motor and maximum acceleration and maximum grade at low speed values give the maximum torque value of the electric motor. Then, starting from the idea that engine-generator couple supplies steady state power, grade at high speed and maximum speed performance values are used for engine and s generator sizing. Also maximum speed could be used

for gear ratio determination for electric motor considering the speed limited case. The whole flow diagram of the sizing procedure is given in Figure 3-23. The flow diagram of the procedure is given in Appendix A in more detail.

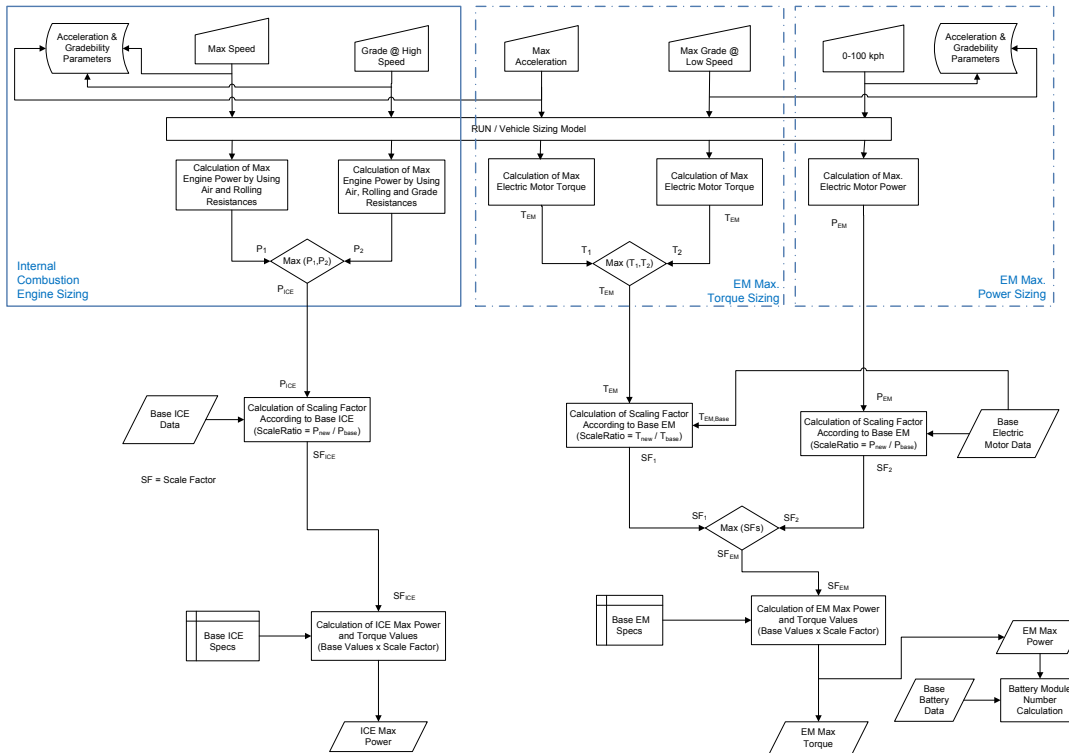


Figure 3-23: Series drivetrain power component sizing flow diagram

Here the first step is to determine the traction motor power sizing by using 0-100 kph performance value. The electric motor has different torque speed and power characteristic from the combustion engine. Generally, the speed-torque characteristic of electric motor is identified by the so-called base speed, below which the motor has a constant torque, and above which constant power. In a more generalized way, the motor speed can be identified by a speed ratio,  $x$ , which is defined as the ratio of maximum speed of the motor to its base speed [38]. A typical electric motor torque and power curve with speed is given in Figure 3-24.

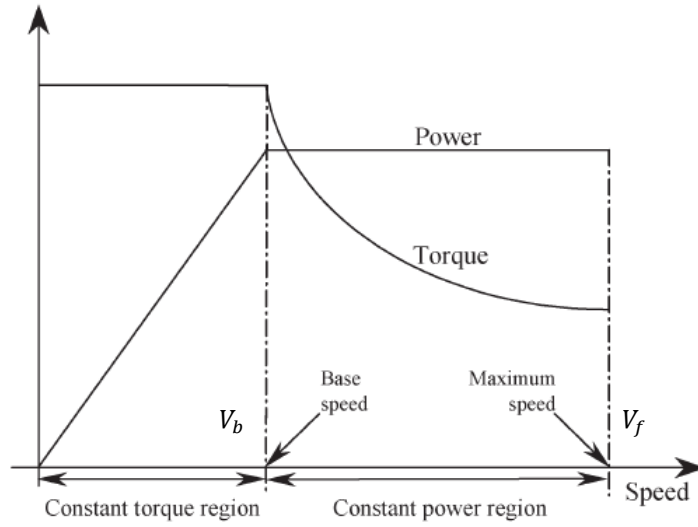


Figure 3-24: Typical characteristics of traction motor

As shown on the figure, there two regions to be included separately with different formulas into the equations used in the power estimation calculations. Acceleration performance as time elapsed in seconds during speeding up from 0 to 100 kph, the equation for an electric motor could be formed as integration with two regions of electric motor with air and rolling resistances and inertial effects [39].

$$t_a = \int_0^{v_b} \frac{M_v \delta * dV}{F_{max} - M_v g f_r - \frac{1}{2} \rho C_d A_f V^2} + \int_{v_b}^{v_f} \frac{M_v \delta * dV}{\frac{F_{max} V_m}{V} - M_v g f_r - \frac{1}{2} \rho C_d A_f V^2} \quad (3.46)$$

However it is hard to obtain an analytical solution from the equation given above. As an initial estimation of power sizing of the electric motor, a simplified form of equation (3.47) by ignoring rolling and air resistances is used [2].

$$P_{em} = \frac{M_v \delta}{2 \eta_t t_a} (V_b^2 + V_f^2) \quad (3.47)$$

The final speed of the vehicle is taken as 100 kph for 0-100 kph acceleration rating and the base speed is determined as one fourth of the final speed since the “x Factor” of the motor is defined as in the base electric motor file as “4”.

$$V_b = \frac{V_f}{4} \quad (3.48)$$

In addition to maximum power estimation of the traction motor, sizing according to maximum torque rating is also carried by using two performance demand values: “maximum acceleration” and “maximum grade at low speed”. As it is done in case of parallel configuration the same formula is used for electric motor maximum torque determination.

$$F_{max} = M_v * a_{max} \quad (3.49)$$

Where

$$F_{max} = \frac{T_{em,max}}{r_{wheel}} \quad (3.50)$$

and while determining from the maximum gradeability at vehicle velocity close to zero, the equations become

$$F_{max} = M_v * g * \sin(\text{atan}(\alpha)) \quad (3.51)$$

and

$$F_{max} = \frac{T_{em,max}}{r_{wheel}} \quad (3.52)$$

The second element to size is the internal combustion engine and generator couple. They are sized as a couple since when pure series configuration is the concern; generator is directly connected to engine output shaft and converts all mechanical energy into the electrical energy. Different from the parallel configuration, engine and the electric motor could be sized as decoupled and total vehicle traction ability is directly specified by electric traction motor. Main hybrid strategy that takes battery as a power peaking source, and engine-generator couple is used as energy source for continuous and steady state power needs. So, engine-generator couple specifications are defined according to maximum speed and grade at high speed values. The equation is same with the one used in engine sizing in parallel drivetrain.

$$P_e = \frac{V}{\eta_{t,e}} \left( M_v g f_r + \frac{1}{2} \rho_{air} C_d A_f V^2 + M_v g \sin(\alpha) \right) \quad (3.53)$$

In addition to the usage of maximum speed in engine and generator sizing, it could be also be used for transmission ratio determination considering the speed limited case of electric motor while reaching the top speed.

There are three different data (2 maximum torque and 1 maximum power) for the determination of power rating of the electric motor and two data (2 maximum power) for the engine. For the engine, direct comparison between the power values give the result of maximum power rating and then scaling is performed with respect to base engine parameters. Again the same procedure is carried out after the determination of the maximum torque value of the electric motor, by using maximum power and maximum torque ratings two torque scaling factors are found by using the equation (3.40). Final electric motor specifications are found by directly comparing the two scaling factors. All scaling and determination of component power ratings calculations are made on Simulink platform and its diagram is given in Figure 3-27.

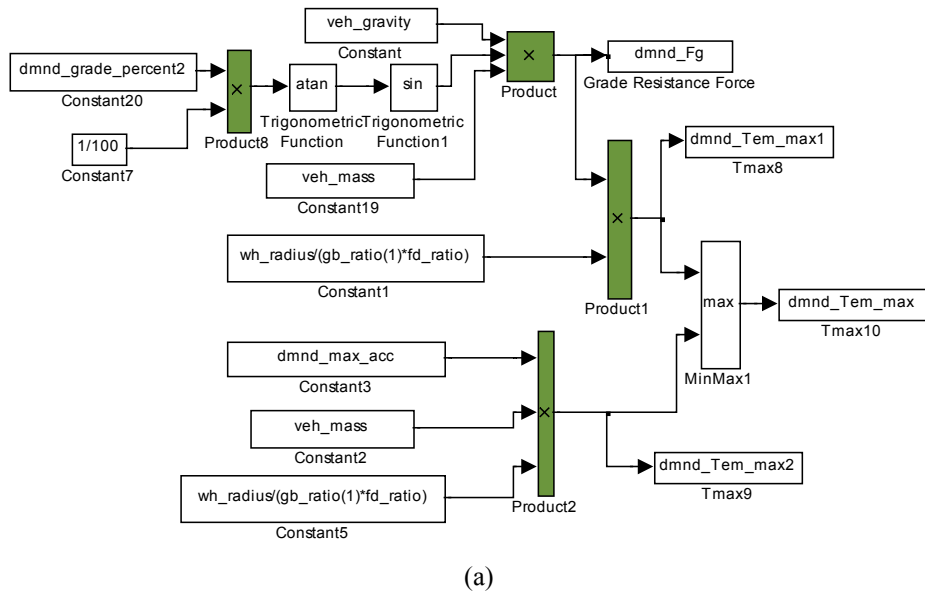
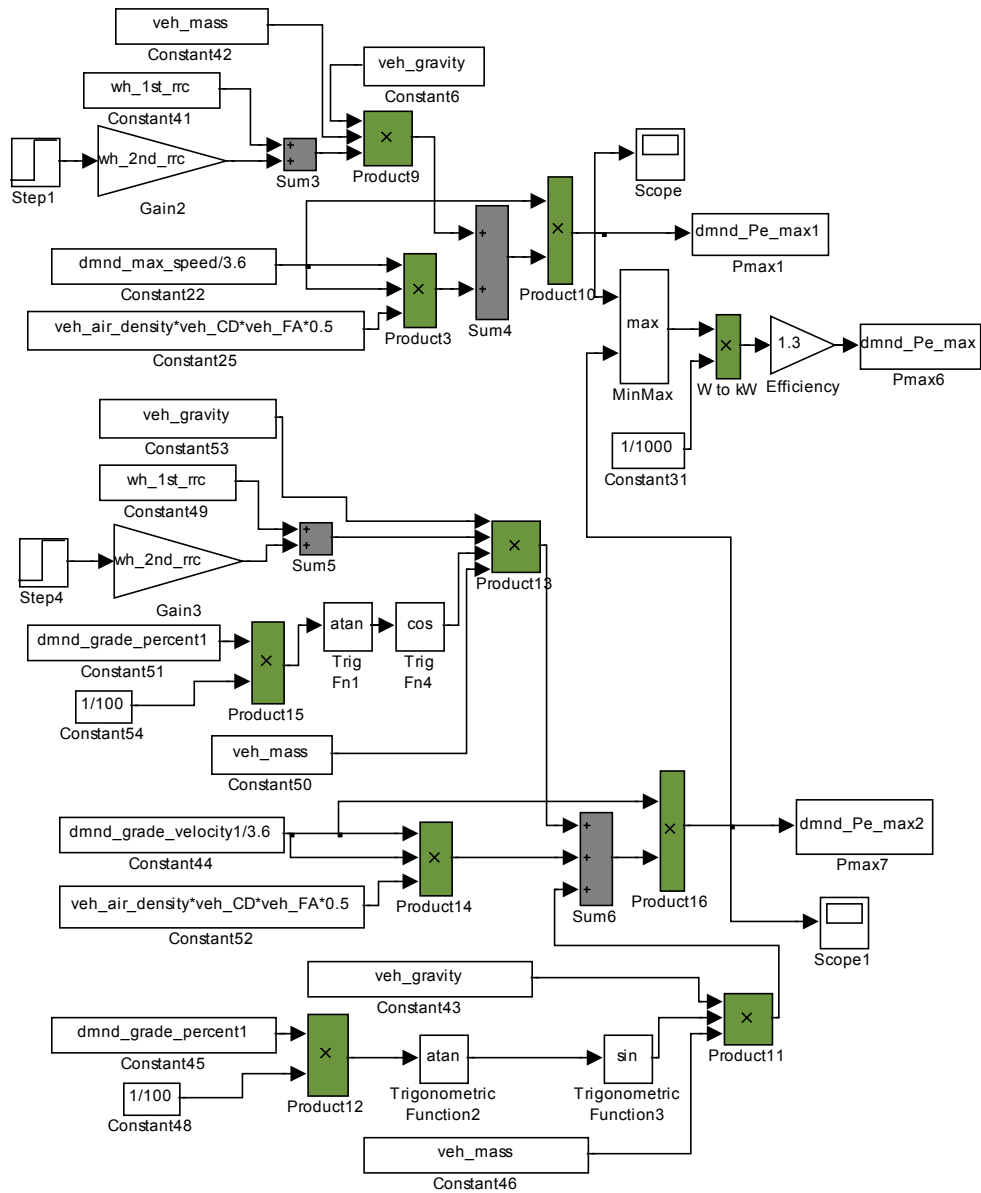


Figure 3-25: Block diagram representation of series drivetrain components sizing



(b)

Figure 3-26: Block diagram representation of series drivetrain components sizing

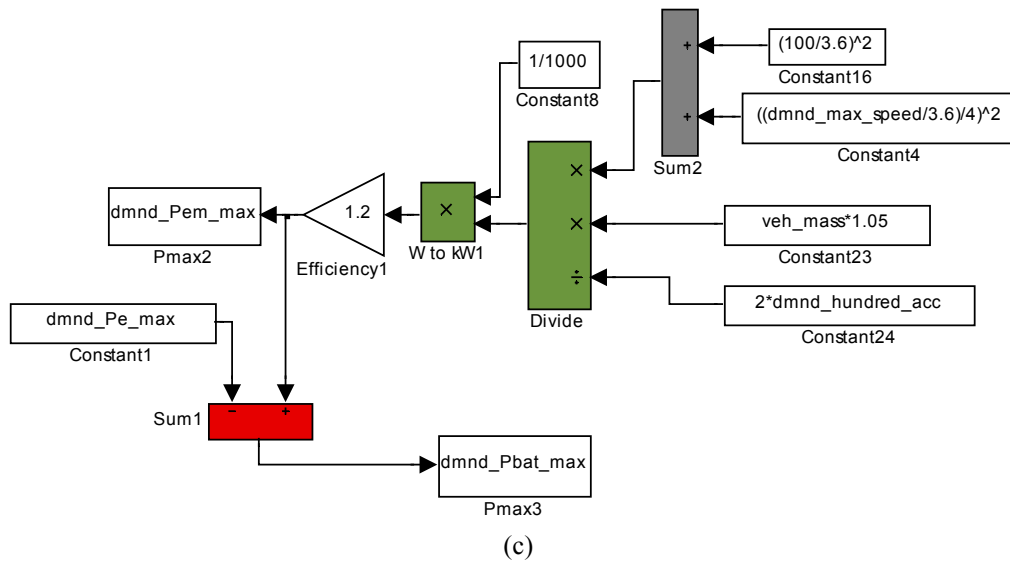


Figure 3-27: Block diagram representation of series drivetrain components sizing

After the engine and electric motor power sizing is completed, the next step is to estimate the battery power and capacity sizing. Similar to parallel structure these two key parameters are to be sized according to drive cycle characteristics and are dependent on other elements power sizing. Although capacity scaling is totally the same with parallel configuration which is defined in equation (3.44) and power value assignment in terms of module number has the same procedure which is given in equation (3.45); power value determination is different from the parallel drivetrain. It is determined as the difference between the electric motor and engine/generator couple.

$$P_{bat} \geq P_{em} - P_{e/g} \quad (3.54)$$

However battery ratings should also meet with the electric motor ratings. The most important point is the satisfaction of the electric motor minimum voltage value. Moreover since the electric motor data are mostly defined by the operating voltage around 320V, battery ratings should also satisfy it. The types of batteries used have 6V and 12V a cell values. So for 6V battery pack minimum 50 cells and for 12V pack minimum of 25 cells are defined. If the calculated value exceeds total power of the defined minimums, the maximum power rating is updated. This procedure is applied for both series and parallel configurations. Then the battery power rating is optimized by using its capacity scaling value as explained in energy storage modeling section. The rest of the procedure flows in the same way for mass and resistance effects inclusion to the model and optimization process.

### 3.4 CONTROL STRATEGY IMPLEMENTATION

A control strategy is a rule that is implemented to the vehicle via a controller and commands the operation and coordination of each component over drivetrain. The driver gives drive commands through acceleration and brake pedals as positive or negative torque demands and the controller gets this information together with the feedback from drivetrain and all necessary components and finally makes a decision to use proper operation modes and regions. The performance of the drivetrain is highly dependent on control strategy in the aspect of satisfying the performance demands and best efficiency values with emission considerations.

In commercial, internal combustion engine powered vehicles, control is simple as engine provides all tractive torque and frictional brakes fulfill the deceleration demand. However in hybrid drive train, there is an additional power source and propeller as battery and electric motor which give lots of different operation alternatives over a drive cycle. The main objectives of hybrid drivetrain energy management system are during the vehicle operation, meeting the tractive power demand while sustaining the battery charge due its life time consideration and optimization of drivetrain efficiency and the parameters for fuel consumption and emission.

Simple approaches in order to maximize the efficiency do not give the optimal solution. Simply applying as much electric torque while propelling as possible will give a temporary minimization and when overall cycle or trip is considered it will result in battery depletion. Some other approaches considering only determination of the engine most efficient operating points without regarding previous operating history and also current battery state could not give the overall efficiency performance improvement. The hybrid vehicle efficiency is highly dependent on satisfying the optimum operation point of the engine together with the battery restoring performance.

In addition to common applications as satisfying the most efficient operating point for the engine and keeping the battery in between defined SOC limits, series and parallel drive trains differ in control strategy techniques and contents. Series configuration could be controlled via a simpler control strategy due its simpler design in drivetrain with electrical energy flow. On the other hand parallel configuration needs more complicated systems since coupling the mechanical power coming from EM and ICE.

In the following sections implemented control strategies with their algorithms, parameters and rules are given. Further comparison with other alternative strategies that could be used, including their advantages and disadvantages together with basic implementation procedures, is made.

### **3.4.1 Parallel Hybrid Control Strategy Parameters and Rules**

The available operation modes are already defined in introduction part for parallel configuration. During the operation, the convenient operation modes should be used so as to meet the traction torque requirement, achieve high overall engine efficiency, maintain a reasonable level of battery SOC and recover braking energy as much as possible [40].

As a base control strategy, a rule based strategy which includes predetermined parameters and working regions is used [41]. The main idea behind the rule based strategy is “load leveling” between the power components. The load-leveling strategy is to shift the actual ICE operating point as close as possible to the optimal point of efficiency, fuel economy, or emissions at a particular engine speed. Generally, the best fuel economy for this system is found at a lower torque and a lower engine speed than the best point of efficiency. This means that better fuel economy will be attained by having smaller accelerator commands [42]. The difference between the driver’s commanded power and the power generated by ICE will be compensated by the EM or used in replenishing the battery based on the measured SOC.

Deterministic rule based strategies include different alternatives such as on-off control, SOC maximization algorithm, etc. In the current study, a rule based static control strategy which attempts to minimize fuel use and keep the SOC level balanced is implemented. The control strategy is named as “baseline static control strategy” [43]. This strategy uses ICE as primary power source and motor power as supplemental. So it could also be called as parallel electric assist control strategy. The main idea of the strategy depends on limiting engine working region and keeping the working region higher from a defined base speed and a torque value, and satisfying the power demands corresponding to below-defined region by using electric motor and battery. Similar strategies are used in Toyota Prius and Honda Insight [44] [45]. Here the electric motor could be used for different purposes:

1. The motor can be used for all driving torque below a certain minimum vehicle speed.
2. The motor is used for torque assist if the required torque is greater than the maximum producible torque by the engine at recent engine operating speed.
3. The motor charges the batteries by regenerative braking.
4. When the engine would run inefficiently at the required engine torque at a given speed, the engine will shut off and the motor will produce the required torque.
5. When the battery SOC is low, the engine will provide excess torque which will be used by the motor to charge the battery.

There are six variables defined in order to determine the operation procedures. These are given in Table 3-9.

Table 3-9: Baseline control strategy variables [27]

Variable	Description
cs_hi_soc	[-] highest desired battery SOC
cs_lo_soc	[-] lowest desired battery SOC
cs_electric_launch_spd	[m/s] vehicle speed below which vehicle operates as a ZEV
cs_off_trq_frac	[-]off torque threshold = fraction* $T_{max}$ (SOC > low limit)
cs_min_trq_frac	[-] minimum torque threshold = fraction* $T_{max}$ (SOC < low limit)
cs_charge_trq	$cs\_charge\_trq * ((cs\_lo\_soc + cs\_hi\_soc) / 2 - SOC)$ = an accessory like torque loading on the engine to recharge the battery pack

And their influence on defining the working region of the ICE during the operation is given in the Figure 3-28 and Figure 3-286 for SOC is higher than the lower limit of the battery and SOC is lower than the lower limit cases separately.

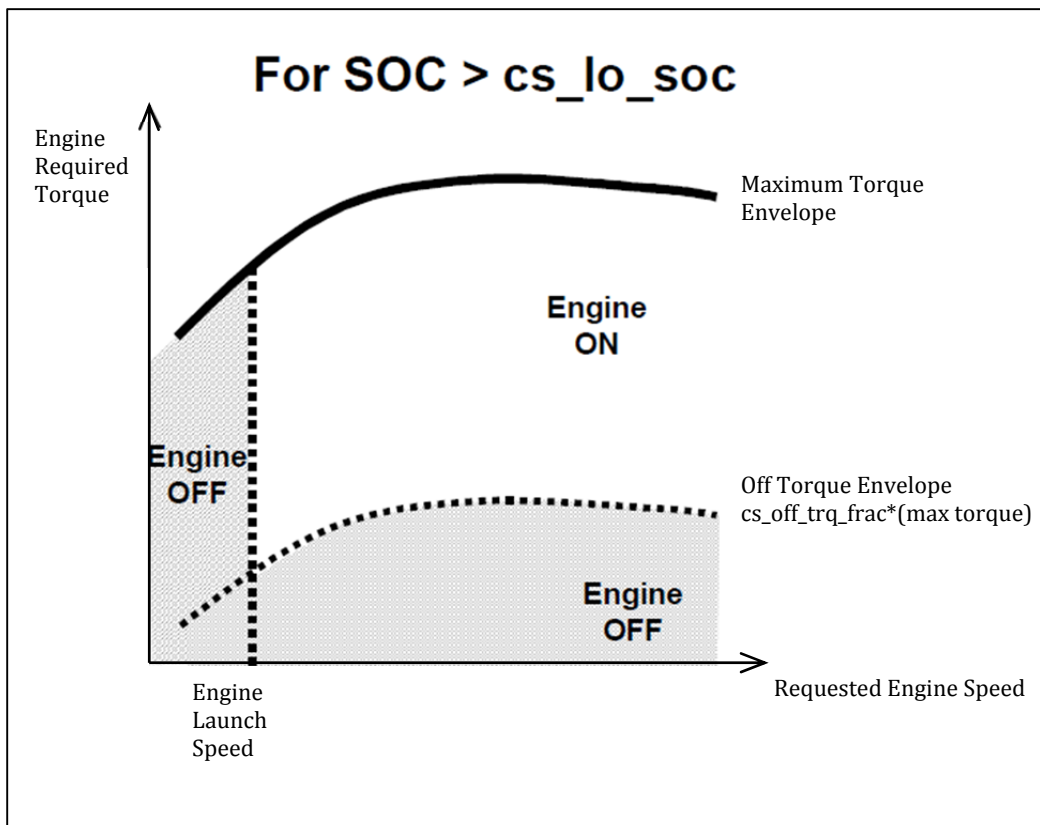


Figure 3-28: Control strategy when SOC > low limit [43]

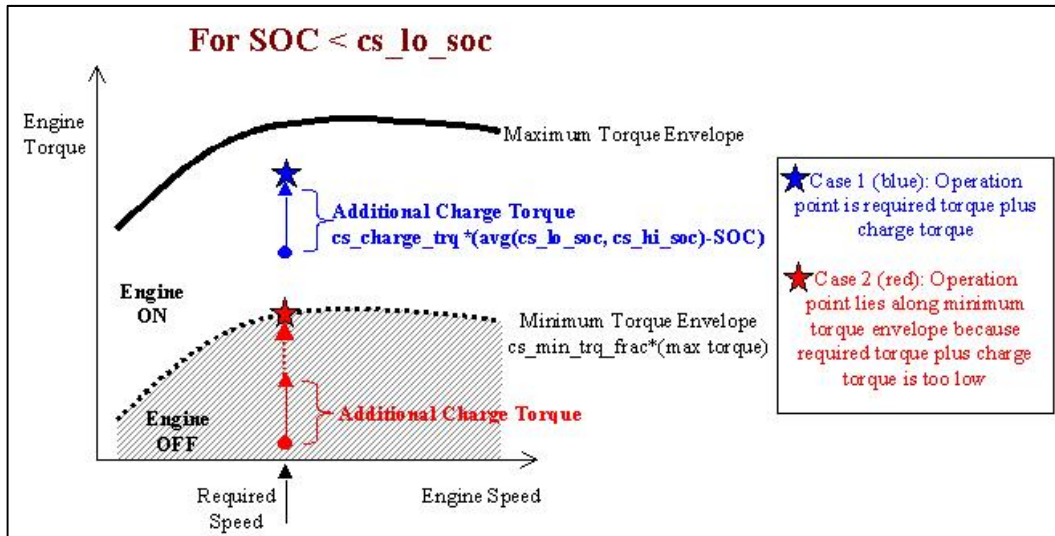


Figure 3-26: Baseline control strategy for low SOC [27]

There are two block diagrams structured in order to simulate this control algorithm. First one is named as “electric assist control block diagram” which determines torque distribution between supplied from the engine and electric motor to produce the required torque while keeping the charge of the battery between predefined limits according to torque and speed demand presented to engine through the clutch. The block diagram is given in Figure 3-. The diagram could be described in three steps as:

- “When the battery SOC is below  $cs\_soc\_lo$ , additional torque is required from the engine to charge the battery. This additional charging torque is proportional to the difference between SOC and the average of  $cs\_lo\_soc$  and  $cs\_hi\_soc$ .”
- “This engine torque is prevented from being below a certain fraction,  $cs\_min\_trq\_frac$ , of the maximum engine torque at the current operating speed. This is intended to prevent the engine from operating at an inefficiently low torque.”
- “Engine torque is only requested when the engine is on.”

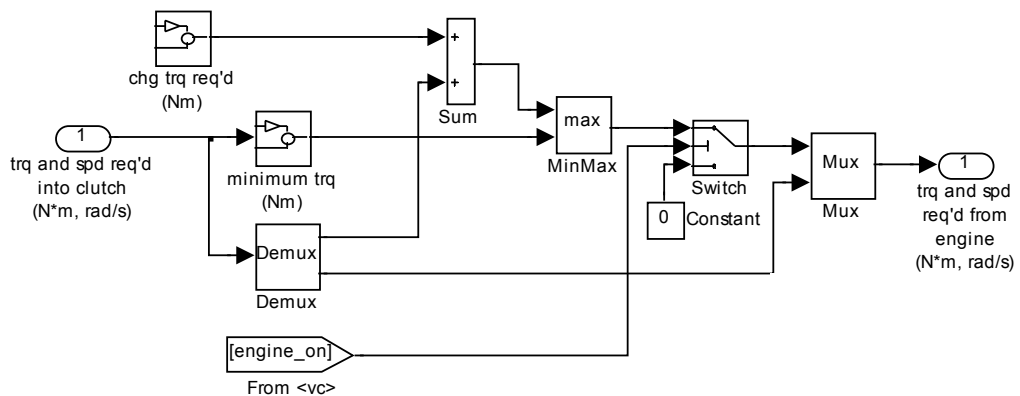


Figure 3-27: Electric assist control strategy block diagram

Then the second block diagram which controls the state of engine as on and off timings. The diagram is given in Figure 3-. It works by using the principles described below.

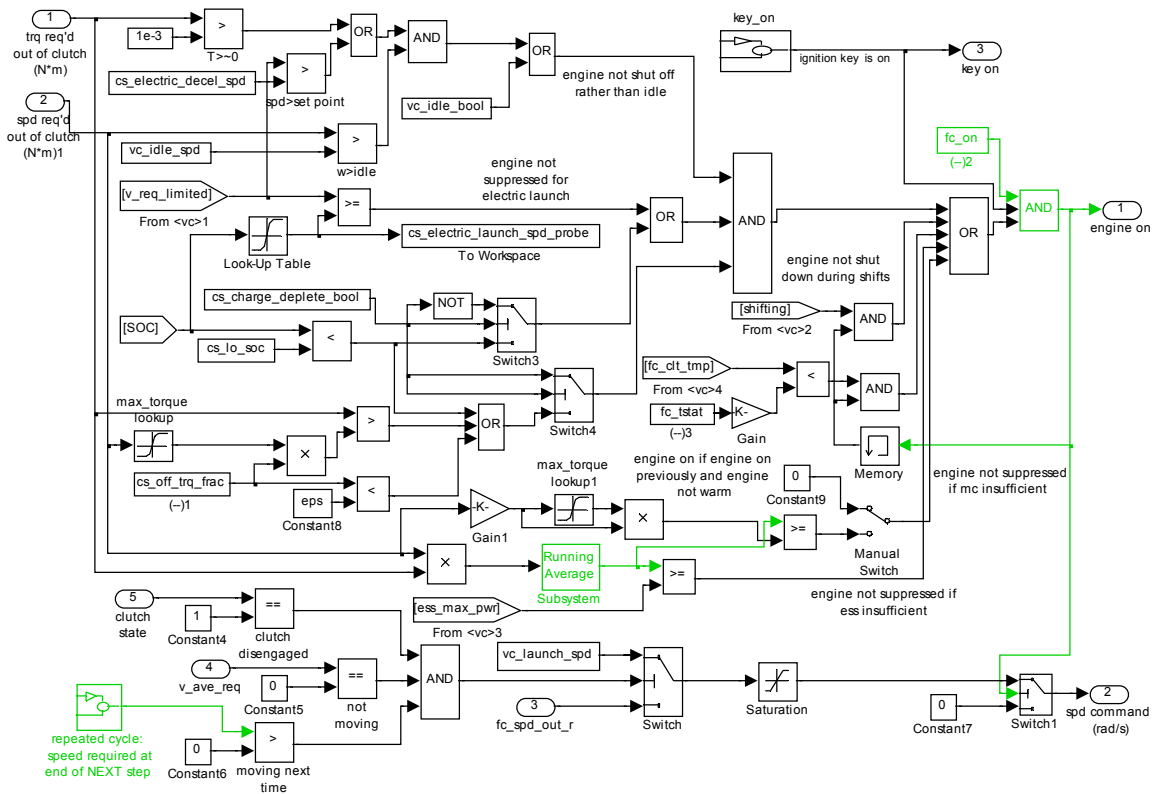


Figure 3-28: Engine on/off control block diagram [27]

- “If the speed required is less than the electric launch speed, `cs_electric_launch_spd`, the engine could turn off.”
- “If the SOC is higher than its low limit, the engine could turn off. If both the requested speeds are less than the launch speed and the SOC is higher than the low limit, the engine will turn off.”
- “If the torque required is less than a cutoff torque, `cs_off_trq_frac` fraction of the maximum torque, the engine could turn off. If both the requested torques is lower than this cutoff and the SOC is higher than the lower limit, the engine will turn off.”

The main aspect that determines the control strategy performance is the values of these six variables and their convenience with the power distribution between EM and ICE and the energy capacity of the battery. The base values of ADVISOR [27] and the values were used as a base of genetic algorithm optimization study done by Lincun Fang et. al. [19]. These values are actually determined according to some basic specifications and parameters of power components. The low SOC and high SOC values are defined to satisfy the minimum discharge/charge resistance and an example graph is given in Figure 3-29.

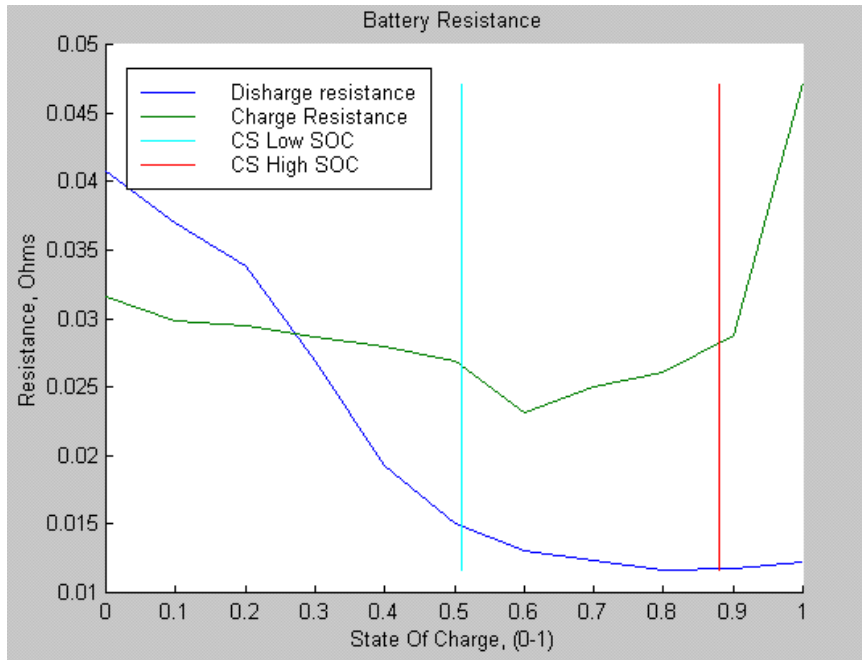


Figure 3-29: Battery resistance vs. SOC [27]

The minimum torque fraction that defines the minimum level that the engine should operate when lower torque demands are present and engine off torque limit which defines the limit below which torque demands engine will not operate, are defined according to the efficiency maps for which an example is given in Figure 3-30.

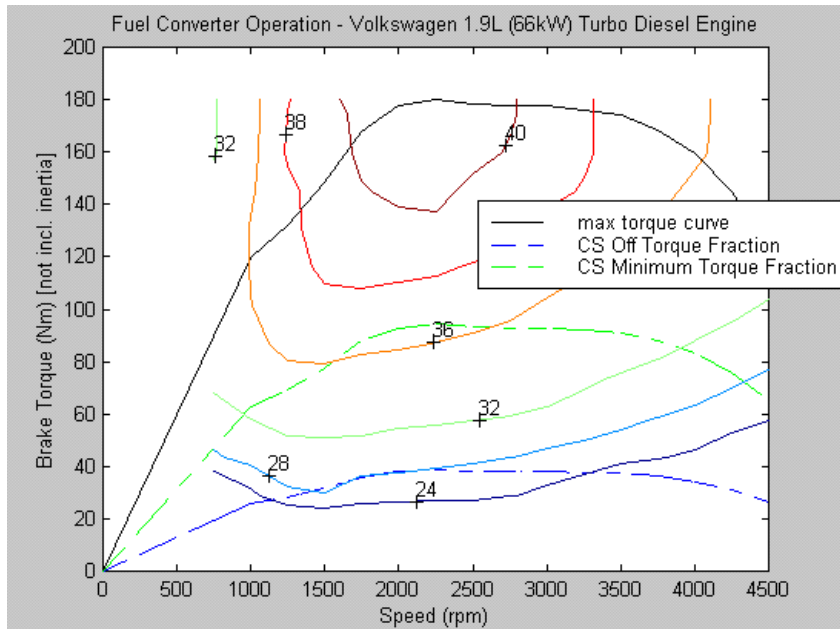


Figure 3-30: ICE Efficiency map and cs\_off\_trq\_frac and cs\_min\_trq\_frac values

The initial values of the six control parameters are assigned as given in Table 3-10.

Table 3-10: Base values of control strategy parameters

cs_hi_soc	0.7
cs_lo_soc	0.6
cs_electric_launch_spd [m/s]	0
cs_off_trq_frac	0
cs_min_trq_frac	0.4
cs_charge_trq [Nm]	15

These initial values for the six control variables are used as base values of the optimization procedure, since these parameters are used simultaneously as optimization variables together with the power ratings of the hybrid vehicles. This process will be explained in detail in the optimization process section.

### 3.4.2 Series Hybrid Control Strategy Parameters and Rules

Although most of the works on hybrid technology, especially regarding control strategies, are devoted to the parallel structure, series structure has some alternatives for the control strategy application environment. Since the system structure is simpler, a control system with a low complexity will give considerable reduction in fuel economy and emissions while satisfying the performance demands.

Similar to parallel structure and all hybrid vehicles, in series configuration too overseeing the battery life in terms of its SOC and trying to keep ICE running in its optimal region are the most basic criteria while designing the control algorithm. Starting from this point, as the simplest power split strategy is the on/off control for series power train. In the literature there are studies starting from improvement of on-off control strategy in some aspects like adding forecasting the road characteristics [46] going up to real time optimization by dynamic programming [47], instead of directly using a rule based strategy with a pre-implemented static rules. For example, Jalil [48] gives a rule based control strategy as an improvement over on-off control with addition of extra rules and defining new working alternatives for ICE and battery.

The control strategy used in the study is similar to the one suggested by Jalil. The control strategy determines the torque and speed that the engine should operate while examining the battery electric motor and engine itself conditions and states. This strategy is used to optimize the fuel consumption and also emission values. The block diagram is given in Figure 3-31.

Adjustment of the engine is made by on and off states and power required from the engine. The engine power is adjusted according to the demand from traction motor including the losses in the generator.

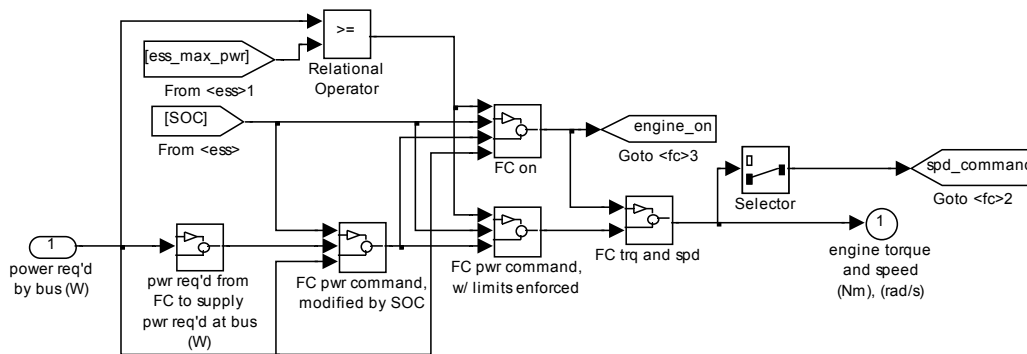


Figure 3-31: Series configuration controller block diagram

The algorithm which gives some flexibility for the engine is given as [27]:

- “The engine may be turned off if the SOC becomes too high.”
- “The engine may be turned on again if the power required by the bus becomes high enough.”
- “The engine may be turned on again if the SOC becomes too low.”
- “The engine output power may be adjusted by SOC, in order to bring the SOC back to the center of its operating range.”
- “The engine output power may be kept above some minimum value.”
- “The engine output power may be kept below some maximum value (which is enforced unless the SOC gets too low).”
- “The engine output power may be allowed to change no faster than a prescribed rate.”

These conditions are all implemented to the system by using 11 different variables defined. These parameters are given in Table 3-11.

Table 3-11: Series control strategy parameters [27]

Variable	Description
cs_hi_soc	highest desired battery state of charge
cs_lo_soc	lowest desired battery state of charge
cs_charge_pwr	$cs\_charge\_pwr * fc\_spd\_scale * fc\_trq\_scale * ((cs\_soc\_hi + cs\_soc\_lo) / 2 - SOC)$ is the SOC-stabilizing adjustment made to the bus power requirement
cs_fc_init_state	1=>fuel converter (FC) is initially on; 0=>FC initially off
cs_max_pwr	$cs\_max\_pwr * fc\_spd\_scale * fc\_trq\_scale$ is the maximum power commanded of the fuel converter unless $SOC < cs\_lo\_soc$
cs_min_pwr	$cs\_min\_pwr * fc\_spd\_scale * fc\_trq\_scale$ is the minimum power commanded of the fuel converter
cs_max_pwr_fall_rate	$cs\_max\_pwr\_fall\_rate * fc\_spd\_scale * fc\_trq\_scale$ is the fastest the fuel converter power command can decrease (this number < 0)
cs_max_pwr_rise_rate	$cs\_max\_pw\_rise\_rate * fc\_spd\_scale * fc\_trq\_scale$ is the fastest the fuel converter power command can increase
cs_min_off_time	the shortest allowed duration of a FC-off period; after this time has passed, the FC may restart if high enough powers are required by the bus
cs_pwr	$cs\_pwr * fc\_spd\_scale * fc\_trq\_scale$ is the vector of FC powers that define the locus of best efficiency points throughout the genset map
cs_spd	$cs\_spd * fc\_spd\_scale$ is the vector of FC speeds in locus of best efficiency points, indexed by $cs\_pwr * fc\_spd\_scale * fc\_trq\_scale$

Engine power required is computed by two main cases as estimating the ICE output power converted to electrical power through the generator which meets with the one needed from electric power system for the propulsion and accessory loads together with the addition of a SOC-dependent correction factor.

$$ChargePower = cs\_charge\_pwr * fc\_trq\_scale * ((cs\_hi\_soc + cs\_lo\_soc) / 2 - SOC) \quad (3.55)$$

$$ChargePower = Battery\ charging\ power [W]$$

This equation implies that SOC value is tried to bring the mid of the predefined limits when it is lower than that value. Instead of using a direct pass between on and off states; there is a transition state

which is determined according to previous state of the engine and also according to power demand from the engine and SOC limits. The overall algorithm is illustrated in Figure 3-32 [27]. If the ICE was lastly on and SOC is lower than the upper limit, the engine will stay on regardless of power command. However, if the ICE was previously off, and “(the average of the last 5 s of fuel converter power command) > (1.2\*cs\_min\_pwr\*fc\_trq\_scale\*fc\_spd\_scale)”, AND “(the time since the ICE was last on) > cs\_min\_off\_time”, the ICE will start. This algorithm is not shown in the Figure 3-23. Finally, regardless of all other conditions, if the power required by the electric motor is greater than the battery capability, the ICE will turn/stay on.

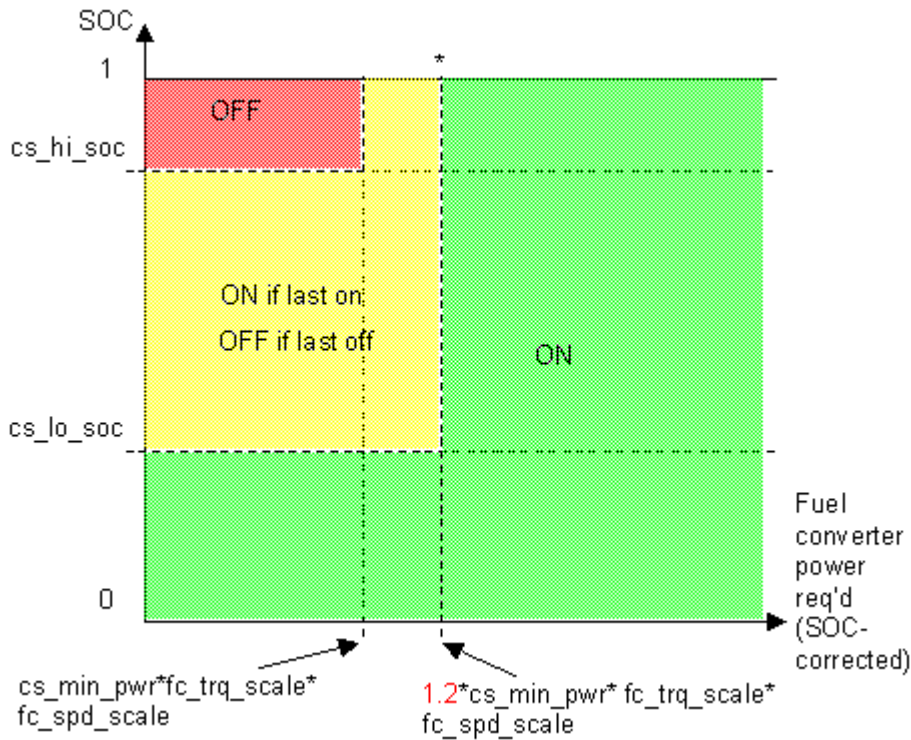


Figure 3-32: Series control strategy [27]

As an alternative to power follower method explained above, the same structure could be used also for the simpler on/off control strategy. Simply changing the control strategy parameters could convert the whole controller. It could be satisfied basically by setting cs\_max\_pwr and cs\_min\_pwr equaling to each other and half of the maximum power of the scaled internal combustion engine which provide only one power supply level instead of a region. Then cs\_min\_off\_time is set to infinity in order to set the generator-engine such that it won't come until SOC becomes lower than the cs\_lo\_soc. Moreover cs\_charge\_pwr value is set to zero which makes the engine-generator power zero until SOC gets lower than the defined minimum value. Finally, engine-generator couple power maximum rise and fall rates are set to zero to get a constant power when the engine is turned on.

For power follower strategy, some of the control strategy parameters are also used as optimization variables similar to parallel configuration. This procedure and the values with initials and lower-upper bounds are given in detail in the optimization chapter.

## CHAPTER 4

### GUI DEVELOPMENT

#### 4.1 INTRODUCTION

Design step of a HEV requires lots of additional variables should be included into the data structure. Also change in one variable necessitates modifying others with different functions. When it comes to the sizing and optimization procedures which need simultaneous run of variables, these cross relations and a large number of parameters make it hard, if not impossible, to handle the process using only written texts and workspaces.

Graphical user interface aims to provide a compact and flexible way to interact users with the simulation tool by using images instead of dealing with rows of texts and bulk of data. By using push buttons, textboxes, radio buttons and selection check boxes provided by MATLAB GUIDE, a user friendly HEV and its simulation parameters, and configuration selection platform is provided.

In literature there are various simulation platforms with GUI. Some of them only include component type modeling which is simply close to MATLAB Simulink platform but with specific pre-modeled structures like battery and engine. Most popular and detailed GUI is generated by ADVISOR simulation platform. It is a highly flexible platform with lots of vehicle and its components. Also it gives chance for performance test procedures, parametric studies, test procedures and driving cycles and also optimization procedure. However, while provision of lots of choices together gives flexibility, the system gets too complex for users focusing on some specific cases and those who do not have sufficient data required and just aim to get a preliminary design.

#### 4.2 INTERFACE DEVELOPMENT

Interface development procedure focuses on that user who can define a HEV with very basic steps starting from vehicle type, then performance criteria, and lastly to optimization parameters. It consists of three consecutive steps divided to separate base decisions like vehicle type and numerical values such as acceleration demand and thesis focus: optimization procedure and a result screen where battery SOC, fuel consumption and emission values during the simulation over a drive cycle are shown. Every step has options to save and/or load which give opportunity to save the data and selections to a user defined file over dialog screen and call the previously saved ones in the same way. Also optimization screen and parameter screen have back buttons when the parameters/selections in the previous screen is needed to be modified. The returned screen by using the back button has the last state that user selected. Moreover in parameters screen and optimization screen the edit boxes used for modification of the values checks the new defined value whether it is a number or not and if not it shows a modal warning dialog box.

##### 4.2.1 Type Selection Screen

First step includes 4 basic selections: 1.Vehicle type, 2.Engine type, 3.Driving area, 4.Application emphasis. Figure 4-1 shows type selection screen. There are six different vehicle type selection named as saloon “car”, “suv”, “light truck”, “heavy truck”, “bus”, and “others”. It is followed by fuel converter type selection that consists of two internal combustion engine types: “compression ignition” and “spark ignition”, mostly known as diesel and gasoline engines and electric motor for all-electric vehicle. The third and the last parameter that specify the base vehicle is the drivetrain selection. There are 4 alternatives of selection: “parallel”, “series”, “pure electric”, and “conventional”. In the study only parallel and series configurations are used and pure electric vehicle and conventional drivetrain

optimization is not included since their sizing procedures are straight forward when compared to hybrid ones.

The next block is constructed for driving cycle selection from standard cycles according to driving are “urban” or “highway” or “mixed”. Urban and highway cycles are mixed in standard test procedures such as FTP-75 [49] or NEDC [50] and according to radio button selection pop-up menu content changes.

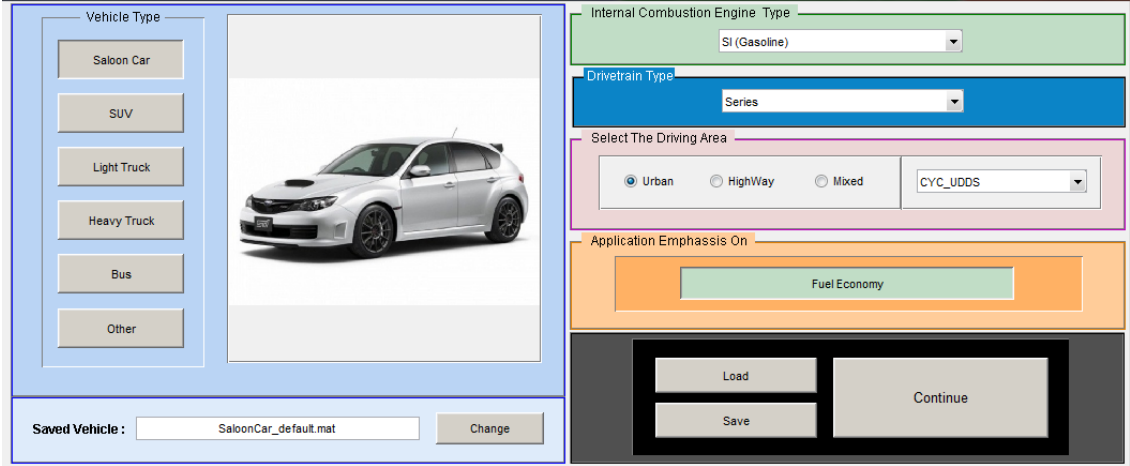


Figure 4-1: Type Selection Screen GUI

After all selections are made on the screen, pushing the “continue” button the next step for parameter and performance sizing is started. If at least one selection is missed, the program will show a message to make all the selections and unless all types are defined continue, the button will not function.

#### 4.2.2 Parameters Screen

The second step for HEV configuration is the Parameters Screen. The second screen is designed to take entries for performance demands and give the pre-selected vehicle parameters in a well-organized form of edit boxes providing easy entry and modification. In Figure 4.2, the parameters screen is given. The edit boxes group on the left shows the vehicle parameters: vehicle mass, load fraction, wheelbase, center of gravity position, frontal area, drag coefficient, differential ratio, gear ratios, tire info (it is not editable), tire radius, and rolling resistance coefficients. These values are loaded when the continue button on the type selection screen is pressed.

The screenshot displays a software interface for configuring vehicle parameters and performance demands. It is divided into two main vertical panels.

**Vehicle Parameters (Left Panel):**

- Vehicle Mass [kg]: 1259
- Vehicle Cargo Mass [kg]: 136
- Wheelbase [m]: 2.6
- CenterofGravity Height [m]: 0.5
- Frontal Area [m<sup>2</sup>]: 2
- Drag Coeff.: 0.335
- Differential Ratio: 1
- Gear Ratios:
 

1st	5.00491
2nd	5.00491
3rd	
4th	
5th	
- Wheel/Tire Info: WH\_SMCAR
- Tire Radius [m]: 0.282
- 1st Rolling Resistance Coef.: 0.009
- 2nd Rolling Resistance Coef.: 0

**Acceleration & Gradeability Demand (Right Panel):**

**Vehicle Performance**

- Speed:** Max. Speed  $\geq$  [ ] kph
- Desired Acceleration:**
  - 0 - 100 km/h time  $\leq$  [ ] s
  - Max. Acceleration  $\geq$  [ 4 ] m/s<sup>2</sup>
- Max. Grade (@Cruising):**
  - Grade  $\geq$  [ ] %
  - @ Speed  $\geq$  [ ] kph
- Max. Grade (@Low Speed):**
  - Max. Grade  $\geq$  [ ] %

**Optimization (Bottom Right):**

- Optimization (Blue button)
- Back (Blue button)
- Run (Green button)
- Load (Grey button)
- Save (Grey button)

Figure 4-2: Parameters Screen GUI

The “acceleration and gradeability demand” group on the right side allows the user to enter maximum speed of the vehicle in kph, 0-100 kph and max acceleration values, and electric only mode gradeability values in the available edit boxes. For desired acceleration, 0-100 kph or maximum acceleration value could be selected through checkbox selection placed left of each value. They are disabled as default and could not be edited unless the checkbox in front is ticked. The values set by the user in acceleration and gradeability demand block is going to be used in initial sizing procedure which determines the starting power and torque values of electric motor, engine, and battery sizing. This procedure is given in detail in section 3.3. Power component sizing.

After all the parameters are entered and performance demands are defined as acceleration and gradeability, “run” button is pressed to decide initial power sizing of the HEV. It is a simulation

process in Simulink platform on a separate simpler vehicle model. The optimization process could not be started before initial sizing operation

### 4.2.3 Optimization Screen

The focus of the current study is the optimization procedure which is initiated on the optimization screen. The procedure will be given in detail in chapter 5, but a brief explanation about the process as handled in GUI side and the relevant button and boxes are going to be given in this section. There are two separate screens for series and parallel configurations. These are shown in Figure 4-3 and Figure 4-4.

The optimization procedure needs three sets of variables and equations, and their values. The first set contains the design parameters. The design parameters are given in the first block with their initial values, lower bounds and upper bounds. Parameter values are changed during the optimization process between upper and lower bounds to get the minimum of the objective function. Here on the GUI, basic design parameters are determined as electric motor power, engine power, and battery voltage. Also electric motor torque and engine torque could also be modified instead of power because they are not independent. In addition to these three parameters, control parameters are used as optimization variables for both of the configurations. While the electric motor and engine power and battery sizing are active as default, other parameters could be enabled by ticking the checkboxes in front.



Figure 4-3: Optimization Screen GUI for series configuration

Second step of the procedure includes cost function variables: fuel consumption, NO<sub>x</sub>, CO, and HC emission values and their weighting factors. These four variables could be included in the cost function by checking the related boxes. After modifying the values by pushing the “Update Objective Function” button the function that will be minimized is printed on the text box.

The last step is designed to change the given constraints for the minimization process. The performance criteria already defined in the previous GUI screen are given as default values. Again the constraints are implemented as gradeability and acceleration performance. The gradeability performance is evaluated as maximum grade at a certain speed with certain duration, while acceleration is directly needed to be entered as the maximum acceleration desired.

The overall flow diagram of the optimization screen and process is given in the Figure 4-6 and Figure 4-7. The whole process starting from step1 figure to optimization ends is given in Appendix A.



Figure 4-4: Optimization Screen GUI for parallel configuration

#### 4.2.4 Results Screen

The last step of the optimization process is showing the optimization results on a appropriate platform. The result screen is designed to show initial and final values of cost function value, selected design parameters such as engine or electric motor power sizes and optimization parameters such as fuel consumption and also changes of the variables during the optimization process. The designed GUI is given in Figure 4-5.

The left column is prepared to show all changes in design and optimization parameters during the optimization process in a graphical manner. It makes easier to follow the process and decide whether the optimization process is effective and/or how initial sizing process performed. The resulting plots observed in case studies are given Appendix B.

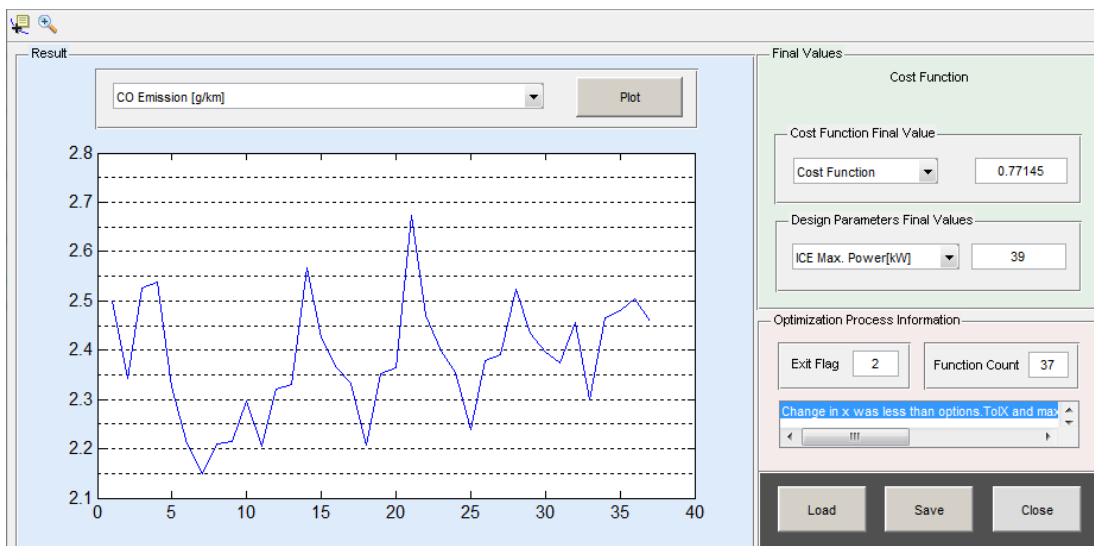


Figure 4-5: Results Screen GUI for parallel configuration

The right side column includes final values of design and optimization variables such as fuel consumption, emission values and internal combustion engine, electric motor and battery power sizing and also controls strategy parameters in order to provide easy to obtain platform for final values of the optimization. Moreover “fmincon” function exit flag number with its brief information is provided on the screen with total number of function count for the optimization process.

The result screen becomes enabled automatically when the optimization process is over and it is directly opened when the button on the optimization screen is pressed. In addition to that, similar to other screens, all save and load options are also available for result screen also.

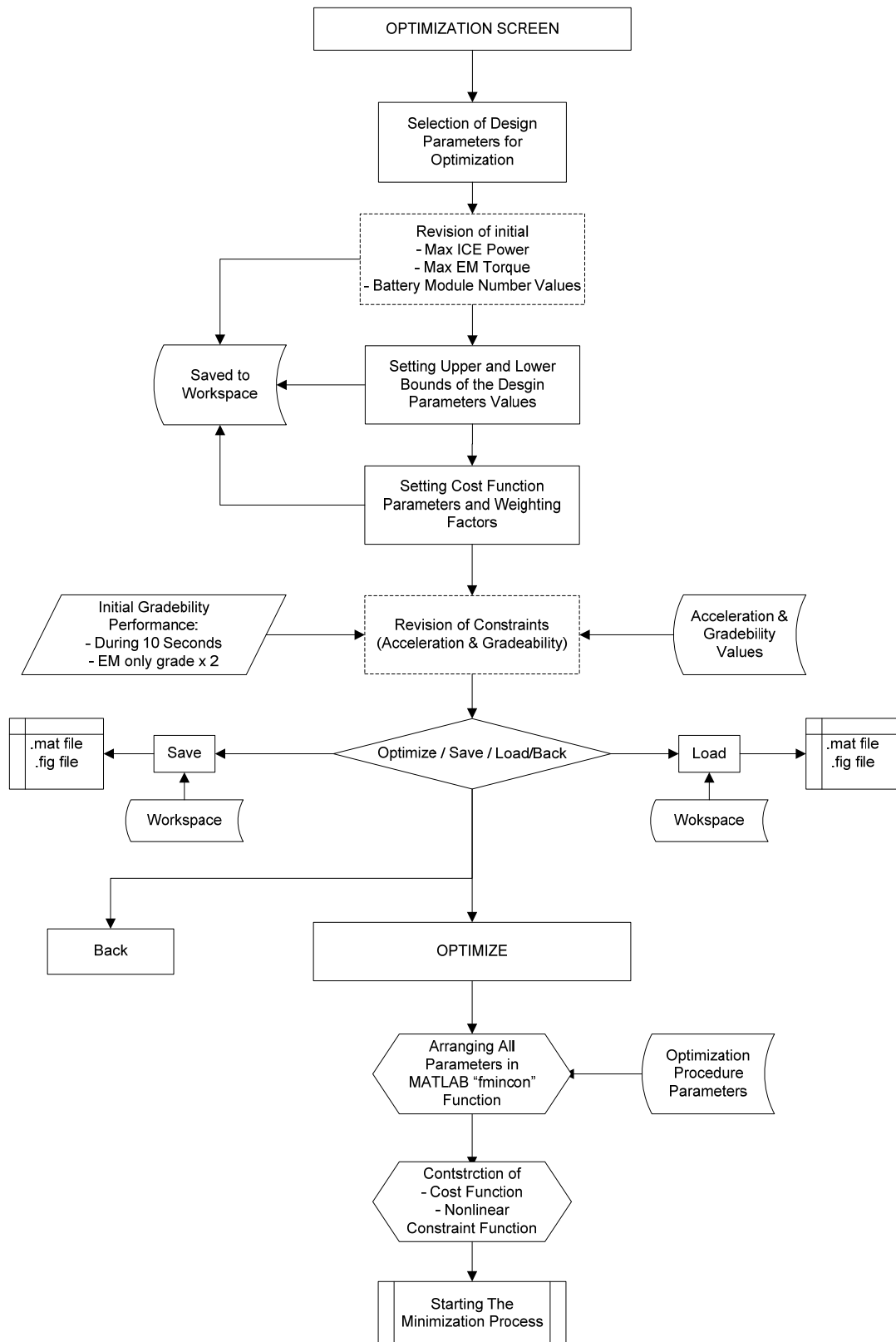


Figure 4-6: Flow diagram of the optimization process (a)

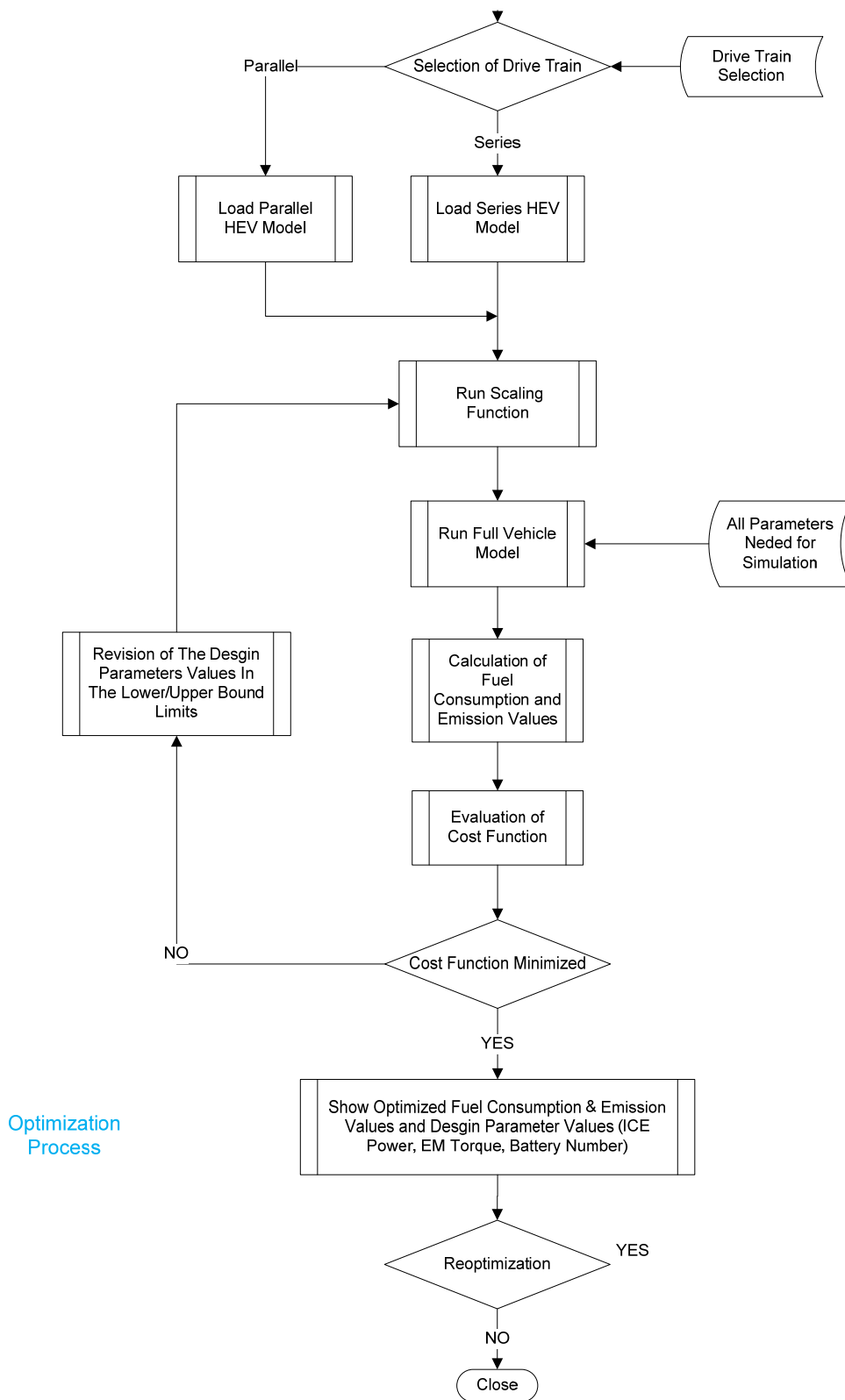


Figure 4-7: Flow diagram of the optimization process (b)

## CHAPTER 5

### OPTIMIZATION PROCESS

#### 5.1 INTRODUCTION

Designing a hybrid vehicle is certainly more complex than the process of specifying power rating of a single power source of a conventional vehicle and determining the gear box and final drive ratios according to performance demands. It has the potential to satisfy varying requirements in many different configurations and parameter sets. Since hybrid technology is widely recognized as a promising technology for the next generation vehicles which offer low emission and fuel consumption values, optimization of the design of a HEV is one of the key elements in the design process.

Hybrid electric vehicles are complex electromechanical systems involving hundreds of design parameters. A successful HEV design requires optimal sizing of its key mechanical and electrical components. In addition, for more HEV efficiency, optimal management of the energy flow (control strategy) is required. Therefore, in the design process of a HEV, there is a large variety of design variable choices, including HEV configuration, key mechanical and electrical components sizes, and control parameters that must be taken into account.

HEVs have multiple design objectives which are usually conflicting as well as a large number of design variables. Further, many design constraints must also be fulfilled simultaneously. Moreover, the sizes of powertrain components and control system parameters are coupled and have simultaneous impacts on the performance of the vehicle. The effects of these design parameters on the objectives are non-monotonic. Therefore, the optimization of a HEV can be formulated as a multi-objective constrained nonlinear optimization problem.

There are two different approaches for the optimization process categorized as gradient or derivative base approach and derivative free optimization methods. The main disadvantage of a non-derivative base optimization is the requirement of long time due to huge amount of data matrices have to be computed. Considering the time issue, gradient base optimization methodology is implemented through MATLAB software. In the following sections, starting from the method and working principles of the process are given in detail, and then those variables are selected for the optimization are listed with reasoning and effects, and finally the related case studies are carried out in order to show the performance of the process as a comparison of related examples in literature. Two types of drivetrain alternatives are also compared with each other with respect to their performances with respect to fuel consumption and emission values as another case study.

#### 5.2 METHOD

Constrained minimization is the problem of finding a vector “x” that is a local minimum to a scalar function  $f(x)$  subject to constraints on the allowable x. Here the scalar function that is defined as the cost function consist of “fuel consumption”, “CO”, “HC” and “NO<sub>x</sub>” emission values with their weighting factors defined by the user. And the “x” variables are defined as basically power component sizes in terms of engine and electric motor power ratings, and battery capacity scale. In addition to that control strategy parameters are also included into optimization procedure since they have substantial effects on fuel economy and emission values as illustrated by Burch [51].

The simulation and evaluation process of optimum HEV fuel and emission values needs a tool that could handle nonlinearities for performance constraints and that could handle medium-large scale data. For those purposes, MATLAB based “fmincon” function is used through the optimization process. This built-in function calculates minimum of the desired cost function with initial values,

lower bounds, and upper bounds of design variables defined in order as vectors “x”, “lb” and “ub”. These values are specified or obtained by using the GUI and initial sizing process as explained in the previous sections.

The syntax representation of the fmincon function is [52]

$$fmincon(@objective\_fun, x0, A, b, Aeq, beq, lb, ub, @objective\_constraint, options) \quad (5.1)$$

where

$$\min_x(objective\_fun(x)) \text{ such that } \begin{cases} c(x) \leq 0 \\ ceq(x) \leq 0 \\ A \cdot x \leq b \\ Aeq \cdot x = beq \\ lb \leq x \leq ub \end{cases} \quad (5.2)$$

A, b, Aeq, and beq are matrices and not used in the process since whole model is formed as Simulink diagrams and works with data input and outputs.

The theory behind the definition of first-order optimality measure for constrained problems is defined as Lagrangian function.

$$L(x, \lambda) = f(x) + \sum \lambda_{g,i} g_i(x) + \sum \lambda_{h,i} h_i(x) \quad (5.3)$$

where

$$\nabla_x L(x, \lambda) = 0 \quad (5.4)$$

$$\lambda_{g,i} \geq 0 \quad (5.5)$$

There are three different basic algorithms used in fmincon tool [52]. Since the system defined with nonlinear inequality constraints, default “trust region reflective” is not used as it only accepts equality constraints. The “interior point” algorithm is used. The algorithm is suggested for initial step. However for smaller sized problems the third algorithm “active set” could also be used for faster minimization process.

The cost\_function = objective\_fun(x) is where the simulation is performed according to selected drivetrain configuration and drive cycle information. As an output, fuel consumption emission values are handled and written in a cost function with their weighting factors defined in optimization screen GUI in normalized form and it equals the cost function which is the output value objective\_fun(x).

$$C = w_f * fuel + w_{NOx} * NO_x + w_{CO} * CO + w_{HC} * HC \quad (5.6)$$

where

$w_f$  = Fuel consumption weighting factor

$w_{CO}$  = CO emission weighting factor

$w_{NOx}$  = NOx emission weighting factor

$w_{HC}$  = HC emission weighting factor

The functions and variables defined for fmincon function are given in Table 5-1. They are explained in the section 5.3 in detail.

Table 5-1: Fmincon function parameters

<i>objective_fun</i>	$w_f * fuel + w_{NOx} * NO_x + w_{CO} * CO + w_{HC} * HC$
<i>objective_constraint</i>	6.5 % Gradeability @ 90 kph, 1200 s Maximum acceleration rate > 4 m/s <sup>2</sup> 0 – 100 kph acceleration in s Maximum speed > 140 kph
<i>x0</i>	Initially sized values of electric motor power, battery power, engine power Default control parameters
<i>lb, ub</i>	Given section 5.3
<i>A, b, Aeq, beq</i>	Not used

Since the emission values and fuel consumption values are in different units and different order of magnitude, a simple normalization procedure is implemented. Normalization is made directly by division of the output values of fuel consumption (l/100 km) and emission (g/km) values by the average values taken from EPA [53] and US Department of Energy [54] according to vehicle type. Emission values are grouped for light duty trucks, SUVs and passenger cars and secondly for heavy trucks and buses. Also for fuel consumption similar grouping is also made. Then the normalization factors are defined as

$$\begin{aligned} f_{fuel} &= 7.85 \text{ [l/100 km]} \\ f_{CO} &= 6.52 \text{ [g/km]} \\ f_{NOx} &= 0.186 \text{ [g/km]} \\ f_{HC} &= 0.186 \text{ [g/km]} \end{aligned} \quad (5.7)$$

Where

- $f_{fuel}$  = Fuel usage normalization factor
- $f_{CO}$  = CO emission normalization factor
- $f_{NOx}$  = NOx emission normalization factor
- $f_{HC}$  = HC emission normalization factor

As the fmincon changes the variables within the lower and upper bounds, fuel consumption and emission change due working region changes, electric only propulsion time changes, regenerative braking performance changes, etc. Especially power rating values change the overall mass of the vehicle which effects considerably the fuel consumption while also affects emission values due speed/torque value changes. In order to include these mass change effects into system, in every iteration a new mass calculation is run. After new variable values are set by fmincon, “recomputed\_mass” function is run just before the drive cycle is loaded for the new simulation. Mass calculation is made for engine block, electric motor, battery total mass, generator (for series), exhaust system, transmission and wheel/axle system [27]. The mass scaling functions are formed in terms of torque and speed scaling functions.

$$1) \quad f_{c\_mass\_scale} = f_{c\_trq\_scale} * f_{c\_spd\_scale} * (f_{c\_base\_mass} + f_{c\_acc\_mass}) + f_{c\_fuel\_mass} \quad (5.8)$$

where

$$fc\_base\_mass = 1.8 * fc\_max\_pwr [55] \quad (5.9)$$

$$2) \quad mc\_mass\_scale = mc\_trq\_scale * mc\_spd\_scale * mc\_mass \quad (5.10)$$

$$3) \quad gc\_mass\_scale = gc\_trq\_scale * gc\_spd\_scale * gc\_mass \quad (5.11)$$

where

$$gc\_mass = gc\_max\_pwr / 0.8663 [27] \quad (5.12)$$

$$4) \quad ess\_mass\_scale = ess\_module\_num * ess\_cap\_scale * ess\_module\_mass \quad (5.13)$$

and also the exhaust aftertreatment system mass changes related to fuel converter maximum power rating [27]

$$5) \quad ex\_mass\_scale = fc\_pwr\_scale * ex\_mass \quad (5.14)$$

### 5.3 OPTIMIZATION VARIABLES AND CONSTRAINTS

The conventional vehicles, the lower fuel consumption the lower the exhaust emission values, since emission value is correlated with fuel consumed. So the fuel economy and emission are semi-dependent for the HEV case. For SI and CI engines low emission regions are shown in Figure 5-1 and Figure 5-2.

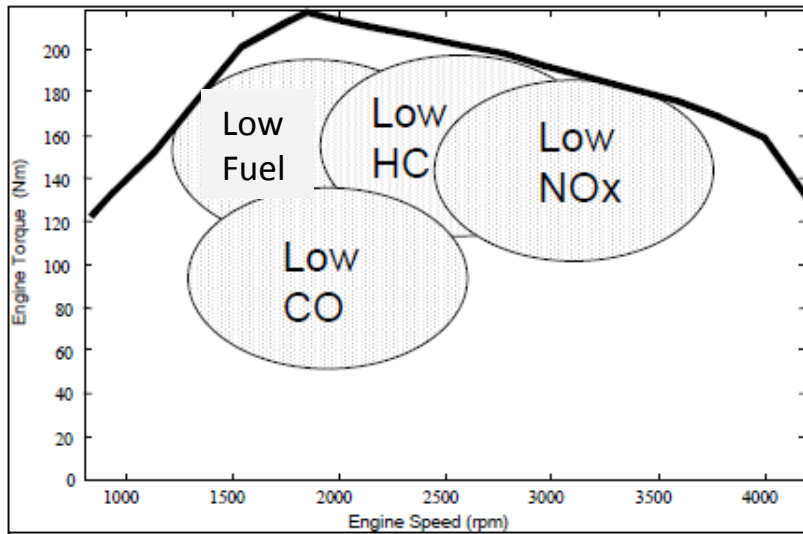


Figure 5-1: Fuel economy and emission tradeoffs for a SI engine [43]

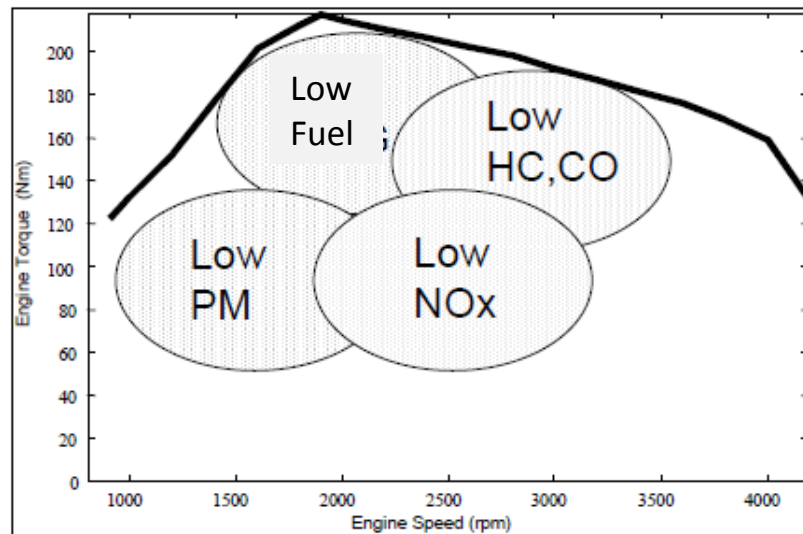


Figure 5-2: Fuel economy and emission tradeoffs for a CI engine [43]

Considering that different cities and different users mean different levels of the fuel economy and emissions, a set of trade-off solutions that represent a wide range of each issue (the fuel economy, and the HC, CO, NO<sub>x</sub> emissions) is useful for the designers, in that it provides a set of optimal alternatives. PM emissions are not included into the cost function.

While calculating the fuel consumption value over a drivecycle, HEV has an initial SOC value that supplies energy to electric system during the simulation and only constraint for SOC value is the lower limit checked by the controller. By definition, fuel economy is a measure of fuel consumption over a drive cycle with balanced SOC [56]. In order to eliminate the influence of the energy supplied for vehicle propulsion through electrical system on fuel consumption, a procedure is carried just before the optimization process starts which adjust the initial SOC such that final value of SOC will be same with the initial one with a tolerance of 0.5 % [57]. So the entire output energy for the cycle is sourced from engine. It is only run early in the optimization process and defines the initial SOC for every cycle in the optimization as estimation. In order reduce the optimization time, corrected SOC value for initially sized vehicle is used as initial SOC in every step of the optimization as an approximation.

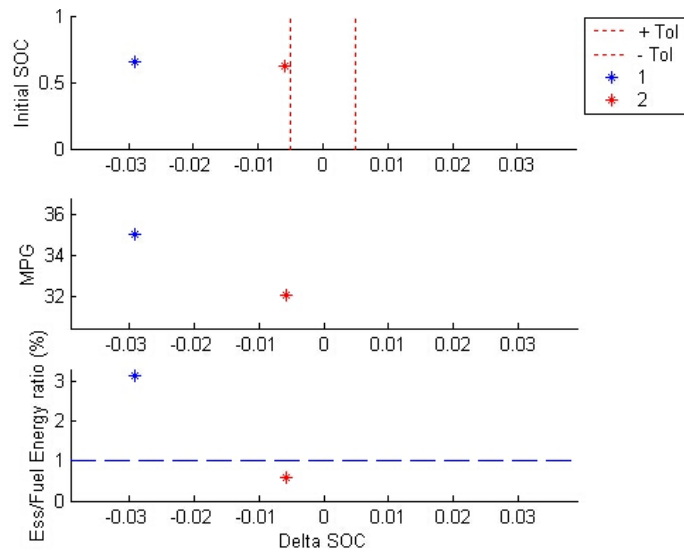


Figure 5-3: SOC correction procedure graphical representation.

It is obvious that sizes of the power components have substantial effects on fuel economy and emissions. The first group of optimization variables and the energy management system parameters also affect results and they become the second group of optimization variables. The third group is optional and only includes final drive ratio which directly affects the maximum speed of the vehicle and acceleration and gradeability performance of the vehicle. For the parallel and series drivetrains, although the first group of variables and final drive ratio as an optimization variable are the same (power components), control parameters are different since totally different energy management techniques and algorithms are used for these two configurations.

The optimization variables for parallel and series configurations are given in Table 5-2 and Table 5-3. For series configuration there are some other control parameters that could be included in the optimization process.

Table 5-2: Parallel configuration optimization variables

	Variable Name	Description
<b>POWER</b>	fc_trq_scale	Maximum Engine Power
	mc_trq_scale	Maximum Electric Motor Power
	ess_cap_scale	Battery Capacity
<b>CONTROL</b>	cs_electric_launch_spd [m/s]	Electric Only Launch Speed Limit
	cs_min_trq_frac	Engine Minimum Working Torque Ratio Compared to Max. Torque Curve
	cs_off_trq_frac	Engine Off Torque Ratio Compared to Max. Torque Curve
	cs_hi_soc	Highest SOC value of battery
	cs_lo_soc	Lowest SOC value of battery
<b>OTHER</b>	Fd_ratio	Final Drive Ratio

Table 5-3: Series configuration optimization variables

	Variable Name	Description
<b>POWER</b>	fc_trq_scale	Maximum Engine Power
	mc_trq_scale	Maximum Electric Motor Power
	ess_cap_scale	Battery Capacity
<b>CONTROL</b>	cs_min_pwr	Engine Min. operating power (when SOC > ess_lo_soc)
	cs_max_pwr	Engine Max. operating power (when SOC > ess_lo_soc)
	cs_charge_pwr	Charging power when SOC < mean(ess_hi_soc,ess_lo_soc)
	cs_hi_soc	Highest SOC value of battery
	cs_lo_soc	Lowest SOC value of battery
<b>OTHER</b>	fd_ratio	Final Drive Ratio

In order to define a complete nonlinear optimization, constraints should be well defined. The performance demands are directly taken from the data defined by the user over parameters screen GUI. However in order to get a comparative result, standard performance demands are defined taken from US Consortium for Automotive Research (USCAR) for PNGV effort [9] [58]. These performance requirements are as followings

- $t1 \leq 12$  s for 0–100 kph
- $t2 \leq 5.3$  s for 60–100 kph
- $t3 \leq 23.4$  s for 0–140 kph
- 0 to 140 kph acc.in s.  $\leq 23.4$  s
- The gradeability at 90 kph for 1200 s Grad  $\geq 6.5\%$
- Maximum speed:  $\geq 140$  kph
- Maximum acceleration:  $>0.5$  g
- Distance in 5 s:  $>42.7$ m

Moreover vehicle final velocity during the drive cycle is saved as an output and the difference between the drive cycle and simulation output value should be below 2.5 kph.

In order to implement this performance values as constraints to the optimization process and define them as in the format of inequality as

$$c \leq 0 \tag{5.15}$$

an acceleration test procedure and a grade test procedure is implemented to fmincon function as “optimization\_const.m”.

The acceleration test measures acceleration performance of the current vehicle in optimization function calculation. It works on the same model that the main routine runs but with a new drive

cycle. The drive cycle is defined as a step input of a 300 kph velocity for 100s duration. The 300 kph value is set as a higher value that a vehicle could achieve and it provides the vehicle components to work at their limits since the vehicle current velocity could not reach the desired speed at any time instant. By application of this cycle, vehicle will try to request as much power as it could supply through the drivetrain to the wheels. At the end of the cycle, acceleration times for different speed ratings, maximum acceleration and maximum vehicle velocity are calculated from the vehicle speed trace data.

Similarly, the grade test measures the gradeability of the vehicle with current parameters in optimization function calculation. Again the grade test runs in the same model but in this case vehicle is simulated with a constant speed which is defined by the user (e.g. 90 kph) at first. Then again drive cycle is modified as a step input with a value of the desired speed applied to the model. If at the end of the cycle the vehicle is within a specified tolerance of the speed goal it is said to be able to maintain this grade and speed indefinitely.

**5.4 CASE STUDIES AND RESULTS**

In order to find the optimum power ratings and capacities and also controller parameters that satisfy the minimum fuel consumption and/or emission and/or combination of these with weighting factors, a couple of studies are carried out with city and highway driving cycles for different vehicles and with different starting points of variables. The case studies are prepared for parallel and series configurations separately. The fuel consumption values are compared for two configurations and for each simulation, a separate run is made over ADVISOR platform by using the final values of variables as simulation inputs in order to get reference value as fuel consumption and emission value of conventional vehicle with the same type of internal combustion engine (SI or CI) with the same total propulsion power that the hybrid vehicle has.

For the simulations two vehicles are used in order to define the baseline vehicle assumptions. First one is 2000 Honda Insight and the other is 1994 Saturn SL1. Both have 5-speed gearbox. The vehicles are defined as “Vehicle 1” and “Vehicle 2” in Table 5-4 and will be referred to with these names in the following part of the section. The cargo mass value is used to adjust the total initial vehicle mass in order to get same values with the values defined in published papers and standards.

Table 5-4: Base vehicle parameters

Vehicle 1 (2000 Honda Insight)	
Vehicle Body Mass	520 kg
Wheel Radius	0.275 m
Rolling Resistance (1 <sup>st</sup> )	0.0054
Frontal Area	1.9 m <sup>2</sup>
Aerodynamic Drag Coefficient	0.25
Differential Ratio	3.28
Vehicle 2 (1994 Saturn SL1)	
Vehicle Body Mass	592 kg
Wheel Radius	0.282 m
Rolling Resistance (1 <sup>st</sup> )	0.009
Frontal Area	2.0 m <sup>2</sup>
Aerodynamic Drag Coefficient	0.335
Differential Ratio	3.28

As defined in chapter 3, for a small hybrid car, base internal combustion, electric motor, and battery pack are selected. Different from the parallel configuration, additionally a generator is added in the series configuration. The descriptions of the all base components are given in Table 5-5.

Table 5-5: Base power components specifications

	Vehicle 1	Vehicle 2
Engine	1991 Geo Metro 1.0L SI engine. Max. Power 41 kW @ 5700 rpm. Peak Torque 81 Nm @ 3477 rpm.	1991 Geo Metro 1.0L SI engine. Max. Power 41 kW @ 5700 rpm. Peak Torque 81 Nm @ 3477 rpm.
Electric Motor	Westinghouse, 75 kW, AC Induction motor Efficiency/loss data appropriate for a 320 V system	Westinghouse, 75 kW, AC Induction motor Efficiency/loss data appropriate for a 320 V system
Battery	Ovonic, 6V28Ah NiMH high power intermediate energy battery (50 Modules)	Ovonic, 12V45Ah NiMH intermediate energy battery (25 Modules)
Generator	-	32kW Permanent Magnet Motor with 90 % efficiency

For optimization simulation both in city and highway driving conditions, 3 different drive cycles are used. These are Japanese 10-15 mode driving cycle, Urban Dynamometer Driving Schedule (UDDS), which is equivalent to the first two bags of the Federal Test Procedure (FTP-75) and used for light duty vehicle testing and Highway Fuel Economy Test (HFET) driving cycle used by the US EPA for Corporate Average Fuel Economy (CAFE) certification of passenger vehicles in the US [59]. These driving cycles are given in Figure 5-4, Figure 5-5 , and Figure 5-6.

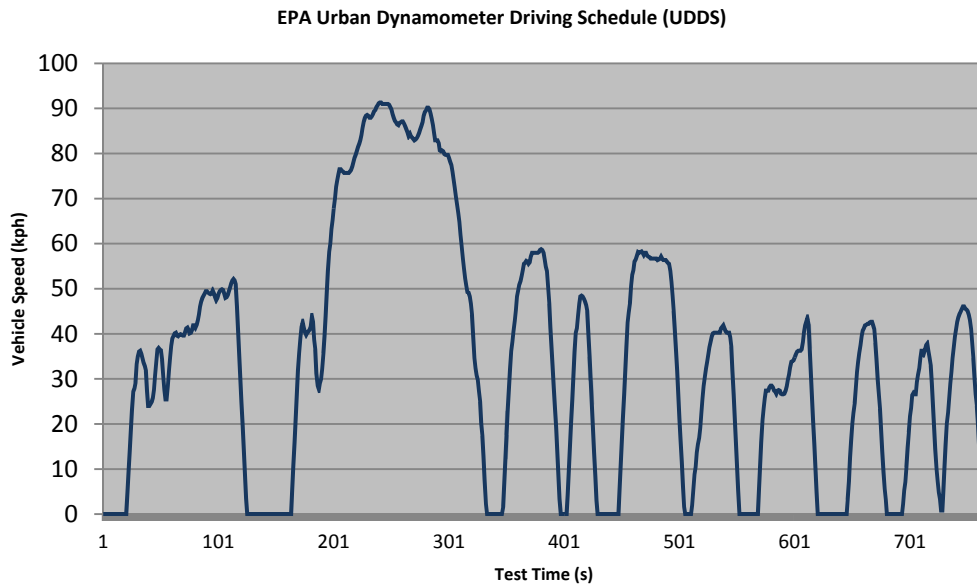


Figure 5-4: Speed profile of the UDDS drive cycle

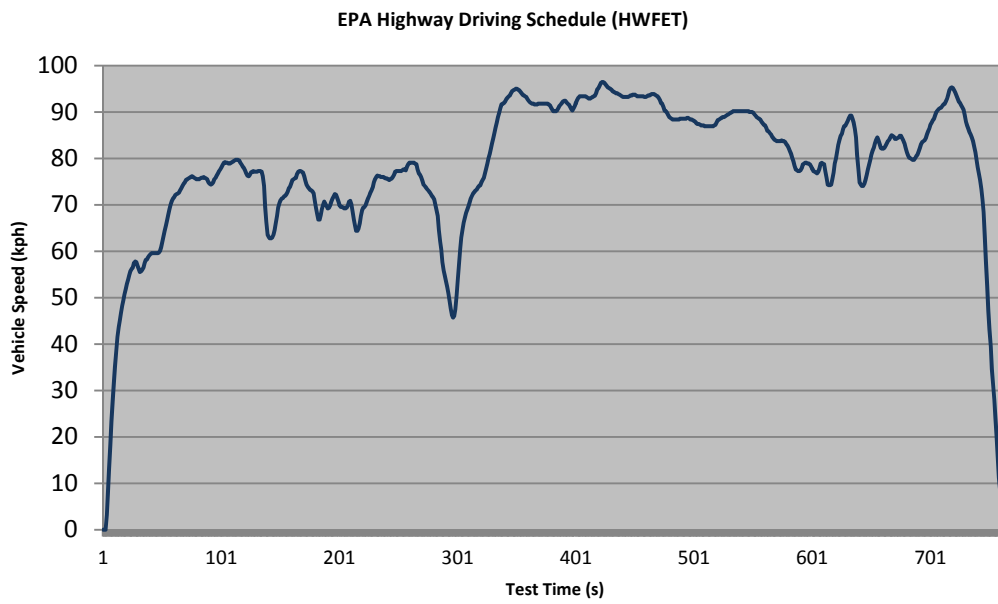


Figure 5-5: Speed profile of the HWFET drive cycle

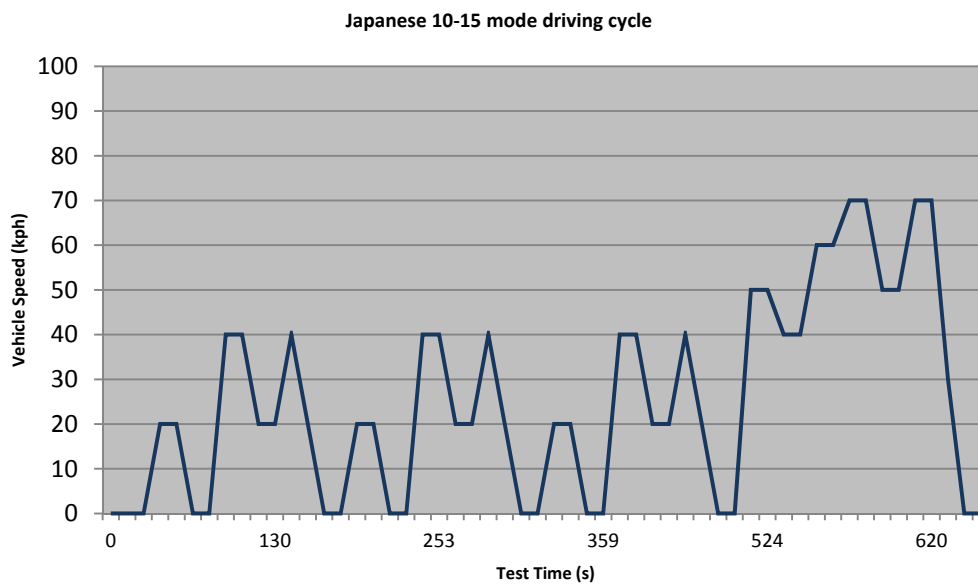


Figure 5-6: Speed profile of the J1015 drive cycle

By using these data, different combinations are made to prepare different case study alternatives and to validate the performance of the gradient base algorithm by using fmincon tool and to compare the study with some other previous works in literature. These studies are listed below in Tables 5-7 to 5-19 with brief descriptions and in the following sections each case is given in detail with reasoning and related result and comparison if applicable.

- Case 1 :

Table 5-6: Case 1 data

Vehicle Parameters	Optimization Parameters	Optimization Variables
Vehicle 1	Drive Cycle: UDDS	1) Engine Max. Power, Initial: 41 kW
Parallel Drivetrain	Initial Mass: 1366 kg	2) Motor Max. Power Initial: 75 kW
Cargo Mass: 320 kg	Lower Bounds: [20,20,0.2]	3) Battery Capacity Initial: 1
SI Engine	Upper Bounds: [80,80,3]	
	Cost Function: 1*Fuel Usage	

- Case 2 :

Table 5-7: Case 2 data

Vehicle Parameters	Optimization Parameters	Optimization Variables
Vehicle 1	Drive Cycle: UDDS	1) Engine Max. Power, Initial: 35 kW
Parallel Drivetrain	Initial Mass: 1366 kg	2) Motor Max. Power Initial: 56 kW
Cargo Mass: 320 kg	Lower Bounds: [20,20,0.2]	3) Battery Capacity Initial: 1
SI Engine	Upper Bounds: [80,80,3]	
	Cost Function: 1*Fuel Usage	

- Case 3 :

Table 5-8: Case 3 data

Vehicle Parameters	Optimization Parameters	Optimization Variables
Vehicle 1	Drive Cycle: UDDS	1) Engine Max. Power, Initial: 70 kW
Parallel Drivetrain	Initial Mass: 1549 kg	2) Motor Max. Power Initial: 75 kW
Cargo Mass: 320 kg	Lower Bounds: [20,20,0.2]	3) Battery Capacity Initial: 1.5
SI Engine	Upper Bounds: [80,80,3]	
	Cost Function: 1*Fuel Usage	

- Case 4 :

Table 5-9: Case 4 data

Vehicle Parameters	Optimization Parameters	Optimization Variables
Vehicle 2	Drive Cycle: UDDS	1) Engine Max. Power, Initial: 37 kW
Parallel Drivetrain	Initial Mass: 1204 kg	2) Motor Max. Power Initial: 45 kW
Cargo Mass: 136 kg	Lower Bounds: [20,20,0.2]	3) Battery Capacity Initial: 1
SI Engine	Upper Bounds: [80,80,3]	
	Cost Function: 1*Fuel Usage	

- Case 5 :

Table 5-10: Case 5 data

Vehicle Parameters	Optimization Parameters	Optimization Variables
Vehicle 2	Drive Cycle: UDDS	1) Engine Max. Power, Initial: 41 kW
Parallel Drivetrain	Initial Mass: 1255 kg	2) Motor Max. Power Initial: 75 kW
Cargo Mass: 136 kg	Lower Bounds: [20,20,0.2]	3) Battery Capacity Initial: 1
SI Engine	Upper Bounds: [80,80,3]	
	Cost Function: 1*Fuel Usage	

- Case 6 :

Table 5-11: Case 6 data

Vehicle Parameters	Optimization Parameters	Optimization Variables
Vehicle 2	Drive Cycle: HWFET	1) Engine Max. Power, Initial: 39 kW
Parallel Drivetrain	Initial Mass: 1310 kg	2) Motor Max. Power Initial: 49 kW
Cargo Mass: 230 kg	Lower Bounds: [20,20,0.2,0,0,0]	3) Battery Capacity Initial: 1
SI Engine	Upper Bounds: [80,80,3,9,1,1]	4) Electric Only Speed Initial: 6
	Cost Function: 1*Fuel Usage	5) Minimum Charge Torque Fraction Initial: 0.2
		6) Engine Off Torque Fraction Initial: 0.1

- Case 7 :

Table 5-12: Case 7 data

Vehicle Parameters	Optimization Parameters	Optimization Variables
Vehicle 2	Drive Cycle: UDDS	1) Engine Max. Power, Initial: 41 kW
Parallel Drivetrain	Initial Mass: 1350 kg	2) Motor Max. Power Initial: 75 kW
Cargo Mass: 230 kg	Lower Bounds: [20,20,0.2,0,0,0]	3) Battery Capacity Initial: 1
SI Engine	Upper Bounds: [80,80,3,9,1,1]	4) Electric Only Speed Initial: 6
	Cost Function: 1*Fuel Usage	5) Minimum Charge Torque Fraction Initial: 0.2
		6) Engine Off Torque Fraction Initial: 0.1

- Case 8 :

Table 5-13: Case 8 data

Vehicle Parameters	Optimization Parameters	Optimization Variables
Vehicle 2	Drive Cycle: UDDS	1) Engine Max. Power, Initial: 39 kW
Parallel Drivetrain	Initial Mass: 1310 kg	2) Motor Max. Power Initial: 49 kW
Cargo Mass: 230 kg	Lower Bounds: [20,20,0.2,0,0,0]	3) Battery Capacity Initial: 1
SI Engine	Upper Bounds: [80,80,3,9,1,1]	4) Electric Only Speed Initial: 6
	Cost Function: 1*Fuel Usage + 1*CO + 1*NO <sub>x</sub> + 1*HC	5) Minimum Charge Torque Fraction Initial: 0.2
		6) Engine Off Torque Fraction Initial: 0.1

- Case 9 :

Table 5-14: Case 9 data

Vehicle Parameters	Optimization Parameters	Optimization Variables
Vehicle 2	Drive Cycle: J1015	1) Engine Max. Power, Initial: 39 kW
Parallel Drivetrain	Initial Mass: 1310 kg	2) Motor Max. Power Initial: 55 kW
Cargo Mass: 230 kg	Lower Bounds: [20,20,0.2,0,0,0]	3) Battery Capacity Initial: 1
SI Engine	Upper Bounds: [80,80,3,9,1,1]	4) Electric Only Speed Initial: 1
	Cost Function: 1*Fuel Usage + 1*CO + 1*NO <sub>x</sub> + 1*HC	5) Minimum Charge Torque Fraction Initial: 0.4
		6) Engine Off Torque Fraction Initial: 0.135

- Case 10 :

Table 5-15: Case 10 data

Vehicle Parameters	Optimization Parameters	Optimization Variables
Vehicle 2	Drive Cycle: UDDS	1) Engine Max. Power, Initial: 45 kW
Parallel Drivetrain	Initial Mass: 1620 kg	2) Motor Max. Power Initial: 59 kW
Cargo Mass: 408 kg	Lower Bounds: [20,20,0.2]	3) Battery Capacity Initial: 1
SI Engine	Upper Bounds: [80,80,3]	
	Cost Function: 1*Fuel Usage	

- Case 11 :

Table 5-16: Case 11 data

Vehicle Parameters	Optimization Parameters	Optimization Variables
Vehicle 2	Drive Cycle: UDDS	1) Engine Max. Power, Initial: 37 kW
Parallel Drivetrain	Initial Mass: 1170 kg	2) Motor Max. Power Initial: 46 kW
Cargo Mass: 65 kg	Lower Bounds: [20,20,0.2]	3) Battery Capacity Initial: 1
CI Engine	Upper Bounds: [80,80,3]	
	Cost Function: 1*Fuel Usage	

- Case 12 :

Table 5-17: Case 12 data

Vehicle Parameters	Optimization Parameters	Optimization Variables
Vehicle 2	Drive Cycle: UDDS	1) Engine Max. Power, Initial: 35 kW
Series Drivetrain	Initial Mass: 1250 kg	2) Motor Max. Power Initial: 78 kW
Cargo Mass: 136 kg	Lower Bounds: [20,50,0.2]	3) Battery Capacity Initial: 1
SI Engine	Upper Bounds: [60,90,3]	
	Cost Function: 1*Fuel Usage	

- Case 13 :

Table 5-18: Case 13 data

Vehicle Parameters	Optimization Parameters	Optimization Variables
Vehicle 2	Drive Cycle: UDDS	1) Engine Max. Power, Initial: 35 kW
Series Drivetrain	Initial Mass: 1260 kg	2) Motor Max. Power Initial: 82 kW
Cargo Mass: 136 kg	Lower Bounds: [20,50,0.2]	3) Battery Capacity Initial: 1
CI Engine	Upper Bounds: [60,90,3]	
	Cost Function: 1*Fuel Usage	

- Case 14:

Table 5-19: Case 14 data

Vehicle Parameters	Optimization Parameters	Optimization Variables
Vehicle 2	Drive Cycle: UDDS	1) Engine Max. Power, Initial: 39 kW
Parallel Drivetrain	Initial Mass: 1310 kg	2) Motor Max. Power Initial: 49 kW
Cargo Mass: 230 kg	Lower Bounds: [20,20,0.2,0,0,0]	3) Battery Capacity Initial: 1
CI Engine	Upper Bounds: [80,80,3,9,1,1]	4) Electric Only Speed Initial: 6
	Cost Function: a*Fuel Usage + b*CO + c*NOx + d*HC	5) Minimum Charge Torque Fraction Initial: 0.2
		6) Engine Off Torque Fraction Initial: 0.1

- Case 15:

Table 5-20: Case 15 data

Vehicle Parameters	Optimization Parameters	Optimization Variables
Vehicle 2	Drive Cycle: UDDS	1) Engine Max. Power, Initial: 39 kW
Parallel Drivetrain	Initial Mass: 1310 kg	2) Motor Max. Power Initial: 49 kW
Cargo Mass: 230 kg	Lower Bounds: [20,20,0.2,0,0,0]	3) Battery Capacity Initial: 1
CI Engine	Upper Bounds: [80,80,3,9,1,1]	4) Electric Only Speed Initial: 6
	Cost Function: a*Fuel Usage + b*CO + c*NOx + d*HC	5) Minimum Charge Torque Fraction Initial: 0.2
		6) Engine Off Torque Fraction Initial: 0.1

### 5.4.1 Case 1, 2 & 3

The first three case studies are carried out in order to get a reference performance analysis for gradient base optimization by the fmincon tool using different starting points for optimization variables. While doing so, convergence to the global minimum solution and moreover total time needed by means of total function counts through the optimization process are observed. For that purpose 2000 Honda Insight vehicle parameters are used and also the found results are compared with the original fuel consumption value of the Insight.

During these 3 cases, only power components are defined as optimization variables and cost function is directly equal to fuel consumption. Different from the original Honda Insight vehicle additional cargo weight is used as 4 passenger and cargo. All specified values are given in Table 5-6, Table 5-7 and Table 5-8.

The initial configuration fuel consumption values are 5.05 L/100 km, 4.62 L/100 km and 6.53 L/100 km. The comparison of the results observed by using created GUI and ADVISOR GUI platform for initial parameters and also optimized parameters are also given for three cases one by one. In Figure 5-7 the fuel consumption value for case initial parameters are given as 5.1 L/100 km. The other two cases 2 and 3 results with ADVISOR platform is given in Figure 5-8 and Figure 5-9 and the fuel consumption results are 4.9 L/100km and 6.4 L/100 km.

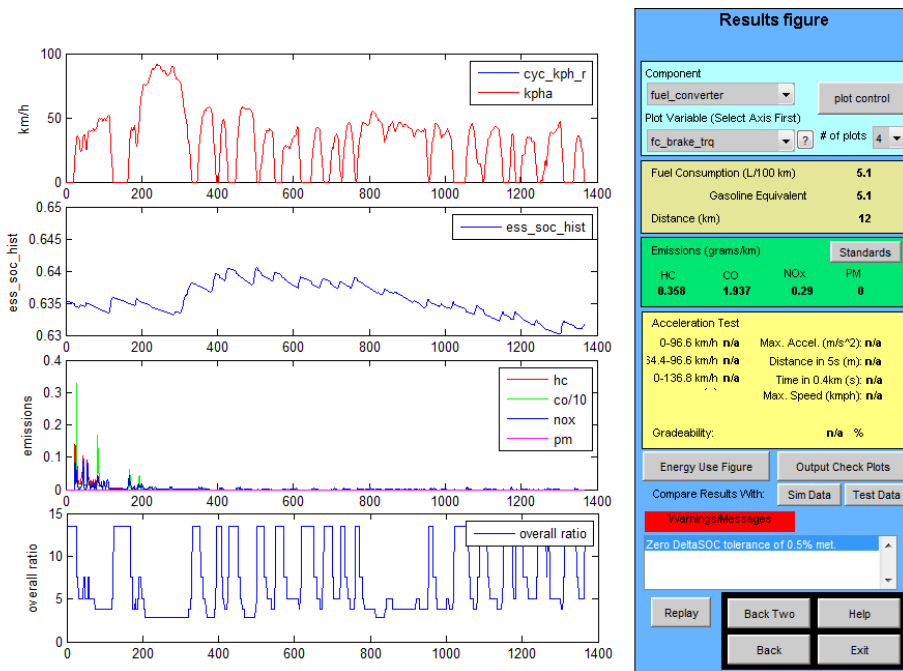


Figure 5-7: ADVISOR result screen for simulation with case 1 initial parameters

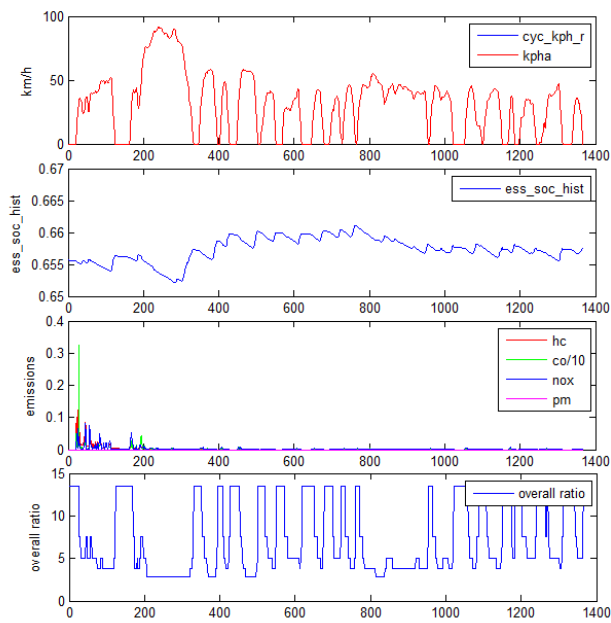


Figure 5-8: ADVISOR result screen for simulation with case 2 initial parameters

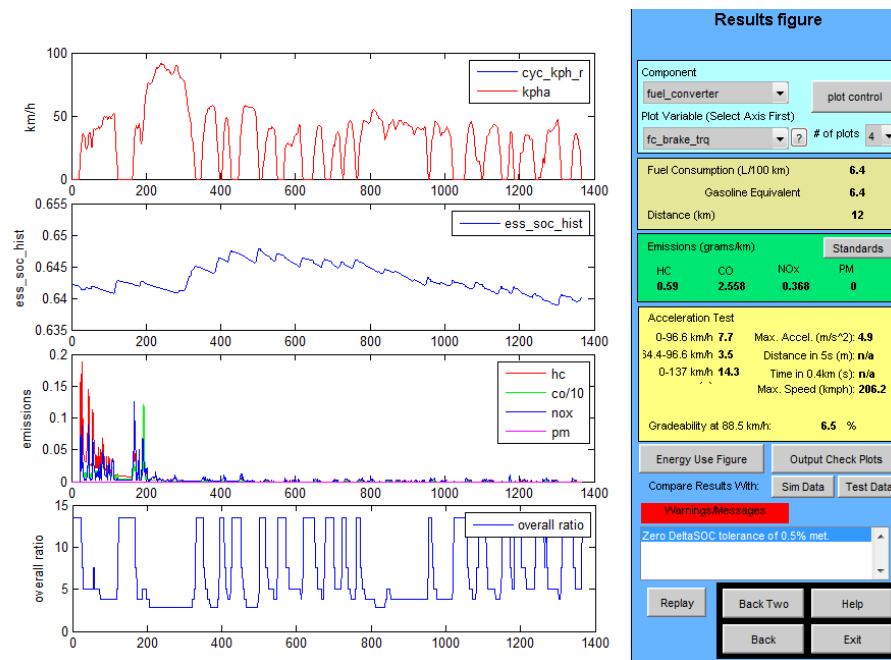


Figure 5-9: ADVISOR result screen for simulation with case 3 initial parameters

The results of the three cases are given in Table 5-21 and whole data table which includes the variable changes, cost function values, constraint satisfaction condition and also mass changes for each function count is given in the Appendix B.

Table 5-21: Case 1, 2 & 3 optimization results

	Fuel Consumption [L/100 km]	Total Function Count	Variable Final Values	Final Mass [kg]
Case 1	4.741	13	- Max. Engine Power: 34 kW - Max. Motor Power: 75 kW - Battery Capacity Scale : 0.95	1336
Case 2	4.620	45	- Max. Engine Power: 33 kW - Max. Motor Power: 56 kW - Battery Capacity Scale : 1.18	1319
Case 3	4.773	58	- Max. Engine Power: 37 kW - Max. Motor Power: 72 kW - Battery Capacity Scale : 0.83	1317

The results show that, the procedure with initial sizing according to performance demands satisfy a close approximation to the optimal solution which is also shown in the following cases. Cases 1 and 3 which have different starting values have close fuel consumption values to the one in Case 2 but slightly worse. However these results could be acceptable also when compared to Case 2, with only 3.5 % difference. In addition to cost function results, function counts also differ. While Case 2 has a lower function value than the Case 3 as expected, Case 1 has much lower value than the other two which could be explained as initial values' closeness to the local minimum value.

Also separate ADVISOR runs are made for optimized parameters in order to measure the accuracy of the optimization procedure. The result figures are given in Figure 5-10, Figure 5-11 and Figure 5-12.

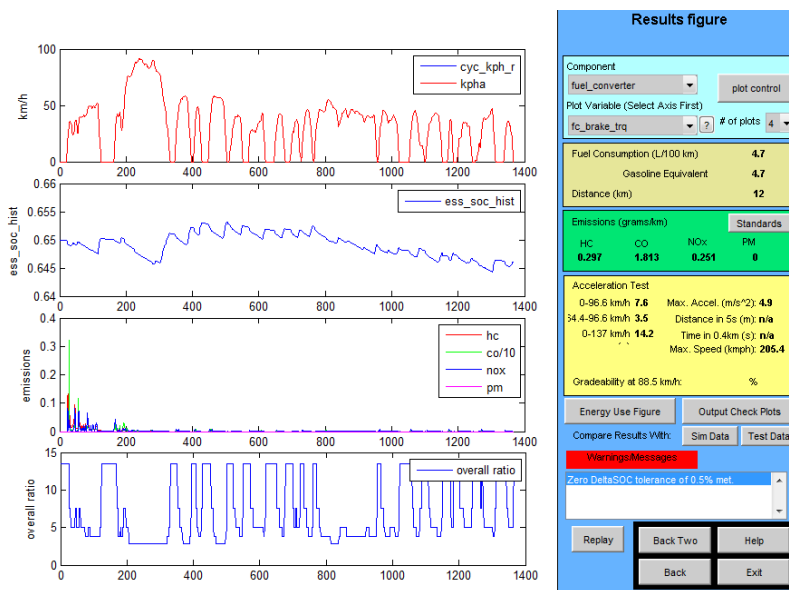


Figure 5-10: ADVISOR result screen for simulation with case 1 optimized parameters

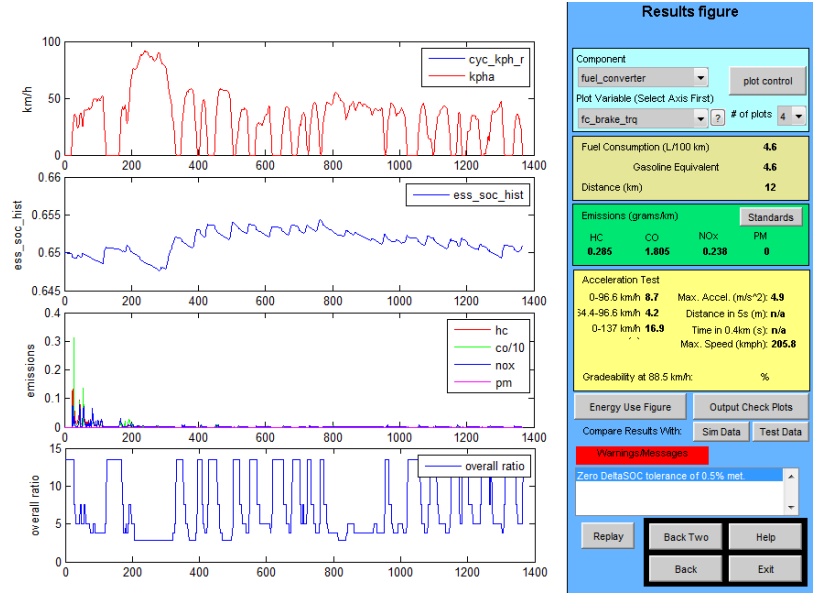


Figure 5-11: ADVISOR result screen for simulation with case 2 optimized parameters

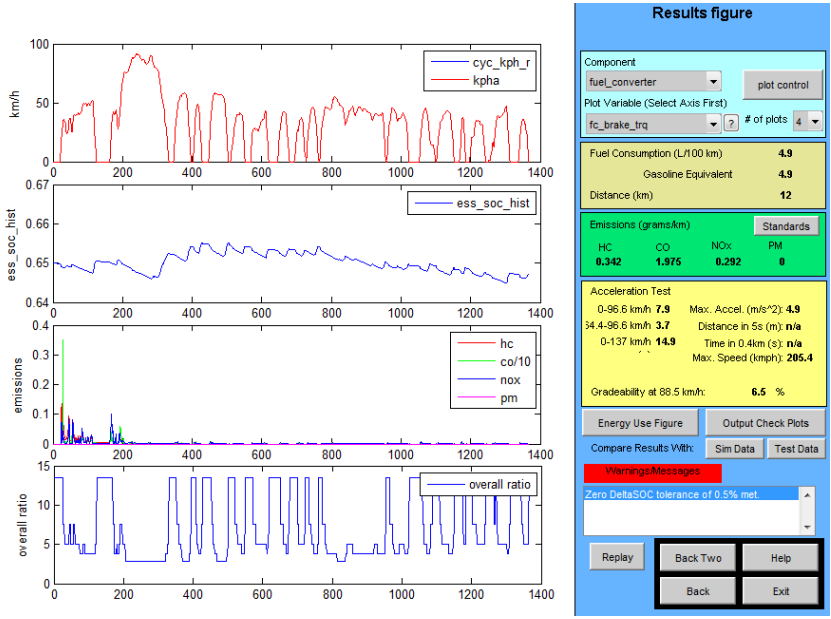


Figure 5-12: ADVISOR result screen for simulation with case 3 optimized parameters

The ADVISOR results are 4.7 L/100 km, 4.6 L/100 km and 4.9 L/100 km which are very close to ones observed by using optimization process.

The original fuel consumption rating of the 2000 Honda Insight is given as 49 mpg = 4.9 L/100km [60] in city driving condition which is very close to the calculated values.

#### 5.4.2 Case 4 & 5

These two simulations are carried in order to get a reference values for the other cases simulations and also starting point effect on the cost function and final values are examined for second vehicle configuration. Moreover a separate ADVISOR simulation is carried out with initial and the final values of the design variables (only power components here, and control parameters are set as default values which is explained in cases 6 and 7) to control the final value of the cost function.

The initial fuel consumption values before the optimization process are 5.66 L/100 km for case 4 (it was not satisfying the constraints) and 6.13 L/100 km for case 5. The ADVISOR results with the same parameters are given in Figure 5-13 and Figure 5-14. The fuel consumption values are 5.6 L/100 km and 6.3 L/100 km.

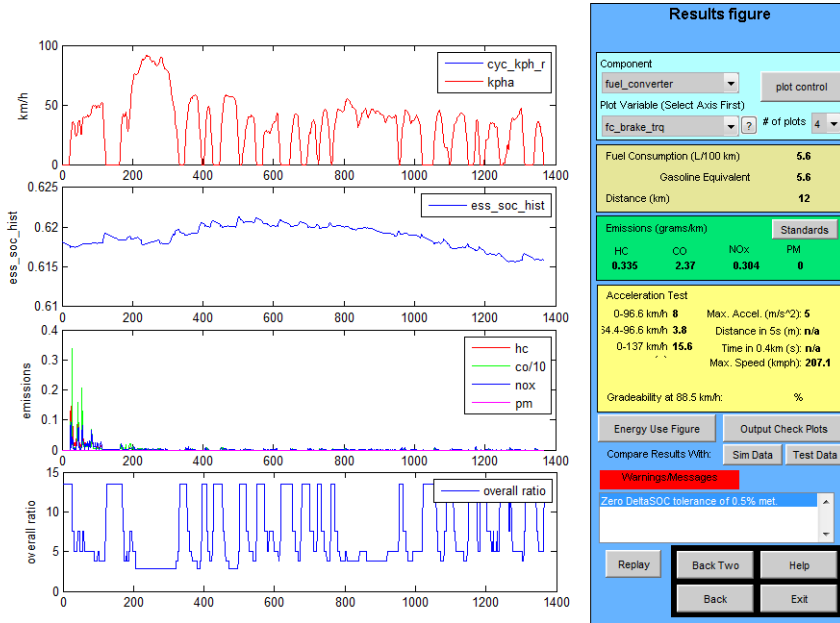


Figure 5-13: ADVISOR result screen for simulation with case 4 initial parameters

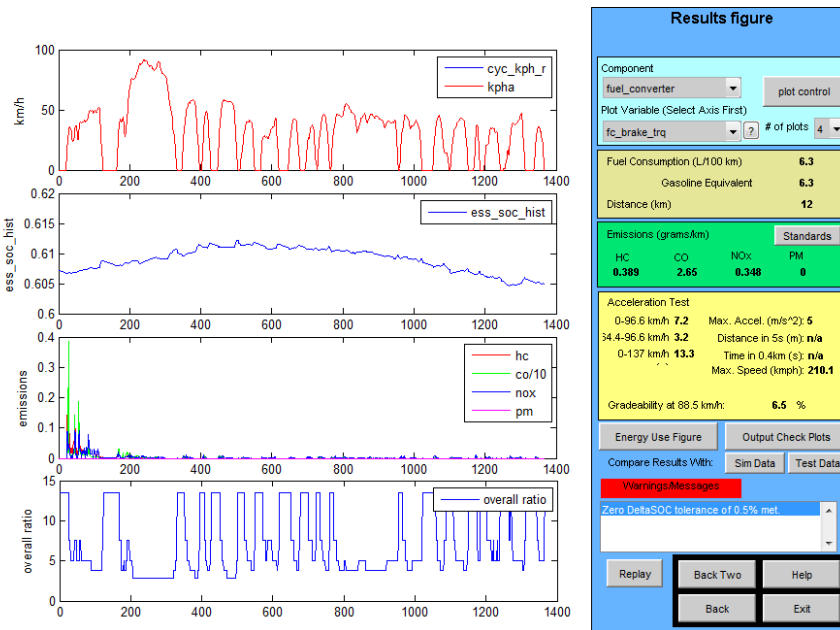


Figure 5-14: ADVISOR result screen for simulation with case 5 initial parameters

Table 5-22: Case 4 & 5 optimization results

	Fuel Consumption [L/100 km]	Total Function Count	Variable Final Values	Final Mass [kg]
Case 4	5.761	13	- Max. Engine Power: 37 kW - Max. Motor Power: 50 kW - Battery Capacity Scale : 0.9	1200
Case 5	5.832	45	- Max. Engine Power: 35 kW - Max. Motor Power: 70 kW - Battery Capacity Scale : 1	1227

Similar to first three cases, starting point changes the cost function final value little bit and initially sized vehicle has a better performance. Although it does not guarantee that the global maximum is satisfied, it could be used as a good approximation.

To prepare a reference value for the next cases, only fuel consumption is minimized and for that purpose only power sizing values are used as design variables. With the final values of the optimization, a basic ADVISOR run is carried out and the results are shown in Figure 5-15. Fuel consumption value of the simulation is 5.7 L/100km which is very close to the one found in Case 4. Also for case 5 another ADVISOR run is made with optimized parameters. The result is given in Figure 5-16 and the result is 5.9 L/100 km. Also emission values meet the values observed in the optimization which are given in Appendix B.

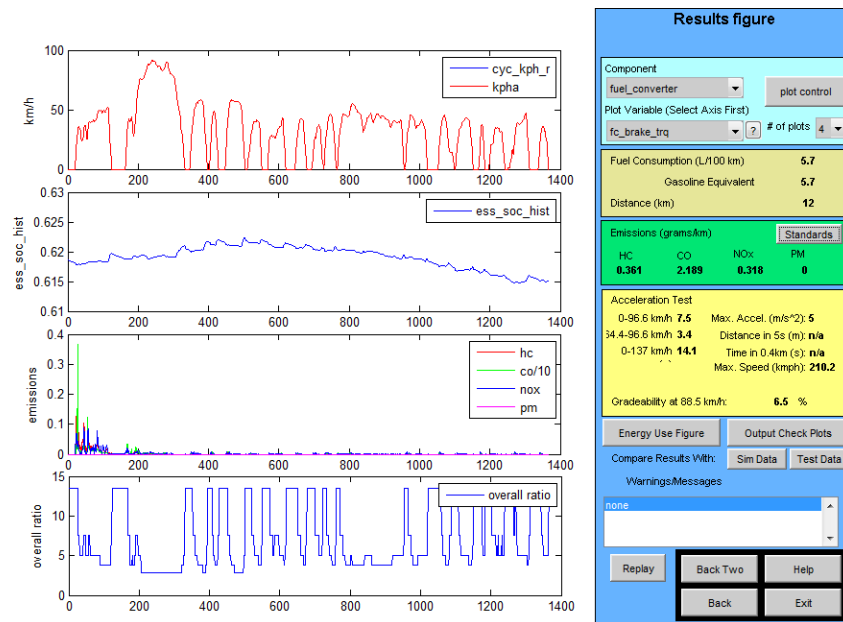


Figure 5-15: ADVISOR result screen for simulation with case 4 optimization result parameters

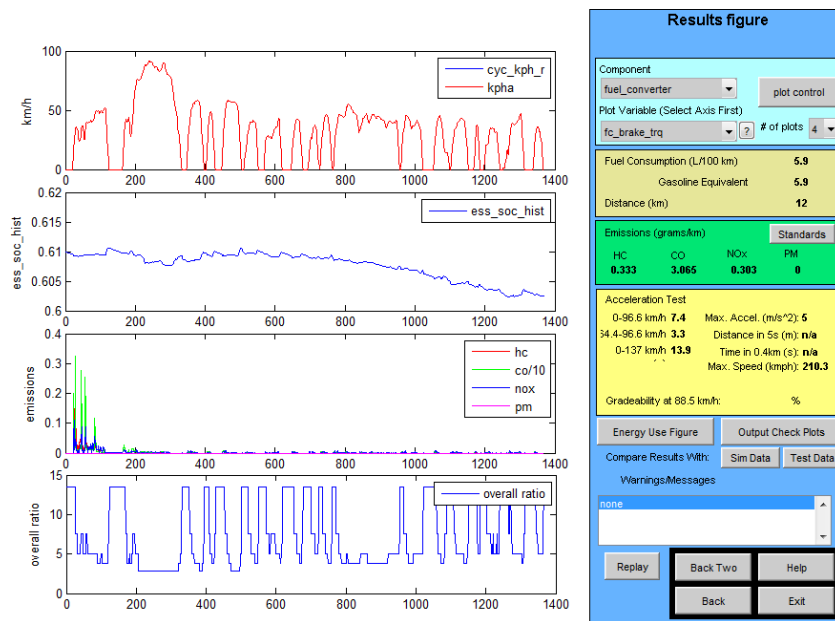


Figure 5-16: ADVISOR result screen for simulation with case 5 optimization result parameters

### 5.4.3 Case 6

This is the only case for parallel configuration which is performed over a highway drive cycle HWFET. As in the previous cases only fuel consumption is taken as cost function and variables are defined as power ratings plus control parameters.

Table 5-23: Case 6 optimization results

	Fuel Consumption [L/100 km]	Total Function Count	Variable Final Values	Final Mass [kg]
Case 6	4.432	65	<ul style="list-style-type: none"> <li>- Max. Engine Power: 45 kW</li> <li>- Max. Motor Power: 57 kW</li> <li>- Battery Capacity Scale : 1.29</li> <li>- Electric Launch Speed: 5.85 m/s</li> <li>- Charge Torque Fraction: 0.54</li> <li>- Off Torque Fraction: 0.46</li> </ul>	1393

The result show that the optimization process provides a 12 % improvement compared to initial fuel consumption value which was 5.02 L/100 km and also it provides a 32 % improvement compared to a same total power conventional vehicle.

In the next case includes the result of the same vehicle over UDSS drive cycle. It provides a 19 % improvement over the HEV with initial power ratings and provides a 40 % improvement over same power conventional vehicle. This result shows that hybrid technology could achieve better improvement for city cycle compared to highway cycle and there is a two times difference between city and highway drive cycles in these cases.

Moreover, as comparison, ADVISOR simulation runs for initial and final parameters are given in Figure 5-17 and Figure 5-18. The initial fuel consumption value is 5 L/100 km where the final one is 4.4 L/100 km.

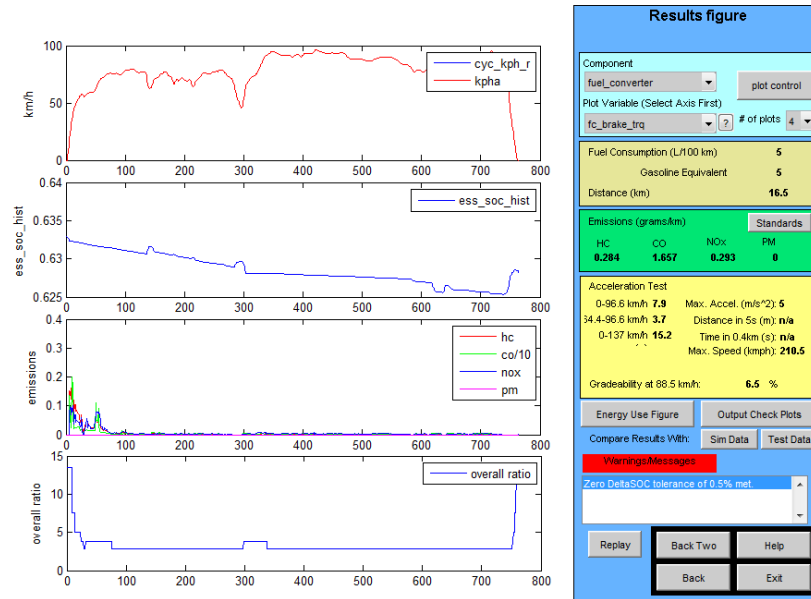


Figure 5-17: ADVISOR result screen for simulation with case 6 initial parameters

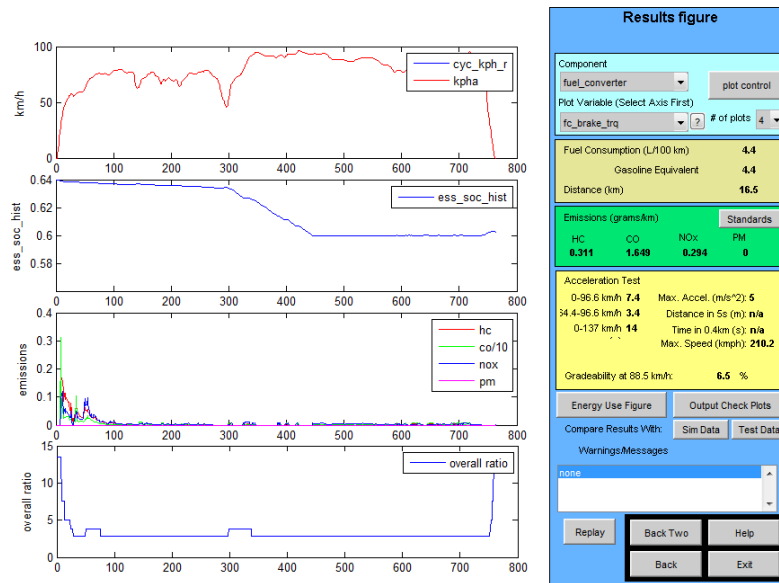


Figure 5-18: ADVISOR result screen for simulation with case 6 optimization result parameters

#### 5.4.4 Case 7 & 8

The next step is adding controller parameters to optimization variables and then defining the cost function not only for fuel consumption but also emission values with equal weightings. 3 most important parameters “electric launch speed”, “engine off torque fraction” and “charge torque fraction” which define the characteristic of the controller are used as additional design parameters in case 7. Furthermore, in case 8 emission values are also added to cost function and the tradeoff between fuel consumption and emission values is tried to be examined.

Table 5-24: Case 7 & 8 optimization results

	Fuel Consumption [L/100 km]	Emission Values [g/km]	Total Function Count	Variable Final Values	Final Mass [kg]
Case 7	5.083		90	- Max. Engine Power: 41 kW - Max. Motor Power: 36 kW - Battery Capacity Scale : 1.14 - Electric Launch Speed: 5.85 m/s - Charge Torque Fraction: 0.44 - Off Torque Fraction: 0.39	1330
Case 8	5.473	NOx: 0.2965 CO: 3.3132 HC: 0.3008	37	- Max. Engine Power: 31 kW - Max. Motor Power: 53 kW - Battery Capacity Scale : 0.86 - Electric Launch Speed: 5.95 m/s - Charge Torque Fraction: 0.39 - Off Torque Fraction: 0.22	1266

Case 7 shows that addition of the controller parameters as optimization variables into the process could reduce the fuel consumption of the vehicle. The fuel consumption value at case 7 becomes 5.083 L/100km while the initial fuel consumption is 6.34 L/100 km and fuel consumption at case 4 is 5.761 L/100km although its total mass is lower than the one in case 7. Power ratings of the propulsion system also differ too with the inclusion of the control parameters as design variables. While the engine and battery capacity get larger, electric motor power rating gets smaller.

On the other hand, as a next step addition of the emission values to cost function in case 8 results in an increase in the fuel consumption as expected as it is explained in [43]. While the control strategy parameters values differ from the case 6 it is closer to initial assumptions of 6 m/s, 0.2 charge and 0.1 off torque fractions. Further power ratings are closer to case 4. The better fuel consumption performance of case 8 compared to case 4 could be explained as control parameters addition to optimization procedure.

A similar study is performed by Xiaolin Hu [20] investigates the optimum values of power sizing and controller parameters in order to minimize the fuel consumption and emission values by using multi objective genetic algorithm found that with the 41 kW engine and 75 kW motor initial ratings and unity capacity scale, fuel consumption and emission values changes as

Fuel: [5.155, 6.137] L/100km  
 NOx: [0.246, 0.322] g/km  
 HC: [0.341, 0.391] g/km  
 CO: [1.253, 3.008] g/km

The results for fuel consumption and HC emission optimization are just below the results given above, while NOx emission value is placed in the upper part of the given interval. The CO is at the highest value. On the other hand, while the engine power rating is very close to 41 kW, the electric motor rating is in the range of 25-30 kW and battery capacity scale is directly 0.8.

In addition to comparison with the literature as in the previous cases comparison to analyze the accuracy of the results, ADVISOR simulation results are shown for initial and optimized cases. In Figure 5-19 and Figure 5-20 results with initial parameters for case 7 and case 8 is given. The values are 6.5 L/100 km and 6 L/100 km.

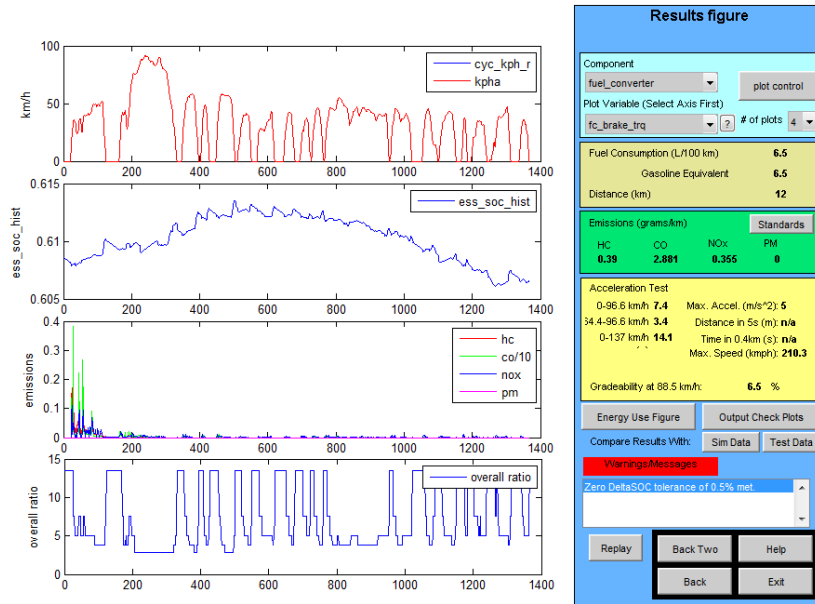


Figure 5-19: ADVISOR result screen for simulation with case 7 initial parameters

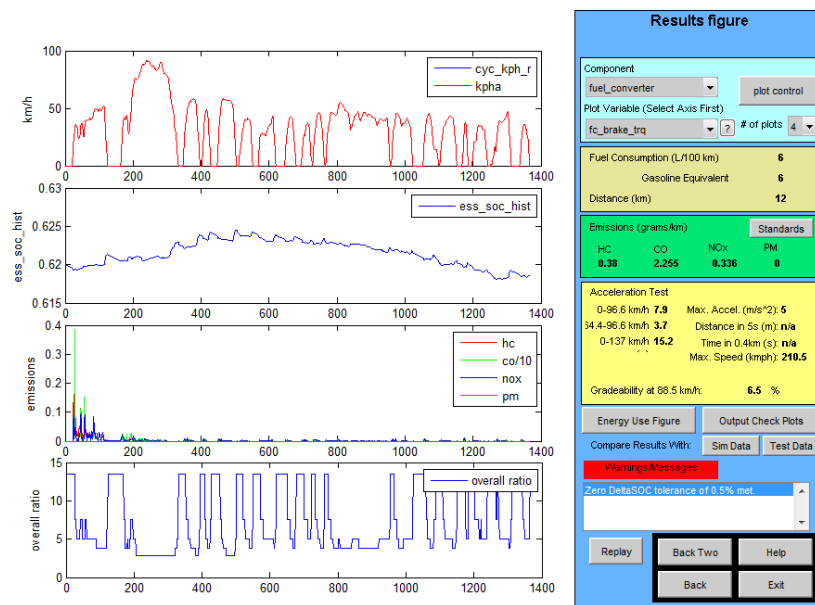


Figure 5-20: ADVISOR result screen for simulation with case 8 initial parameters

Then the results for optimized parameters are given in Figure 5-21 and Figure 5-22. The resultant values are 5 L/100 km and 5.4 L/100 km which meet with the ones observed by using developed GUI. Also emission values for case 8 are NOx: 0.27 g/km, CO: 3.231 g/km and HC: 0.298 g/km which are also very close to ones found in optimization process.

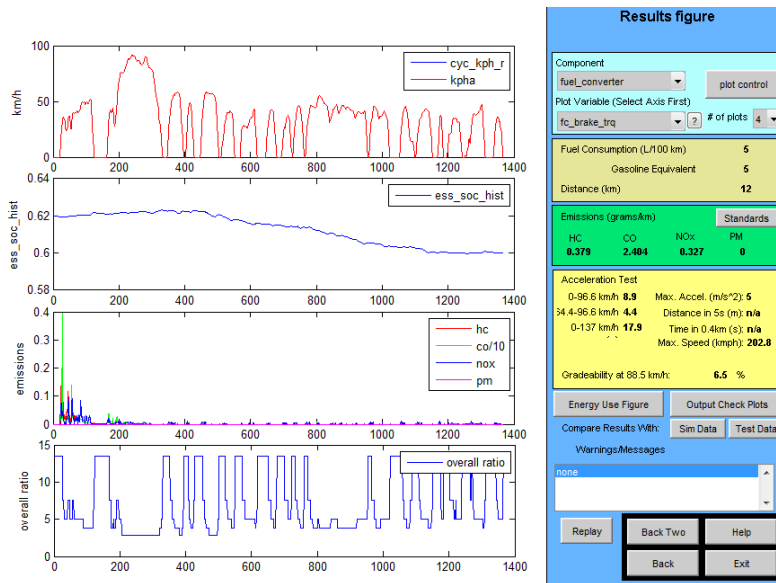


Figure 5-21: ADVISOR result screen for simulation with case 7 optimization result parameters

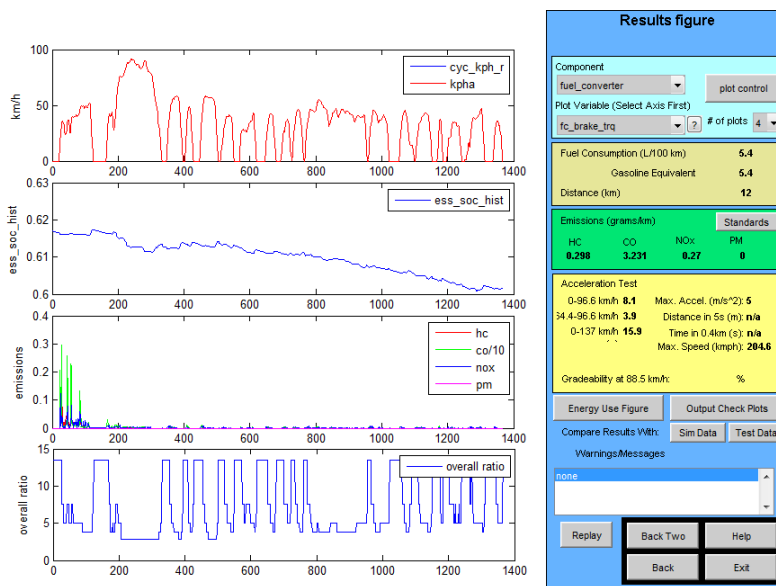


Figure 5-22: ADVISOR result screen for simulation with case 8 optimization result parameters

### 5.4.5 Case 9

Another city cycle Japan 10-15 is used for comparison with UDDS drive cycle results and also comparison with another early study made by using genetic algorithm. The optimization is made for all control plus power component parameters in order to optimize both emission and fuel consumption. After the initial sizing process initial mass of the vehicle is 1310 kg and initial fuel consumption emission values are

Fuel: 6.6 L/100 km, CO: 3.4458 g/km, HC: 0.7986 g/km, NOx: 0.5175 g/km

Also they are compared with the ones that observed from ADVISOR simulation. They are given in Figure 5-23.

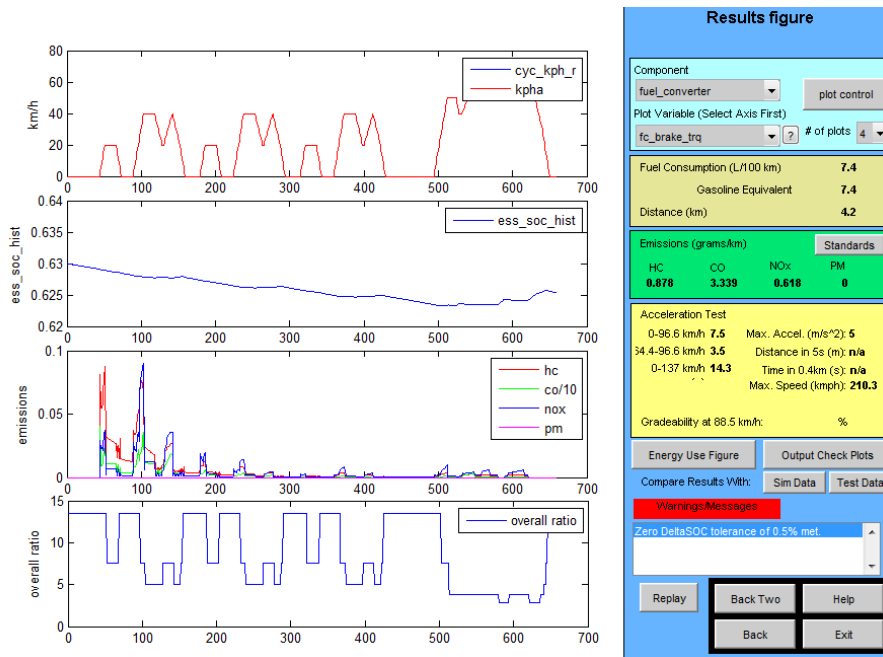


Figure 5-23: ADVISOR result screen for simulation with case 9 initial parameters

Table 5-25: Case 9 optimization results

	Fuel Consumption [L/100 km]	Emission Values [g/km]	Total Function Count	Variable Final Values	Final Mass [kg]
Case 9	5.882	NOx: 0.3985 CO: 3.403 HC: 0.7217	32	- Max. Engine Power: 38 kW - Max. Motor Power: 49 kW - Battery Capacity Scale : 0.77 - Electric Launch Speed: 1.07 m/s - Charge Torque Fraction: 0.46 - Off Torque Fraction: 0.14	1266

Although engine power and electric motor power remain nearly same with the initials, battery power capacity is reduced in magnitude by 25 % and control parameters are changed considerably in between the bounds. All emission and fuel consumption values are reduced. However when looked at the other values collected during the process which are given in Appendix B, at some points, while fuel consumption decreases especially NOx emission value increases a little which is coincides with the working region effect of engine shown in Figure 5-1.

A similar study is made by Fang [19], shows different parameter alternatives for fuel consumption and emission value minimization. The power components and control parameters have similar values. The results found in this study is given below

“Fuel: [5.9, 6.5] (L/100km)”  
 “CO: [1.960, 3.179] (g/km)”  
 “HC: [0.291, 0.374] (g/km)”  
 “NOx: [0.289, 0.329] (g/km)”

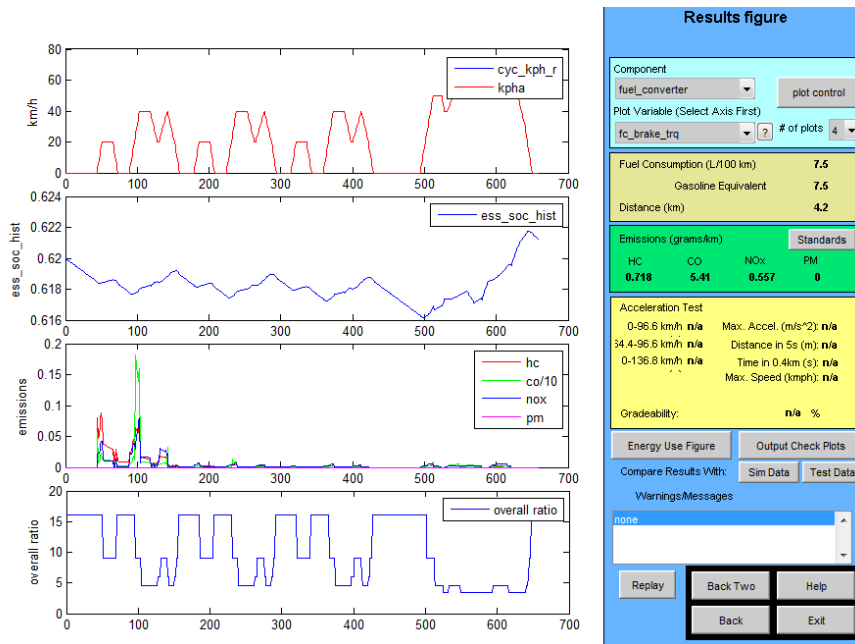


Figure 5-24: J1015 Drive cycle results for reference study

Although fuel consumption value is a little bit higher, emission values are lower than those found in the current study. Especially there is a big difference in HC emission value. When a separate simulation with given parameters of the study is made, the results show that emission values are higher than the given values as shown in Figure 5-24.

The discrepancy between the results could be due to lack of some initial conditions which are not given in the study. In the current study, cold start initial conditions are used for all simulations. When the hot start conditions are applied, the result is given in Figure 5-25. The emission values are HC:0.111 g/km, CO:0.418 g/km, NOx:0.174 g/km. The results show the effect of hot start conditions especially on emission values.

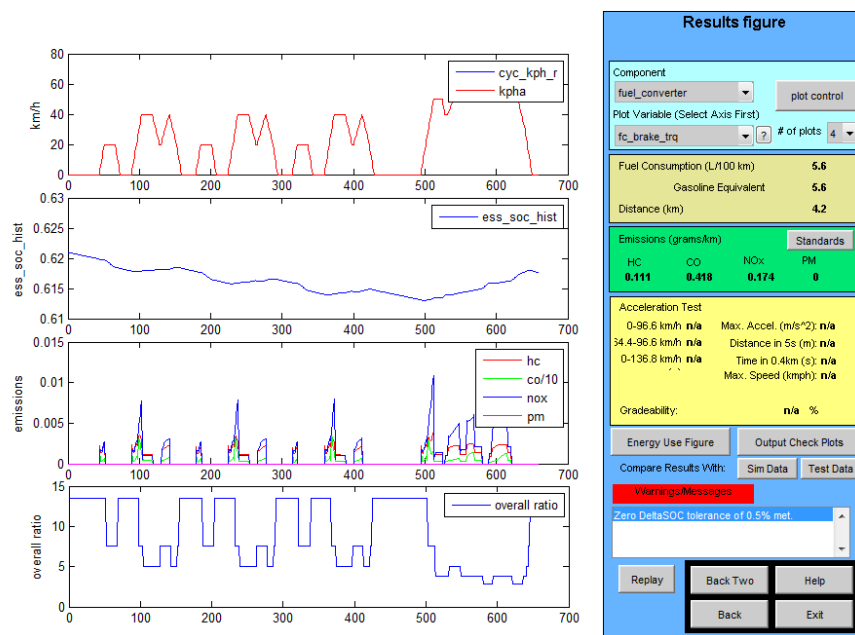


Figure 5-25: J1015 Drive cycle results for reference study with hot initial conditions

### 5.4.6 Case 10

This case is carried out for comparison with case 5 and also for comparison with early similar studies. In the simulation only fuel consumption minimization is made with 3 power unit rating sizing with an additional mass. It could be taken for additional cargo or a larger saloon car and effect of mass on power sizing and fuel consumption is investigated.

Table 5-26: Case 10 optimization results

	Fuel Consumption [L/100 km]	Emission Values [g/km]	Total Function Count	Variable Final Values	Final Mass [kg]
Case 10	7.83		26	- Max. Engine Power: 48 kW - Max. Motor Power: 35 kW - Battery Capacity Scale : 1.19	1644

The final value of the fuel consumption value is very close to initial one which was 7.89 L/100 km but the initial configuration does not satisfy the performance constraints. Constraints satisfaction is achieved with the configuration which has initially 8.14 L/100 km fuel consumption. Also result by using ADVISOR platform with initial parameters is given in Figure 5-26 and the fuel consumption value is 7.8 L/100 km.

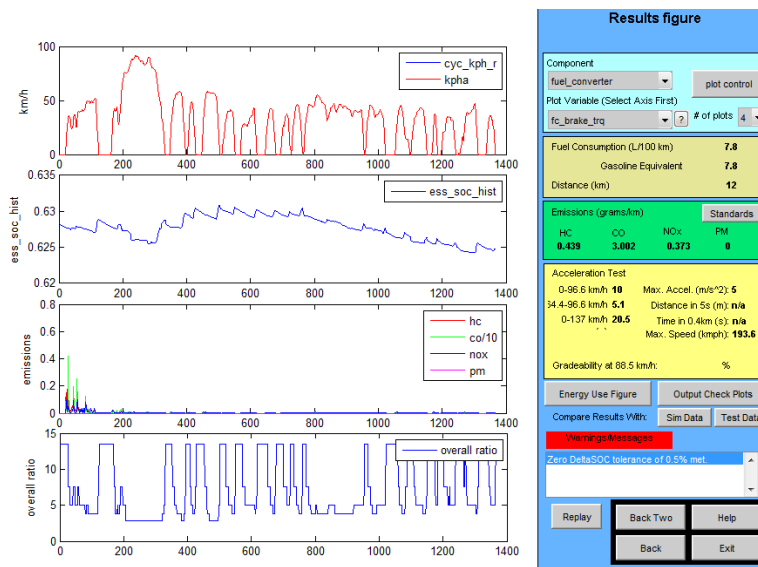


Figure 5-26: ADVISOR result screen for simulation with case 10 initial parameters

Early studies for parallel drivetrain with same total vehicle weight are made by Gao [21], [10]. 4 different optimization algorithms are used for the optimization process. The results are close to each other, so as an example the results from simulated annealing algorithm are used here. The power components' ratings are 82.4 kW engine, 22 kW motor and 311 modules (1.8 capacity scale value). The fuel consumption value is 5.85 L /100 km for HWFET and UDDS combined drive cycle (45 % + 55 %). There are considerable differences between the results. That could be a result of SOC correction procedure not being applied although there is no information on this aspect. Further control strategy is not given. In order to show the difference between SOC corrected and non-corrected results' difference a separate simulation is made with the study's parameters and basic control strategy.

Also as a comparison, ADVISOR result for the parameters have the same values with the optimization results is given in Figure 5-27 and result, 7.8 L/100 km is very close to one found in optimization process 7.83 L/100 km.

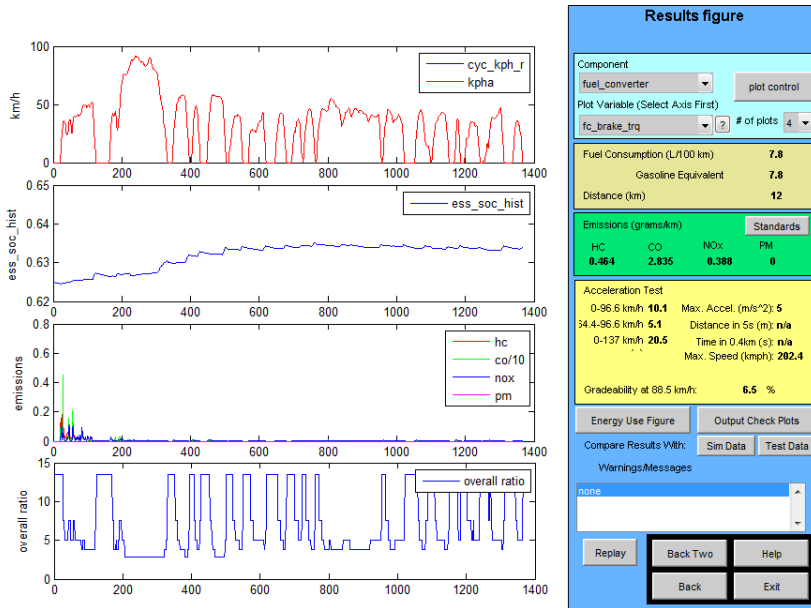


Figure 5-27: ADVISOR result screen for simulation with case 10 optimization result parameters

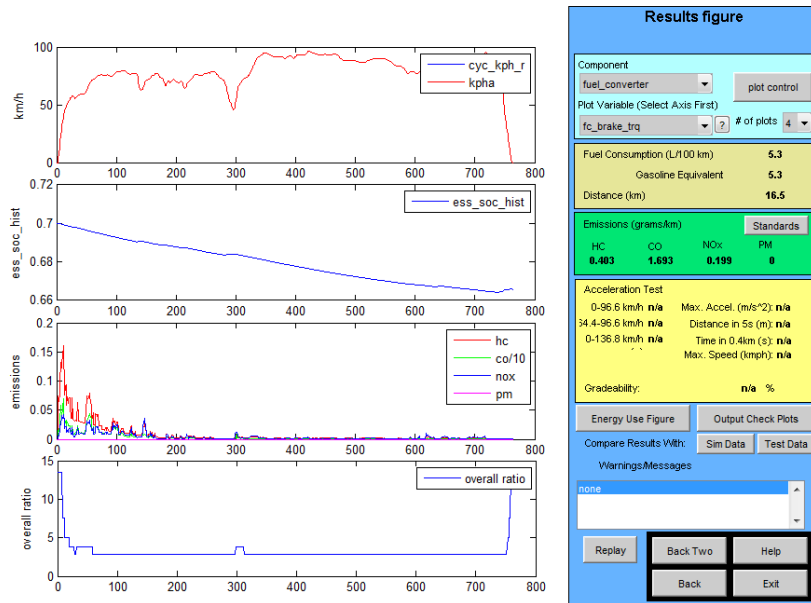


Figure 5-28: HWFET Drive Cycle without SOC correction

The results are shown in Figure 5-28 and Figure 5-29. For HWFET the value is 5.3L/100 km and for UDDS it is 7.3 L/100 km. So the combined fuel consumption becomes  $5.3 \cdot 0.45 + 7.3 \cdot 0.55 = 6.4$  L/100 km. The given value in the study is 40 mpg = 5.9 L/100 km. The result is high little than the given one. Effect of another criterion should be shown also when SOC is not corrected. It highly effects the resultant fuel consumption since it increases the battery energy usage alternative. The initial SOC was 0.7 for the previous runs. For this time 0.80 initial SOC value is set. The simulation is made only for UDDS driving cycle and comparison is directly made with 0.7 SOC valued UDDS cycle simulation. The result is given in Figure 5-30.

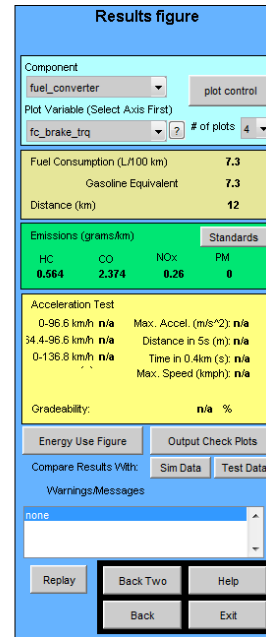
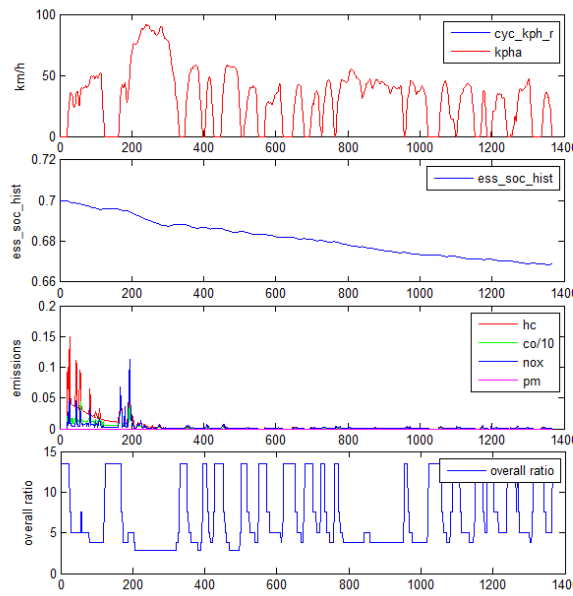


Figure 5-29: UDDS Drive cycle without SOC correction

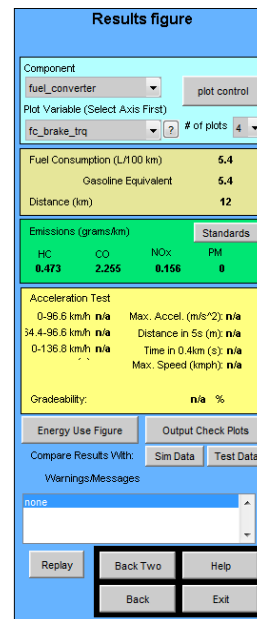
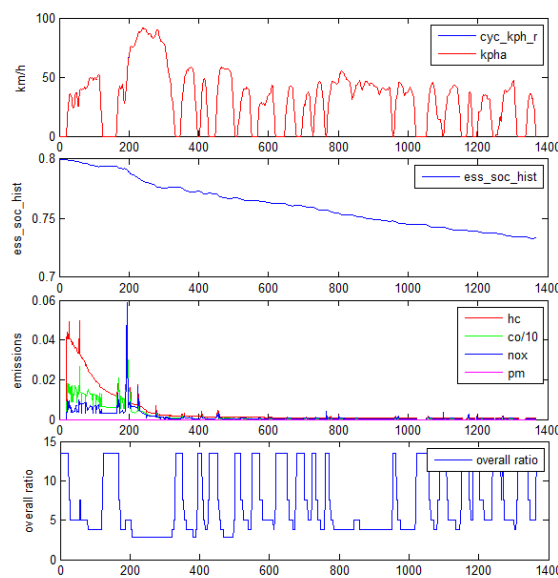


Figure 5-30: UDDS Drive cycle without SOC correction and initial SOC = 0.8

The resultant fuel consumption becomes 5.4 L/100 km which indicates a 25 % reduction. This shows that simulations without SOC correction are highly dependent on initial SOC, and high and low SOC values and they do not give dependable results. Since all simulations are made for standard hybrid configuration not plug-in ones, the battery should be charged from engine, the simulation without SOC correction could be considered as non-realistic and non-implementable.

The optimization results by using `fmincon` tool give another option of hybrid vehicle sizing. It is the hybridization factor which is defined in the introduction section. Lukic [18] made a study on finding optimum hybridization factor according to total vehicle power. Although total mass of the vehicle changes with the power components sizing, average vehicle mass is taken as 1450 kg. The study

shows that for a total power of 100 kW power vehicle optimum hybridization factor is 0.48 and for a 150 kW power vehicle it becomes 0.3. When this result is compared with the case 6 where engine power is 45 kW and motor power is 57 kW so the total power is 102 kW and total vehicle mass is 1393 kg which is a little lower than the given vehicle, the hybridization factor is 55 %. When the case 7 is taken, total weight of 1330 kg vehicle with total power is 77 kW the hybridization factor is 0.48. When the case 2 is considered total weight 1319 kg and total power is 89, the hybridization factor is 0.63. Lastly for case 10 where total mass is 1644 kg and total power is 83 kW, hybridization factor becomes 0.42. This could indicate that optimum hybridization factor could also changes with the changing vehicle mass for the same total powered vehicles, since as the mass increases the hybridization factor decreases. And also it could change with the changing driving conditions. However in order get more reliable results a more specific simulation procedure should be prepared which focuses on only hybridization factor with changing drive cycle and changing mass for the same total power vehicles.

**5.4.7 Case 11**

In the previous all configurations are carried by using spark ignition engines. In this case a parallel drivetrain with compression ignition engine is performed over a UDDS drive cycle and only power ratings are used as optimization variables and cost function again just equal to fuel consumption.

Table 5-27: Case 11 optimization results

	Fuel Consumption [L/100 km]	Total Function Count	Variable Final Values	Final Mass [kg]
Case 11	4.418	25	- Max. Engine Power: 33 kW - Max. Motor Power: 45 kW - Battery Capacity Scale : 0.96	1200

When compared to conventional diesel engine powered vehicle with the same power rating and the fuel consumption is 6.2 L/100 km (diesel), there is a 29 % improvement in fuel consumption and when compared to case 4 which has similar vehicle mass and configurations but with gasoline powered vehicle with nearly same power rating (85 kW) which has a fuel consumption value of 5.76 L/100 km, there is a 10 % increase in fuel consumption where 4.42 L/100 km diesel consumption is equal to 5.1 L/100 km gasoline. Also 14% improvement is observed compared to vehicle with initial sizing. As in the previous cases with SI engine vehicles, separate simulations are made in order to compare the both results for parameters with initial and final values. These results are given in Figure 5-31 and Figure 5-32 for initial and final values. Although initial value which is 4.6 L/100 km does not match exactly with 5.1 L/100 km, final value which is 4.4 L/100 km closely meet the one observed from the optimization process.

An early study published by Cuddy [9], the improvement relative to conventional is given as 30 % which is nearly same with 29 % value for UDDS cycle. There are also other comparisons as series and parallel performances on UDDS and series and conventional fuel consumption performances. These are given in the next case studies.

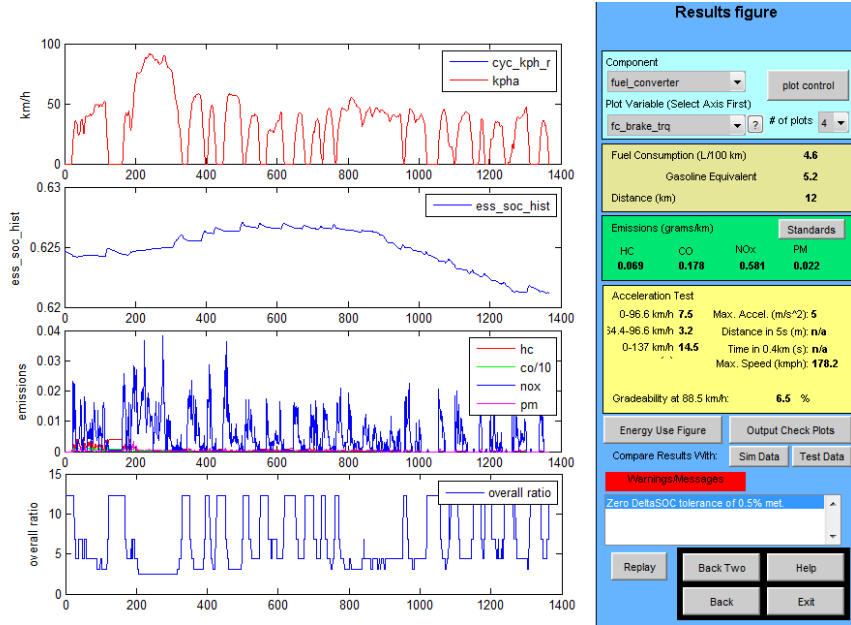


Figure 5-31: ADVISOR result screen for simulation with case 11 initial parameters

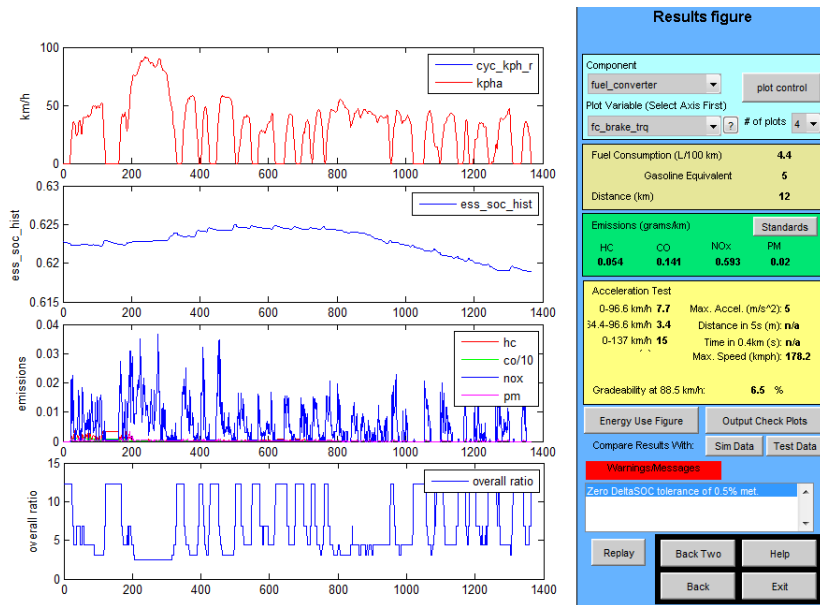


Figure 5-32: ADVISOR result screen for simulation with case 11 optimization result parameters

### 5.4.8 Case 12 & 13

Up to here, all cases are carried with parallel configuration and fuel consumption emission values are optimized with gasoline and diesel powered parallel vehicles. Since in most of the studies, UDSS cycle is referenced, for the series configuration again UDSS cycle is implemented. Since the initial sizing effect is showed that it could give better approximation for the optimization, initial sizing procedure defined in power component sizing part is used.

Table 5-28: Case 12 optimization results

	Fuel Consumption [L/100 km]	Total Function Count	Variable Final Values	Final Mass [kg]
Case 12 CI Series	5.118	21	- Max. Engine Power: 32 kW - Max. Motor Power: 78 kW - Battery Capacity Scale : 1.03	1250

Table 5-29: Case 13 optimization results

	Fuel Consumption [L/100 km]	Total Function Count	Variable Final Values	Final Mass [kg]
Case 13 SI Series	6.691	28	- Max. Engine Power: 46 kW - Max. Motor Power: 77 kW - Battery Capacity Scale : 1	1230

Case 12 results in a 5.12 L/100 km diesel fuel consumption which is 18 % better than the conventional one which was 6.2 L/100 km (however it could be considered as 20-22 % improvement a coarse assumption is made on fuel consumption – mass relation since conventional total mass is 4 % lower than the series one). Also the result shows that series configuration with compression ignition engine is 7% worse than parallel one (If 4 % mass increase is included this value will be lower). In addition to that when compared to case 13, 12 % decrease in fuel consumption with diesel power where the gasoline equivalent of 5.118 L/100 km diesel fuel in energy aspect is 5.84 L/100 km.

In Cuddy’s study [9], parallel configuration with diesel engine is 4 % better than the series configuration with diesel engine and series configuration gets 26 % fuel consumption increase compared to conventional one at UDDS cycle. Here, the improvement relative to conventional is nearly 20 % and the reduction in fuel performance compared to parallel configuration is 5 % with mass effect included assumption. However, both configurations given in case 11 and case 12 could not satisfy the values 64.5 mpg = 3.65 L/100 km and 62.6 mpg = 3.76 L/100 km for the parallel and series configurations and also 49.6 mpg = 4.74 L/100 km for the conventional vehicle.

Case 13 shows that the series configuration with gasoline fuel has a fuel consumption improvement of 22 % compared to conventional vehicles’ 8.5 L/100 km consumption value. In addition to that, when compared with parallel configuration with the same total mass value which is given in case 5, parallel configuration shows 12 % better performance. It could be concluded that by using parallel configuration instead of series configuration higher improvement can be achieved in gasoline engine compared to diesel engine equipped HEV.

In addition to those comparisons, in order to verify the optimization process with their initial and final values, simulations by using ADVISOR GUI with same parameter values are made and their result screen captures are given in Figure 5-33 and Figure 5-35 for case 12 and Figure 5-34 and Figure 5-36 for case 13. For case 12 initial fuel consumption is found as 6.6 L/100 km while it is 8 L/100 km for case 13 and the final fuel consumption values are 5.1 L/100 km for case 12 and 7 L/100 km for case 13 and they are very close to ones found in optimization process.

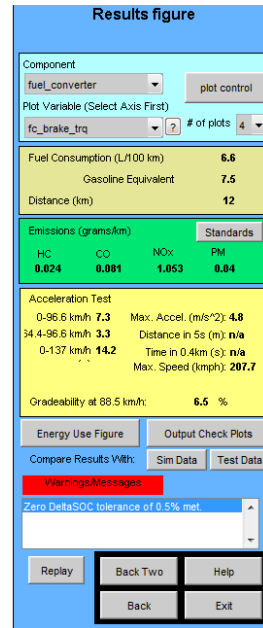
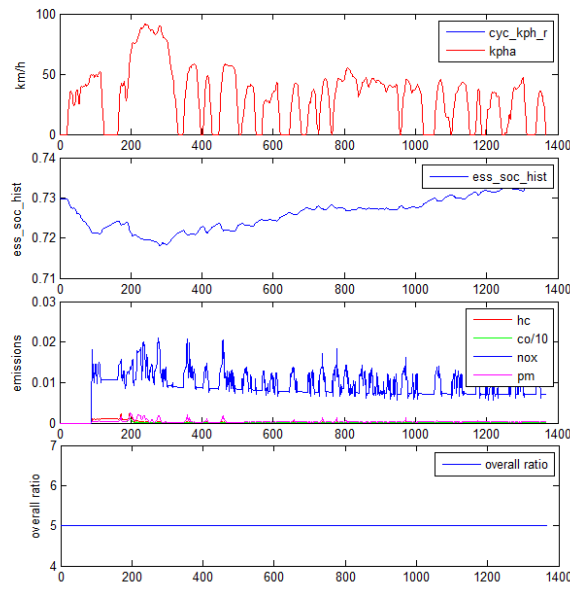


Figure 5-33: ADVISOR result screen for simulation with case 12 initial parameters

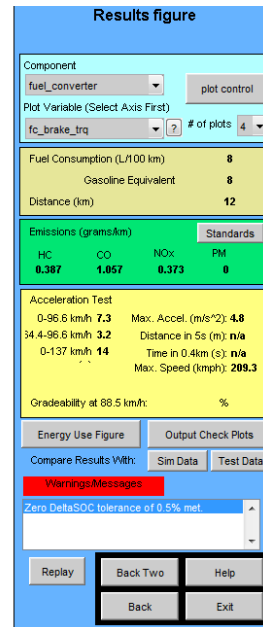
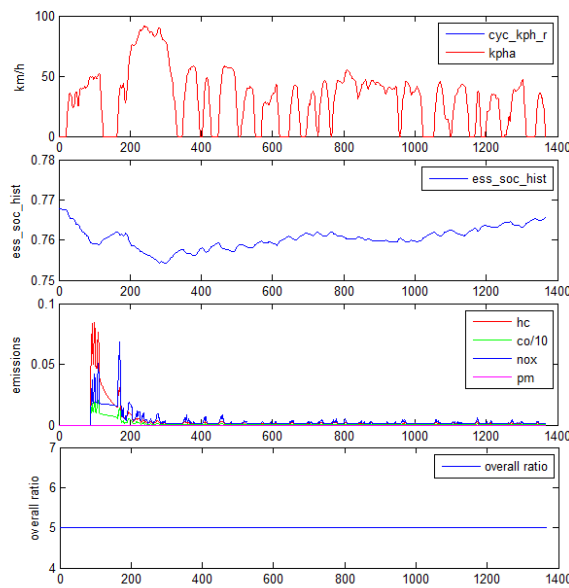


Figure 5-34: ADVISOR result screen for simulation with case 13 initial parameters

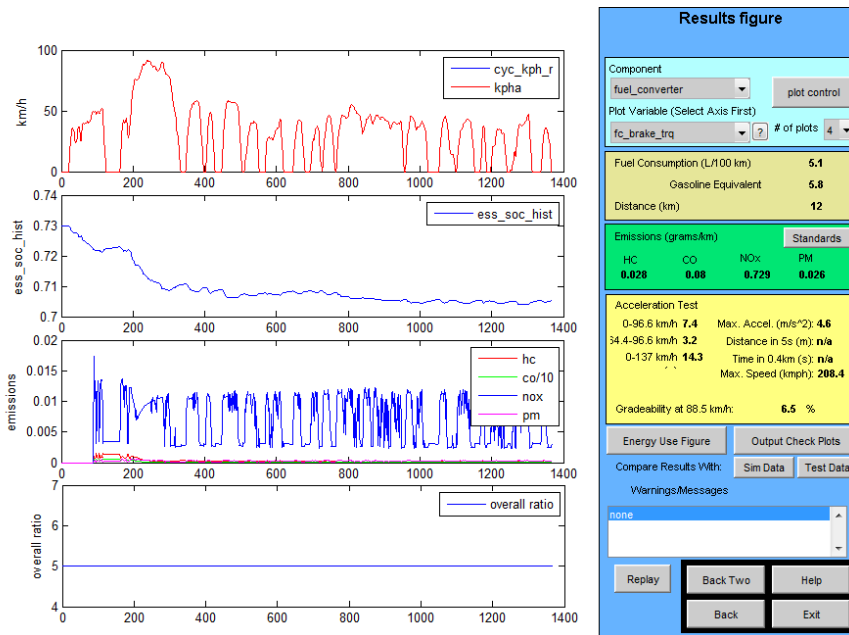


Figure 5-35: ADVISOR result screen for simulation with case 12 optimization result parameters

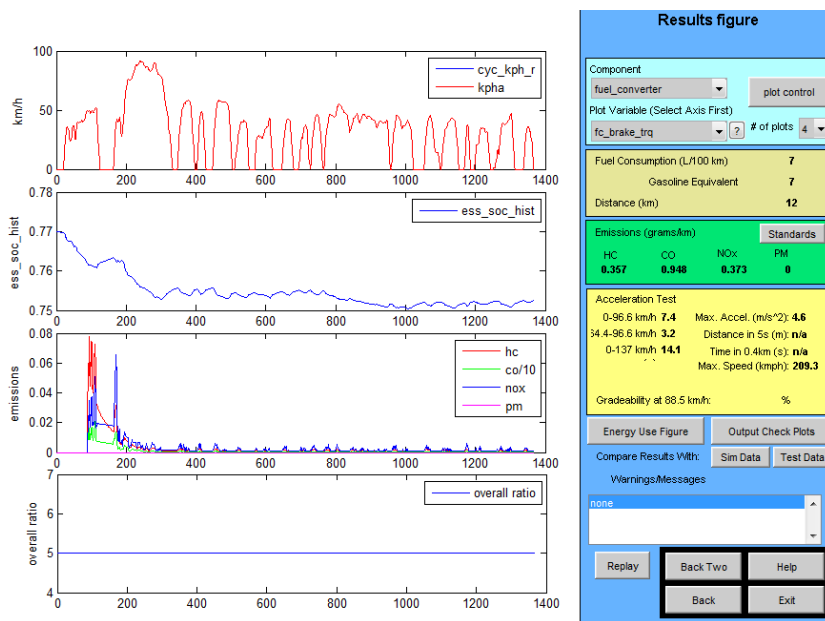


Figure 5-36: ADVISOR result screen for simulation with case 13 optimization result parameters

#### 5.4.9 Case 14 & 15

Last two cases includes optimization according to different cost functions for parallel drivetrain for SI and CI engines. There are total of ten (five for each type of engine) different cases are simulated. The aim is to investigate the effects of emission and it is observed by changing their weighting factor values instead of using equal factor values. All weighting factor values are given in Table 5-30.

Table 5-30: Case 14 and case 15 weighting factors

SI	Fuel	CO	NOx	HC
Run #1	0.2	0.6	0.1	0.1
Run #2	0.4	0.4	0.1	0.1
Run #3	0.6	0.2	0.1	0.1
Run #4	0.8	0.1	0.05	0.05
Run #5	0	0.8	0.1	0.1
CI	Fuel	CO	NOx	HC
Run #1	0.2	0.1	0.6	0.1
Run #2	0.4	0.1	0.4	0.1
Run #3	0.6	0.1	0.2	0.1
Run #4	0.8	0.05	0.1	0.05
Run #5	0	0.1	0.8	0.1

Since CO emission value is critical for SI engines, only fuel consumption and CO weighting factors are changed accordingly while NOx and HC emission values are kept constant (except for case 4) and equal. Different from the SI engines, in CI engines NOx emission has the priority while emission reduction. So, similar to SI engine cases, only fuel consumption and NOx emission weighting factor values changed accordingly. The results of the all cases are given in Table 5-31.

Cost function value changes during the optimization process are given in APPENDIX B.

Table 5-31: Case 14 results

Case Number	Cost Function	Initial Values	Final Values
SI	Run #1	0.2Fuel+0.6CO+0.1NOx+0.1HC Cost Function:0.7532	Fuel: 5.93L/100 km CO: 2.611g/km NOx: 0.326g/km HC: 0.346g/km Cost Function:0.7320
	Run #2	0.4Fuel+0.4CO+0.1NOx+0.1HC Cost Function:0.8311	Fuel: 6.00 L/100 km CO: 2.530 g/km NOx: 0.323 g/km HC: 0.353 g/km Cost Function:0.8307
	Run #3	0.6Fuel+0.2CO+0.1NOx+0.1HC Cost Function:0.9091	Fuel: 6.08L/100 km CO: 2.530 g/km NOx: 0.328 g/km HC: 0.364 g/km Cost Function:0.8856
	Run #4	0.8Fuel+0.1CO+0.05NOx+0.05HC Cost Function:0.8418	Fuel: 6.00 L/100 km CO: 2.530 g/km NOx: 0.323 g/km HC: 0.353 g/km Cost Function:0.7898
	Run #5	0.8CO+0.1NOx+0.1HC Cost Function:0.4934	Fuel: 6.00 L/100 km CO: 2.530 g/km NOx: 0.328 g/km HC: 0.353 g/km Cost Function: 0.4002

Table 5-32: Case 15 Results

CI	Run #1	0.2Fuel+0.1CO+0.6NOx+0.1HC	Fuel: 5.66 L/100 km CO: 0.259 g/km NOx: 0.572 g/km HC: 0.104 g/km Cost Function:2.0490	Fuel: 5.95 L/100 km CO: 0.385 g/km NOx: 0.533 g/km HC: 0.161 g/km Cost Function:1.9627
	Run #2	0.4Fuel+0.1CO+0.4NOx+0.1HC	Fuel: 5.36 L/100 km CO: 0.256 g/km NOx: 0.533 g/km HC: 0.102 g/km Cost Function:1.4795	Fuel: 5.24 L/100 km CO: 0.268 g/km NOx: 0.523 g/km HC: 0.107 g/km Cost Function:1.4392
	Run #3	0.6Fuel+0.1CO+0.2NOx+0.1HC	Fuel: 5.61 L/100 km CO: 0.267 g/km NOx: 0.556 g/km HC: 0.107 g/km Cost Function:1.0878	Fuel: 4.68 L/100 km CO: 0.221 g/km NOx: 0.507 g/km HC: 0.086 g/km Cost Function:0.9531
	Run #4	0.8Fuel+0.05CO+0.1NOx+0.05HC	Fuel: 5.66 L/100 km CO: 0.259 g/km NOx: 0.572 g/km HC: 0.104 g/km Cost Function:2.5198	Fuel: 4.43 L/100 km CO: 0.243 g/km NOx: 0.511 g/km HC: 0.097 g/km Cost Function: 2.253
	Run #5	0.1CO+0.8NOx+0.1HC	Fuel: 5.61 L/100 km CO: 0.267 g/km NOx: 0.556 g/km HC: 0.107 g/km Cost Function:2.4523	Fuel: L/100 km CO: 0.266 g/km NOx: 0.474 g/km HC: 0.106 g/km Cost Function:2.0418

The change in cost function and changes in fuel consumption and purposed emission reduction is achieved according to the given weightings. For HEV with SI engine has considerable amount of CO reduction in run#5 where CO has a 0.8 weighting factor. And also tradeoff between the fuel consumption and emission values is observed according to the change in weighting factors. Similar to SI engine powered vehicle, for HEV with CI, relative change in NOx emission reduction according to weighting factor is observed.

## CHAPTER 6

### DISCUSSION AND CONCLUSION

The objective of this thesis was to analyze the improvement of the fuel consumption and emission values simultaneously by optimization of the power and capacity ratings of the energy suppliers of the HEV, as well as the power control strategy parameters. Two hybrid configurations: series and parallel were used for the investigation of the fuel consumption and emission performance improvement upon the baseline vehicle and also a conventional vehicle with a similar total power rating value.

In the study, two vehicle models were used for parallel and series drivetrains. The Matlab Simulink platform was used for the entire simulation and optimization process. The vehicle modeling was based on integration of separate component models according to drivetrain selection. In the study, component models were adopted from ADVISOR. The integration of the component models were achieved as forward/backward modeling where each component takes the previous component's desired velocity and torque output value as input. This flow named as backward flow and starts from vehicle model and goes to power sources, engine and battery. Then achievable speed and torque values those calculated in power source models are fed back to the components. Again the flow occurs in component based. At each component calculations are made with model losses and some control algorithms and new value is sent to next component. This flow is named as forward flow. Final step is to calculate the vehicle speed with achievable torque and speed values. So it could be stated that all components have basically 2 input and 2 output ports both including speed and torque information. Desired input data was taken from standard drive cycles in the form of speed and time tables.

In order to determine the approximate initial power ratings of the vehicle according to maximum speed, maximum acceleration, and 0-100 kph acceleration, and maximum gradeability at a defined speed, a three step GUI was formed which included vehicle type, engine type, drivetrain selection options, and optimization parameters. The optimization results showed that although the parameter set for the optimum fuel consumption and emission values is not unique an some alternative combinations could also provide similar performances, the results of initial sizing procedure could produce ICE ratings which are very close to optimum values with a difference less than 5 % for parallel drivetrain. The maximum change in the engine power rating was observed 15 % according to the initial sizing value again in parallel drivetrain. However, the same performance could not be achieved in EM ratings.

In the main stage of the study, the optimization process was implemented by using sequential quadratic programming as an iterative method for nonlinear optimization by using Matlab built-in `fmincon` function. The performance of the gradient based optimization procedure was investigated by means of starting point effect on final value. Five cases were used to analyze the effect and it was concluded that starting with initially sized values give better results in most cases, although optimization with values somewhat far from the final ones might also end up with similar optimum values. Also there was no advantage in time elapsed to complete the optimization process. On the other hand gradient based optimization used in the current study could give successive results in less time compared to non-gradient base optimization such as genetic algorithm reported in literature.

13 different cases were formed to investigate effects of changing parameters on fuel consumption and emission values. In simulations, PNGV performance requirement standards were used for all cases and they were implemented as constraint functions and they are also used as performance requirements in initial sizing process. Throughout the case studies, the improvement of fuel consumption with the optimization process was determined by comparison to the performance of the initial specifications. The result showed that when only fuel consumption value reduction is the only aim, optimization could provide up to 21 % improvement in fuel consumption compared to initially

sized vehicle, and up to 40 % improvement compared to the same total power conventional vehicle. These results were observed with UDDS drive cycle and for SI engine powered hybrid vehicle. When the drive cycle changed to J1015 with SI engine hybrid vehicle, the fuel consumption improvement compared to initially sized vehicle becomes 14 % and the improvement compared to conventional vehicle could reach 50. Further, when a highway cycle was used for comparison, the vehicle with optimized parameters showed a 12 % improvement compared to initially sized vehicle and a 28 % improvement with respect to the conventional. From these results it could be concluded that hybrid vehicle fuel consumption improvement compared to conventional vehicle is highly dependent on drive cycle and for urban cycles a higher fuel consumption reduction can be obtained.

Since it is desired to minimize the fuel consumption and the emissions simultaneously considering the tradeoff between them, another case study was made with the same vehicle over a UDDS cycle. The cost function was formed with equal weightings for fuel and emission values. The fuel consumption value turned out to be 6 % higher than the only fuel optimized case. On the other hand, NO<sub>x</sub> value was reduced from 0.3283 g/km to 0.2965 g/km and HC value became 0.3008 g/km where it was 0.3662 g/km. However, simulation resulted in an increase in CO emission value from 2.318 g/km to 3.313 g/km. On the other hand, in simulations with fuel consumption objective only, the value went down to 2.201 g/km value where the fuel consumption became 5.1 L/100 km.

In addition to optimization with only power ratings, implemented basic power split control strategy parameters were also included to the optimization process. A rule based control strategy was used for power split between the electric motor and engine for parallel configuration and battery and engine-generator set for series configuration. The rules basically control the engine operating region according to battery SOC value and torque demand. The effect of control parameter optimization on fuel consumption was investigated only for the parallel configuration. Again with the same vehicle on UDDS drive cycle, the fuel consumption value reduction corresponded to a 12 % reduction in fuel consumption. For the optimization 3 main parameters of the control parameters were used which are “electric only speed”, “charge torque fraction” and “engine off torque fraction” The study shows how control parameters values effected on fuel economy.

The second drivetrain alternative, series hybrid configuration was also considered for fuel consumption and emission improvement alternative. All simulations included basic control strategy parameters and power ratings of battery, engine and electric motor as optimization variables. It was run for the same vehicle again and simulation results were evaluated with comparison to the parallel configuration. Again initial sizing procedure is implemented for the series configuration. Results showed that series configuration could satisfy a 22% improvement over conventional vehicle, but is 12 % worse than the parallel configuration for a SI engine powered vehicle. Moreover another simulation showed that series drivetrain with CI engine could give, on the UDDS cycle, a 20% improvement over conventional vehicle, while it is only 7% worse than the parallel hybrid vehicle consumption performance. This shows that diesel and gasoline powered hybrid vehicles could give different improvements according to drivetrain configuration and compared to conventional vehicles.

The last analysis was made for optimum hybridization factor of a hybrid vehicle in the region of full hybrid class. As stated earlier, optimum hybridness value changed with changing total power of the vehicle, e.g. 0.48 for a 100 kW vehicle and 0.3 for a 150 kW vehicle. But the optimum hybridness value is also affected by total vehicle mass for the same total power vehicles, and decreases with increasing total mass.

In this study, power component ratings and basic control parameters were used as optimization variables to observe optimum fuel consumption and emission values for parallel and series configurations. Although different scenarios were examined there are lots of alternatives that could be tried and investigated since hybrid technology has a high degree of freedom in design and parameter determination. Some of the future work that could validate and improve the results of the current study and analyze different aspects of hybrid technology are listed below.

- 1) Different rules may be used in the rule-based control strategy implemented in the current study. Other strategies such as Fuzzy Logic based controller strategies or real time optimization strategy may be implemented used to analyze the effect of the controller.

Further, controller effects on different drive cycles, different vehicle and engine types may also be examined.

- 2) Instead of using a single cycle with delta SOC correction technique, consecutive cycles may be used to see both how the cold start effect diminishes on a longer cycle and combined cycle fuel consumption and emission values.
- 3) The rest of the control parameters may also be included in the optimization process, and especially the effect of high and low SOC values on fuel consumption and emission values may be investigated.
- 4) The simulations may be carried out for different drive cycles and different vehicle types such as truck or city bus in order to see the optimization options according to special purpose cases.
- 5) Final drive and gearbox ratio could also be used as optimization variables and effect of this inclusion on different drivetrain configurations could be observed.
- 6) Instead of using charge sustaining mode, effect of combined charge depleting and charge sustaining mode might be implemented to use it for the optimization of parameters. Moreover plug-in hybrid technology could be included into system to see the different alternatives of optimization parameters with addition of longer electric only mode alternative.
- 7) Engine with hot initial conditions case also may be simulated to see the relative change according to cold start condition.



## REFERENCES

- [1] K. T. Chau and Y. S. Wong, "Overview of power management in hybrid electric vehicles," *Energy Conversion and Management*, vol. 43, pp. 1953-1968, 2002.
- [2] Mehrdad Ehsani, Yimin Gao, Sebastien E. Gay, and Ali Emadi, *Modern Electric, Hybrid Electric, and Fuel Cell Vehicles: Fundamentals, Theory, and Design.*: CRC Press, 2004.
- [3] US Department of Energy. Last accessed in September, 2012 [Online]. [http://www1.eere.energy.gov/vehiclesandfuels/technologies/systems/hybrid\\_electric\\_vehicles.html](http://www1.eere.energy.gov/vehiclesandfuels/technologies/systems/hybrid_electric_vehicles.html)
- [4] C.C. Chan, "The State of the Art of Electric, Hybrid and Fuel Cell Vehicles," in *Proceedings of IEEE*, vol. 95, 2007.
- [5] Allen E. Fuhs, *Hybrid Vehicles and The Future of Personal Transportation*. Florida, United States of America: CRC Press, 2009.
- [6] Ian John Albert, Elvir Kahrmanovic, and Ali Emadi, "Diesel Sport Utility Vehicles With Hybrid Electric Drive Trains," *IEEE TRANSACTIONS ON VEHICULAR TECHNOLOGY*, vol. 53, no. 4, pp. 1247-1256, July 2004.
- [7] D. Karbowski, S Pagerit, J Kwon, and A Rousseau, "'Fair' Comparison of Powertrain Configurations for Plug-In Hybrid Operation Using Global Optimization," SAE International, ISSN 0148-7191, 2009.
- [8] Vincent Freyermuth, Aymeric Rousseau, and Eric Fallas, "Comparison of Powertrain Configuration for Plug-in HEVs from a Fuel Economy Perspective," in *Proceedings of SAE World Congress, Detroit*, 2008.
- [9] Matthew R. Cuddy and Keith B. Wipke, "Analysis of the Fuel Economy Benefit of Drivetrain Hybridization," in *Proceedings of SAE International Congress & Exposition*, Detroit, Michigan, 1997.
- [10] D. W. Gao, C. Mi, and A. Emadi, "Modeling and simulation of electric and hybrid vehicles," in *Proceedings of Proceedings of IEEE*, 2007, pp. 729-745.
- [11] K.B. Wipke, M.R. Cuddy, and S.D. Burch, "ADVISOR 2.1: A User-Friendly Advanced Powertrain Simulation Using a Combined Backward/Forward Approach," *IEEE Transactions on Vehicular Technology: Special Issues on Hybrid and Electric Vehicles*, vol. 48, pp. 1751-1761, November 1999.
- [12] T. Markel et al., "ADVISOR: a systems analysis tool for advanced vehicle modeling," *Journal of Power Sources*, vol. 110, pp. 255-266, 2002.
- [13] D. Assanis et al., "Optimization Approach to Hybrid Electric Propulsion System Design," *Mechanics of Structures and Machines: An International Journal*, vol. 27, no. 4, pp. 393-421, April 2007.
- [14] F. Rajaei Salmasi, "Control Strategies for Hybrid Electric Vehicles: Evolution, Classification, Comparison," *IEEE TRANSACTIONS ON VEHICULAR TECHNOLOGY*, vol. 56, no. 5, pp. 2393-2404, September 2007.
- [15] Niels J. Schoutena, Mutasim A. Salmanb, and Naim A. Kheir, "Energy management strategies for parallel hybrid vehicles using fuzzy logic," *Control Engineering Practice*, vol. 11, pp. 171-177, 2003.
- [16] A. Rajagopalan, G. Washington, G. Rizzoni, and Y. Guezennec, "Development of Fuzzy Logic and Neural Network Control and Advanced Emissions Modeling for Parallel Hybrid Vehicles," National Renewable Energy Laboratory, Golden, Colorado, Tech. Report NREL/SR-540-32919, 2003.
- [17] Reza Langari and Jong-Seob Won, "Intelligent Energy Management Agent for a Parallel Hybrid Vehicle—Part I: System Architecture and Design of the Driving Situation Identification Process," *IEEE TRANSACTIONS ON VEHICULAR TECHNOLOGY*, vol. 54, no. 3, pp. 925-936, May 2005.
- [18] Srdjan M. Lukic and Ali Emadi, "Effects of Drivetrain Hybridization on Fuel Economy and

- Dynamic Performance of Parallel Hybrid Electric Vehicles," *IEEE TRANSACTIONS ON VEHICULAR TECHNOLOGY*, vol. 53, no. 2, pp. 385-389, March 2004.
- [19] L. Fang, S Qin, G Xu, T Li, and K Zhu, "Simultaneous Optimization for Hybrid Electric Vehicle Parameters Based on Multi-Objective Genetic Algorithms," *Energies*, vol. 4, pp. 532-544, March 2011.
- [20] Xiaolin Hu, Zhongfan Wang, and Lianying Liao, "Multi-Objective Optimization of HEV Fuel Economy and Emissions using Evolutionary Computation," SAE International, 2004-01-1153, 2004.
- [21] W. Gao and S. K. Porandla, "Design Optimization of a Parallel Hybrid Electric Powertrain," in *Proceedings of Proceedings of IEEE Vehicle Power Propulsion Conference*, Chicago, IL, 2005, pp. 530-535.
- [22] Jun Hou and Xuexun Guo, "Modeling and Simulation of Hybrid Electric Vehicles Using HEVSIM and ADVISOR," in *Proceedings of IEEE Vehicle Power and Propulsion Conference (VPPC)*, Harbin, China, 2008.
- [23] M.A. Tamor, "Hybrid Vehicle Modeling," in *Proceedings of ENV*, 1996.
- [24] K. Wipke and M Cuddy, "Using an Advanced Vehicle Simulator (ADVISOR) to Guide ," in *Proceedings of NESEA Sustainable Transportation Conference*, New York, 1996.
- [25] W. T. Mason and U. Kristiansson, "Hybrid EVs versus Pure EVs: Which Gives Greater Benefits?," in *Proceedings of INTERNATIONAL CONGRESS ON TRANSPORTATION ELECTRONICS*, Dearborn, 1994.
- [26] John M. Miller, *Propulsion Systems for Hybrid Vehicles*. London, United Kingdom: Institution of Electrical Engineers, 2004.
- [27] Aaron Brooker et al., "Advanced Vehicle Simulator(ADVISOR) Documentation," National Renewable Energy Laboratory, User Manual 2002.
- [28] Mojtaba Shams-Zahraei, Abbas Z Kouzani, Stefan Kutter, and Bernard Baker, "Integrated thermal and energy management of plug-in hybrid electric vehicles," *Journal of Power Sources*, no. 216, pp. 237-248, May 2012.
- [29] V. Johnson, M. Zolot, and A. Peseran, "Development and validation of a temperature-dependent resistance/capacitance battery model for ADVISOR," in *Proceedings of 18th Electric Vehicle Symposium*, Berlin, 2001.
- [30] V. Johnson, T. Pesaran, and T. Sack, "Temperature-dependent battery models for high-power lithium-ion batteries," in *Proceedings of 17th Electric Vehicle Symposium*, Montreal, 2000.
- [31] V.H. Johnson, "Battery performance models in ADVISOR," *Journal of Power Sources*, no. 110, pp. 321-329, 2002.
- [32] Andreas Malikopoulos, Zoran Filipi, and Dennis Assanis, "Simulation of an Integrated Starter Alternator ( ISA ) System for the HMMWV," in *Proceedings of SAE World Congress*, Detroit, April 2006.
- [33] "Induction versus permanent magnet motors," *Industry applications magazine*, pp. 28-35, December 2009.
- [34] M. Ehsani, K.L. Butler, Y. Gao, K.M. Rahman, and D. Burke, "Toward a sustainable transportation without sacrifice of range, performance, or air wuality: the ELPH car concept," in *Proceedings of International Federation of Automotive Engineering Society Automotive Congress*, Paris, 1998.
- [35] L. Guzella and A. Sciarretta, *Vehicle Propulsion Systems Introduction to Modeling and Optimization*. New York, United States of America: Springer, 2005.
- [36] D Stock and R. Bauder, "The New Audi 5-Cylinder Turbo Diesel Engine: The First Passenger Car Diesel Engine with Second Generation Direct Injection," *SAE*, vol. Paper No. 900648, 1990.
- [37] Chan-Chiao Lin, Huei, Grizzle, Jessie W. Peng, and Jun-Mo Kang, "Power Management Strategy for a Parallel Hybrid Electric Truck," *IEEE Transactions on Control System Technology*, vol. 11, no. 6, pp. 839-849, November 2003.
- [38] M Ehsani, Y Gao, and S Gay, "Characterization of Electric Motor Drives for Traction Applications," in *Proceedings of Industrial Electronics Society, IECON*, 2003, pp. 891-896.

- [39] Z. Rahman, M. Ehsani, and K.L. Butler, "An Investigation of Electric Motor Drive Characteristics for EV and HEV Propulsion Systems," in *Proceedings of SAE Technical Paper Series Future Transportation Technology Conference*, Costa Mesa, 2000.
- [40] M. Ehsani, Y. Gao, and K. Butler, "Application of electric peaking hybrid (ELPH) propulsion system to a full size passenger car with simulation design verification," *IEEE Transactions on Vehicular Technology*, vol. 48, June 1999.
- [41] L. Guzzella, A. Amstutz, and F. Grob, "Optimal operation strategies for hybrid power-trains," in *Proceedings of 1st Int. Fed. Autom. Control Workshop*, 1995.
- [42] B. M. Bauman, G. Washington, B. C. Glen, and G. Rizzoni, "Mechatronic design and control of hybrid electric vehicles," *IEEE/ASME Trans. Mechatronics*, vol. 5, no. 1, pp. 58-71, March 2000.
- [43] V. H. Johnson, B. K. Wipke, and D.J. Rausen, "HEV Control Strategy for Real-Time Optimization of Fuel Economy and Emissions," *SAE*, April 2000.
- [44] David Hermance and Shoichi Sasaki, "Hybrid electric vehicles take to the streets," *IEEE Spectrum*, November 1998.
- [45] Jack Yamaguchi, "Insight by Honda," *Automotive Engineering International*, October 1999.
- [46] S. Barsali, M. Ceraolo, and A. Possenti, "Techniques to control the electricity generation in a series hybrid electrical vehicle," *IEEE Transactions, Energy Conversion*, vol. 17, no. 2, pp. 260-266, June 2002.
- [47] A. Brahma, Y. Guezennec, and G. Rizzoni, "Optimal energy management in series hybrid electric vehicles," in *Proceedings of American Control Conference*, Ohio, 2000, pp. 60-64.
- [48] N. Jalil, M. Salman, and N.A. Kheir, "A rule-based energy management strategy for a series hybrid vehicle," in *Proceedings of American Control Conference*, Albuquerque, NM, 1997, pp. 689-693.
- [49] Environmental Protection Agency. Last accessed in October, 1996 [Online]. <http://www.epa.gov/oms/regs/ld-hwy/ftp-rev/sftp-fr.pdf>
- [50] P. Mock, J. German, and A. Bandivadekar, "Discrepancies between typeapproval and "real-world" fuelconsumption and CO2," *The International Council on Clean Transportation*, p. 13, February 2012.
- [51] S.D. Burch, "Trading off HEV Fuel Economy and Emissions through Optimization," NREL, 1999.
- [52] Mathworks, "MATLAB Product Help," Mathworks, User Manual 2010.
- [53] EPA. Last accessed in January, 2013 [Online]. <http://www.epa.gov/otaq/standards/light-duty/tier2interimstds.htm>
- [54] Fueleconomy. Last accessed in January, 2013 [Online]. <http://www.fueleconomy.gov/feg/calculatorSelectEngine.jsp?year=2007&make=Toyota&model=Prius>
- [55] "Saving Energy in US Transportation," U.S. Congress, Office of Technology Assessment, Washington DC, OTA-ETI-589, 1994.
- [56] K. Wipke, T. Markel, and D. Nelson, "Optimizing energy management strategy and a degree of hybridization for a hydrogen fuel cell SUV," in *Proceedings of 18th Electric Vehicle Symp.*, Berlin, 2001, pp. 20-24.
- [57] K. Morita and K. Shimamura, "Fuel Economy and Exhaust Emissions Test Procedure for Hybrid Electric Vehicles," International Energy Agency, Review Report 2000.
- [58] T.C. Moore and A.B. Lovins, "Vehicle design strategies to meet and exceed PNGV goals, Electric and Hybrid Vehicles—Implementation of Technology," *SAE*, pp. 79-121, 1995.
- [59] EPA. United States Environmental Protection Agency. Last accessed in November, 2012 [Online]. <http://www.epa.gov/otaq/standards/light-duty/udds.htm>
- [60] US Department of The Energy. EPA. Last accessed in January, 2013 [Online]. <http://www.fueleconomy.gov>
- [61] M. Zeraoulia, M. E. H. Benbouzid, and D. Diallo, "Electric Motor Drive Selection Issues for HEV Propulsion Systems: A Comparative Study," *IEEE TRANSACTIONS ON VEHICULAR*

*TECHNOLOGY*, vol. 55, no. 6, pp. 1756-1764, November 2006.

## APPENDIX A

### SIZING PROCEDURE FLOWCHARTS

a) Parallel Drivetrain Configuration Initial Sizing Flow Diagram

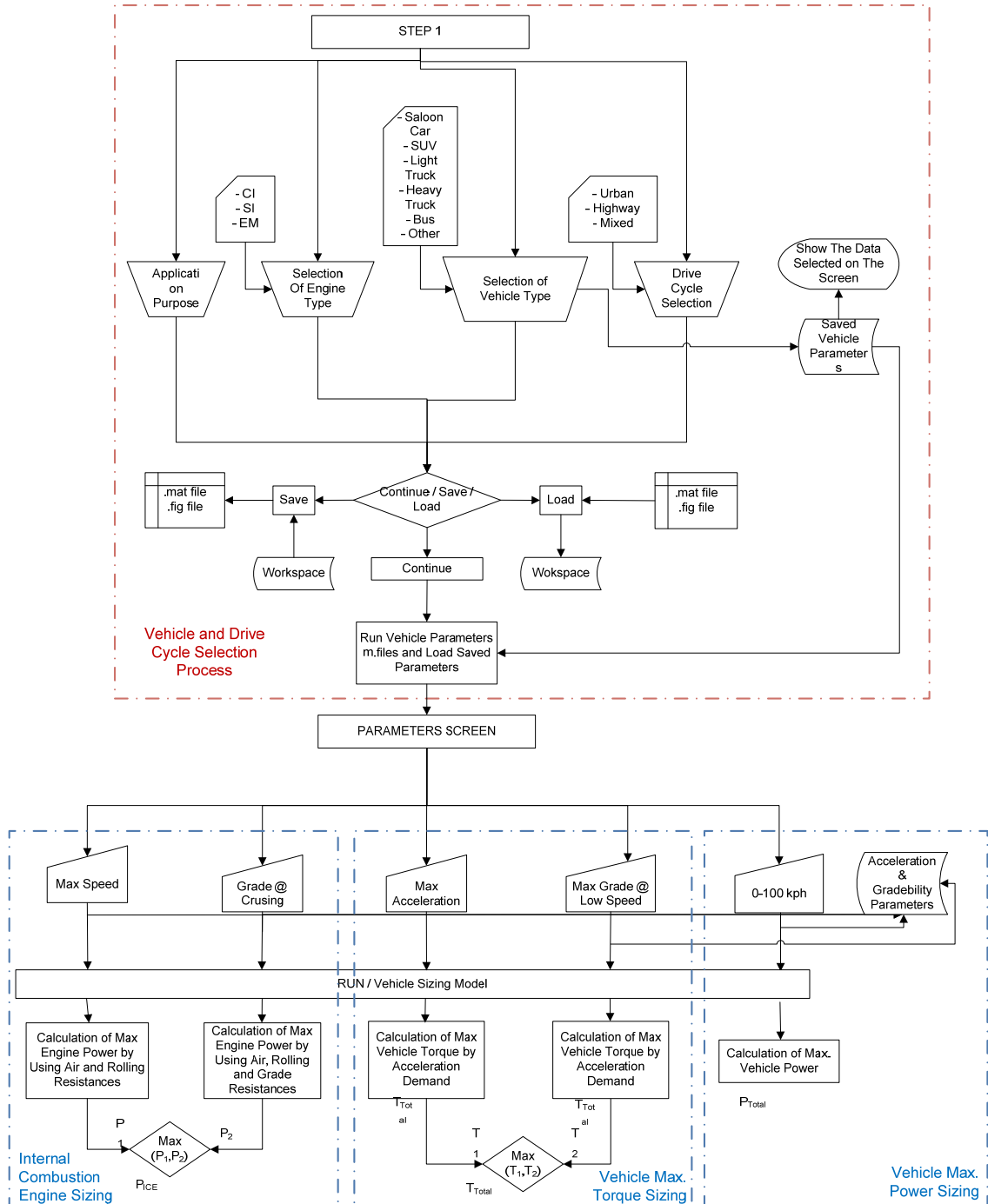


Figure A-1: Flowchart for parallel drivetrain sizing procedure – part1

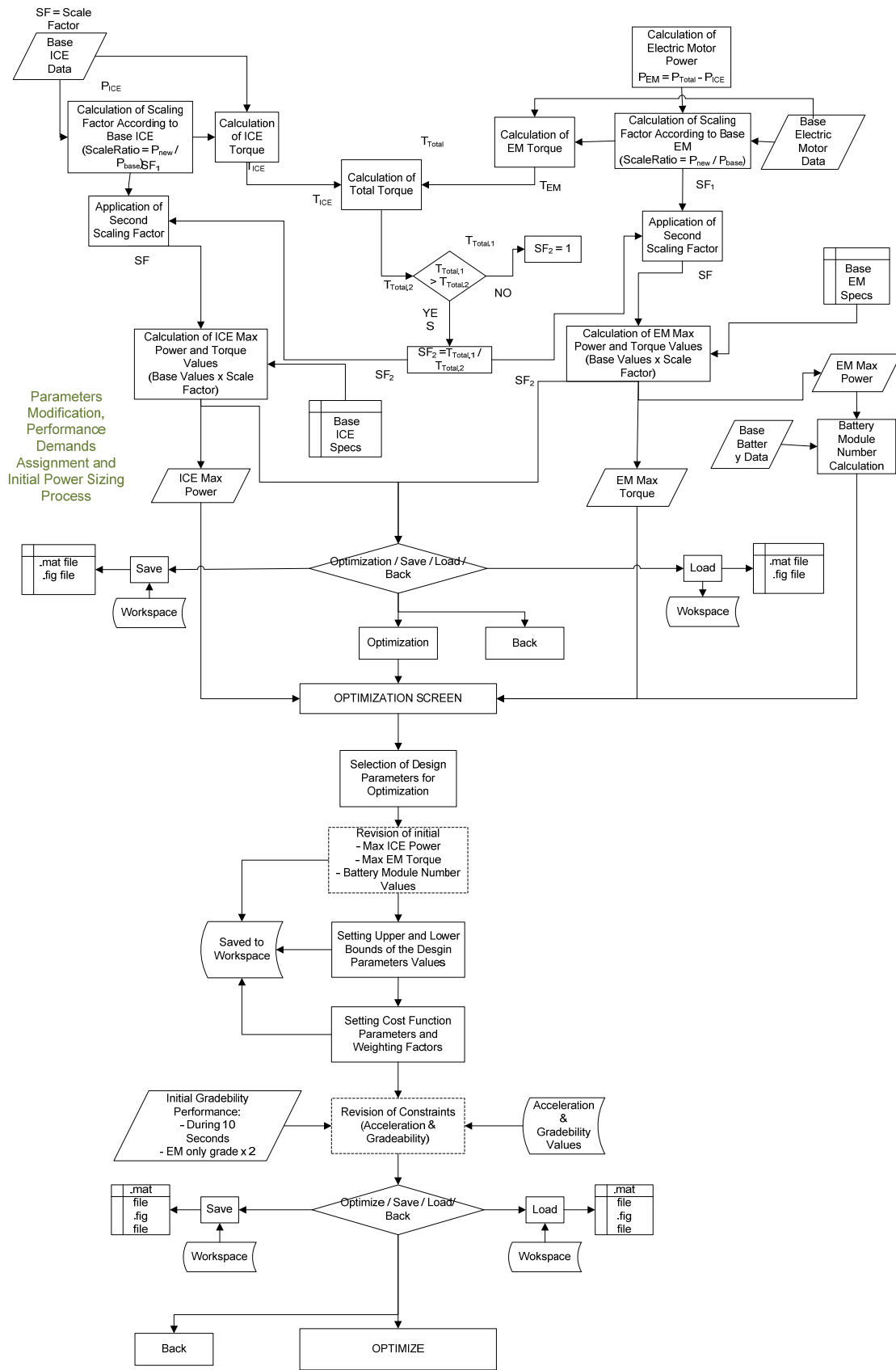


Figure A-2: Flowchart for parallel drivetrain sizing procedure – part2

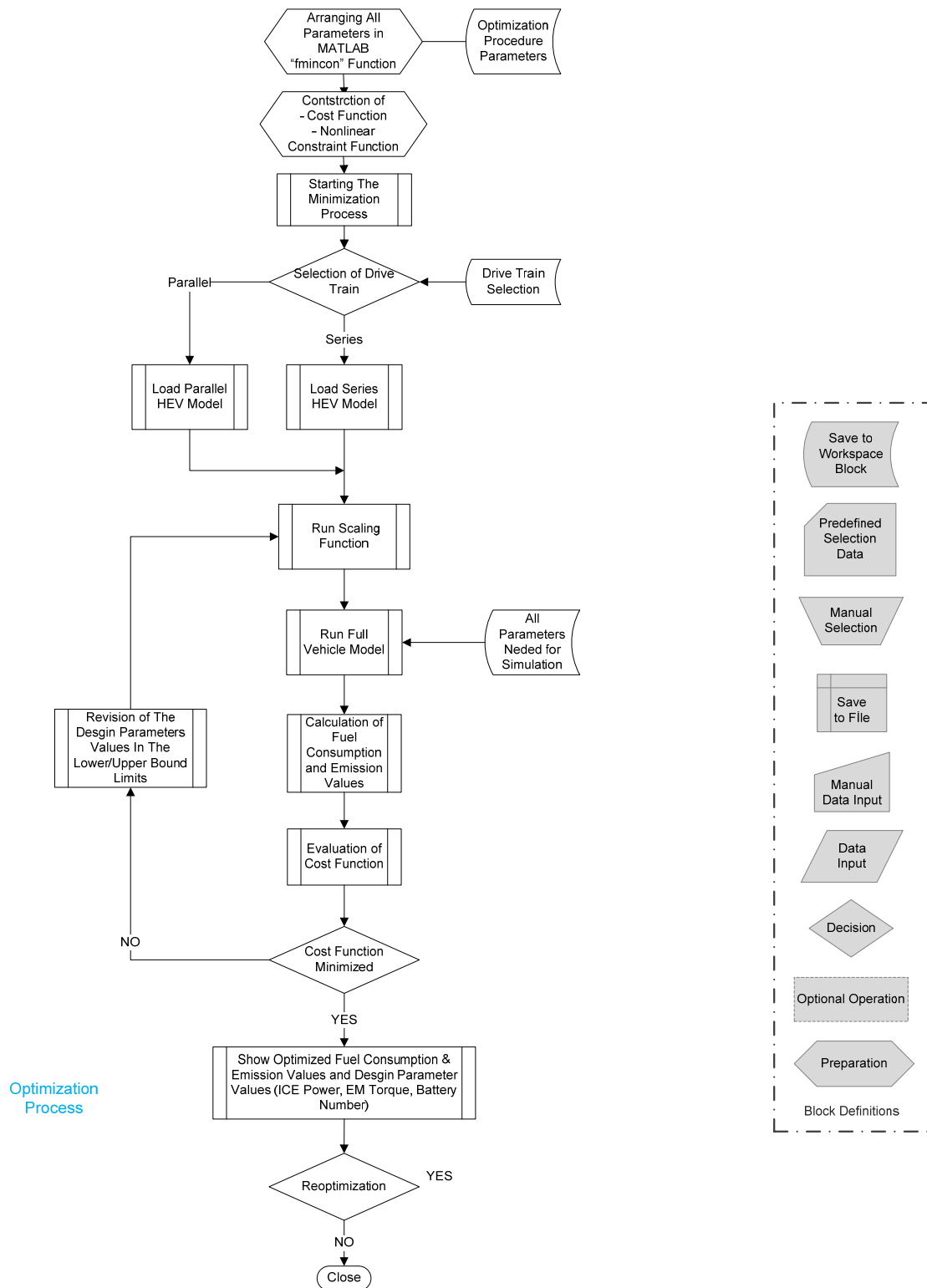


Figure A-3: Flowchart for parallel drivetrain sizing procedure – part3

b) Series Drivetrain Configuration Initial Sizing Flow Diagram

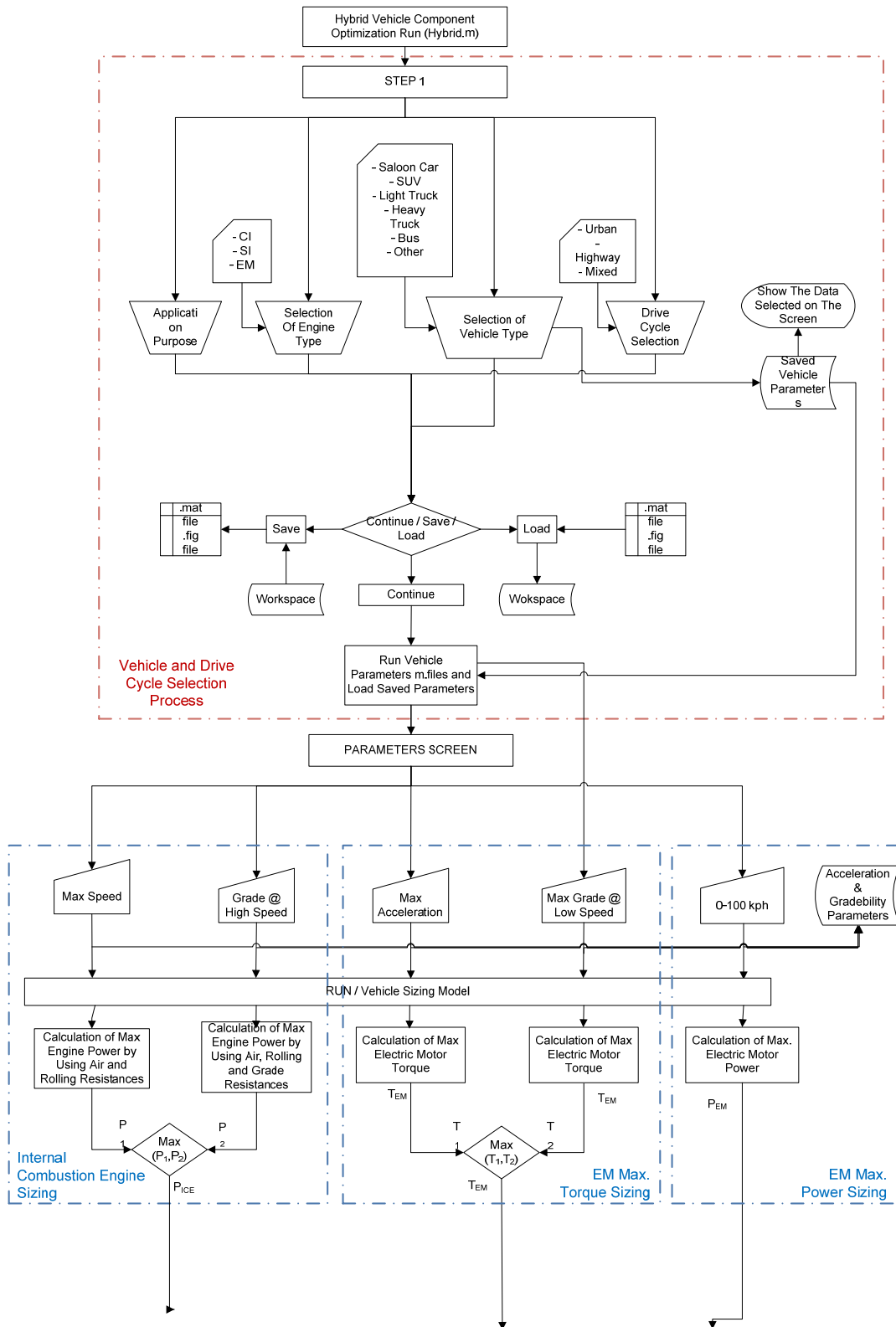


Figure A-4: Flowchart for series drivetrain sizing procedure – part1

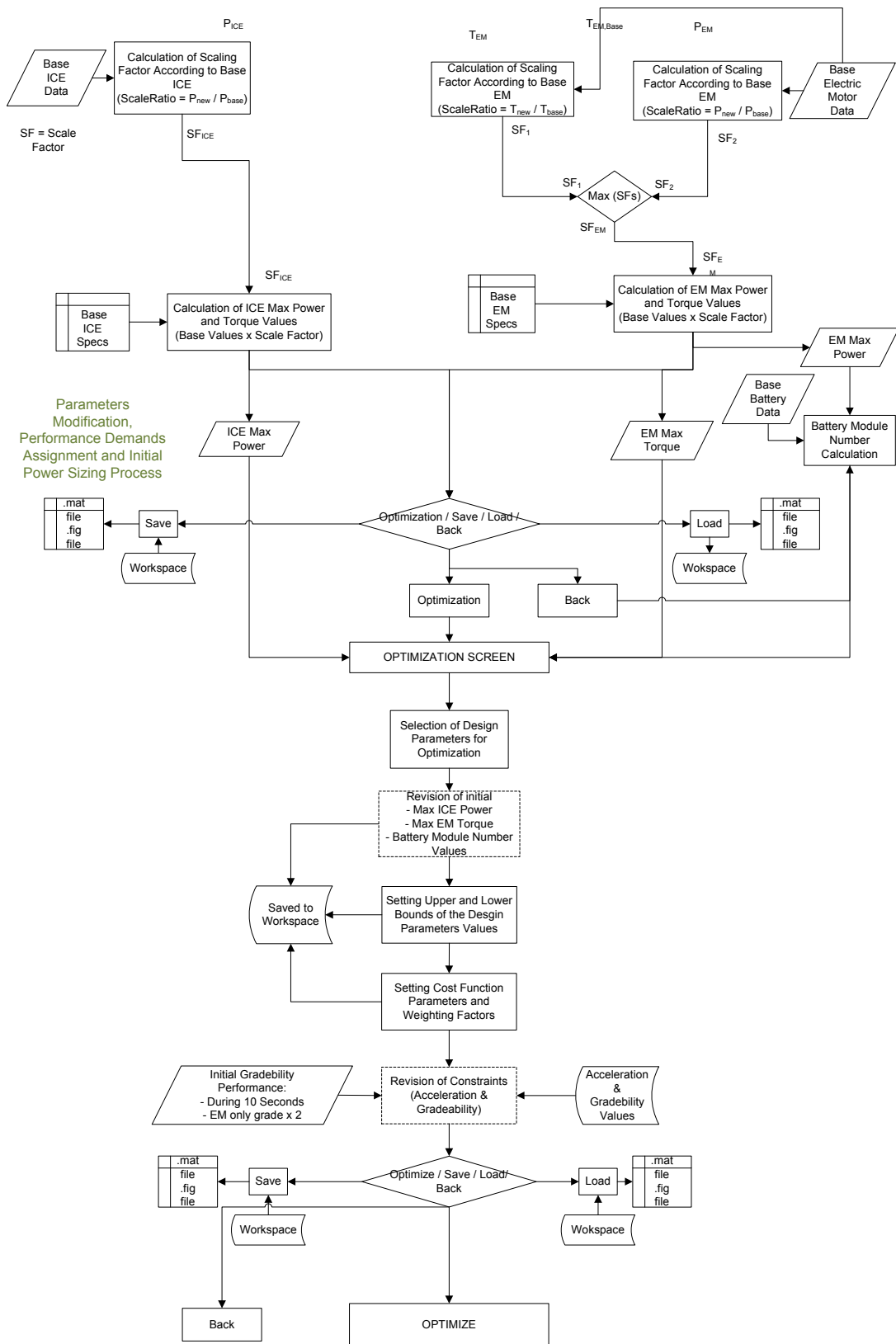


Figure A-5: Flowchart for series drivetrain sizing procedure – part2

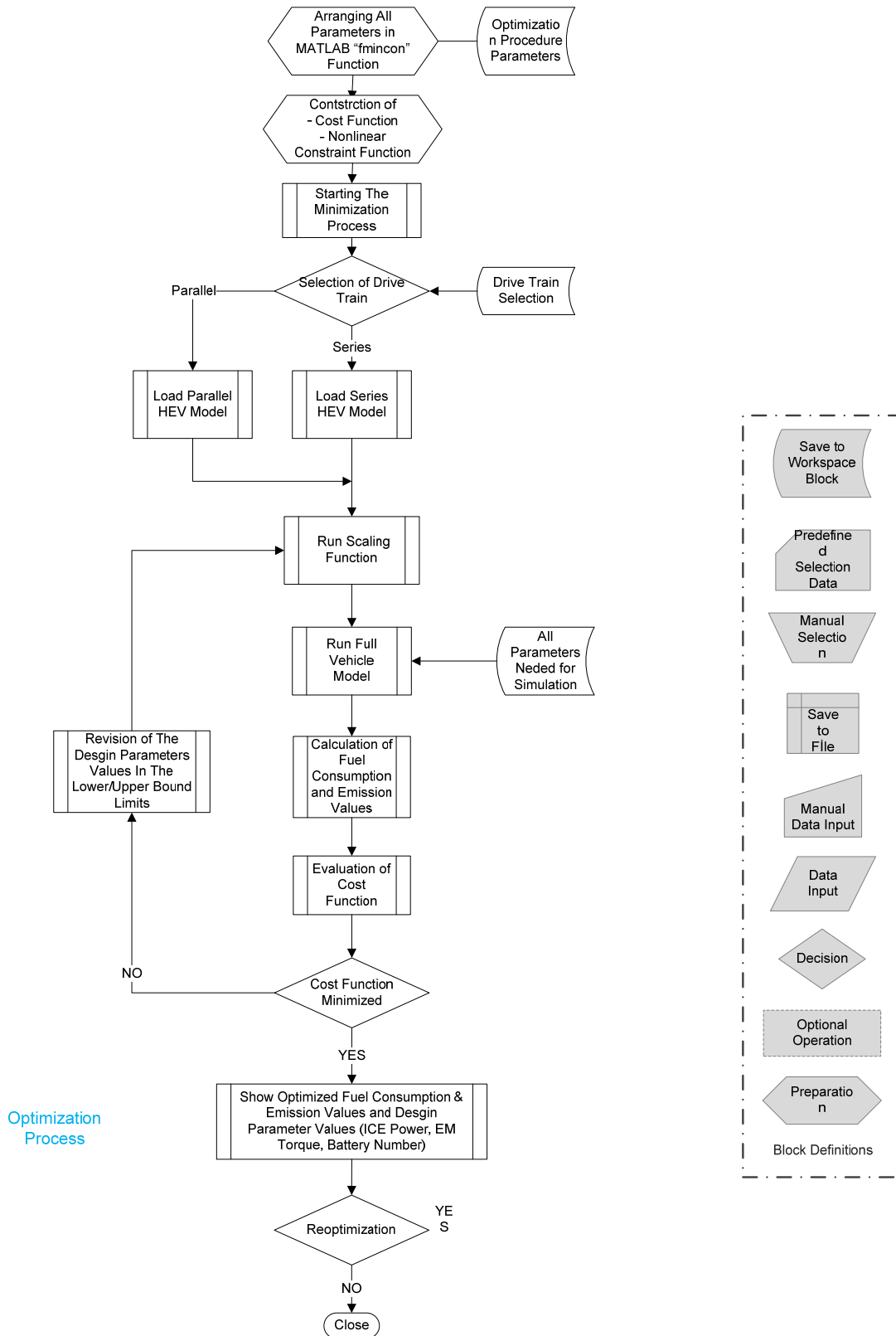


Figure A-6: Flowchart for series drivetrain sizing procedure – part3

## APPENDIX B

### OPTIMIZATION PROCESS RESULT DATA

#### a) Case 1

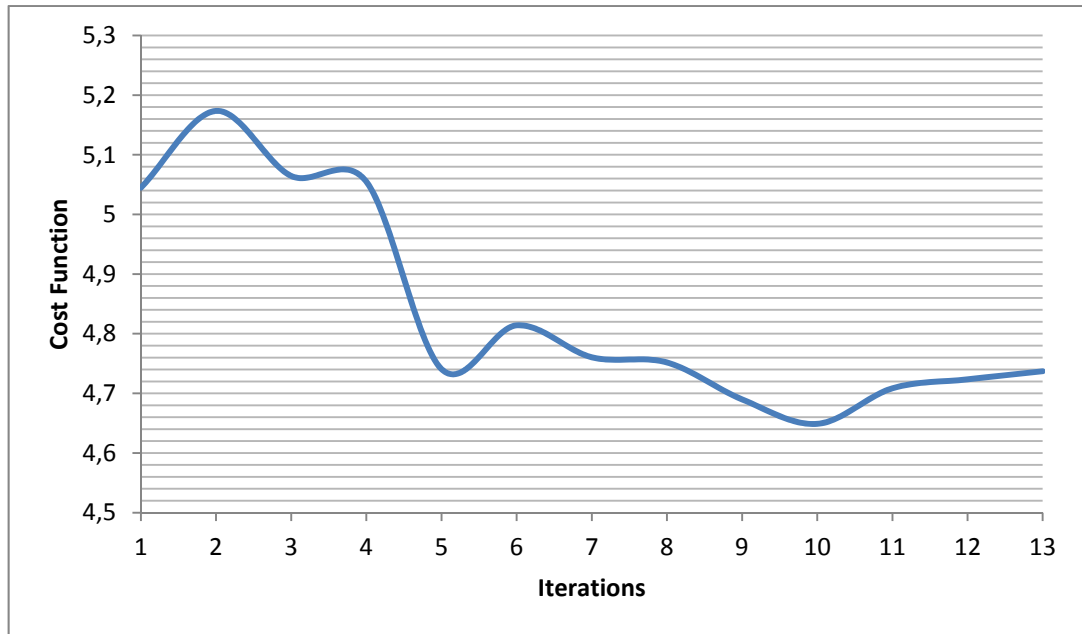


Figure B-1: Case 1 cost function value change during optimization

#### b) Case 2

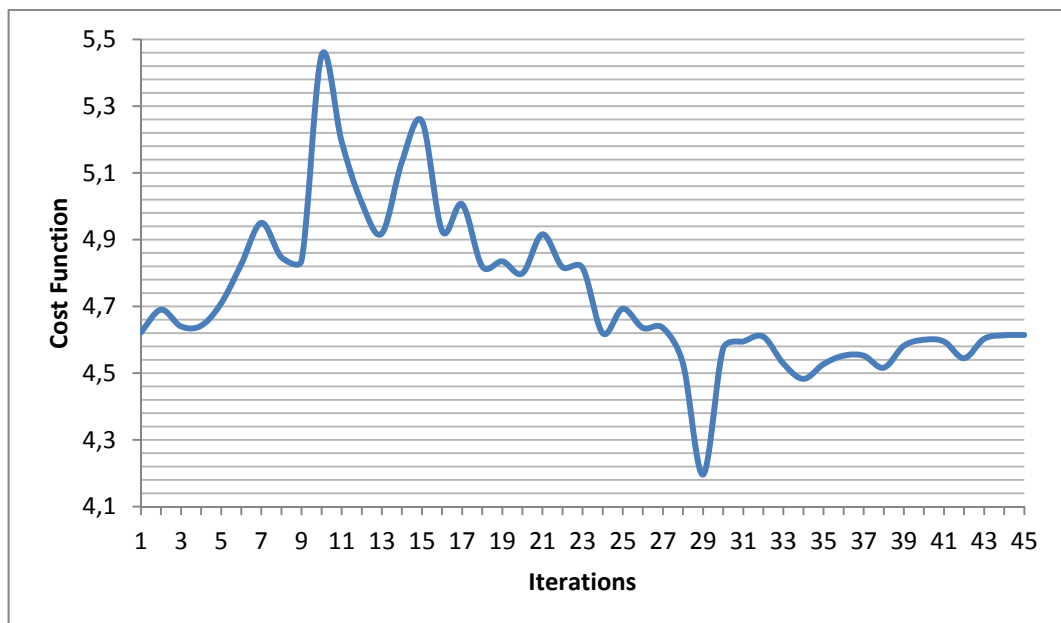


Figure B-2: Case 2 cost function value change during optimization

c) Case 3

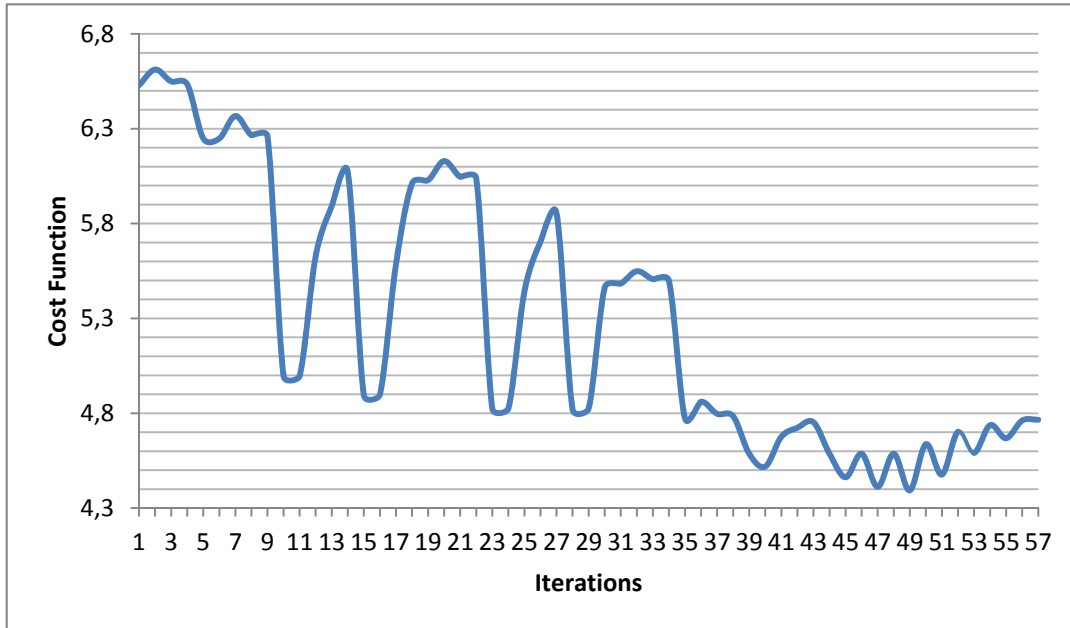


Figure B-3: Case 3 cost function value change during optimization

d) Case 4

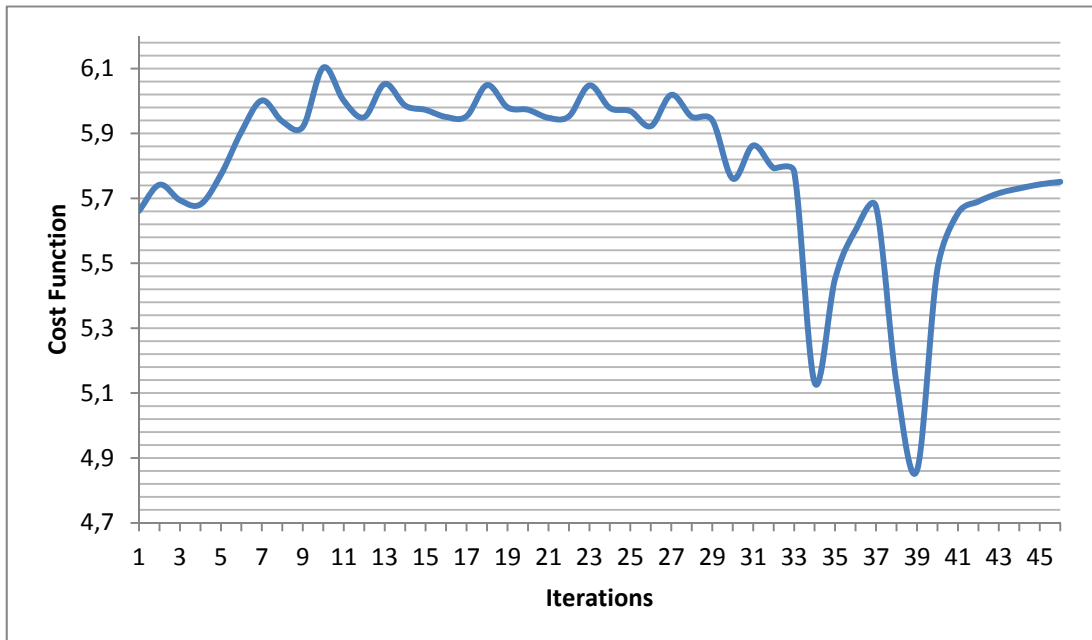


Figure B-4: Case 4 cost function value change during optimization

e) Case 5

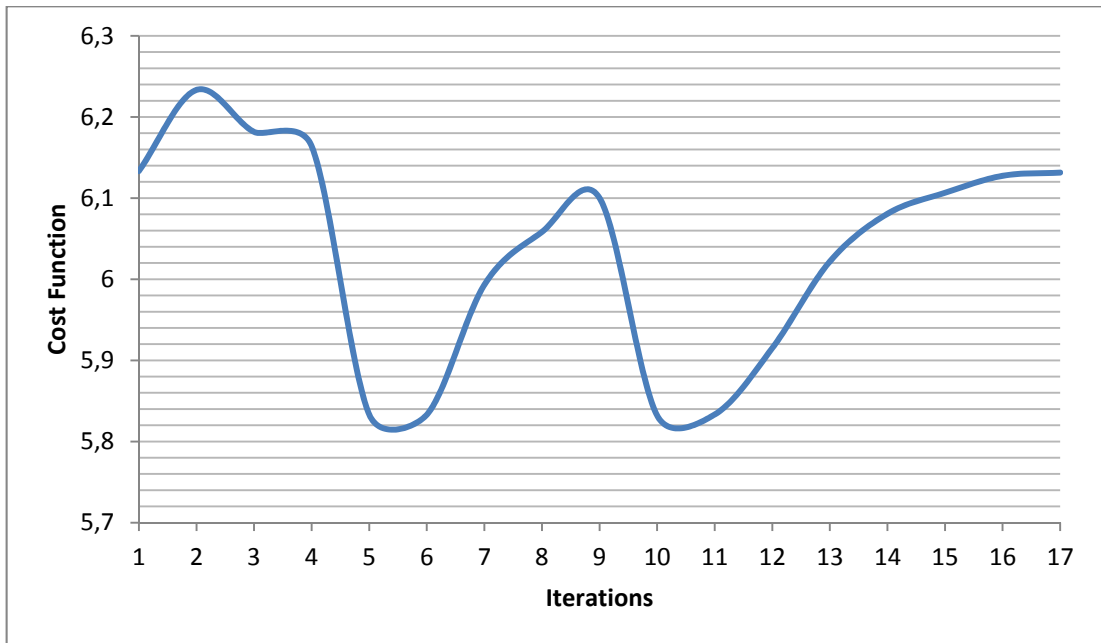


Figure B-5: Case 5 cost function value change during optimization

f) Case 6

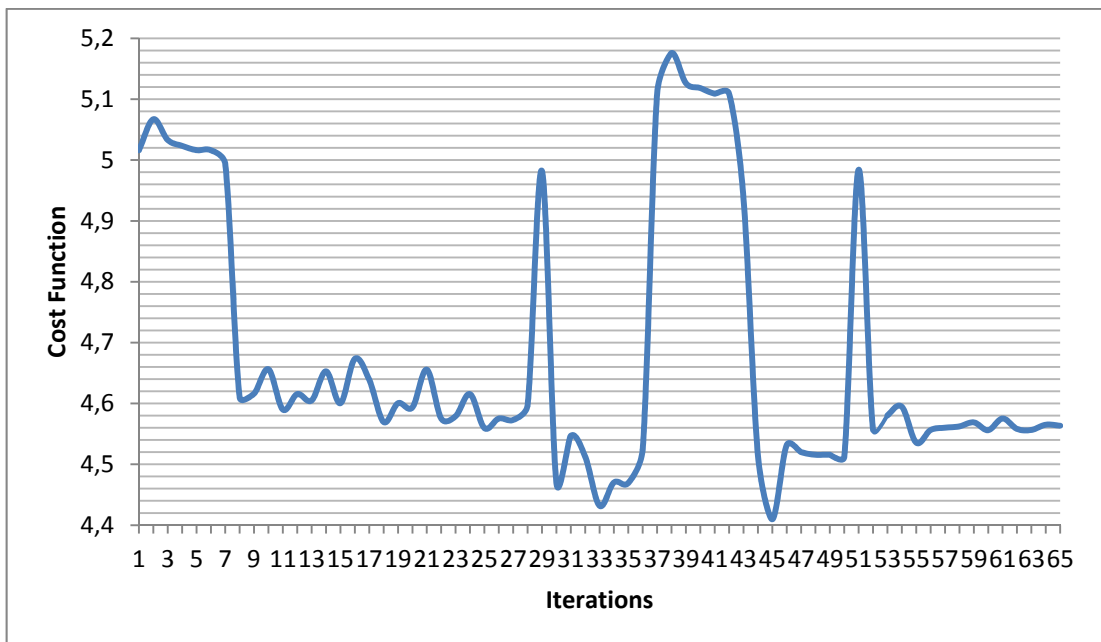


Figure B-6: Case 6 cost function value change during optimization

**g) Case 7**

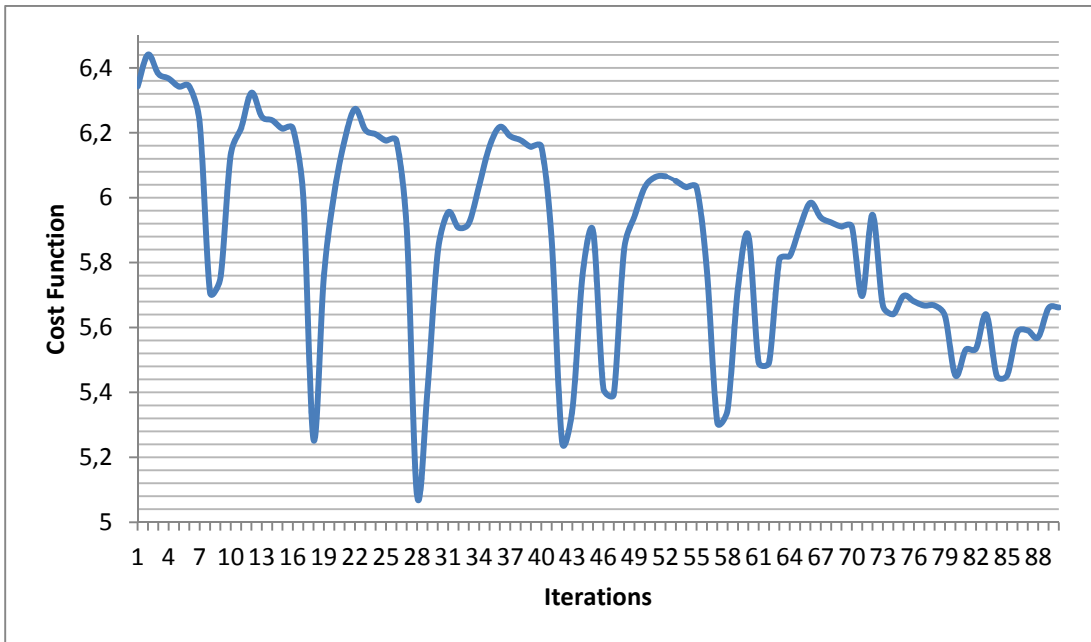


Figure B-7: Case 7 cost function value change during optimization

**h) Case 8**

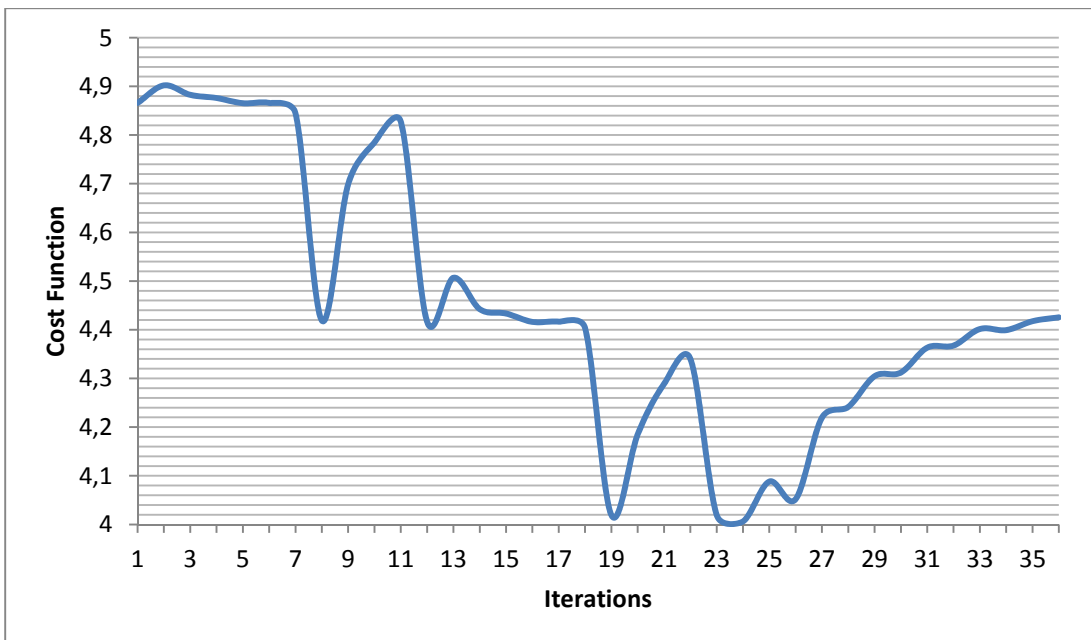


Figure B-8: Case 8 cost function value change during optimization

**i) Case 9**

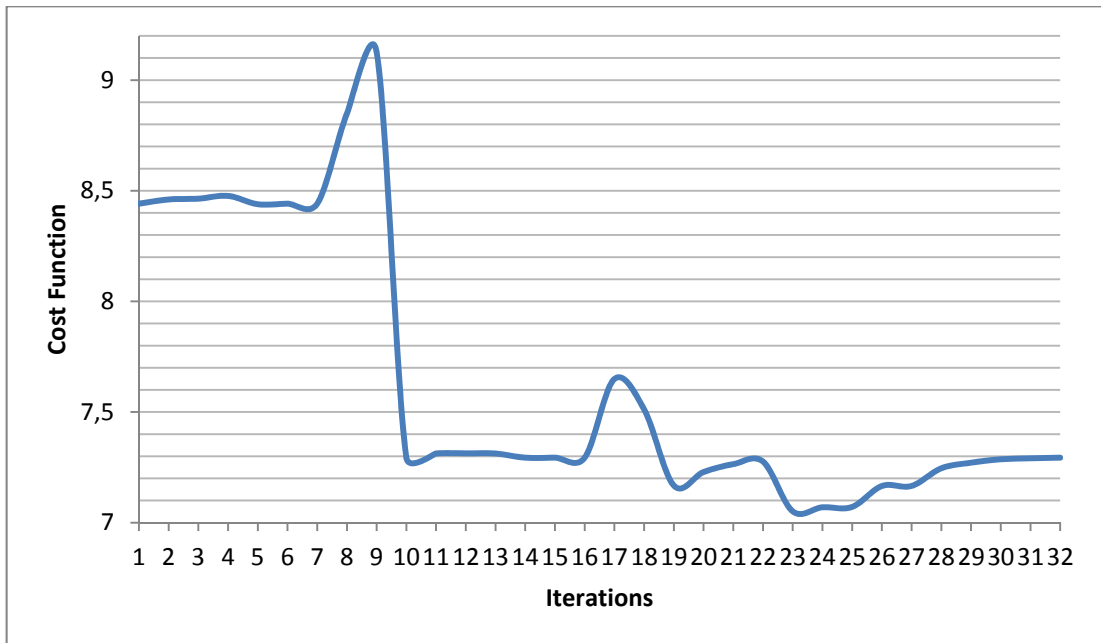


Figure B-9: Case 9 cost function value change during optimization

**j) Case 10**

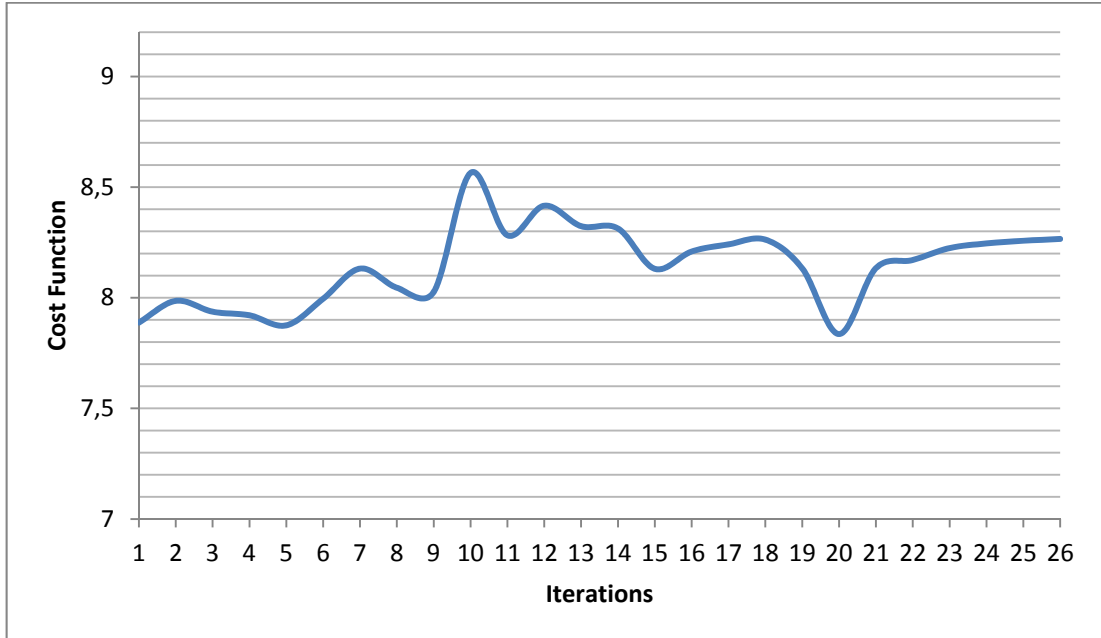


Figure B-10: Case 10 cost function value change during optimization

k) Case 11

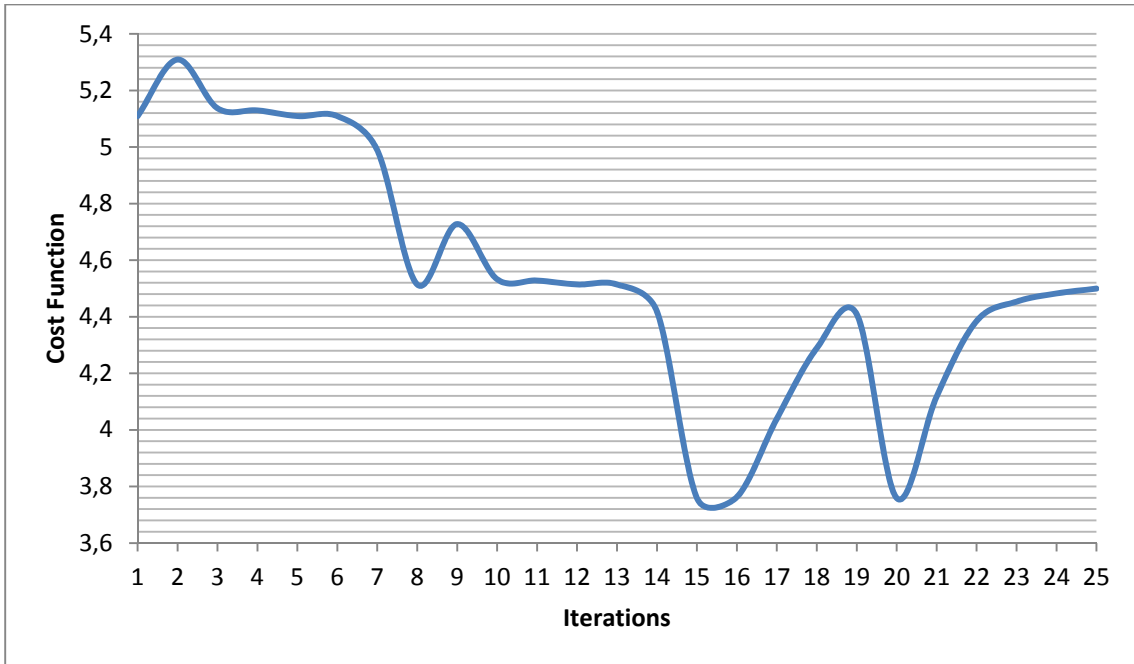


Figure B-11: Case 11 cost function value change during optimization

l) Case 12

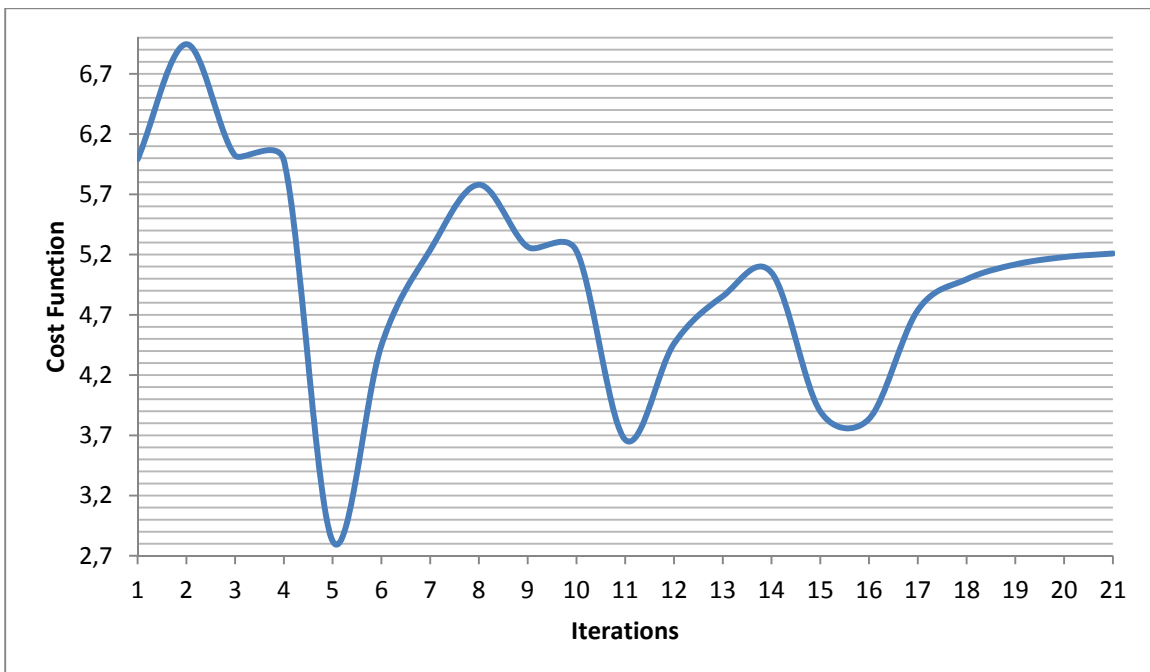


Figure B-12: Case 12 cost function value change during optimization

**m) Case 13**



Figure B-13: Case 13 cost function value change during optimization

**n) Case 14**

- **Run #1**

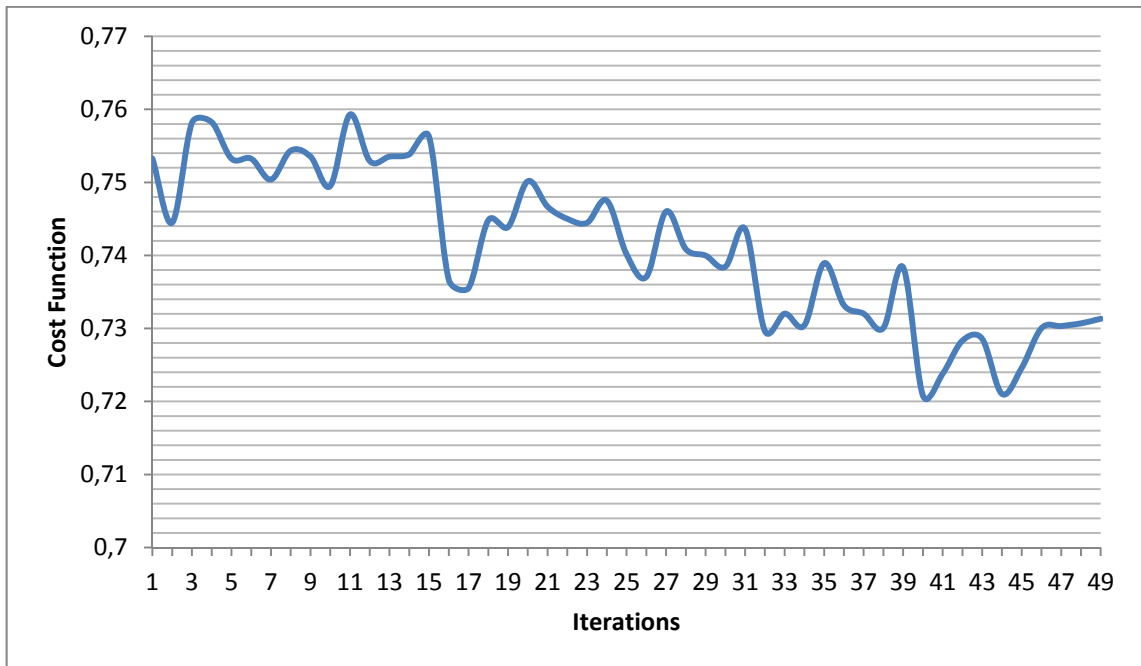


Figure B-14: Case 14 – Run #1 cost function value change during optimization

- **Run #2**

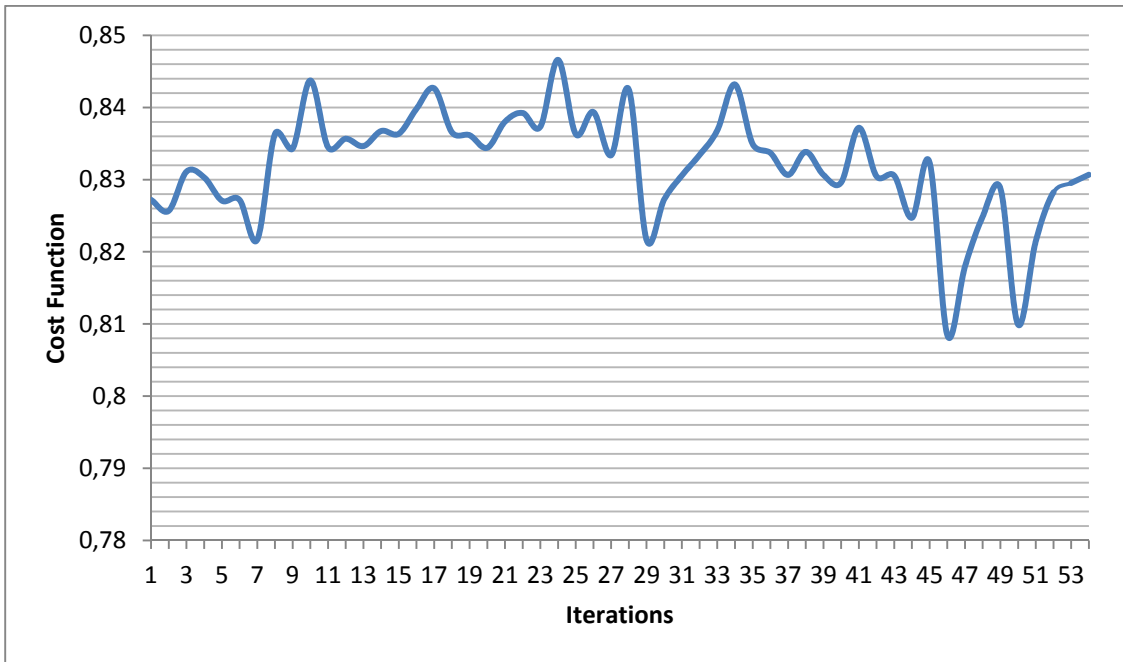


Figure B-15: Case 14 – Run #2 cost function value change during optimization

- **Run #3**

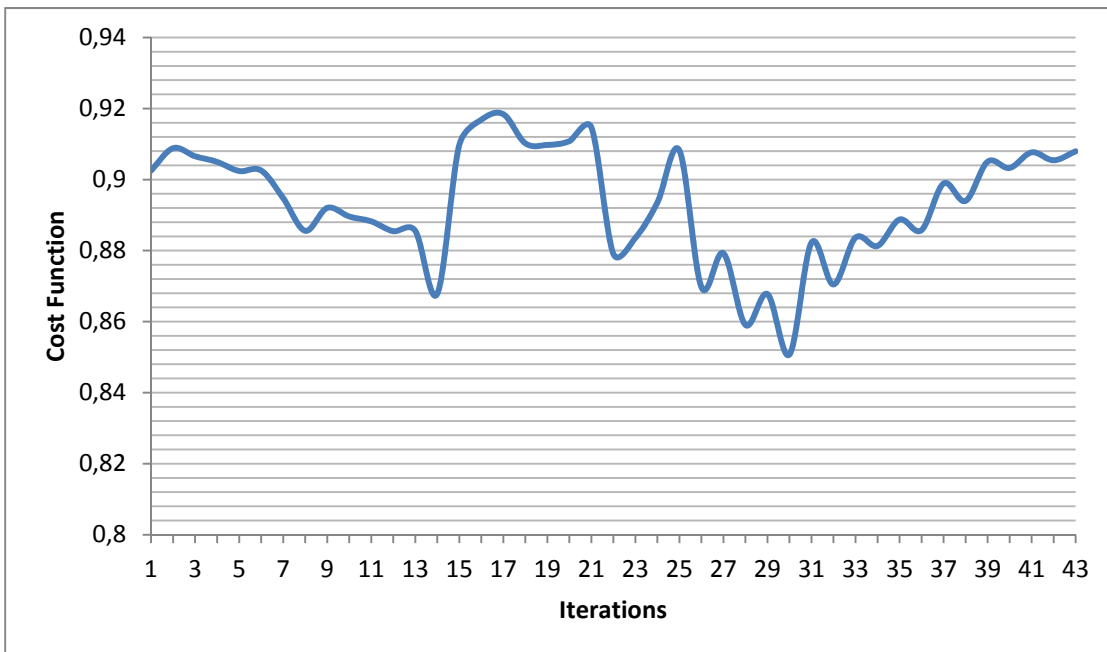


Figure B-16: Case 14 – Run #3 cost function value change during optimization

- **Run #4**

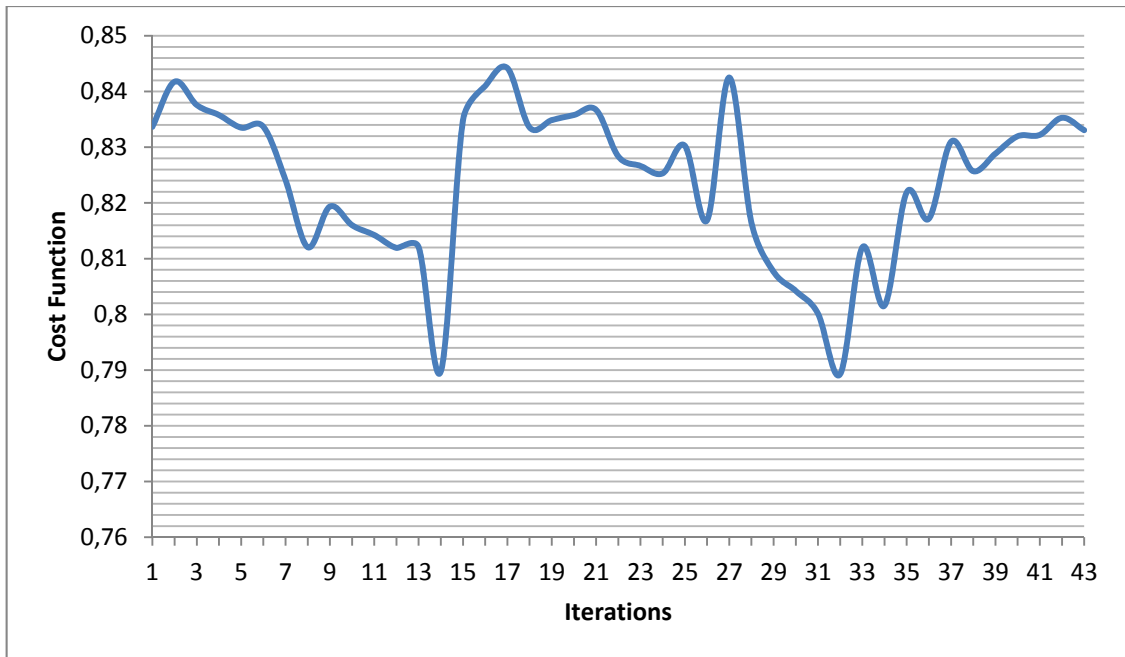


Figure B-17: Case 14 – Run #4 cost function value change during optimization

- **Run #5**

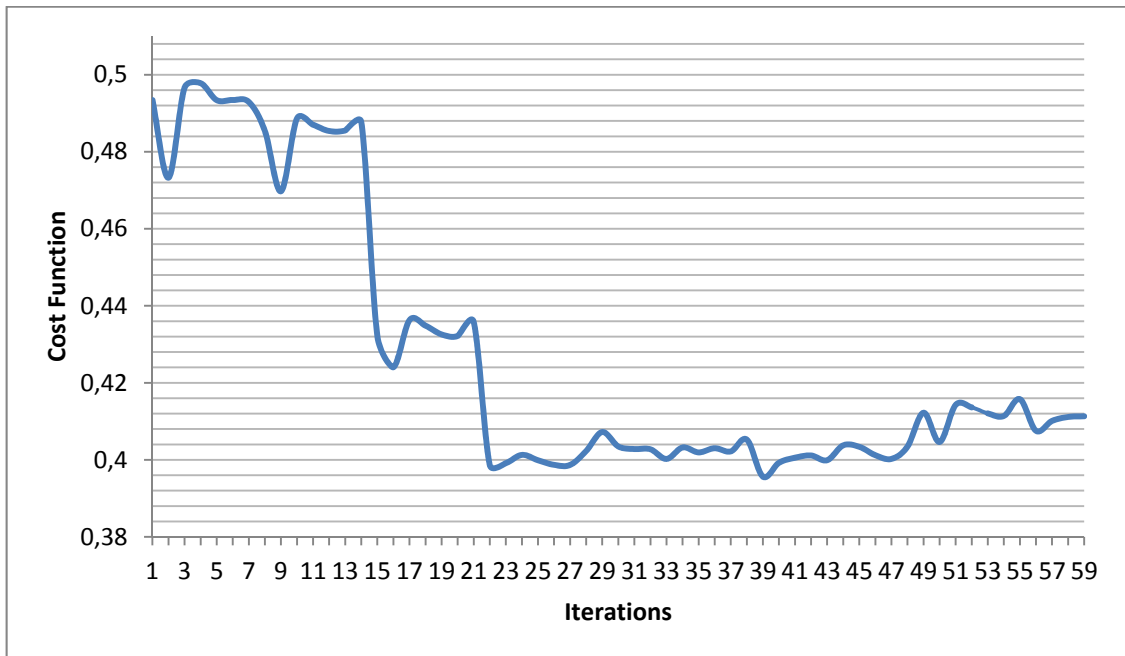


Figure B-18: Case 14 – Run #5 cost function value change during optimization

o) Case 15

- Run #1

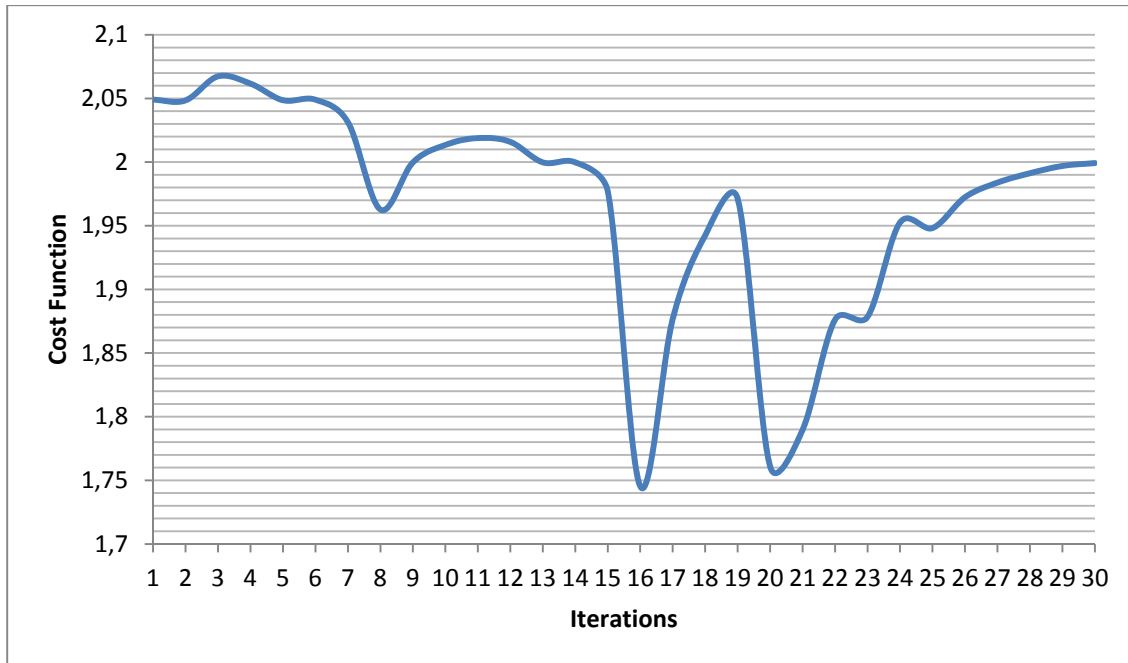


Figure B-19: Case 15 – Run #1 cost function value change during optimization

- Run #2

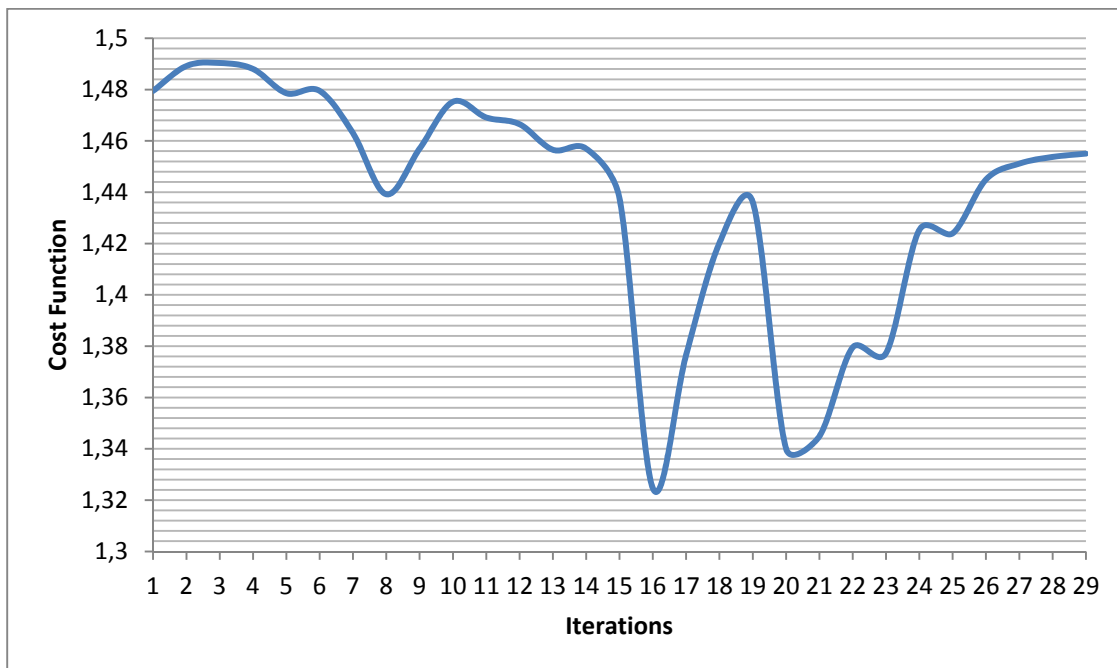


Figure B-20: Case 15 – Run #2 cost function value change during optimization

- **Run #3**

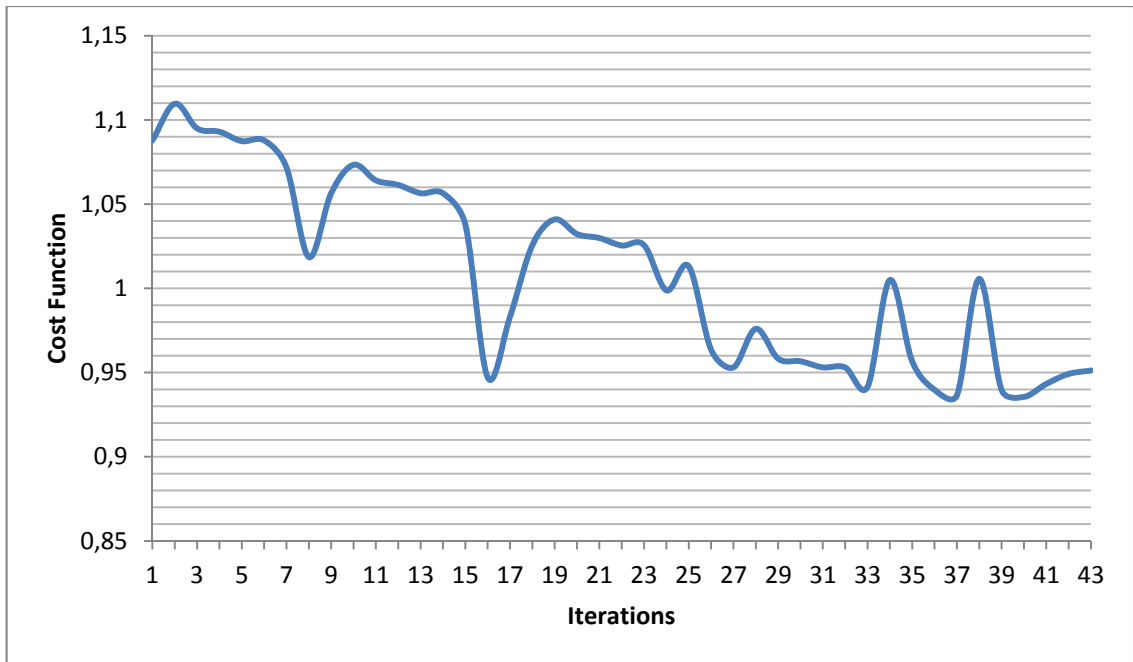


Figure B-21: Case 15 – Run #3 cost function value change during optimization

- **Run #4**

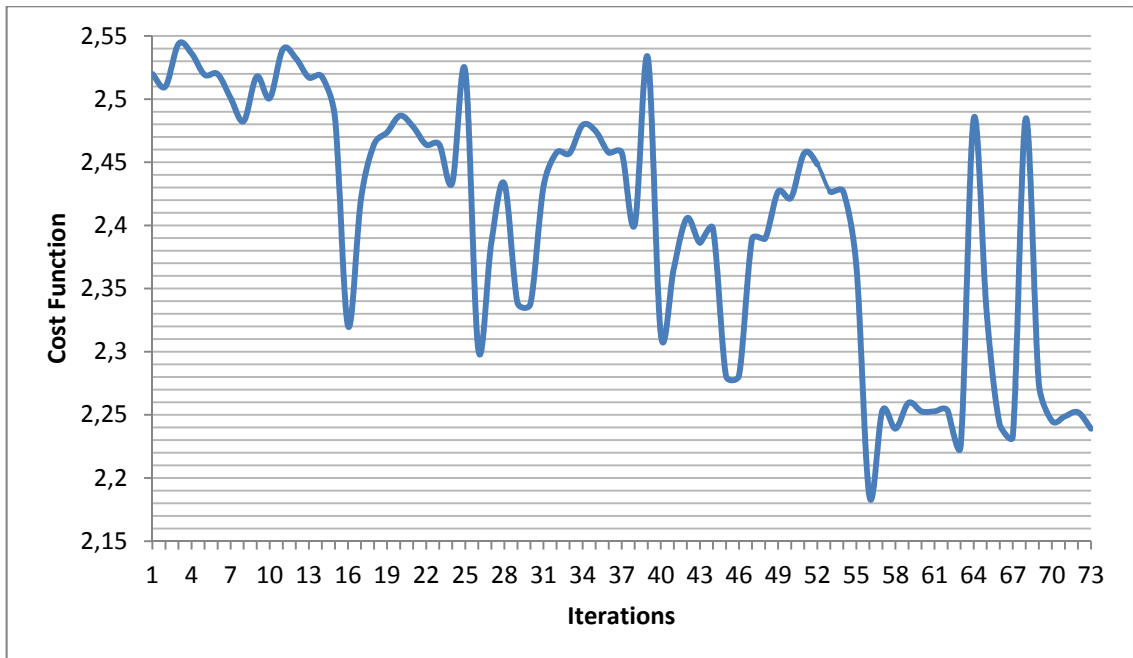


Figure B-22: Case 15 – Run #4 cost function value change during optimization

- **Run #5**

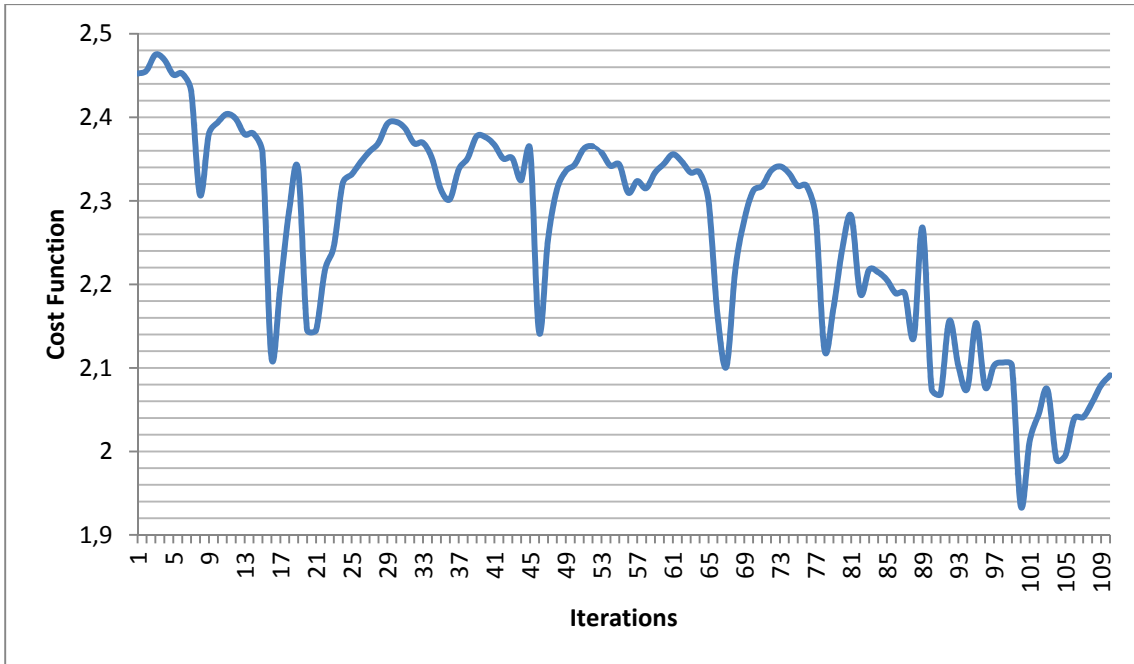


Figure B-23: Case 15 – Run #5 cost function value change during optimization

## APPENDIX C

### SIMULATION RESULTS FOR CONVENTIONAL VEHICLES

Here the conventional vehicle fuel consumption values are given. The simulations are carried on ADVISOR platform. The mass and power rating values are adjusted such that they closely meet the ones in cases (total power of parallel vehicle). There are 5 different simulation results for different drive cycles and different engine types.

a) UDDS Drive Cycle \_ 85kW SI \_ 1625 kg vehicle mass

The result is 9.3 L/100 km which is equal to 25.3 mpg. The emission value are HC = 0.397 g/km  
 CO = 1.789 g/km  
 NOx = 0.197 g/km  
 (All results are for cold start conditions)

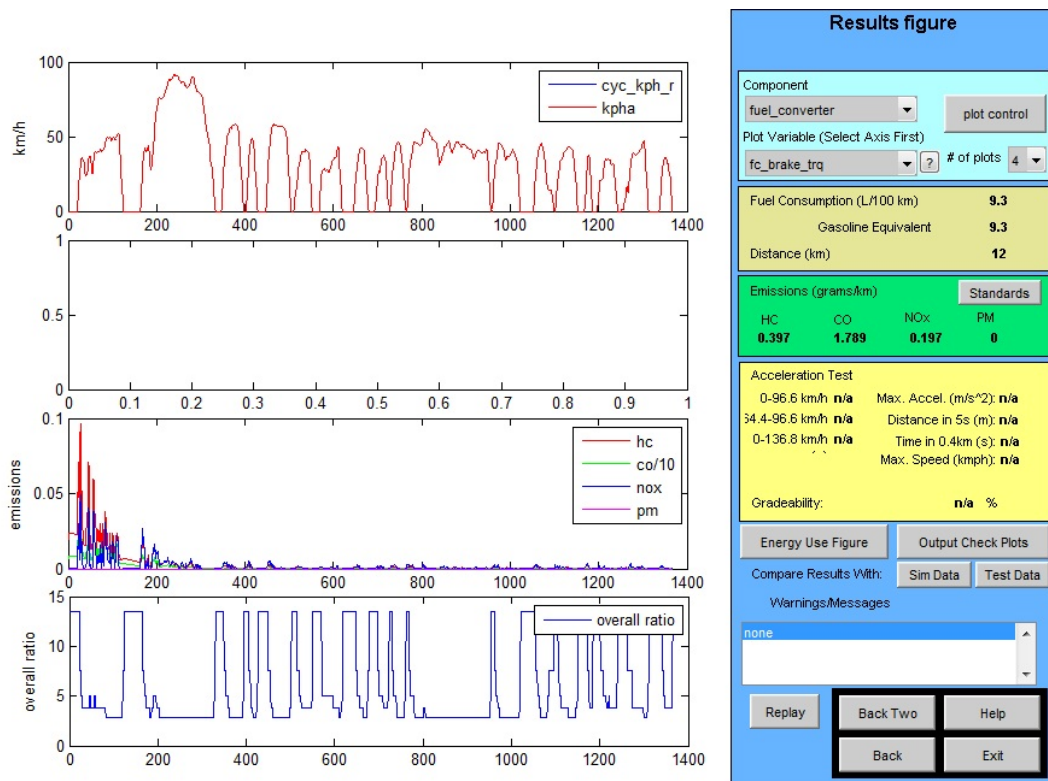
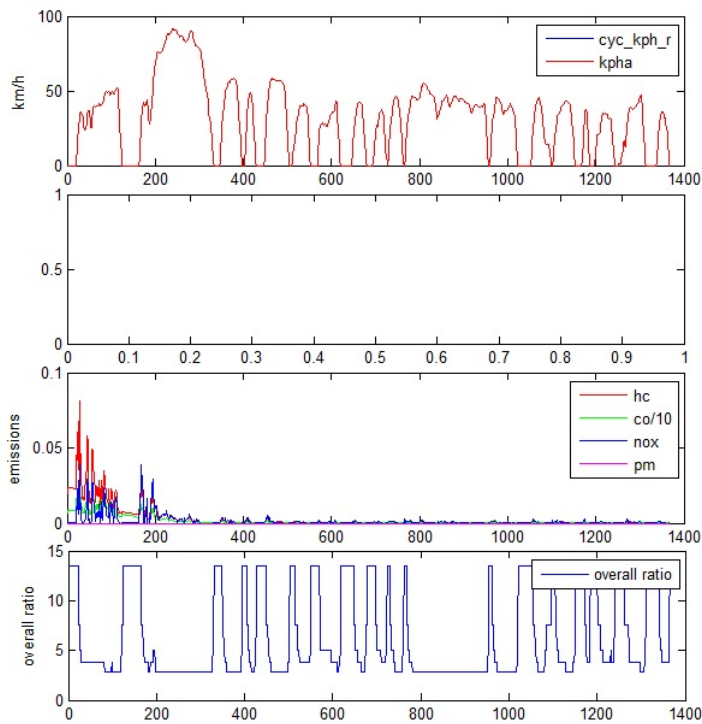


Figure C-1: Results for UDDS - 85kW SI - 1625 kg

b) UDDS Drive Cycle \_ 85kW SI \_ 1265 kg vehicle mass

The result is 8.5 L/100 km which is equal to 27.7 mpg. The emission value are HC = 0.396 g/km  
 CO = 1.867 g/km  
 NOx = 0.180 g/km  
 (All results are for cold start conditions)



### Results figure

Component: fuel\_converter plot control

Plot Variable (Select Axis First): fc\_brake\_trq # of plots: 4

Fuel Consumption (L/100 km)	8.5
Gasoline Equivalent	8.5
Distance (km)	12

Emissions (grams/km) <span>Standards</span>			
HC	CO	NOx	PM
0.396	1.867	0.18	0

Acceleration Test	
0-96.6 km/h	Max. Accel. (m/s <sup>2</sup> ): n/a
34.4-96.6 km/h	Distance in 5s (m): n/a
0-136.8 km/h	Time in 0.4km (s): n/a
	Max. Speed (kmph): n/a

Gradeability: n/a %

Energy Use Figure Output Check Plots

Compare Results With: Sim Data Test Data

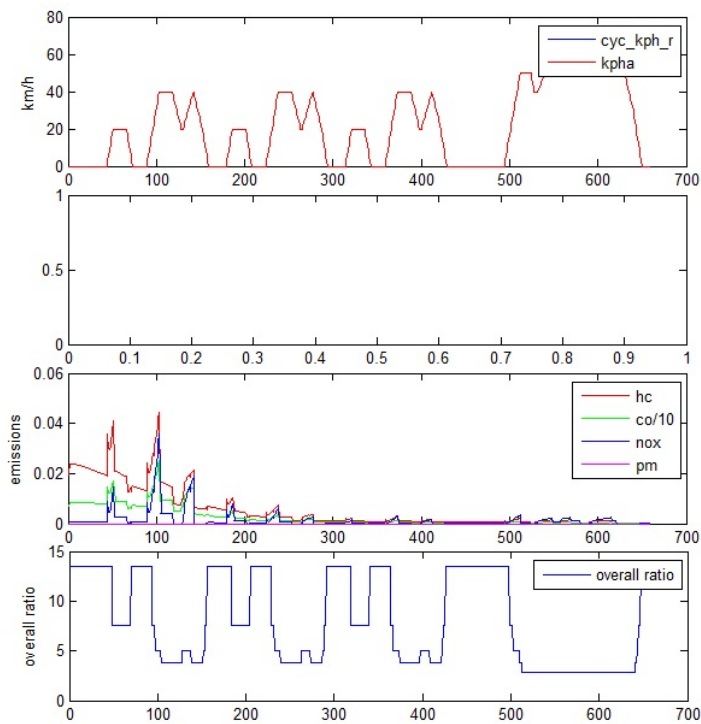
Warnings/Messages: none

Replay
Back Two Help  
Back Exit

Figure C-2: Results for UDDS - 85kW SI - 1265 kg

c) J1015 Drive Cycle \_ 85kW SI \_ 1265 kg vehicle mass

The result is 10.6 L/100 km which is equal to 22.2 mpg. The emission value are HC = 0.898 g/km  
 CO = 4.278 g/km  
 NOx = 0.222 g/km  
 (All results are for cold start conditions)



### Results figure

Component: fuel\_converter plot control

Plot Variable (Select Axis First): fc\_brake\_trq # of plots: 4

Fuel Consumption (L/100 km)	<b>10.6</b>
Gasoline Equivalent	<b>10.6</b>
Distance (km)	<b>4.2</b>

Emissions (grams/km)				Standards
HC	CO	NOx	PM	
<b>0.898</b>	<b>4.278</b>	<b>0.222</b>	<b>0</b>	

Acceleration Test

0-96 km/h	n/a	Max. Accel. (m/s <sup>2</sup> )	n/a
34.4-96.6 km/h	n/a	Distance in 5s (m)	n/a
0-136.8 km/h	n/a	Time in 0.4km (s)	n/a
		Max. Speed (kmph)	n/a

Gradeability: n/a %

Energy Use Figure Output Check Plots

Compare Results With: Sim Data Test Data

Warnings/Messages

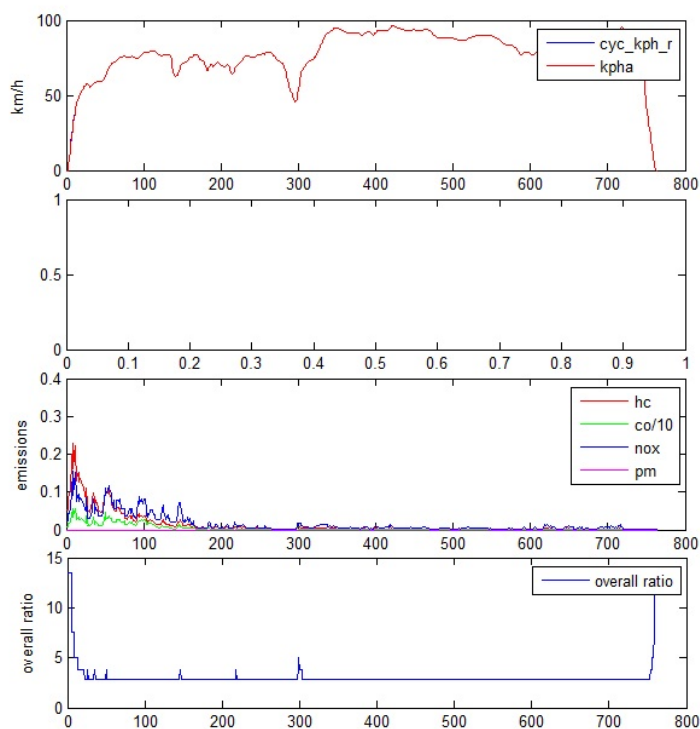
none

Replay
Back Two Help  
Back Exit

Figure C-3: Results for J1015 - 85kW SI - 1265 kg

d) HWFET Drive Cycle \_ 102kW SI \_ 1390 kg vehicle mass

The result is 6.8 L/100 km which is equal to 34.6 mpg. The emission value are HC = 0.616 g/km  
 CO = 2.106 g/km  
 NOx = 0.735 g/km  
 (All results are for cold start conditions)



### Results figure

Component: fuel\_converter plot control

Plot Variable (Select Axis First): fc\_brake\_trq ? # of plots: 4

Fuel Consumption (L/100 km)	<b>6.8</b>
Gasoline Equivalent	<b>6.8</b>
Distance (km)	<b>16.5</b>

Emissions (grams/km)				Standards
HC	CO	NOx	PM	
<b>0.616</b>	<b>2.106</b>	<b>0.735</b>	<b>0</b>	

Acceleration Test

0-96.6 km/h	n/a	Max. Accel. (m/s <sup>2</sup> ):	n/a
34.4-96.6 km/h	n/a	Distance in 5s (m):	n/a
0-136.8 km/h	n/a	Time in 0.4km (s):	n/a
		Max. Speed (kmph):	n/a

Gradeability: n/a %

Energy Use Figure Output Check Plots

Compare Results With: Sim Data Test Data

Warnings/Messages: none

Replay
Back Two Help  
Back Exit

Figure C-4: Results for HWFET - 102kW SI - 1265 kg

e) UDDS Drive Cycle\_ 85W CI\_ 1200 kg vehicle mass

The result is 6.2 L/100 km which is equal to 37.9 mpg. The emission value are HC = 0.852 g/km  
 CO = 2.462 g/km  
 NOx = 0.489 g/km  
 PM = 0.055 g/km  
 (All results are for cold start conditions)

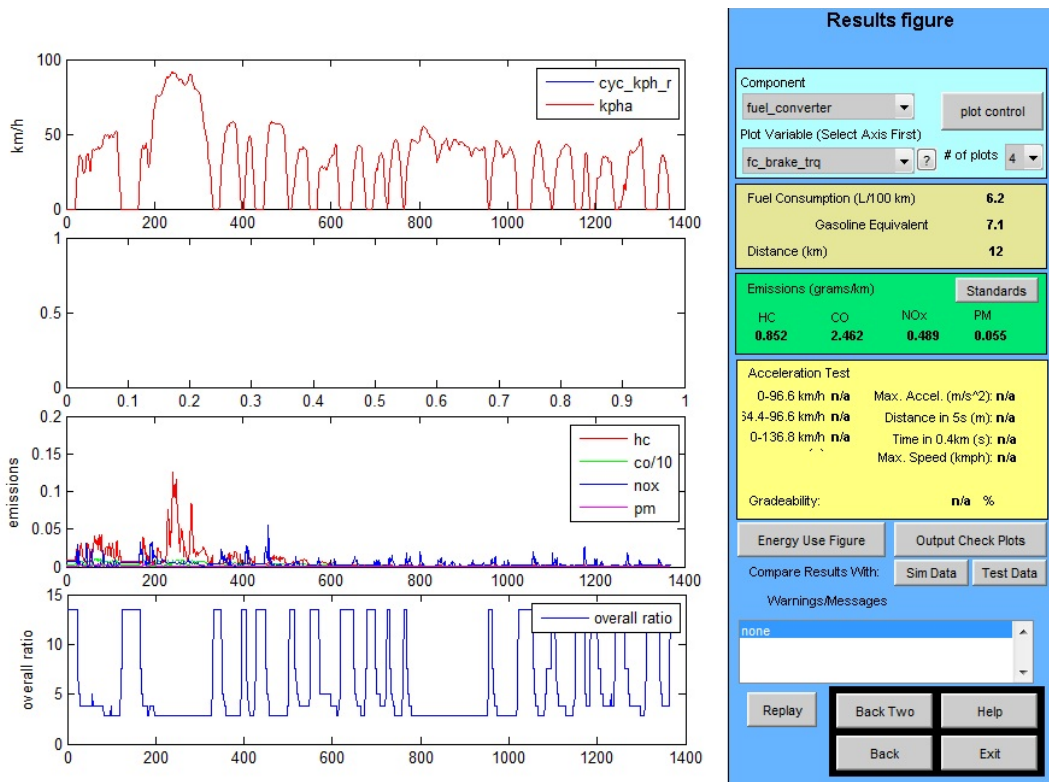


Figure C-5: Results for UDDS - 85kW CI - 1200 kg